Néprilysine et dysfonction d'organe : biomarqueur et déterminant de la vasoréactivité en condition physiopathologique

Thibault Michel

Université Paris Cité

École doctorale Hématologie, Oncogenèse et Biothérapies (ED 561)

Marqueurs cardiovasculaires en situation de stress (UMR-S 942)

Néprilysine et dysfonction d'organe : biomarqueur et déterminant de la vasoréactivité en condition physiopathologique

Par Thibault MICHEL

Thèse de doctorat de Biothérapies et Biotechnologies

Dirigée par Nicolas VODOVAR
Et co-encadrée par Hélène NOUGUÉ

Présentée et soutenue publiquement le 27 novembre 2023
Devant le jury composé de :

Anne-Claire LUKASZEWICZ, PU-PH, Université Claude Bernard Lyon 1	Rapportrice
Guillaume BESCH, PU-PH, Université de Franche-Comté	Rapporteur
Anaïs CAILLARD, MD-PhD, Université de Bretagne Occidentale	Examinatrice
Kada KLOUCHE, PU-PH, Université de Montpellier	Examinateur
Bernard CHOLLEY, PU-PH, Université Paris Cité	Examinateur
Nicolas VODOVAR, CR-HDR, Université Paris Cité	Directeur de thèse
Hélène NOUGUÉ, MD-PhD, Université Paris Cité	Membre invité

RESUME

Néprilysine et dysfonction d'organe : biomarqueur et déterminant de la vasoréactivité en condition physiopathologique

L'inhibition de la néprilysine (NEP) dans l'insuffisance cardiaque (IC) est un axe thérapeutique prometteur. En effet le sacubitril/valsartan (S/V) a montré son efficacité dans le traitement de l'IC chronique avec fraction d'éjection du ventricule gauche (FEVG) réduite en réduisant la morbi-mortalité. Cependant le mode d'action de cette molécule reste peu connu.

Tout d'abord, j'ai étudié l'impact du S/V sur le métabolisme des peptides natriurétiques (ANP et BNP) qui sont des biomarqueurs très utilisés en cardiologie. Cette étude a été réalisée sur une cohorte de 73 atteints d'IC à FEVG réduite chez lesquels le S/V a été introduit. Cette étude a montré que la glycosylation des précurseurs des peptides natriurétique (proANP et proBNP) était impactée par la S/V, avec des conséquences importantes sur les dosages de ces biomarqueurs, expliquant en partie leur évolution inattendue chez les patients atteints d'IC à FEVG réduite traités par S/V. Ce travail a également conduit à une étude approfondie du métabolisme du proANP qui a permis de montrer que : i) la production d'ANP dans l'IC à FEVG réduite est freinée par des mécanismes épigénétiques qui implique des miRNAs, ii) que l'action du sacubitril n'est pas restreint à la NEP, et que iii) le S/V permet de rétablir un métabolisme normal du proANP. L'ensemble de ces travaux a permis de mieux comprendre le mode d'action du S/V et éclaire sur la physiopathologie de IC à FEVG réduite.

La seconde partie de mon projet s'est intéressé aux conséquences de l'inhibition de la NEP dans le choc septique. L'inhibition de la NEP provoque une vasodilatation et une diminution de la pression artérielle (PA) qui sont des aspects majeurs de la physiopathologie du choc septique. Chez les primates, le BNP est un inhibiteur endogène de la NEP quand > 916 pg/mL, et nous avons postulé que cette inhibition de la NEP par le BNP pouvait jouer un rôle dans l'aggravation du choc septique. Dans un modèle de choc septique chez le rat, j'ai montré que l'administration de BNP humain à des concentrations inhibitrice de la NEP provoquait une diminution brutale de la PA, récapitulant les formes les plus graves de choc septique chez l'homme. Nous avons identifié une molécule (X.Y.U.) qui prévient cette inhibition et la réverse partiellement in vitro. Chez le rat, X.Y.U. prévient également les effets vasoplégiants du BNP dans le choc septique. Ce travail a permis de montrer que l'inhibition endogène de la NEP par le BNP humain jouait un rôle physiopathologique majeur dans les formes les plus sévères de CS et que X.Y.U. est un option thérapeutique prometteuse.

Enfin dans la dernière partie de ce travail j'ai étudié le rôle de la NEP comme biomarqueur de l'insuffisance rénale aiguë (IRA) et comme participant à sa physiopathologie. L'activation du système rénine-angiotensine-aldostérone (SRAA) comme voie physiopathologique de l'agression rénale dans le contexte de chirurgie cardiaque reste débattu. La NEP urinaire étant un biomarqueur potentiel de la survenue d'une IRA et la NEP limitant l'activation du SRAA, j'ai exploré le rôle potentiel de la NEP dans le contrôle du SRAA dans l'IRA dans une cohorte de patients ayant subi une chirurgie cardiaque élective ave circulation extracorporelle. Les résultats montrent que la NEP plasmatique est un biomarqueur précoce de la survenue de l'IRA, que le SRAA est activé dans l'IRA, mais que la NEP ne semble pas impacter l'activation du SRAA dans ce contexte. Néanmoins, ces travaux suggèrent un intérêt possible du S/V dans le traitement de l'IRA dans ce contexte.

En conclusion, ce travail a permis de préciser le rôle physiopathologique de la NEP dans différents contextes cliniques et montre que son inhibition est bénéfique dans l'IC à FEVG réduite, possiblement dans l'IRA, mais est délétère dans le choc septique. Ces travaux devraient permettre d'ouvrir de nouvelles voies thérapeutiques, en particulier dans le choc septique.

Mots clés : Néprilysine, insuffisance cardiaque, choc septique, insuffisance rénale aigue, chirurgie cardiaque

SUMMARY

Neprilysin and organ dysfunction: biomarker and role on vasoreactivity in pathophysiological conditions

Neprilysin (NEP) inhibition appears to be a promising therapeutic approach in heart failure (HF). Indeed, sacubitril/valsartan (S/V) has shown its effectiveness in the treatment of HF with reduced ejection fraction (HFrEF) by reducing morbidity and mortality by ~20%. However, S/V mode of action remains partially unclear.

Firstly, I studied the impact of S/V on the metabolism of natriuretic peptides (ANP and BNP) which are biomarkers routinely used in cardiology. This study was carried out on a cohort of 73 patients with HFrEF who were transitioned to S/V, and a population of healthy volunteers. This study showed that the glycosylation of natriuretic peptide precursors (proANP and proBNP) was impacted by S/V, with significant consequences on their measurements, partly explaining their unexpected evolution in patients treated with S/V. This work also led to an in-depth study of the metabolism of proANP which showed that: i) the production of ANP in HFrEF is sub-optimal due to epigenetic mechanisms which involve miRNAs, ii) that the action sacubitril is not restricted to NEP, and that iii) S/V restored and enhanced proANP. All of this work has not only provided a better understanding of the mode of action of S/V but also shed light on the pathophysiology of HFrEF.

The second part of my project focused on the consequences of inhibition of NEP in septic shock. Inhibition of NEP causes vasodilation and low blood pressure, which are hallmarks of septic shock. In primates, BNP is an endogenous NEP inhibitor when > 916 pg/mL, and we hypothesised that this BNP-mediated NEP inhibition may play a role in worsening septic shock. In a rat model of septic shock, I showed that administration of human BNP at NEP-inhibitory concentrations caused an abrupt decrease in blood pressure, recapitulating the most severe forms of septic shock in humans. We have identified a molecule (X.Y.U.) which prevents this inhibition and partially reverses it in vitro. In rats, X.Y.U. also prevented the vasoplegic effects of BNP in septic shock. This work showed that BNP-mediated NEP inhibition could play a major pathophysiological role in the most severe forms of septic shock and that X.Y.U. is a promising therapeutic option.

Finally, in the last part of this work of thesis I studied the role of NEP both as a biomarker of acute kidney injury (AKI) but also as a participant in its pathophysiology. Indeed, the activation of the renin-angiotensin-aldosterone system (RAAS) as a pathophysiological pathway of renal aggression in the context of cardiac surgery remains debated. Urinary NEP being a potential biomarker of the occurrence of AKI and NEP limiting the activation of the RAAS, I explored the potential role of NEP in the control of RAAS in AKI in a cohort of patients hospitalized in intensive care following elective cardiac surgery with extracorporeal circulation (ECC). The results obtained show that plasma NEP is an early biomarker of the occurrence of AKI, that the RAAS is activated in AKI, but that NEP does not seem to impact the activation of the RAAS in this context. Nevertheless, this work suggests a possible benefit of sacubitril/valsartan in the treatment of AKI in this context.

In conclusion, this work has clarified the pathophysiological role of NEP in different clinical contexts and shows that its inhibition is beneficial in HFrEF, possibly in AKI, but is harmful in septic shock. This work should open new therapeutic avenues, particularly in septic shock.

Keywords: Neprilysin, heart failure, septic shock, acute kidney injury, cardiac surgery

Table des matières

INTRODUCTION

1 Peptides natriurétiques et néprilysine

1.1 Peptides natriurétiques

1.1.1 De la production à la libération

Les peptides natriurétiques constituent une famille de peptides conservés qui présente un structure identique caractérisée par une boucle fermée par un pont disulfure qui est essentielle à leur signalisation [1] **(Figure 1)**. Chez les mammifères, il existe trois peptides natriurétiques : le peptide natriurétique de type A (ANP initialement appelé Atrial Natriuretic Peptide), le peptide natriurétique de type B (BNP, initialement appelé Brain Natriuretic Peptide), et le peptide natriurétique de type C (CNP). Les peptides natriurétiques ont initialement été identifiées pour leurs propriété natriurétique, diurétique et vasodilatatrice mais présentent également des activités anti-fibrosante[2] ; anti-hypertrophique [3] ; anti-inflammatoire [4] ; et pro-angiogénique [5]. En condition aiguë, ils s'opposent également au système sympathique [6] et au système rénine-angiotensine-aldostérone (SRAA) [7].

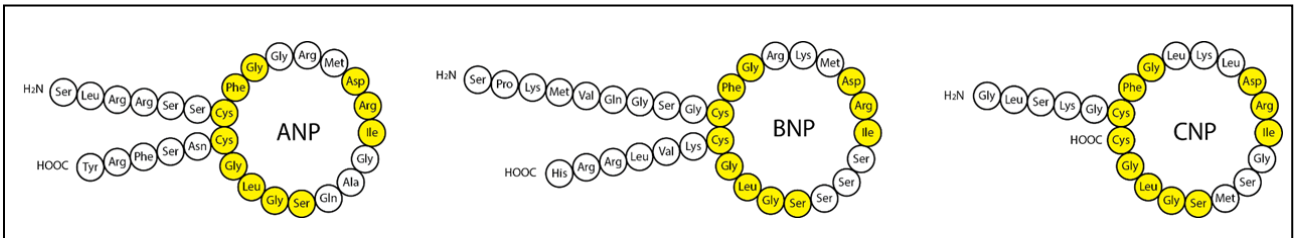

Figure 1 : Structure des trois peptides natriurétiques ANP, BNP et CNP. Les acides aminés en jaunes sont identiques dans les trois peptides.

Les peptides natriurétiques sont produits sous forme de pré-pro-hormone (proANP, proBNP et proCNP). Après clivage du peptide signal, la pro-hormone transite via le réticulum endoplasmique et l'appareil de Golgi, où elles vont être *O*-glycosylées [8, 9]. Le clivage des pro-hormones a lieu au moment de leur sécrétion pour donner les peptides natriurétiques (ANP, BNP et CNP) et le fragment N-terminal des pro-hormones (NT-proANP, NT-proBNP et NT-proCNP). Les trois peptides présents chez les mammifères diffèrent de par la longueur et la composition de leurs extrémités N- et C-terminales. De plus, même si les peptides natriurétique partagent de nombreux aspects métaboliques, ils diffèrent également tant du point de vue de leur biologie que de leur métabolisme.

En condition physiologique, le proANP est principalement synthétisé au niveau des cardiomyocytes auriculaires de manière constitutive et est stocké dans des granules de sécrétion [10] ; ce stockage permettant une libération immédiate en réponse à une augmentation de pression au niveau des oreillettes. En condition pathologique, le proANP est également produit au niveau des ventricules [11]. Par conséquent l'augmentation de l'ANP dans le plasma est plus rapide que celle du BNP. L'ANP est la première adaptation physiologique en cas de surcharge de pression au niveau des oreillettes, y compris en conditions physiologique. D'un point de vue métabolique, le proANP ($proANP_{1-126}$) est principalement clivé par la corine en $proANP_{1-98}$ (NT-proANP) et $proANP_{99-126}$ (ANP) [12, 13]. Le NT-proANP est ensuite clivé en trois peptides actifs : le $proANP_{1-30}$ (peptide natriurétique d'action prolongée), le $proANP_{31-67}$ (vasodilatateur) et le $proANP_{79-98}$ (kaliurétique) [14, 15] ; le $proANP_{68-78\ quant}$ à lui n'a jamais été détecté **(Figure 2).** A noter que les enzymes impliquées dans le clivage du NT-proANP n'ont pas été identifiées. Étant donné la demi-vie très courte de l'ANP, le MR (midregional)-proANP a été développé comme biomarqueur « surrogate » pour la production de proANP et d'ANP [16]. Au sens strict, le MR-proANP correspond au $proANP_{31-}$

98. Cependant, des différences de valeurs entre la mesure plasmatique du proANP et du MR-proANP ont été observées pouvant suggérer que des modifications post-traductionnelles pourraient interférer avec le dosage du MR-proANP [17]. L'identification récente de site d'O-glycosylation dans le proANP pourrait donc être responsable des différences observées entre les différents dosages [8].

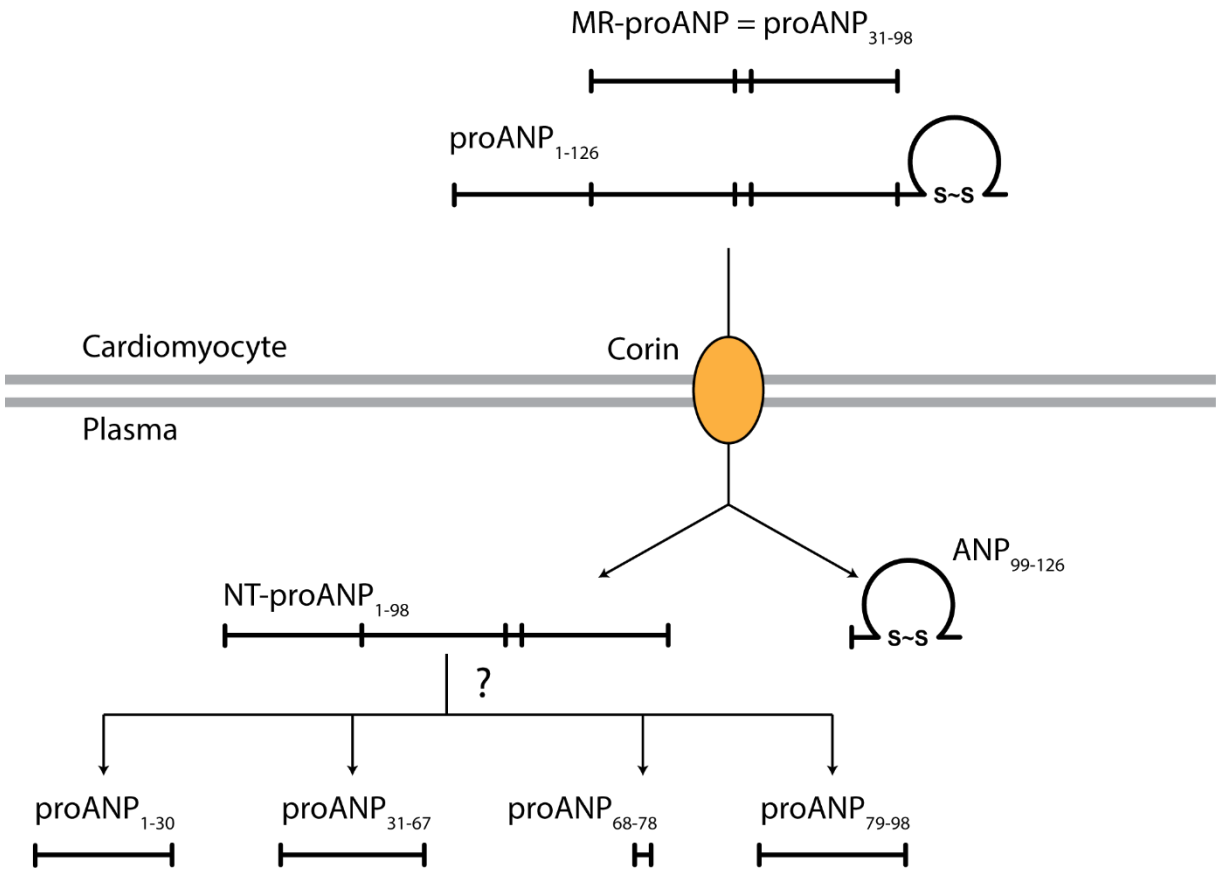

Figure 2 : Métabolisme du proANP chez l'homme.

Le BNP est principalement produit au niveau des cardiomyocytes ventriculaires en réponse à l'étirement des cardiomyocytes par augmentation des pressions dans les cavités cardiaques. Il est sécrété de façon continue, sans stockage dans des granules [18, 19]

contrairement à l'ANP. Par conséquent son augmentation plasmatique est plus lent et il constitue la deuxième réponse physiologique en cas de surcharge [20]. D'un point de vue métabolique, le proBNP ($proBNP_{1-108}$) est principalement clivé par la furine entre l'arginine76 et la sérine 77 en $proBNP_{1-76}$ (NT-proBNP) et BNP_{1-32} actif **(Figure 3)** [21]. Contrairement au NT-proANP, il ne semble pas que le NT-proBNP soit clivé en peptides actifs. La glycosylation sur la thréonine 71 (T71) empêche le clivage du proBNP par la furine [22]. Cette glycosylation est exclusivement réalisée dans les cardiomyocytes ventriculaires [23, 24], et uniquement chez les primates. En conditions aigues, la glycosylation du proBNP en T71 diminue fortement et favorise ainsi la production de BNP_{1-32} actif en augmentant la population de proBNP non glycosylée en T71 et donc le clivable par la furine. Dans l'insuffisance cardiaque chronique, la glycosylation du proBNP en T71 ne semble pas moduler la production de BNP_{1-32} [25].

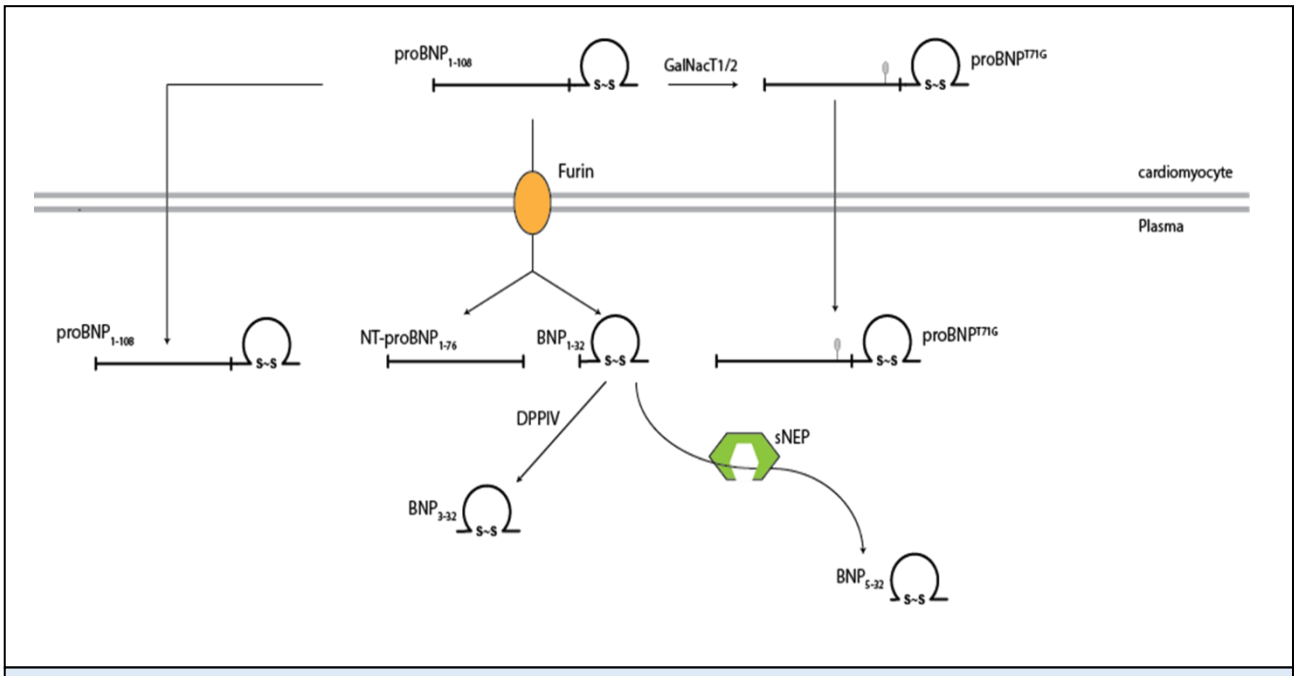

Figure 3 : Métabolisme du proBNP chez l'homme.

1.1.2 Signalisation et dégradation

Il existe trois récepteurs aux peptides natriurétiques : NPR-A (NPR1, GC-A), NPR-B (NPR2, GC-B), NPR-C (NPR3, GC-C) **(Figure 4)** [1, 26, 27]. Le NPR-A est le récepteur de l'ANP et du BNP mais présente une affinité supérieure pour l'ANP que pour le BNP [1, 28, 29]. Il est présent dans de nombreux organes tels que le poumon, le rein, le tissu adipeux, les surrénales et l'œil. Le NPR-B est le récepteur du CNP et est principalement impliqué dans l'ossification endochondrale [30]. Le NPR-C a une affinité équivalente pour les trois peptides natriurétiques et a été qualifié de récepteur de clairance. D'un point de vue fonctionnel, NPR-A et NPR-B possèdent une activité guanylate cyclase intrinsèque. La fixation des peptides natriurétiques sur le NPR-A et NPR-B entraine donc la production directe de GMPc (guanosine monophosphate cyclique) [31, 32] qui est à l'origine de leurs effets biologiques. Le NPR-C ne possède pas d'activité guanylate cyclase mais est couplé à des petites protéines G [33], ce qui suggèrent qu'il n'est pas seulement impliqué dans la clairance des peptides natriurétique mais est également capable de signalisation. De manière importante, la fixation des peptides natriurétiques à leurs récepteurs nécessite la présence de la boucle fermée par le pont disulfure.

La clairance des peptides natriurétique est assurée par 1) leur fixation à leurs récepteurs NPR-A et NPR-B, 2) de leur fixation au NPR-C si on ne le considère que comme un récepteur de clairance, 3) leur élimination rénale, et 4) leur clivage protéolytique. Concernant ce dernier, la néprilysine (NEP) joue un rôle majeur puisqu'elle inactive les peptides natriurétiques chez la plupart des espèces et clivant entre la phénylalanine et la glycine en aval de la première cystéine, ouvrant ainsi la boucle et rendant les peptides inactifs **(Figure 1)**.

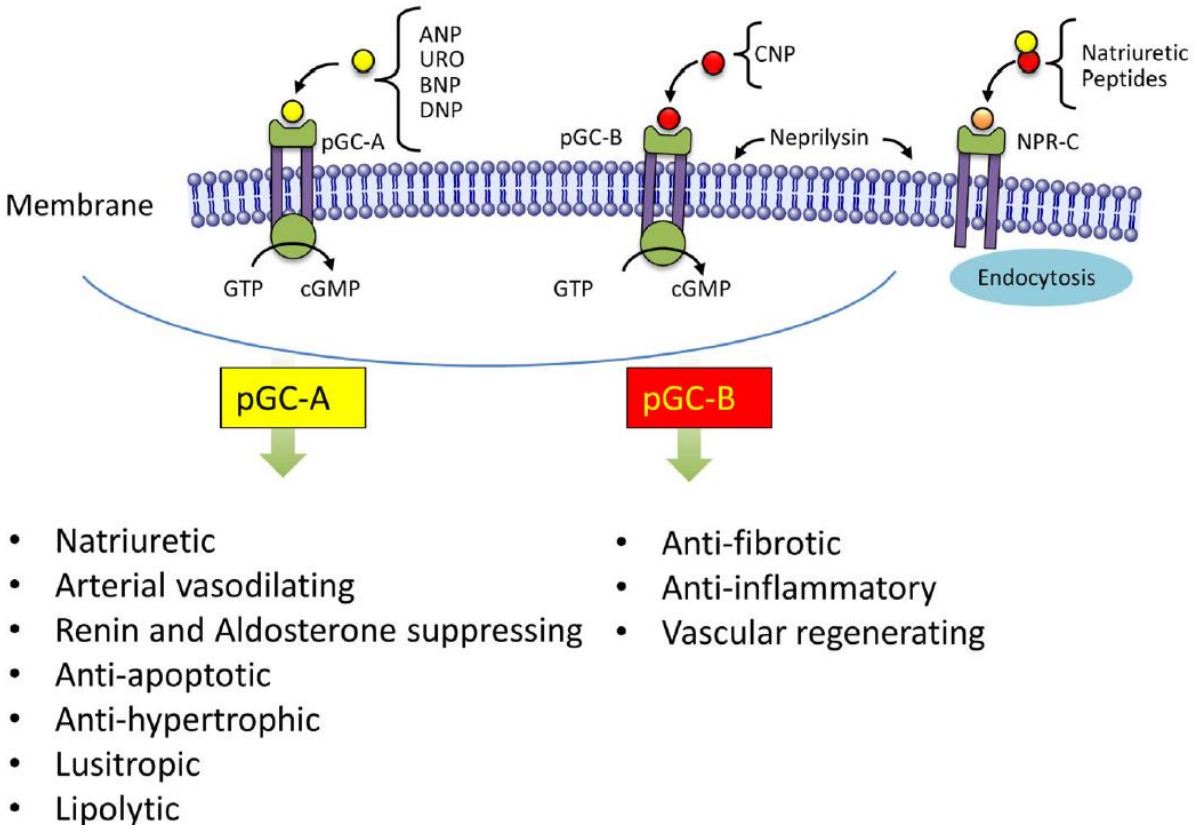

Figure 4 : Récepteurs aux peptides natriurétiques : NPR-A, NPR-B et NPR-C. D'après [27]

1.2 La néprilysine

La néprilysine (NEP, EC 3.4.24.11) est une métallopeptidase transmembranaire au Zn^{2+} [34] codée par le gène *MME*. La NEP a plusieurs dénominations : atriopeptidase, CALLA, CD10 (neutrophil antigen cluster differenciation antigen 10), endopeptidase 21.11, enkephalinase, fibroblast metalloelastase, kidney-brush-border du fait de son identification indépendante dans différentes conditions. Elle fait partie de la famille des endopeptidases de la famille M13 qui comprend six membres : la NEP, ECE-1 et ECE-2 (enzymes de conversion de l'endothéline 1 et 2), PHEX (phosphate regulating gene with homologies to endopeptidase on the X chromosome, ou PEX), le complexe antigénique Kell des érythrocytes, NEP2 et ECEL-1 (enzyme de conversion-like1) [35]. La NEP hydrolyse les liaisons peptidiques préférentiellement en

amont des résidus hydrophobes telle qu'une phénylalanine, une tyrosine, une leucine ou une valine. Même si la NEP est transmembranaire, une fraction est détectable dans la circulation [36]. L'activité de la NEP est hautement régulée. En effet la NEP contient de nombreux site de *N*-glycosylation et de phosphorylation. Les sites de glycosylation sont impliqués dans la régulation de son activité et de son transport à la surface des cellules [37]. La phosphorylation de son domaine intracellulaire module l'internalisation de la NEP, et ce mécanisme a été mis en cause dans certaines maladies neurodégénératives [38, 39]. En conséquence, l'activité ainsi que la concentration de la NEP sont régulées afin de permettre une adaptation à des conditions particulières.

1.3 Actions de la néprilysine

La NEP comprend plus de 40 substrats **(Tableau 1)** [40] parmi lesquels de nombreux substrats vasoactifs, à la fois vasoconstricteurs (angiotensines, endothéline-1) et vasodilatateurs (peptides natriurétiques, bradykinines, substance P, adrenomédulline). Parmi les peptides vasodilatateurs, la NEP joue un rôle majeur dans l'inactivation des peptides natriurétiques. La NEP inactive l'ANP chez tous les mammifères par clivage entre la Cystéine 7 et la Phénylalanine 8 qui sont localisées dans la boucle formée par le pont disulfure, le rendant ainsi inactif **(Figure 1)**. Chez les murins, la NEP clive le BNP au même endroit le rendant inactif. Cependant, contrairement à l'ANP, le BNP_{1-32} doit être préalablement clivé par la méprine A au niveau de sa terminaison N-terminale en BNP_{7-32} qui possède toujours la boucle et reste actif, avant que la NEP ne puisse cliver au niveau de la boucle. Chez l'Homme, le BNP est insensible à l'action de la méprine A [41], et la NEP n'est pas non plus capable de cliver le BNP_{7-32} humain, malgré la présence du site de clivage consensus au niveau de la boucle [42, 43]. Néanmoins, la NEP clive le BNP_{1-32} en BNP_{5-32} qui possède toujours la boucle mais dont

l'activité physiologique reste incertaine. Il est important de noter, que le BNP humain est un inhibiteur endogène de la NEP quand sa concentration plasmatique dépasse 916 pg/mL [44].

Peptide	Fonctions
hormone adrénocorticotrope (ACTH)	Stimule la sécrétion surrénale de glucocorticoïdes
adrenomédulline	vasodilatateur
Peptide β-amyloïde	Synaptogénèse, migration neuronale. Agrégation dans la maladie d'Alzheimer
Angiotensine-I	Précurseur des autres angiotensine dont Angiotensine-II et Angiotensine$_{1-7}$
Angiotensine-II	Vasoconstricteur via AT$_1$, vasodilatateur via AT$_2$
Angiotensine$_{1-7}$	vasodilatateur
ANP$_{99-126}$, BNP$_{1-32}$, CNP .et urodilatine	Natriurétique, diurétqiue
Bombésine (= GRP, gastrin releasing peptide)	Mitogène, stimule la sécrétion de gastrine et de cholécystokinine
Bradykinine et kallidine	Vasodilatateur, augmente la perméabilité endothéliale, douleur, inflammation
Peptide relié au gène calcitonine (PRGC)	Vasodilatateur, douleur, inflammation
Formyl-Met-Leu-Phe peptide (fMLP)	inflammation
Cholécystokinine (CCK8)	Stimule la contraction de la vésicule biliaire, la sécrétion pancréatique, péristaltisme intestinal, satiété
Dynorphine	analgésie
β-endorphine	analgésie
Endothéline 1 et 2	Vasoconstriction, mitogénèse, hypertrophie du muscle lisse endothéliale
enkephalines	analgésie
FGF2 (fibroblast growth factor 2)	angiogénèse
Galanine	Inhibe relargage de neurotransmetteur

Peptide	Fonctions
hormone adrénocorticotrope (ACTH)	Stimule la sécrétion surrénale de glucocorticoïdes
adrenomédulline	vasodilatateur
Peptide β-amyloïde	Synaptogénèse, migration neuronale. Agrégation dans la maladie d'Alzheimer
Angiotensine-I	Précurseur des autres angiotensine dont Angiotensine-II et Angiotensine$_{1-7}$
Angiotensine-II	Vasoconstricteur via AT$_1$, vasodilatateur via AT$_2$
Angiotensine$_{1-7}$	vasodilatateur
ANP$_{99-126}$, BNP$_{1-32}$, CNP .et urodilatine	Natriurétique, diurétqiue
Bombésine (= GRP, gastrin releasing peptide)	Mitogène, stimule la sécrétion de gastrine et de cholécystokinine
Bradykinine et kallidine	Vasodilatateur, augmente la perméabilité endothéliale, douleur, inflammation
Peptide relié au gène calcitonine (PRGC)	Vasodilatateur, douleur, inflammation
Formyl-Met-Leu-Phe peptide (fMLP)	inflammation
Cholécystokinine (CCK8)	Stimule la contraction de la vésicule biliaire, la sécrétion pancréatique, péristaltisme intestinal, satiété
Dynorphine	analgésie
β-endorphine	analgésie
Endothéline 1 et 2	Vasoconstriction, mitogénèse, hypertrophie du muscle lisse endothéliale
enkephalines	analgésie
FGF2 (fibroblast growth factor 2)	angiogénèse
Galanine	Inhibe relargage de neurotransmetteur

Tableau 1 : Différents substrats de la NEP. D'après [40]

Parmi les peptides vasoconstricteurs, la NEP intervient au niveau du système rénine-angiotensine-aldostérone (SRAA). Le SRAA joue un rôle majeur dans la régulation de la pression artérielle et l'homéostasie électrolytique. Le SRAA est un système hormonal organisé autour du rein **(Figure 5)**. En réponse à une diminution de la perfusion rénale, l'appareil juxta

glomérulaire sécrète la rénine qui va permettre la transformation de l'angiotensinogène produit par le foie en angiotensine I, peptide inactif. Ensuite l'angiotensine I est transformée en angiotensine II par l'enzyme de conversion de l'angiotensine (ECA), elle-même issue de l'endothélium pulmonaire et rénal.

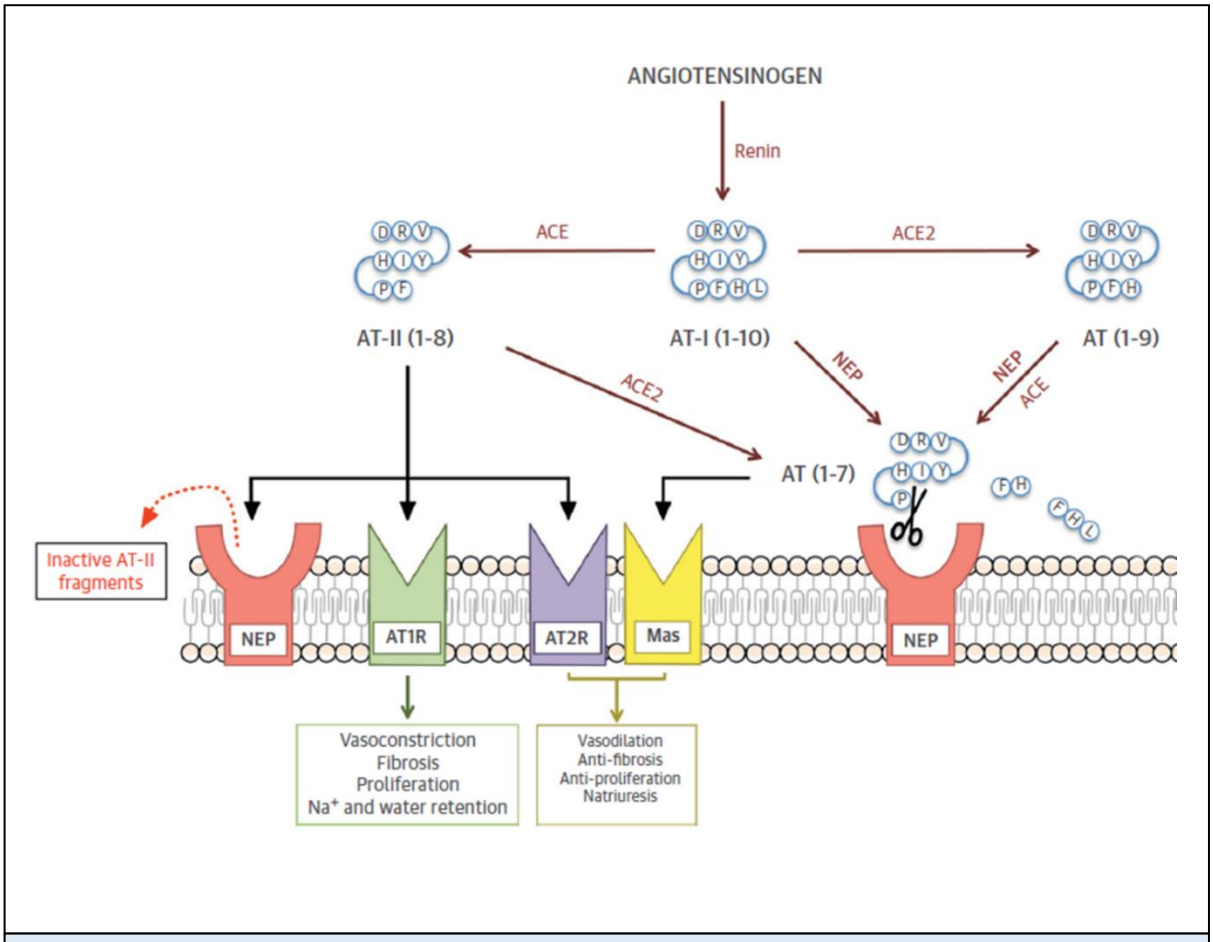

Figure 5 : Rôle de la NEP dans le SRAA. D'après [36]

Dans ce contexte, la NEP semble jouer un rôle tampon en clivant l'angiotensine 1 en angiotensine 1-7, au dépend de la production d'angiotensine 2 [36, 45]. Ce rôle de la NEP dans le SRAA a été à l'origine des échecs des premiers inhibiteurs spécifiques de NEP qui bien qu'augmentant de nombreux peptides vasodilatateurs, provoquait également l'augmentation d'angiotensine II avec donc un effet hypotenseur attendu modeste [46]. C'est pour cette raison que tous les inhibiteurs de NEP testés ou utilisés par la suite ont toujours été associés

à un inhibiteur du SRAA (inhibiteurs de l'enzyme de conversion, IEC ou antagoniste du récepteur à l'angiotensine II, ATR1, ARA II).

2 L'insuffisance cardiaque

2.1 Définition, épidémiologie et diagnostic

L'insuffisance cardiaque est un problème de santé publique. Sa prévalence est de 2-3% dans la population générale mondiale et atteint 10% chez le sujet âgé (>75 ans) [47]. En France, l'incidence de l'insuffisance cardiaque est de 1 million de personnes [48] et sa prévalence est en constante augmentation due au vieillissement de la population [49] et à l'amélioration de la prise en charge des infarctus du myocarde permettant d'améliorer la survie des patients [50].

L'insuffisance cardiaque est définie comme l'incapacité du cœur à suffire aux besoins des autres organes. Selon la société européenne de cardiologie, il s'agit « d'un syndrome clinique caractérisé par des symptômes typiques qui peuvent s'accompagner de signes cliniques causés par une affection structurelle et/ou fonctionnelle du cœur, entrainant une réduction du débit cardiaque et/ou une augmentation des pressions intracardiaques au repos ou pendant un état de stress » [51]. Il existe deux formes de cette maladie, la forme aiguë caractérisée par la survenue brutale de signes cliniques (dyspnée, œdème) alors que la forme chronique est une dysfonction permanente du cœur dans le temps avec des épisodes récurrents d'insuffisance cardiaque aigue qui impactent le pronostic vital et nécessitent des hospitalisations récurrentes.

Classiquement, la classification de l'insuffisance cardiaque chronique gauche est basée sur la fraction d'éjection du ventricule gauche (FEVG) qui est un indicateur de la capacité contractile du ventricule gauche. Les dernières recommandations internationales distinguent trois groupes d'insuffisance cardiaque gauche : FEVG altérée (≤ 40%), FEVG moyennement altérée (40% < FEVG ≤ 49%) et FEVG préservée (FEVG ≥ 50%) [52] **(Figure 6)**.

Les étiologies de l'insuffisance cardiaques sont multiples, au premier rang desquelles la cause ischémique. L'insuffisance cardiaque peut être multifactorielle.

Type of HF		HFrEF	HFmrEF	HFpEF
CRITERIA	1	Symptoms ± Signs[a]	Symptoms ± Signs[a]	Symptoms ± Signs[a]
	2	LVEF <40%	LVEF 40–49%	LVEF ≥50%
	3	–	1. Elevated levels of natriuretic peptides[b]; 2. At least one additional criterion: a. relevant structural heart disease (LVH and/or LAE), b. diastolic dysfunction (for details see Section 4.3.2).	1. Elevated levels of natriuretic peptides[b]; 2. At least one additional criterion: a. relevant structural heart disease (LVH and/or LAE), b. diastolic dysfunction (for details see Section 4.3.2).

BNP = B-type natriuretic peptide; HF = heart failure; HFmrEF = heart failure with mid-range ejection fraction; HFpEF = heart failure with preserved ejection fraction; HFrEF = heart failure with reduced ejection fraction; LAE = left atrial enlargement; LVEF = left ventricular ejection fraction; LVH = left ventricular hypertrophy; NT-proBNP = N-terminal pro-B type natriuretic peptide.
[a]Signs may not be present in the early stages of HF (especially in HFpEF) and in patients treated with diuretics.
[b]BNP>35 pg/ml and/or NT-proBNP>125 pg/mL

Figure 6 : Classification des insuffisances cardiaques gauches. D'après [51]

Le diagnostic de l'insuffisance cardiaque repose sur l'examen clinique associé à des examens complémentaires tels que l'électrocardiogramme, les biomarqueurs (BNP et NT-proBNP) et une échographie cardiaque. Le diagnostic précoce de l'insuffisance cardiaque permet une introduction précoce des thérapeutiques et une amélioration de la survie des patients [50].

2.2 Peptides natriurétiques et insuffisance cardiaque

2.2.1 Peptides comme biomarqueurs

La production et libération des peptides natriurétiques (ANP et BNP) augmentent en réponse aux contraintes imposées à la surface du myocarde. De ce fait, l'augmentation de leur production/libération est une caractéristique importante de l'insuffisance cardiaque. Cette propriété a conduit à leur utilisation comme biomarqueurs. Plusieurs biomarqueurs ont été développé à partir des peptides natriurétiques : le BNP, le NT-proBNP et le MR-proANP. Ces biomarqueurs ont été initialement développés pour distinguer les dyspnées aiguës d'origine cardiaque ou non-cardiaque aux urgences, et présente de très bonnes performances [51]. Depuis, l'utilisation des peptides natriurétiques comme biomarqueur a été étendue au diagnostic de l'insuffisance cardiaque chronique, ainsi qu'au pronostic et au suivi de l'efficacité des thérapeutiques de l'insuffisance cardiaque [53]. Alors que globalement ces biomarqueurs présentent des évolutions parallèles, la mise sur le marché du sacubitril/valsartan (voir ci-dessous) a remis en question l'utilisation du BNP par rapport au NT-proBNP car, pour la première fois, le NT-proBNP diminuait [54 , 55] alors que le BNP restait stable [55] ou augmentait légèrement [54]. Cette évolution inconsistante du BNP et du NT-proBNP a été attribuée au fait que le BNP était dégradé par la NEP et que l'inhibition de la NEP devait entrainer une augmentation du BNP, mais cette interprétation est basée sur l'idée fausse que le BNP humain est dégradé efficacement par la NEP. De plus, cette interprétation résulte en partie de la méconnaissance des molécules détectées par les différents kits de dosages, ainsi que des interférences potentielles avec des modifications post-traductionnelles [56].

2.2.2 Peptides natriurétiques thérapeutiques

Les peptides natriurétiques ont des effets bénéfiques dans l'insuffisance cardiaque et des approches thérapeutiques visant à augmenter leurs activités ont été développées. Ces approches reposent sur deux principes : l'administration directe de peptides natriurétiques ou l'inhibition de leur dégradation.

L'administration de peptides natriurétiques exogènes a été principalement testée dans le cadre de l'insuffisance cardiaque aigue. Ces approches thérapeutique ont consisté dans le développement de peptides natriurétique recombinants : le Carperitide pour l'ANP [57], l'urodilatin pour l'ularitide, une forme d'ANP exclusivement produite par le rein [58], le nesiritide pour le BNP [59], ou des peptides chimériques : le centeritide (chimère CNP/DNP [60]) ou le vasonastrine (chimère ANP/CNP, [61]). Malgré l'anticipation d'un bénéfice de cette approche thérapeutique, l'utilisation des peptides natriurétiques à viser thérapeutique a été globalement abandonnée dans l'insuffisance cardiaque aigüe. A noter néanmoins que des essais préliminaires avait montré le bénéfice de l'administration sous-cutané de nesiritide dans l'insuffisance cardiaque chronique [62, 63].

L'inhibition de la dégradation des peptides natriurétiques constitue le deuxième axe de recherche. L'inhibition de la NEP a donc été étudiée avec comme objectif d'augmenter les formes actives des peptides natriurétiques chez les patients en insuffisance cardiaque.

Depuis la fin des années 80, la NEP est une cible thérapeutique de choix dans l'insuffisance cardiaque. Le premier inhibiteur de NEP testé chez l'Homme, le candoxatril, augmente les concentrations plasmatiques de peptides natriurétiques chez les patients hypertendus et en insuffisance cardiaque chronique mais sans amélioration des paramètres hémodynamiques [64]. L'absence d'effets hémodynamiques est due à une augmentation

parallèle de l'angiotensine II et de la signalisation à son récepteur AT-1. Par la suite, l'omapatrilate qui est un double inhibiteur de l'enzyme de conversion de l'angiotensine (IEC) et de la NEP a montré son efficacité dans une essai randomisé (OUVERTURE) en réduisant le taux d'hospitalisation et de décès pour causes cardio-vasculaires chez les patients en insuffisance cardiaque avec FEVG altérée [65]. Cependant l'omapatrilate n'était pas plus efficace que l'enalapril seul et dans un essai qui a suivi (OCTAVE), il a été décrit une majoration du risque d'angioœdème, principalement dans la population afro-américaine qui a conduit à l'arrêt des études sur cette molécule [66].

Enfin, récemment Novartis a mis sur le marché une molécule combinant un inhibiteur de NEP (sacubitril)) et un ARA II (valsartan) : sacubitril/valsartan (LCZ696), commercialisé sous le nom Entresto [67]. Le premier essai clinique randomisé comparant le sacubitril/valsartan à une IEC (enalapril) chez les patients en insuffisance cardiaque chronique avec FEVG altérée, principalement de classe NYHA II, (PARADIGM-HF) a été publié en 2014 [68]. Les critères d'inclusion étaient : une insuffisance cardiaque avec FEVG ≤ 40% ; BNP ≥ 150 pg/mL ou NT-proBNP ≥ 600 pg/mL et un traitement stable ≥ 4 mois par IEC ou ARA II. Dans cet essai, 4187 patients ont reçu le sacubitril/valsartan et 4212 patients ont reçu l'énalapril. Le sacubitril/valsartan diminuait de 20% les hospitalisations et décès de cause cardiovasculaire. L'effet indésirable principal retrouvé dans les études initiales était l'hypotension orthostatique [67], mais pas d'angioœdème, probablement lié au design de l'étude.

Cette étude a permis l'obtention de l'AMM pour le sacubitril/valsartan le 24 septembre 2015. Par la suite le sacubitril/valsartan a été testé dans d'autres indications **(Figures 7)**, mais l'insuffisance cardiaque chronique a FEVG réduite reste l'indication principale de l'utilisation du sacubitril/valsartan :

- Insuffisance cardiaque à FEVG conservée, étude PARAGON-HF : pas de supériorité du sacubitril/valsartan [69].
- Insuffisance cardiaque aigue, étude PIONNER-HF : le sacubitril/valsartan réduit le NT-proBNP plus rapidement que le traitement standard [70].

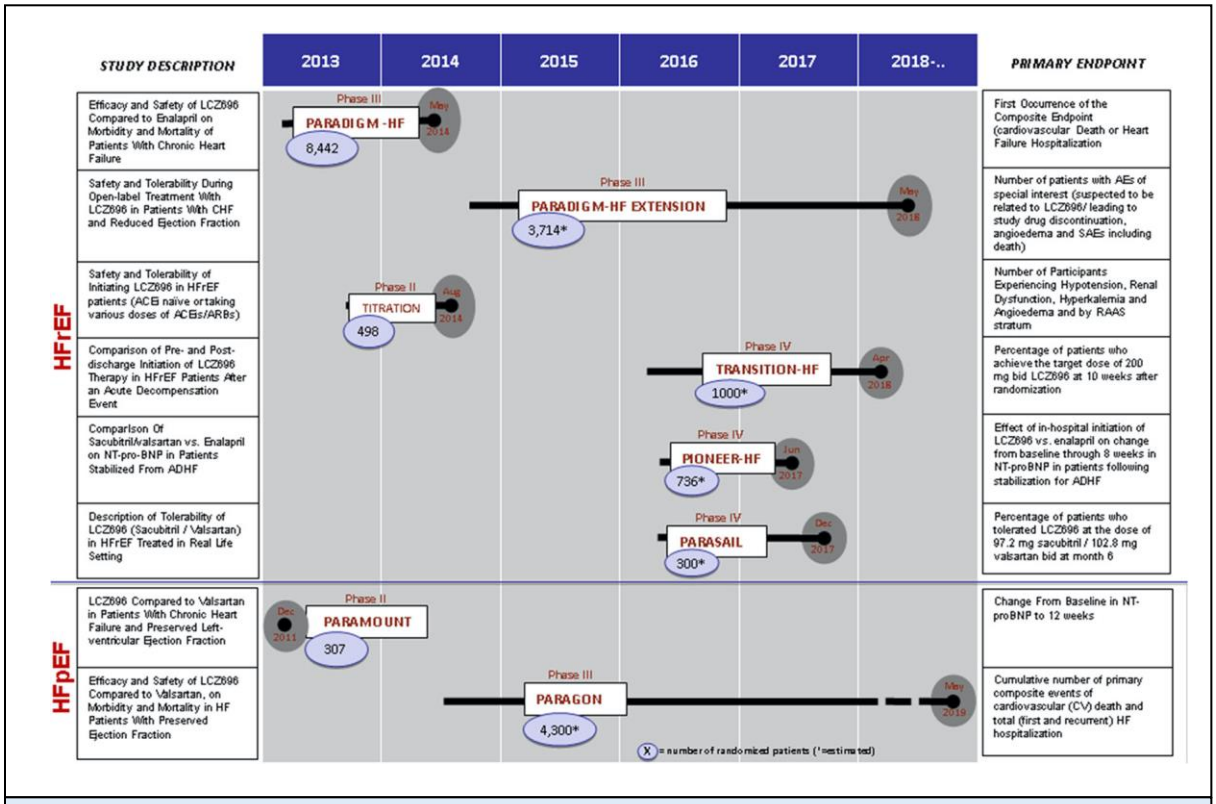

Figure 7 : Etudes cliniques s'intéressant au sacubitril /valsartan. D'après [36]

Récemment, l'étude LIFE qui a testé l'impact du sacubitril/valsartan dans l'insuffisance cardiaque chronique à FEVG réduite avancée n'a pas montré de bénéfice du sacubitril/valsartan par rapport au valsartan [71]. Etant donné que ces patients ont très probablement des taux de BNP élevés, il a été proposé que l'échec de cette étude pouvait résulter d'une inhibition endogène de la NEP par le BNP, rendant l'inhibition pharmacologique de la NEP futile [72].

3 L'insuffisance rénale aiguë

3.1 Le rein : structure et fonctions

Les reins font partie de l'appareil urinaire haut et assurent la filtration du sang permettant ainsi d'éliminer les déchets et toxines en produisant de l'urine. Ils constituent environ 0.4% de la masse corporelle totale mais sont responsables de la filtration en moyenne de 170 à 180 litres de plasma par jour chez l'Homme.

3.1.1 Les fonctions du rein

Le rein a 4 grandes fonctions principales :

La filtration du sang conduisant à la synthèse d'urine : le sang arrive au niveau rénal via l'artère rénale, le sang est filtré au niveau du glomérule rénal permettant la filtration de l'urine primitive. Par la suite l'urine primitive est modifiée tout le long du tubule rénal par des mécanismes de réabsorption et de sécrétion permettant la formation de l'urine définitive. La filtration rénale permet donc de contrôler l'équilibre hydroélectrolytique et l'équilibre acido-basique.

La sécrétion de rénine : La rénine est une enzyme du SRAA responsable du maintien de la pression artérielle **(Figure 1)**.

La sécrétion d'érythropoïétine (EPO) : l'EPO est une hormone sécrétée par le cortex rénal qui stimule la prolifération des cellules souches hématopoïétique au niveau de la moelle osseuse. Sa sécrétion est stimulée en cas d'hypoxie et est diminuée en cas d'hyperoxie.

La transformation de la vitamine D en sa forme active (1-25-dihydroxy-vitamine D ou calcitriol) : la vitamine D compte beaucoup d'actions différentes, elle est responsable en autre

de l'absorption du calcium par l'intestin, la réabsorption du calcium et du phosphore par les reins et la résorption osseuse par les ostéoclastes.

3.1.2 Structure générale du rein

Les reins contiennent des millions d'unités de filtrations appelés « néphrons ». Les néphrons se composent d'un glomérule où s'effectue la filtration du sang et la synthèse de l'urine, et des tubules impliqués dans les modifications de la composition de l'urine. L'architecture rénale se compose de 3 parties distinctes **(Figure 8)** :

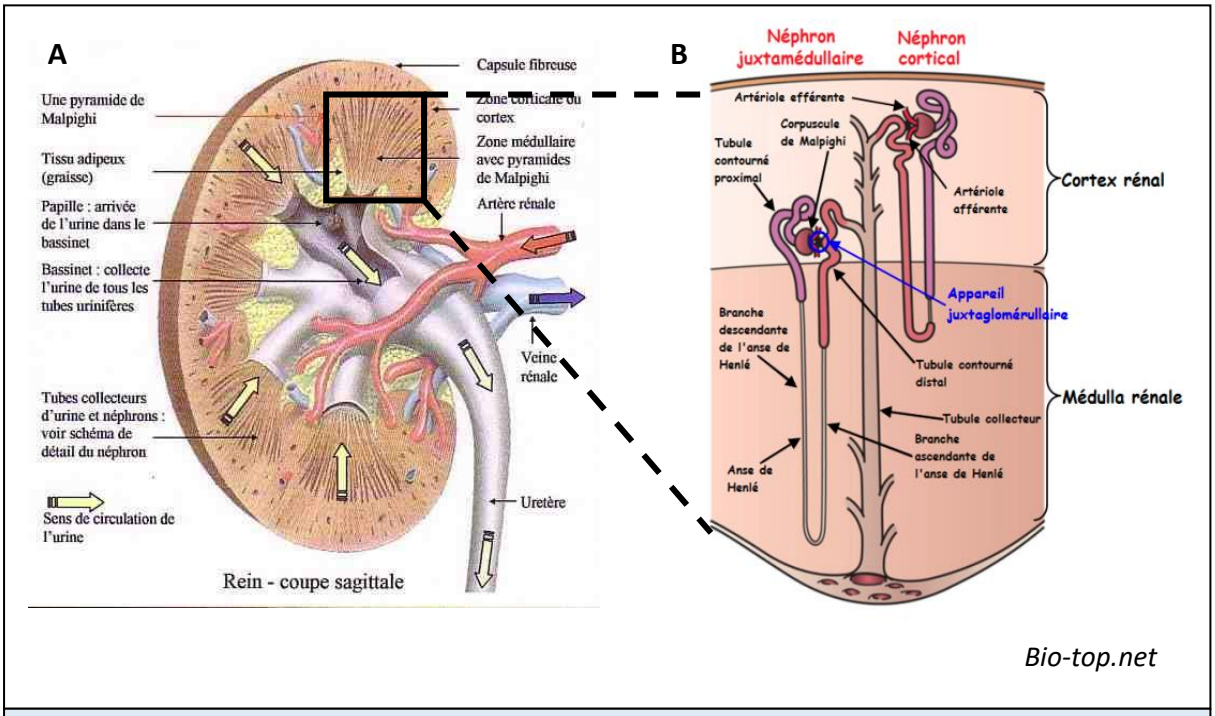

Figure 8 : Structure générale du rein et unité de filtration (le néphron)

- **Le cortex** : partie la plus externe qui recouvre la médullaire (1cm d'épaisseur environ chez l'Homme), siège des glomérules, assurant les fonctions de filtration.

- **La médullaire** : au centre, siège des tubules, assurant les fonctions de concentrations/dilution de l'urine.

- **Les calices et le bassinet** : les calices sont des cavités permettant la collecte de l'urine provenant des néphrons puis l'urine se déverse dans le bassinet pour s'écouler par la suite dans l'uretère jusqu'à l'arrivée dans la vessie où elle sera stockée avant d'être éliminée.

3.1.3 Le néphron

Le néphron est l'unité fonctionnelle et structurelle du rein, il permet la formation d'urine. Chez l'Homme, chaque rein se compose en moyenne d'1 million de néphrons. Le néphron est composé globalement de deux structures :

- Le corpuscule rénal : portion initiale du néphron où la filtration du plasma est effectuée, il réunit une composante vasculaire et épithéliale. Le pôle vasculaire d'un côté, appelé le glomérule et le pôle urinaire (épithéliale) de l'autre, appelé capsule de Bowman. L'ultrafiltrat, liquide obtenu après passage du corpuscule rénal, intègre par la suite le système tubulaire.

- Le système tubulaire : lieu de maturation de l'urine primitive, il est composé d'une succession de tubules droits et contournés (dans l'ordre : tube contourné proximal, anse de Henle et tube contourné distal), lieux des processus de sécrétion et réabsorption tubulaires permettant l'élimination et l'ajout de différentes substances au filtrat. Le tube contourné distal se jette par la suite dans le tube collecteur, ne faisant pas partie du néphron, le fluide résultant sort des reins sous forme d'urine.

3.2 Insuffisance rénale aiguë

3.2.1 Epidémiologie

L'IRA est un problème majeur de santé publique, son incidence ne fait qu'augmenter depuis une dizaine d'années en particulier dans les pays développés. Sa prévalence en milieu hospitalier varie entre 1.9 et 7.2% [73]. Les étiologies principales à l'hôpital sont principalement liées aux sepsis, à l'hypovolémie, aux traitements néphrotoxiques et aux complications post-opératoires. Environ 2 millions de personnes meurent chaque année d'une IRA et les survivants ont un risque accru de développer par la suite une insuffisance rénale chronique [73, 74]. En réanimation, l'IRA est un facteur indépendant de mortalité [73].

3.2.2 Définition

L'insuffisance rénale aigue (IRA) est une notion dont la définition a évolué au cours des dernières années. Elle est définie par la baisse du débit de filtration glomérulaire (DFG) dont les marqueurs les plus couramment utilisés sont la diurèse et la créatinine plasmatique.

Le terme d'insuffisance rénale aiguë (ou acute kidney injury) est centré sur le dysfonctionnement rénal en terme d'incapacité du rein à maintenir l'équilibre hydroélectrolytique due à une baisse du débit de filtration glomérulaire (GFR). Cependant il existe de nombreuses situations durant lesquelles le rein est soumis à une agression pouvant induire des lésions histologiques sans diminution du GFR, du moins à la phase initiale du processus physiopathologique [75]. L'atteinte rénale aiguë (ou acute kidney damage) correspond à une altération du parenchyme rénal qui peut être mis en évidence par des études histologiques, ou de manière non-invasive grâce à des biomarqueurs d'atteinte tissulaire rénale aiguë qui ne reflètent pas nécessairement la fonction rénale **(Figure 10)** [75].

Enfin, l'agression rénale aiguë (ou kidney attack) implique des situations dans lesquelles le rein subit des atteintes rénales conduisant à une insuffisance rénale. Ces situations sont nombreuses et incluent par exemple le sepsis, les chirurgies majeures, les agents dits néphrotoxiques, etc **(Figure 9)** [75].

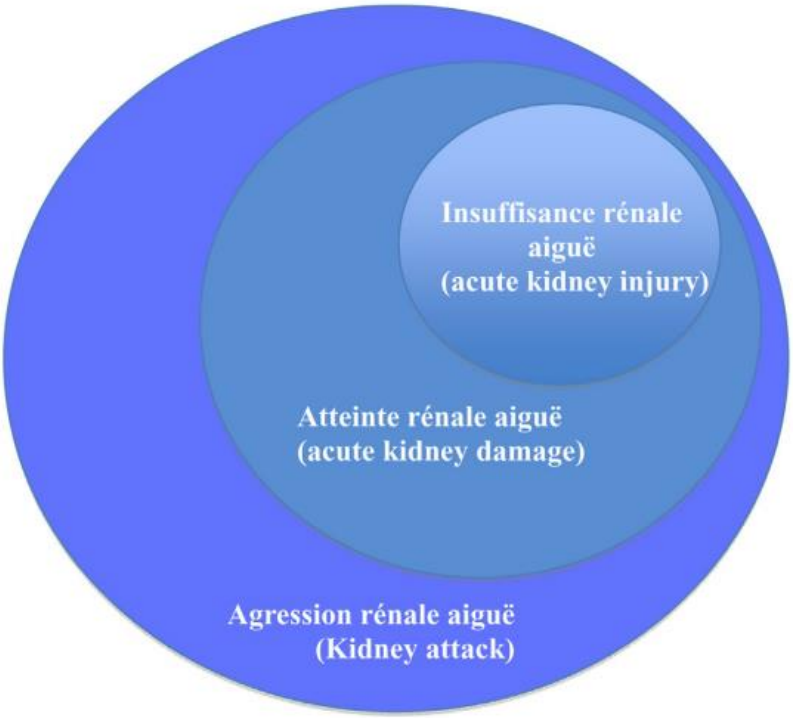

Figure 9 : L'IRA : de l'agression à la dysfonction rénale. D'après [75]

Les notions d'agression et d'atteinte rénale aiguës ont émergé ces dernières années, grâce au développement récent de biomarqueurs rénaux, principalement de structure plutôt que de fonction, et qui permettent d'identifier rapidement l'atteinte rénale aiguë, avant même toute altération de la fonction. On parle alors de « subclinical AKI » **(Figure 10)** [76, 77].

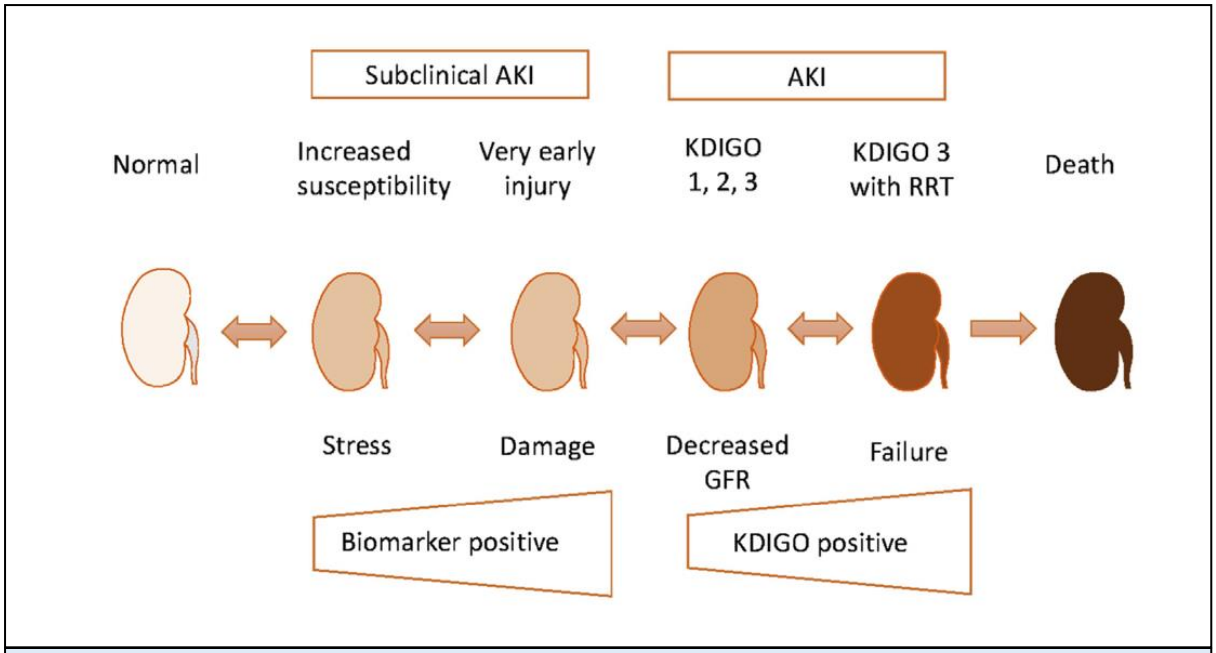

Figure 10 : Place des biomarqueurs dans l'IRA. AKI: Acute Kidney Injury. D'après [77]

3.2.3 Classifications

Historiquement, l'insuffisance rénale a été classée suivant des stades de sévérité en se basant sur le dosage de la créatinine plasmatique et sur la mesure du débit urinaire. La première classification mise au point pour diagnostiquer l'IRA est la classification RIFLE (Risk, Injury, Failure, Loss and End-stage renal disease) [78], établie en 2004. En 2007 une nouvelle version est établie, l'AKIN (Acute Kidney Injury Network) [79], puis en 2012, KDIGO (Kidney Disease : Improving Global Outcomes) qui est la fusion des 2 premières classifications pour ne donner plus qu'une seule définition de l'IRA **(Tableau 2)** [80]**.** Début octobre 2020, de nouvelles recommandations proposent une nouvelle définition de l'IRA combinant des critères fonctionnels (créatinine plasmatique et débit urinaire) et des critères d'atteinte rénale à travers l'utilisation de nouveaux biomarqueurs. Le stade 1S identifie un stade précoce lorsqu'il existe des signes d'atteinte rénale non détecté par les critères fonctionnels. Les anciens stades KDIGO sont catégorisés par la présence ou non de biomarqueurs **(Figure 11)** [81, 82].

Classification selon RIFLE		
Stades RIFLE	**Critères selon taux de créatinine* ou le DFG**	**Critères selon la diurèse**
Risque **Lésion** **Défaillance**	↗ créatinine 1,5 x ou ↘ DFG > 25% ↗ créatinine 2 x ou ↘ DFG > 50% ↗ créatinine 3 x ou ↘ DFG > 75% ou ↗ créatinine > 44 µmol/L si créatinine ≥ 354 µmol/L	Diurèse < 0,5 ml/kg/heure x 6 heures Diurèse < 0,5 ml/kg/heure x 12 heures Diurèse < 0,3 ml/kg/heure x 6 heures Ou anurie x 12 heures
Perte	Perte complète de la fonction rénale > 4 semaines	
Insuffisance rénale terminale	Dépendance de dialyse pendant 3 mois	
Classification selon AKIN		
Stades AKIN	**Critères selon le taux de créatinine ou le DFG**	**Critères selon la diurèse**
1 **2** **3**	↗ créatinine ≥ 26,4 µmol/L ou ↗ créatinine ≥ 1,5 à 2 x ↗ créatinine ≥ 2 à 3 x ↗ créatinine ≥ 3 x ou ↗ créatinine ≥ 44 µmol/L si créatinine ≥ 354 µmol/L	Cf. critères **RIFLE**
Classification selon KDIGO		
Stades KDIGO	**Critères selon le taux de créatinine ou le DFG**	**Critères selon la diurèse**
1 **2** **3**	↗ créatinine 1,5-1,9 x ou ↗ créatinine > 26,5 µmol/L ↗ créatinine 2-2,9 x ↗ créatinine 3 x **ou** créatinine ≥ 353,6 µmol/L **ou** début de l'épuration extrarénale **ou** chez patient < 18 ans, ↘ DFGe < 35mV/min/1,73 m^2	Diurèse < 0,5 ml/kg/heure x 6-12 heures Diurèse < 0,5 ml/kg/heure ≥ 12 heures Diurèse < 0,3 ml/kg/heure ≥ 24 heures **ou** Anurie ≥ 12 heures

Tableau 2 : Classification selon RIFLE, AKIN et KDIGO

RIFLE: Risk Injury Failure Loss End stage renal failure; AKIN: Acute Kidney Injury Network; DFG: débit de filtration glomérulaire; KDIGO: Kidney Disease Improving Global Outcomes. * Créatinine plasmatique. Adapté de [80] et [82].

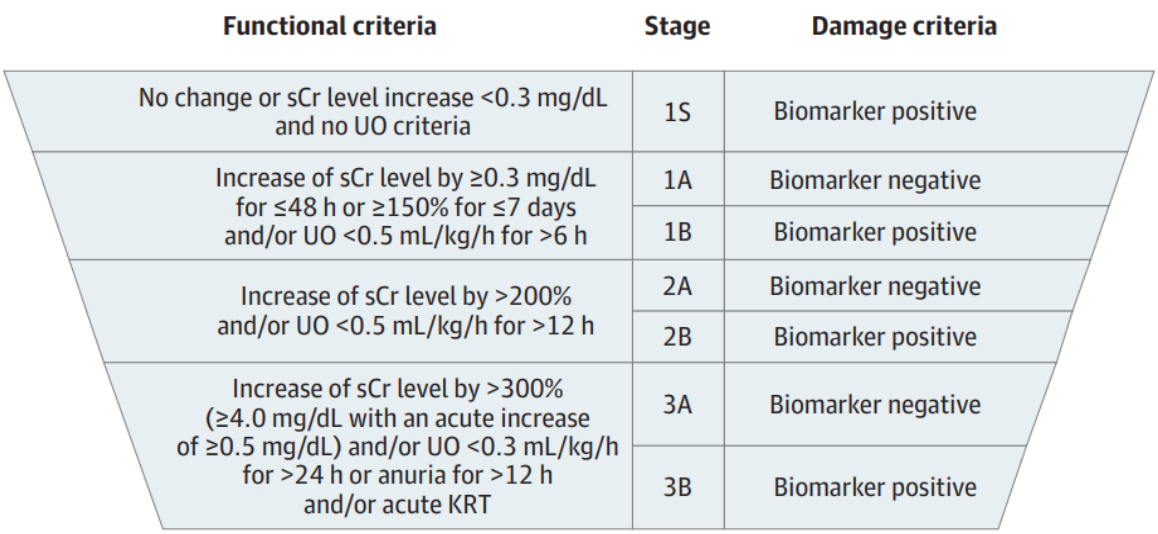

Figures 11 : Nouvelle définition de l'IRA. sCr : serum creatinine; UO : urine output; KRT : kidney replacement therapy. D'après [81]

3.3 Biomarqueurs d'agression rénale aiguë

Le diagnostic de l'insuffisance rénale aiguë (IRA) repose aujourd'hui sur une élévation de la créatinine plasmatique, une baisse du débit de filtration glomérulaire et/ou de la diurèse **(Tableau 2)**.

Le principal défaut de la créatinine est son manque de sensibilité, en particulier quand la filtration glomérulaire est élevée. En effet, la filtration glomérulaire peut diminuer jusqu'à 50% sans pour autant que la créatinémie ne soit modifiée. De plus, la créatinémie peut être influencée par de nombreux facteurs autres que la filtration glomérulaire, tels que l'âge, le sexe, l'état nutritionnel, la volémie et certains médicaments. Finalement, une augmentation de la production endogène de créatine peut provoquer une augmentation de la créatinémie, ce qui peut mimer une baisse de la filtration glomérulaire [83]. De ce fait, la créatinine à évolution lente et est un marqueur tardif dans l'IRA, dont l'utilisation peut entraîner un retard diagnostique. La même problématique se pose avec d'autres outils diagnostiques comme la diurèse ou l'urée.

De nouveaux outils diagnostic plus performants sont donc nécessaires car le seul traitement efficace en dehors de l'épuration extra-rénale repose sur la prévention par l'optimisation des thérapeutiques visant à limiter les effets des facteurs de risque associés à la survenue d'une IRA.

Parmi l'ensemble des biomarqueurs en cours d'étude, le test NEPHROCHECK semble être le plus prometteur. NEPHROCHECK est la combinaison de deux biomarqueurs : l'inhibiteur tissulaire des métalloprotéinases-2 (TIMP-2) et une protéine liant le facteur de croissance analogue à l'insuline (IGFBP7), qui augmentent dans l'urine du patient en réponse au stress des cellules rénales [84]. Ces deux protéines sont induites précocement en cas de

stress rénal afin de mettre en place une réponse adaptée pour protéger le rein et maintenir sa fonction [85].

L'organisation Acute Dialysis Quality Initiative (ADQI), à l'instar de la société médicale professionnelle de chirurgie cardiaque *ERAS® Cardiac Surgery,* a inclus récemment ces deux biomarqueurs dans ses recommandations [86].

3.4 Physiopathologie

3.4.1 Mécanismes inflammatoires

Les agressions rénales aigues (ARA) mettent en jeu un mécanisme central d'inflammation intra-rénale et/ou systémique. Les autres évènements physiopathologiques s'additionnant à l'inflammation sont souvent plus spécifiques de l'étiologie de l'ARA [87].

La phase initiale correspondant à la phase d'agression rénale, conduit à des lésions du parenchyme rénal de manière plus ou moins étendues ainsi qu'à leur mort par nécrose ou apoptose. Cette phase implique plusieurs types cellulaires tels que les cellules endothéliales et épithéliales et elle peut durer plusieurs minutes voire plusieurs heures. L'activation des cellules endothéliales par l'ARA conduit à la production de nombreux facteurs impliqués dans l'initiation de l'inflammation aigüe tels que les DAMP (Damage-associated molecular patterns) et les molécules d'adhésion [88, 89] **(Figure 12).**

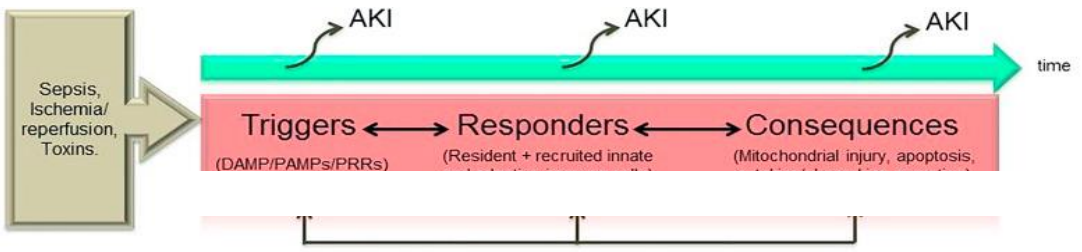

Figure 12 : Effecteurs, cibles et conséquences de l'ARA. AKI: Acute Kidney Injury; **DAMP**: Damage-associated molecular patterns; **PAMP**: Pathogen-associated molecular patterns; **PRR**: Pattern recognition receptor. Daprès [87]

Le recrutement de ces cellules pro-inflammatoires rentre dans la deuxième phase de l'inflammation aigüe qui peut durer plusieurs jours, cette dernière est responsable de la production de cytokines pro-inflammatoires (TNFα, l'IL-6 ou l'IL-1β) et anti-inflammatoires (IL-4, IL-10, resolvines, protectine D1) **(Figure 13)**.

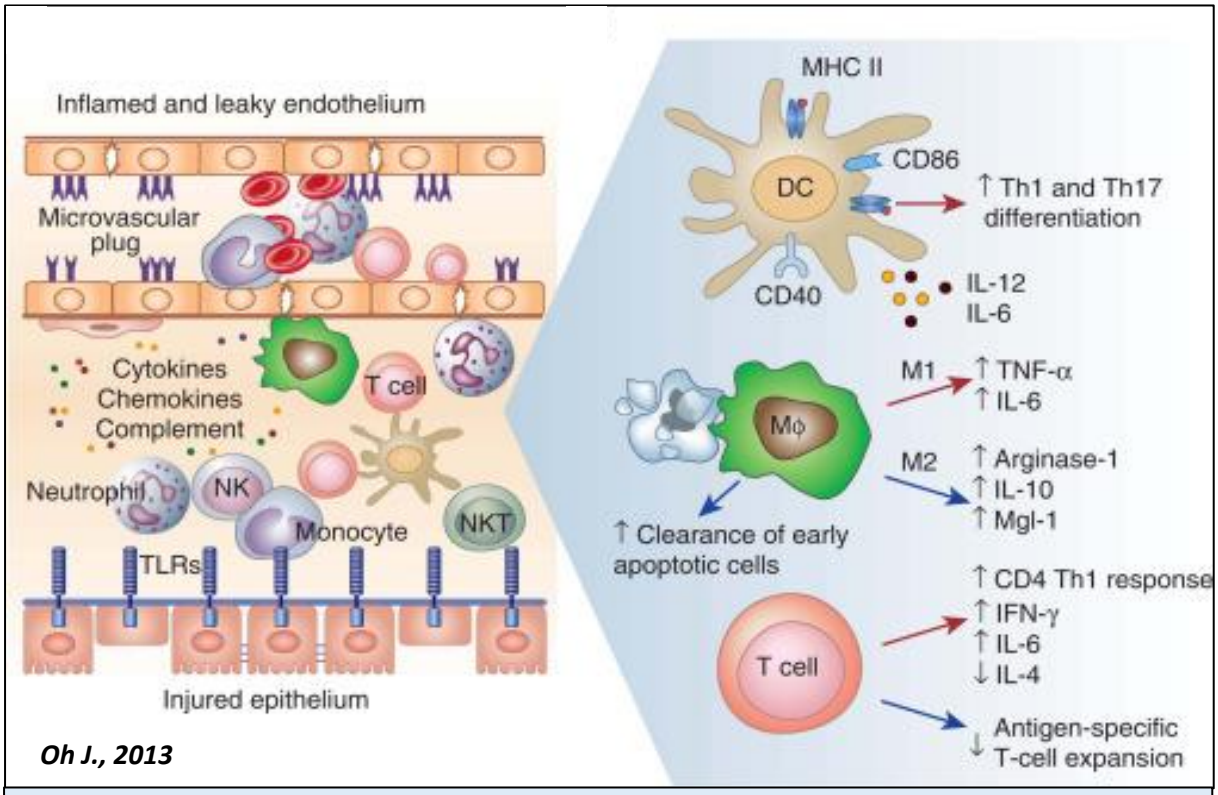

Figure 13 : Réponse inflammatoire et immunitaire après ARA . Mϕ: macrophages, **DC**: Dendritic Cell, **NK**: Natural killer, **TLR**: Toll-Like Receptor, **T cell**: Lymphocytes T.

L'équilibre de cette balance pro et anti-inflammatoire conduit à la réparation du tissu (cicatrisation) et à sa régénération ce qui constitue la phase terminale de la physiopathologie des ARA. Cependant, ce processus de réparation peut devenir inadapté et aboutir au développement d'une fibrose post-ARA pouvant entrainer l'apparition d'une maladie rénale chronique [90, 91].

3.4.2 Le système Rénine – Angiotensine – Aldostérone (SRAA)

En plus des mécanismes inflammatoires suscités, l'activation du système rénine angiotensine aldostérone semble être un processus physiopathologique commun à de nombreux mécanismes d'agression rénale aigue.

Le SRAA est un système hormonal organisé autour du rein comme décrit précédemment (paragraphe 1.3), il aboutit à la formation d'angiotensine II qui agit en se fixant sur des récepteurs transmembranaires. Il en existe deux types : AT1 (majoritaire) et AT2, qui ont des rôles antagonistes. Via le récepteur AT1 (récepteur couplé à la protéine G), l'angiotensine II favorise l'élévation de la pression artérielle par différents mécanismes **(Figure 6)** :

- Stimulation de la vasoconstriction par activation du système nerveux sympathique
- Stimulation de la vasoconstriction artériolaire (directe et indirecte par relargage de noradrénaline)
- Stimulation directe de la réabsorption tubulaire de Na+
- Stimulation de la sécrétion d'aldostérone par le cortex surrénalien entrainant une réabsorption tubulaire de Na+ et d'eau contre une perte de K+
- Stimulation de la sécrétion de l'ADH par la post hypophyse permettant la réabsorption tubulaire d'eau au niveau du tubule contourné distal et du tube collecteur.

3.5 Cas particulier : l'insuffisance rénale aigue en chirurgie cardiaque

3.5.1 Généralités

Près de 2 millions d'actes de chirurgie cardiaque sont réalisés tous les ans dans le monde. L'IRA a été identifiée comme étant le facteur de risque principal de mortalité dans les suites post opératoires. L'ADQI (Acute Disease Quality Initiative) a proposé le terme de CSA-AKI (cardiac surgery-associated acute kidney injury) pour définir les épisodes d'IRA survenant dans les suites d'une chirurgie cardiaque [86]. Basé sur les critères KDIGO **(Tableau 2)**, une CSA-AKI précoce intervient dans les 7 jours suivant une chirurgie cardiaque, une CSA-AKI tardive apparait quant à elle entre 7 à 30 jours après la chirurgie cardiaque.

L'incidence de la CSA-AKI varie selon les études due à l'utilisation de définitions différentes de l'IRA. Deux méta-analyses récentes ont montré que l'incidence de CSA-AKI définie par RIFLE, AKIN et KDIGO était d'environ 22% [92, 93]. La majorité des patients CSA-AKI avaient une AKI légère (stade 1 : 14 à 18% des patients), le stade 2 survenait chez 4% des patients et enfin 3% des patients avaient un stade 3. Le recours à l'EER était nécessaire chez 2,3% à 3,1% des patients. CSA-AKI était associée à une augmentation des coûts et à une augmentation de la durée d'hospitalisation (15 j vs 10,5 j). La sévérité de l'IRA était associée à une augmentation de la durée d'hospitalisation (stade 1 : 14 jours, stade 2 :18 jours et stade 3 : 26,3 jours) [92].

Les patients CSA-AKI présentaient une mortalité à court terme de 10% par rapport à 1,7% chez les patients sans AKI (OR ¼ 8,52, IC à 95% ¼ 8,00 à 9,07), avec une augmentation progressive de la mortalité à court terme en fonction de la sévérité de l'AKI (stade 1 : 5,7%,

stade 2 : 16,2% et stade 3 : 36,7%). La mortalité à long terme était également augmentée chez les patients CSA-AKI en comparaison aux patients sans AKI (30% vs 11,9%). Après ajustement pour d'autres co-variables, il existait un risque accru de mortalité proportionnel à la sévérité de l'AKI [94, 95].

Les mécanismes aboutissant à la survenue d'une IRA dans les suites d'une chirurgie cardiaque sont multiples. On retrouve les mécanismes décrits précédemment (paragraphe 3.4) et on peut citer des mécanismes spécifiques tels que : les néphrotoxiques, l'ischémie reperfusion, la congestion veineuse, l'activation de l'inflammation et du stress oxydant par la circulation extra-corporelle et enfin la prédisposition génétique.

3.5.2 Place de la néprilysine

La néprilysine urinaire a récemment été étudiée comme biomarqueur de l'insuffisance rénale aigue en post opératoire de chirurgie cardiaque. En 2021, Bernardi *et al*, dans une étude monocentrique observationnelle chez 100 patients hospitalisés pour une chirurgie cardiaque élective avec CEC, ont réalisé des mesures répétées de la néprilysine urinaire durant la période peropératoire [96]. Dans cette étude la néprilysine urinaire en fin d'intervention semblait être un biomarqueur prometteur dans la CSA-AKI avec une AUC à 0.77 (0.65-0.90). La néprilysine urinaire comme biomarqueur de l'IRA a été testée dans d'autres cadres nosologiques. En 2017, Pajenda *et al*, ont recueilli quotidiennement pendant cinq jours consécutifs, les urines de 90 patients admis en soins intensifs pour sepsis [97]. La néprilysine urinaire était significativement plus élevée chez les patients avec IRA selon les critères KDIGO en comparaison avec les patients sans IRA et des contrôles sains.

Comme décrit dans le paragraphe 1.1, la néprilysine autrement appelée « kidney-brush-border » est très présente dans les cellules tubulaires rénales. L'hypothèse principales des auteurs dans les études ci-dessus est celle d'une libération urinaire de NEP après agression tubulaire.

3.5.3 Place du SRAA

Récemment, Küllmar *et al* ont démontré qu'une augmentation de la concentration de rénine plasmatique était associée à la CSA-AKI [98], les auteurs ont émis l'hypothèse qu'une telle augmentation de la concentration de rénine était secondaire à un rétrocontrôle négatif par déficit en angiotensine II, entraînant une vasodilatation intrarénale, une perte de pression de filtration glomérulaire, entraînant éventuellement une diminution de la filtration glomérulaire. De plus, un excès relatif d'angiotensine 1-7 pourrait également contribuer à une vasodilatation intra-rénale excessive.

En réponse à cette étude et à l'hypothèse émise par les auteurs, Legrand *et al*, ont proposé une hypothèse alternative afin d'expliquer l'élévation de la concentration de rénine plasmatique dans ce contexte [99]. En effet, une augmentation de la rénine pourrait refléter l'activation complète du SRAA, impliquant une vasoconstriction rénale comme principal moteur physiopathologique de l'IRA (**Figure 14**).

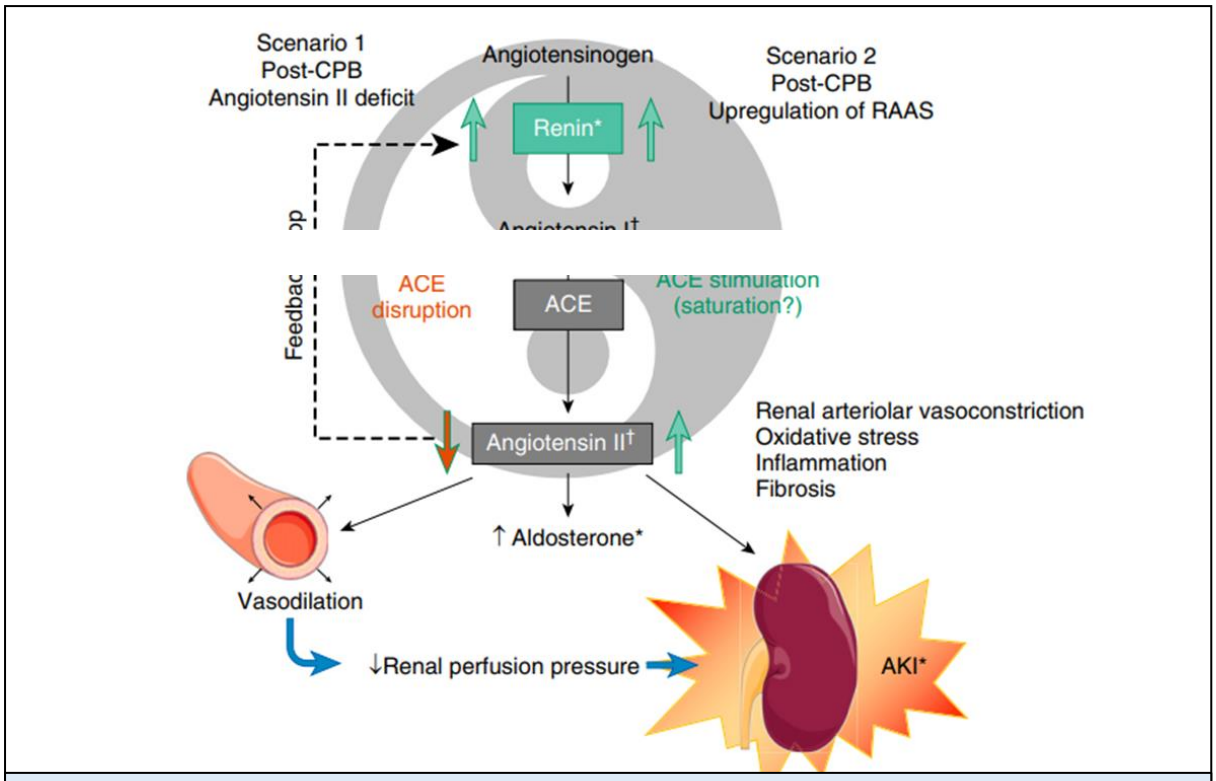

Figure 14 : Scenario de perturbation du RAAS dans les suites d'une chirurgie cardiaque. **ACE** = angiotensin-converting enzyme, **AKI** = acute kidney injury, **CPB** = cardiopulmonary bypass, **RAAS** = renin–angiotensin–aldosterone system. D'après [99]

4 Le choc septique

4.1 Définition

Historiquement le sepsis a été défini comme la réponse inflammatoire de l'organisme ou SIRS (Systemic Inflammatory Response Syndrome) à une infection [100]. Jusqu'en 2016 on distinguait le sepsis sévère du choc septique. Le sepsis sévère était défini comme un sepsis associé à une défaillance d'organe, une hypoperfusion ou une hypotension, alors que le choc septique était défini comme un sepsis associé à une hypotension persistante malgré une expansion volémique adéquate [101].

En 2016, une nouvelle conférence de consensus internationale (SEPSIS-3) a revisité la définition du sepsis et choc septique [102] :

- Le sepsis est maintenant défini comme « une dysfonction d'organe secondaire à une dérégulation de la réponse de l'hôte à l'infection et menaçant le pronostic vital ». La dysfonction d'organe est définie comme une augmentation du score SOFA ≥2.
- Le choc septique est défini comme un « sepsis associé à une hypotension persistante requérant des vasopresseurs pour maintenir une PAM ≥ 65mmHg et une lactatémie > 2 mmol/L ».

4.2 Physiopathologie

La physiopathologie du sepsis et du choc septique est complexe. Ce paragraphe ne prétend pas une exhaustivité mais un rappel des principales voies physiopathologiques [103-105] et tend à décrire la physiopathologie de la vasodilatation constatée dans le choc septique.

4.2.1 Principales voies physiopathologiques

- **Inflammation / Immunosuppression**

En réponse à l'infection, on observe une activation du système immunitaire inné (macrophages et dendrocytes) et l'apparition des motifs moléculaires liés au pathogène : PAMPs (Pathogen-associated Molecular Patterns) et ceux liés aux dégâts cellulaires : DAMPs (Damage-associated Molecular Patterns) qui induisent via leurs récepteurs PRRs (Pattern Recognition Receptors) la transcription de gènes impliqués dans la réponse inflammatoire et l'immunité adaptative. L'activation de ces récepteurs est responsable de la transcription des cytokines pro-inflammatoires (TNFα, l'IL-6 ou l'IL-1β).

Après cette phase pro-inflammatoire, on observe une réponse anti-inflammatoire compensatrice chez les patients présentant un choc septique. Cette phase d'immunosuppression peut se prolonger dans le temps et être à l'origine d'une augmentation de la fréquence de pathologies opportunistes et des réactivations virales.

Ainsi, ce profil inflammatoire décrit dans les suites d'un choc septique a été décrit sous le nom de Persistent Inflammation, immunosuppression and Catabolism Syndrome ou PICS [106, 107].

- **Dysfonction endothéliale et état procoagulant**

La réponse inflammatoire associée au stress oxydant et à l'adhésion leucocytaire et plaquettaire entraine une dysfonction endothéliale responsable d'une perte de l'intégrité de la barrière endothéliale par l'atteinte de son cytosquelette et des jonctions serrées. A cela s'ajoute l'atteinte du glycocalyx qui accentue la perméabilité endothéliale favorisant la fuite capillaire massive responsable de l'œdème tissulaire [108]. On observe également une activation de la voie de coagulation extrinsèque associée à une activation plaquettaire responsable d'un état pro-coagulant. En résulte la formation de microthrombi responsables de troubles de la microcirculation. In fine la consommation excessive de plaquettes et de facteurs de la coagulation, ou coagulation intravasculaire disséminée, induit des saignements incontrôlés.

- **Dysfonction d'organe**

Les défaillances d'organes observées dans le choc septique sont secondaires au défaut d'oxygénation tissulaire par diminution de la délivrance en oxygène en lien avec la vasodilatation et les troubles de la microcirculation. En plus d'un déficit en oxygène s'ajoute

la dysfonction mitochondriale sous l'effet du stress oxydant qui altère la respiration cellulaire. La vasodilatation est l'essence même de la dérégulation d'organe observée lors du choc septique mais elle peut être associée à une composante hypovolémique induite par la fuite capillaire. La vasodilatation peut également être associée à une dysfonction myocardique, on parle alors de cardiomyopathie septique.

4.2.2 Mécanismes de la vasodilatation

Le choc septique est un choc distributif ou choc à « résistances basses ». La vasodilatation observée dans le choc septique est expliquée par trois mécanismes principaux [109]: l'activation des canaux potassiques à ATP des cellules musculaires lisses vasculaires, l'augmentation de la synthèse de NO (Nitric Oxid) et le déficit en vasopressine (**Figure 15**).

- **Activation des canaux potassiques à ATP des cellules musculaires lisses vasculaires**

Le sepsis, l'acidose lactique ou l'hypoxie entraine une activation des canaux potassiques situés sur les membranes des cellules musculaires vasculaire induisant une sortie massive de potassium de la cellule qui entraine une hyperpolarisation de la cellule. Parallèlement, il existe une inactivation des canaux calciques qui empêche l'augmentation de la concentration cytoplasmique en calcium. En l'absence de calcium intracellulaire la diminution de la phosphorylation de la myosine entraine une vasodilatation.

- **Augmentation de la synthèse de NO**

En réponse au sepsis, on observe une augmentation de la production de NO. Cette augmentation est médiée par l'augmentation de l'expression de la NO synthase (NOS) en réponse à l'augmentation des cytokines pro-inflammatoires. L'augmentation de NO induit une vasodilatation par activation directe de la voie GMPc (guanosine monophosphate cyclique) ou

via une activation des canaux potassiques calcium sensible qui accentue le déficit de calcium intracellulaire.

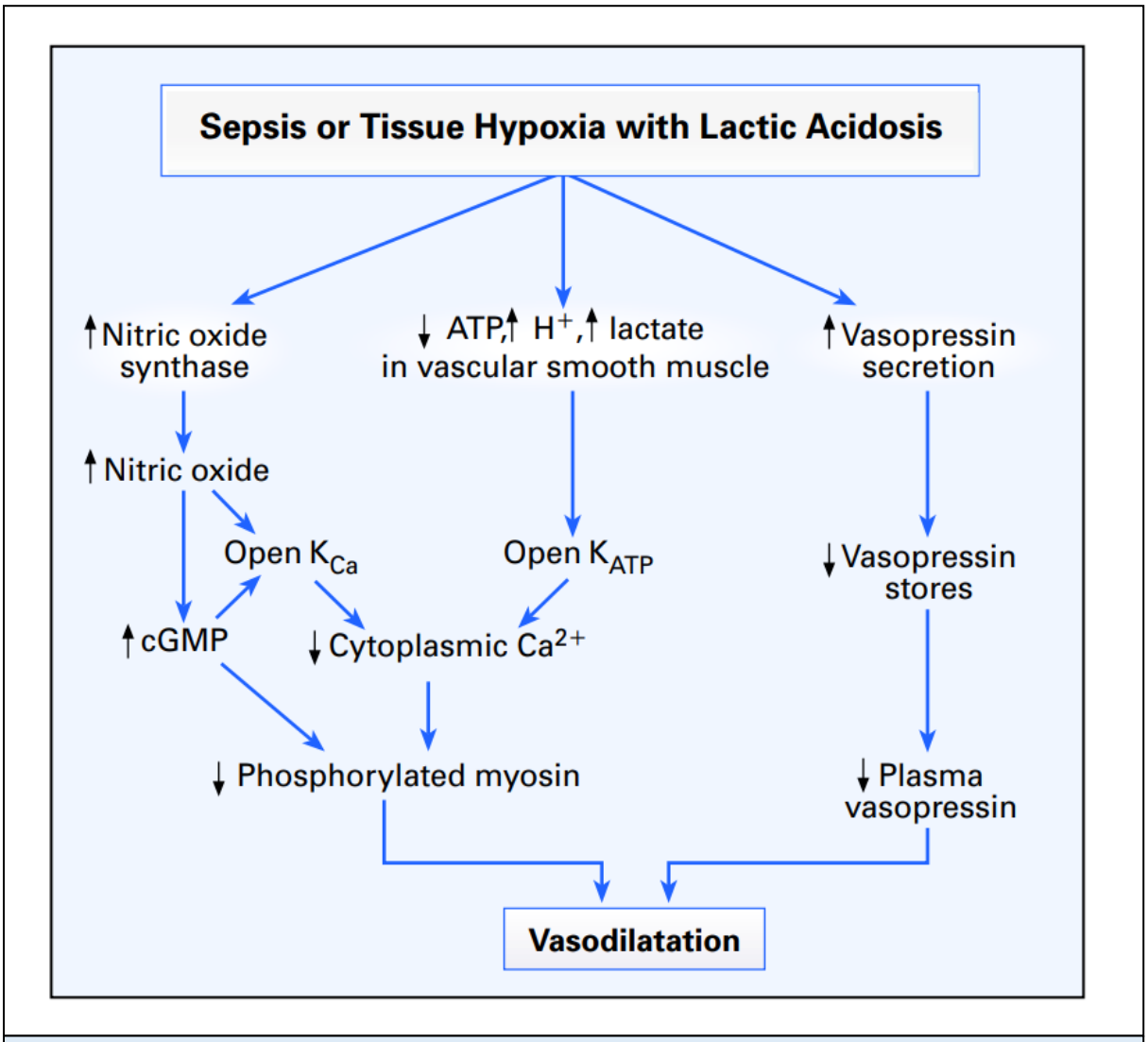

Figure 15 : Mécanismes de la vasodilatation dans le choc septique. D'après [109]

- **Déficit en vasopressine**

Chez le sujet sain la vasopressine joue un rôle mineur dans la régulation de la pression artérielle. Mais en réponse à une hypotension, la concentration plasmatique de vasopressine augmente rapidement afin de maintenir la pression artérielle. Dans le choc septique, il existe

une élévation initiale de la vasopressine plasmatique mais qui diminue rapidement. Les mécanismes responsables de ce déficit secondaire en vasopressine restent mal connus.

- **Augmentation de la production de peptides vasodilatateurs en réponse à l'inflammation**

L'une des conséquences de l'induction de la réponse inflammatoire au niveau vasculaire est la production de peptides vasodilatateurs (bradykinines et substance P) qui augmente la perméabilité vasculaire (substance P) [110]. De manière intéressante, ces peptides sont des cibles de la NEP.

4.3 Cas particulier du choc réfractaire

Le choc septique réfractaire reste une entité obscure dont la définition n'est pas consensuelle. En effet, la littérature évoque un choc septique dans lequel les objectifs de pression artérielle ne répondent plus au traitement vasopresseur conventionnel. Certains auteurs ont tenté de définir des doses-seuil de noradrénaline allant de 0,25 à 4 µg/kg/min au-delà de laquelle un patient doit être considéré en choc septique réfractaire [111, 112]. Leone *et al*, ont défini un seuil de 1 µg/kg/min de noradrénaline au-delà duquel la mortalité dépassait 90% [112]. Par ailleurs, Auchet *et al*, ont conclu qu'une dose de noradrénaline supérieure à 0,75 µg/kg/min et un score SOFA supérieur à 10 étaient des facteurs de risque indépendants de mortalité [113].

En conclusion, le choc septique réfractaire pourrait être défini par une dose de noradrénaline au-delà de laquelle les objectifs de pression sont difficilement atteint et qui est associé avec une augmentation des dysfonctions d'organe et une mortalité accrue. Basé sur l'ensemble de la littérature, il apparait qu'une dose de noradrénaline supérieure à 1

µg/kg/min soit associée à une mortalité supérieure à 80% et pourrait être utilisée comme seuil pour définir le choc septique réfractaire.

4.4 Choc septique, peptides natriurétiques et néprilysine

Chez les patients en état de choc septique les valeurs de BNP et de NT-proBNP sont très élevées [114]. Ces valeurs élevées de BNP et de NT-proBNP ne sont pas corrélées aux pressions de remplissage du ventricule gauche, c'est-à-dire qu'il existe une élévation du BNP et du NT-proBNP indépendante de la fonction cardiaque dans le choc septique [114]. Cette élévation du BNP et du NT-proBNP n'est pas retrouvée dans d'autres modèles de choc [114].

Dans une étude récente, il a été confirmé *in vivo*, dans le plasma de patients en insuffisance cardiaque chronique ou de patients souffrant de dyspnée d'origine cardiaque ou non, que le BNP > 916 pg/mL inhibe l'activité de la néprilysine [44]. Cette inhibition endogène de la néprilysine par le BNP n'est retrouvée que chez les primates. Cette inhibition pourrait avoir de multiples conséquences, en particulier dans le choc septique, la néprilysine ayant de nombreux peptides vasoactifs comme substrats. La néprilysine agit en dégradant ces substrats tels que la substance P, la bradykinine, l'endothéline-1, l'ANP et l'adrenomédulline. De plus, chez des animaux, l'administration de lipopolysaccharide (LPS) entraîne une forte diminution de la pression artérielle, même si le LPS ne reflète pas tous les aspects physiopathologiques du choc septique. L'invalidation génétique ou l'inhibition pharmacologique de cibles de la NEP ont montré une amélioration des animaux [110, 115-122], renforçant un rôle potentiel de la NEP dans la progression du choc septique vers des formes plus graves.

Les taux de BNP dans le choc septique sont supérieurs à 916 pg/mL et devraient donc entrainer une inhibition de la néprilysine. Pirracchio *et al*, a montré des taux d'activité NEP

très bas chez les patients en choc septique[114]. La néprilysine semble donc être inhibée par le BNP dans le choc septique. Cette inhibition entraine une augmentation des substrats de la NEP, comme la substance P qui majore la perméabilité vasculaire induisant une majoration de la fuite capillaire et comme l'ANP, la bradykinine ou l'adrenomédulline qui participent à la défaillance hémodynamique par vasodilatation [110, 115-122].

5 Objectif

L'objectif de ce travail est d'étudier la NEP comme biomarqueur ou acteur physiopathologique dans différents contextes cliniques. Ce travail s'est intéressé :

i) Dans un premier temps aux effets de l'inhibition de la NEP dans l'insuffisance cardiaque chronique à FEVG réduite sur les peptides natriurétiques comme biomarqueurs, afin de mieux comprendre le mode d'action du sacubitril/valsartan.

ii) Dans un second temps à la NEP comme biomarqueur dans la dysfonction rénale aigue dans le contexte de la chirurgie cardiaque et d'étudier son impact sur le SRAA.

iii) Enfin dans un modèle murin de choc septique, ce travail à pour dernier objectif de démontrer l'inhibition de la NEP par le BNP humain, de démontrer les conséquences hémodynamiques de l'inhibition de la NEP dans ce modèle et d'explorer les bénéfices d'un blocage de l'inhibition de la NEP par le BNP humain.

RESULTATS

1 Article I. proANP metabolism provides new insights into sacubitril/valsartan mode of action

La production des peptides natriurétiques (A-type natriuretic peptide : ANP, B-type natriuretic peptide : BNP) augmente lors de l'insuffisance cardiaque et sont couramment utilisé comme biomarqueurs. Le proANP est clivé par la corine en ANP bioactif et en NT-proANP qui est lui-même clivé en trois peptides bioactifs. Cependant, les enzymes impliquées dans le clivage du NT-proANP ne sont pas connues. Comme l'ANP a une demi-vie très courte, la mesure du (mid-regional) MR-proANP a été développé comme substitut afin de différencier les dyspnées d'origine cardiaque ou non. Cependant, des différences de valeurs entre la mesure plasmatique du proANP et celle du MR-proANP ont été identifié pouvant suggérer le rôle de modifications post-traductionnelles. Récemment, il a été montré que le proANP était O-glycosylé et basé sur nos travaux sur le proBNP, nous avons fait l'hypothèse que cette O-glycosylation pouvait interférer avec la mesure du MR-proANP. Afin de répondre à cette question, dans une cohorte de 73 patients en insuffisance cardiaque chronique avec fraction d'éjection du ventricule gauche réduite chez lesquels le sacubitril/valsartan a été introduit en comparaison avec une population de volontaire sain, nous avons comparé les dosages du MR-proANP (Kryptor, ELISA) avec la quantification des espèces moléculaires qui participent au dosage du MR-proANP par spectrométrie de masse. Nous avons observé une diminution du MR-proANP et une augmentation des espèces moléculaires contribuant au signal MR-proANP par spectrométrie de masse. Cette différence était due à l'augmentation de la glycosylation du proANP en S80 qui interfère avec le dosage du MR-proANP, masquant l'augmentation des espèces moléculaires qui contribuent au signal MR-proANP. Ces résultats ont conduit à une étude approfondie du métabolisme du proANP qui a permis :

i) D'identifier les enzymes impliquées dans la cascade enzymatique impliquée dans la production de trois peptides vasoactifs produits à partir du NT-proANP (Meprin B, Enzyme de conversion de l'endothéline 1 [ECE-1], et l'aminopeptidase N [ANPEP]). Cette cascade enzymatique est séquentielle, et la séquence des événements est probablement déterminée par la présence de structures secondaire dans le proANP. Les enzymes

ii) Que l'action du sacubitril n'inhibe pas que la NEP, et inhibe partiellement ECE1 et ANPEP. En particulier, l'inhibition de l'ANPEP est bi-modal avec un effet direct du sacubitril, et un effet indirect par l'accumulation de substance P qui est moins dégradé quand la NEP est inhibée.

iii) Que la production d'ANP dans l'IC à FEVG réduite est limitée par des mécanismes épigénétiques qui implique deux miRNAs dont l'expression est augmentée dans l'IC à FEVG réduite : miR-425 limite la production de proANP, et miR-1-3p limite la production de Corine qui est impliquée dans le clivage du proANP en ANP et NT-proANP. Le sacubitril/valsartan diminue l'expression de ces microRNAs et restore un métabolisme normal du proANP, contribuant à la forte augmentation de l'ANP après traitement par sacubitril/valsartan. L'augmentation de l'ANP résulte également de sa protection contre la dégradation par la NEP.

L'ensemble de ces travaux montrent que l'IC à FEVG réduite est un état suboptimal en ANP, état qui est restauré par le sacubitril/valsartan. Ce travail apporte également de nouveaux éléments sur le mode d'action du sacubitril/valsartan.

Circulation Research

ORIGINAL RESEARCH

proANP Metabolism Provides New Insights Into Sacubitril/Valsartan Mode of Action

Thibault Michel,* Hélène Nougué,* Jérôme Cartailler, Guillaume Lefèvre, Malha Sadoune, François Picard, Alain Cohen-Solal, Damien Logeart, Jean-Marie Launay, Nicolas Vodovar

BACKGROUND: Sacubitril/valsartan (S/V) treatment is beneficial in patients with heart failure with reduced ejection fraction (HFrEF), but its mode of action remains elusive, although it involves the increase in ANP (atrial natriuretic peptide).

METHODS: Combining mass spectrometry and enzymatic assay in the plasma of 73 HFrEF patients treated with S/V and controls, we deciphered proANP processing that converts proANP into 4 vasoactive peptides.

RESULTS: We found that proANP processing is sequential and involved meprin B, ECE (endothelin-converting enzyme) 1, and ANPEP (aminopeptidase N). This processing is limited in HFrEF patients via the downregulation of proANP production, corin, and meprin B activities by miR-425 and miR1-3p. S/V restored or compensated proANP processing by downregulating miR-425 and miR1-3p, hence increasing levels of proANP-derived bioactive peptides. In contrast, S/V directly and indirectly partially inhibited ECE1 and ANPEP. ECE1 partial inhibition resulted in a lower-than-expected increase in ET1 (endothelin 1), tilting the vasoactive balance toward vasodilation, and possibly hypotension. Furthermore, proANP glycosylation interferes with the midregional proANP assay –a clinical surrogate for proANP production, preventing any pathophysiological interpretation of the results. The analysis of S/V dose escalation with respect to baseline treatments suggests S/V-specific effects.

CONCLUSIONS: These findings offer mechanistic evidence to the natriuretic peptide -defective state in HFrEF, which is improved by S/V. These data also strongly suggests that S/V increases plasma ANP by multiple mechanisms that involve 2 microRNAs, besides its protection from NEP (neprilysin) cleavage. Altogether, these data provide new insights on HFrEF pathophysiology and the mode of action of S/V.

GRAPHIC ABSTRACT: A graphic abstract is available for this article.

Key Words: atrial natriuretic factor ■ CD13 antigens ■ endothelin-1 ■ endothelin-converting enzymes ■ humans ■ neprilysin

Meet the First Author, see p 1646

The first-in-class angiotensin receptor NEP (neprilysin) inhibitor sacubitril/valsartan (S/V) combines an NEP (Enzyme Commission Number [EC]: 3.4.24.1) inhibitor (sacubitril) with an angiotensin receptor blocker (valsartan) and has shown benefit in patients with chronic heart failure with reduced ejection fraction (HFrEF).[1] NEP is a ubiquitous metalloprotease responsible for the inactivation of >40 peptides with various functions,[2] including several vasoactive peptides with vasoconstrictive (Ang I [angiotensin I] and ET1 [endothelin-1]) or vasodilatory (natriuretic peptides, adrenomedullin, SP [substance P], bradykinins, and Ang_{1-7} [$angiotensin_{1-7}$]) properties. Besides its effects on natriuresis, hemodynamic and cardiac remodeling, S/V also improved glucose metabolism.[3,4] However, the broad range of NEP substrates and the different neuroendocrine status in healthy and heart failure (HF) individuals renders the understanding of angiotensin receptor NEP inhibitor mode of action difficult.

The cardiac production of ANP (atrial natriuretic peptide) and BNP (B-type natriuretic peptide) increases in patients with HF. While BNP is a poor substrate of

Correspondence to: Jean-Marie Launay, PharmD, PhD, Inserm UMR-S 942, Hôpital Lariboisière, 2 rue Ambroise Paré, Paris 75010, France, Email jean-marie.launay@inserm.fr or Nicolas Vodovar, PhD, Inserm UMR-S 942, Hôpital Lariboisière, 2 rue Ambroise Paré, Paris 75010, France, Email nicolas.vodovar@inserm.fr
*T. Michel and H. Nougué, contributed equally.
Supplemental Material is available at https://www.ahajournals.org/doi/suppl/10.1161/CIRCRESAHA.122.320882.
For Sources of Funding and Disclosures, see page e55 & e56.

Circulation Research is available at www.ahajournals.org/journal/res

Novelty and Significance

What Is Known?

- Sacubitril/valsartan has improved the prognostic of patients with heart failure and reduced ejection fraction, although its mode of action remains mainly unknown.
- Patients with the fastest and greatest increase in ANP (atrial natriuretic peptide) have a better outcome.
- Midregional proANP immunoassay is a surrogate for proANP/ANP production decreased in patients treated with sacubitril/valsartan.

What New Information Does This Article Contribute?

- The decrease in midregional proANP measurements in patients treated with sacubitril/valsartan results from an analytical interference of proANP glycosylation.
- Heart failure with reduced ejection fraction is a proANP-derived peptide suboptimal state that is corrected or compensated by sacubitril/valsartan at multiple regulatory levels.
- Sacubitril is an ECE (endothelin-converting enzyme) 1 and ANPEP (aminopeptidase N) partial inhibitor, which limits the production of vasoconstrictive endothelin-1 and tilts the vasoactive balance toward vasodilation.

Sacubitril/valsartan is beneficial in the treatment of heart failure with reduced ejection fraction, but its pleiotropic mode of action is not clearly understood. In the present study, we deciphered the proteolytic cascade that produces 4 bioactive peptides from proANP, all of which are relevant in HF pathophysiology. We found that proANP metabolism is suboptimal in heart failure with reduced ejection fraction, in part, due to the involvement of miRNAs that downregulate proANP production and enzyme involved early in the cascade. Sacubitril/valsartan had a profound effect on proANP metabolism and overall increased the plasma levels of the 4 peptides that derive from proANP, with anticipated beneficial action. In particular, the increase in ANP that is associated with a better outcome involves 3 independent mechanisms: decrease in ANP degradation by NEP (neprilysin) inhibition, increase in proANP translation, and increase in 2 enzymes involved in proANP processing. In parallel, sacubitril directly and indirectly inhibited ECE1 and ANPEP, indicating that the effects of sacubitril are broader than NEP inhibition alone. Finally, we showed that the decrease in midregional proANP plasma levels resulted from an analytical interference, which precludes any biological interpretation of the results. Altogether, these findings provide mechanistic evidence for heart failure with reduced ejection fraction as the natriuretic peptide suboptimal state and provide new insights into the mode of action of sacubitril/valsartan that go beyond what was originally thought, in particular for the increase in ANP, although other mechanisms are likely at play.

Nonstandard Abbreviations and Acronyms

ACE	angiotensin-converting enzyme
Ang$_{1-7}$	angiotensin$_{1-7}$
Ang I	angiotensin I
Ang II	angiotensin II
ANP	atrial natriuretic peptide
ANPEP	aminopeptidase N
BNP	B-type natriuretic peptide
ECE	endothelin-converting enzyme
ET1	endothelin 1
HF	heart failure
HFrEF	heart failure with reduced ejection fraction
MR-proANP	midregional proANP
MR-proANPir	midregional proANP immunoreactivity
NEP	neprilysin
NF-κB	nuclear factor kappa B
NT-proANP	N-terminal proatrial natriuretic peptide
S/V	sacubitril/valsartan
S63	serine 63
S80	serine 80
SP	substance P

NEP in humans, ANP is inactivated by NEP.[5] Expectedly, ANP plasma levels increased in healthy volunteers[6] and HFrEF patients[3,7] receiving S/V. ANP is produced as a prohormone (proANP$_{1-126}$ or proANP) by cardiomyocytes to mitigate volume and pressure overload. Upon release, proANP$_{1-126}$ is cleaved into ANP and NT-proANP (N-terminal proANP; proANP$_{1-98}$) by corin (EC: 3.4.21.-).[8,9] NT-proANP is further processed into 3 bioactive peptides: proANP$_{1-30}$, proANP$_{31-67}$, and

proANP$_{79-98}$ with natriuretic, vasodilatory, and kaliuretic properties, respectively.[10–12] However, the enzymatic cascade involved in the production of those NT-proANP-derived peptides, their receptors, and the mechanism whereby they exert their physiological action remain unknown.

The midregional proANP (MR-proANP) immunoassay[13] has been developed for clinical use as a surrogate biomarker for proANP production in HF.[14,15] However, discrepancies were observed when using proANP and MR-proANP assays, suggesting that posttranslational modifications may account for the lower MR-proANP immunoreactivity (MR-proANPir).[16] Recently, proANP was found to be *O*-glycosylated, and 2 glycosylation sites are located within the peptides (proANP$_{53-72}$ and proANP$_{73-90}$)[13] that correspond to the epitopes recognized by the antibodies used in the MR-proANP immunoassay.[17] However, the impact of glycosylation on MR-proANPir remains unknown.

The objective of this study was to evaluate the impact of proANP glycosylation on MR-proANP measurements in HFrEF patients whose angiotensin receptor blocker/ACE (angiotensin-converting enzyme) inhibitor treatment was changed to S/V. The results obtained prompted us to decipher the proANP cascade and evaluate the impact of S/V on all its components.

METHODS

Data Availability

Data are available from the corresponding author upon reasonable request.

A description of all Materials and Methods is provided in the Data Supplement.

RESULTS

Deconvolution of the MR-proANPir Signal by Quantitative Mass Spectrometry

As observed previously,[7] MR-proANPir decreased at D30 after initiation of S/V (Figure 1A). To test a potential influence of proANP glycosylation on MR-proANPir, proANP derivatives that could be detected by the 2 antibodies used in the assay[13] (proANP$_{1-126}$, proANP$_{1-98}$, proANP$_{31-98}$, and proANP$_{31-126}$) were quantified by mass spectrometry (Figure 1B). Results showed that proANP$_{1-126}$ and proANP$_{1-98}$ decreased at D30 and D90 (Figure 1C and 1D), while proANP$_{31-98}$ markedly increased at D30 and D90 (Figure 1E); proANP$_{31-126}$ was not detected. Changes in proANP$_{1-126}$, proANP$_{1-98}$, and proANP$_{31-98}$ were observed as soon as D7 after the initiation of S/V (Figure S1). When compared with controls, HFrEF patients at baseline had higher proANP$_{1-126}$ and proANP$_{1-98}$ plasma levels, while proANP$_{31-98}$ was lower (Figure 1C through 1E). At D90, proANP$_{1-126}$ was similar in HFrEF and controls while proANP$_{1-98}$ and proANP$_{31-98}$ were higher (Figure 1C through 1E). Theoretical MR-proANPir, estimated as the sum of proANP$_{1-126}$, proANP$_{1-98}$, and proANP$_{31-98}$ quantified by mass spectrometry, was modestly higher (1.6-folds) in HFrEF patients at baseline when compared with healthy subjects and increased between D0 and D30 conversely to MR-proANPir (Figure 1F). Furthermore, in HFrEF patients at baseline, theoretical MR-proANPir was predominantly (90% [interquartile range, 87%–94%]) composed of proANP$_{1-126}$ and proANP$_{1-98}$, while proANP$_{31-98}$ became predominant at D30 (66% [63%–71%]) and D90 (85% [83%–87%]). In healthy subjects, proANP$_{31-98}$ was the predominant molecular species (Figure 1C through 1E). However, the lack of correlation between measured and theoretical MR-proANPir (Figure 1G) indicates that MR-proANPir does not reflect the true amount of the molecular species that contribute to the signal.

proANP Glycosylation at S80 Interferes With MR-proANPir

The opposite kinetic of measured and theoretical MR-proANPir prompted us to evaluate the impact of proANP$_{31-98}$ glycosylation at S63 (serine 63) and S80 (serine 63) on MR-proANPir. While the former was low and remained unchanged (Figure S2), the latter markedly increased at D30 (Figure 2A). Comparison of the distribution of MR-proANPir and theoretical MR-proANPir not glycosylated at S80 showed a strong correlation at D30 and D90, that is, when proANP$_{31-98}$ is the predominant molecular species (Figure 2B), which was confirmed by the Bland-Altman plot (Figure 2C). Discrepancies were observed above 400 nmol/L, which may result from other analytical interference. The lack of correlation between measured and theoretical nonglycosylated MR-proANPir at baseline (Figure 2B) suggests that the level of glycosylation at S80 differs between proANP$_{1-126}$, proANP$_{1-98}$, and proANP$_{31-98}$. Altogether, these data indicate that the MR-proANPir assay only detects non-S80 glycosylated proANP$_{1-126}$, proANP$_{1-98}$, and proANP$_{31-98}$ and that the decrease in MR-proANPir under S/V treatment results from the analytical interference of S80 glycosylation with the assay.

Deciphering the proANP Proteolytic Cascade

A striking impact of S/V was the rapid and marked increase in proANP$_{31-98}$. However, the enzymes involved in the processing of proANP$_{1-98}$ are unknown. Based on the proANP$_{1-98}$ cleavage sites described previously (between amino acids 30-31, 67-68, and 78-79), we quantified all possible proANP$_{1-126}$ derivatives by mass spectrometry (Figure S3A). The data obtained strongly suggested the cleavage of proANP$_{1-126}$ is sequential (Figure 3A). First,

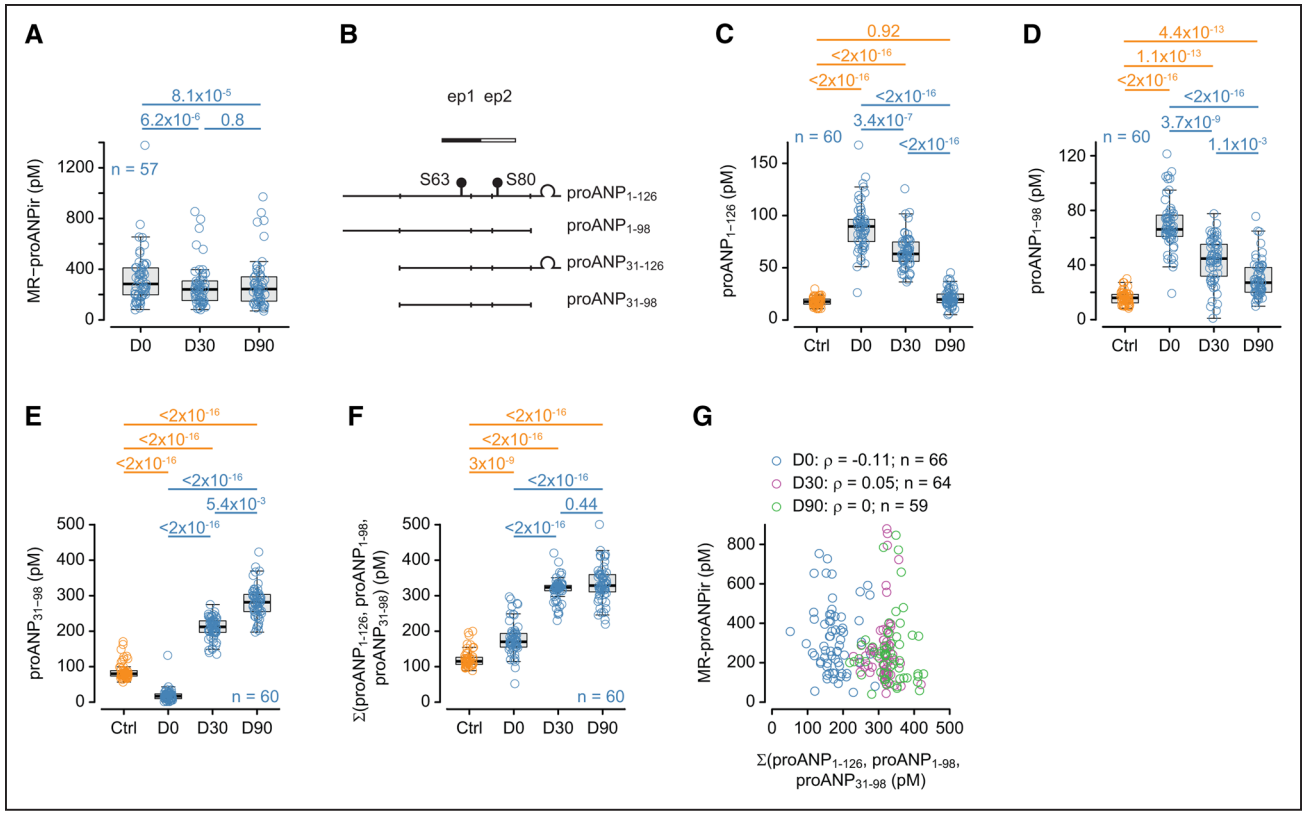

Figure 1. Deconvolution of midregional proANP immunoreactivity (MR-proANPir) by mass spectrometry.
A, MR-proANPir plasma levels of MR-proANPir measured with the Kryptor assay at baseline (D0) and D30 and D90 after the initiation of sacubitril/valsartan (S/V). **B**, proANP derivatives that contain both epitopes recognized by the antibodies of the midregional proANP assay. The glycosylation sites that could interfere with the binding of the antibodies are indicated by black circles and labeled. **C**–**E**, Plasma levels of $proANP_{1-126}$ (**C**), $proANP_{1-98}$ (**D**), and $proANP_{31-98}$ (**E**) quantified by mass spectrometry (MS) in control (Ctrl) heart failure with reduced ejection fraction (HFrEF) patients at baseline and D30 and D90 after the initiation of S/V. **F**, Plasma levels of theoretical MR-proANPir calculated as the sum of $proANP_{1-126}$, $proANP_{1-98}$, and $proANP_{31-98}$ as quantified by MS in controls and HFrEF patients at baseline and D30 and D90 after the initiation of S/V. **G**, Relationship between theoretical and measured MR-proANPir at baseline and D30 and D90 after the initiation of S/V. The Spearman rank correlation coefficient (ρ) is indicated for each time point along with the number of samples. Variables in **A** and **C**–**F** were analyzed using repeated-measures ANOVA on log-transformed data followed by the Tukey honestly significant difference (HSD) test (blue) or using the Wilcoxon rank-sum test corrected for multiple comparisons (holm, orange). The number of subjects included in the analyses is indicated on each panel. The number of healthy subjects was 54.

we never found any $proANP_{1-126}$ derivatives that contains either the first or the last amino acid of $proANP_{1-126}$ but $proANP_{1-98}$ and ANP - $proANP_{31-126}$, $proANP_{68-126}$, or $proANP_{79-126}$ were not detected, indicating that corin always cleaves first. Of note, we detected at baseline $proANP_{1-105}$ the degradation product of $proANP_{1-126}$ by NEP, which could be further cleaved into $proANP_{31-105}$. These data suggest that the disulfide bond present in the ANP moiety prevents the cleavage of $proANP_{1-126}$ within its N-terminal segment. Second, $proANP_{1-98}$ could only be cleaved into $proANP_{1-30}$ and $proANP_{31-98}$ since neither $proANP_{1-68}$ nor $proANP_{1-79}$ was detected. The MEROPS database[18] identified meprin B (EC: 3.4.24.63) as a potential candidate for the cleavage, which was confirmed in vitro by incubating 250 nmol/L $proANP_{1-98}$ with human recombinant meprin B (Figure 3B). Structure prediction algorithms identified an α-helix within $proANP_{1-30}$ (Figure S3B and S3C), which may prevent any cleavage besides between amino acids 30 and 31 to occur in $proANP_{1-98}$. Third, $proANP_{31-98}$ could only be cleaved into $proANP_{31-67}$ and $proANP_{68-98}$ as $proANP_{31-78}$ was not detected. Since $proANP_{31-98}$ increased dramatically after the initiation of S/V, we hypothesized that $proANP_{31-98}$ cleavage could be inhibited by the drug. While human recombinant NEP had little effect on $proANP_{31-98}$ in vitro, ECEs (endothelin-converting enzymes) 1 and 2 (EC: 3.4.24.71), which were found partially inhibited by sacubitril in vitro,[19] cleaved 250 nmol/L $proANP_{1-98}$ rapidly between amino acids 67 and 68 as verified by mass spectrometry (Figure 3C). Finally, $proANP_{68-78}$ was never detected, which suggested that $proANP_{79-98}$ could result from the action of an aminopeptidase on $proANP_{68-98}$. Accordingly, we detected intermediary cleavage products ranging from $proANP_{69-98}$ to $proANP_{78-98}$ with a single N-terminal amino acid difference, predominantly at D7 after the initiation of S/V (Figure S3D). In vitro, incubation of 250 nmol/L $proANP_{68-98}$ with human recombinant ANPEP (aminopeptidase N; EC: 3.4.11.2, also

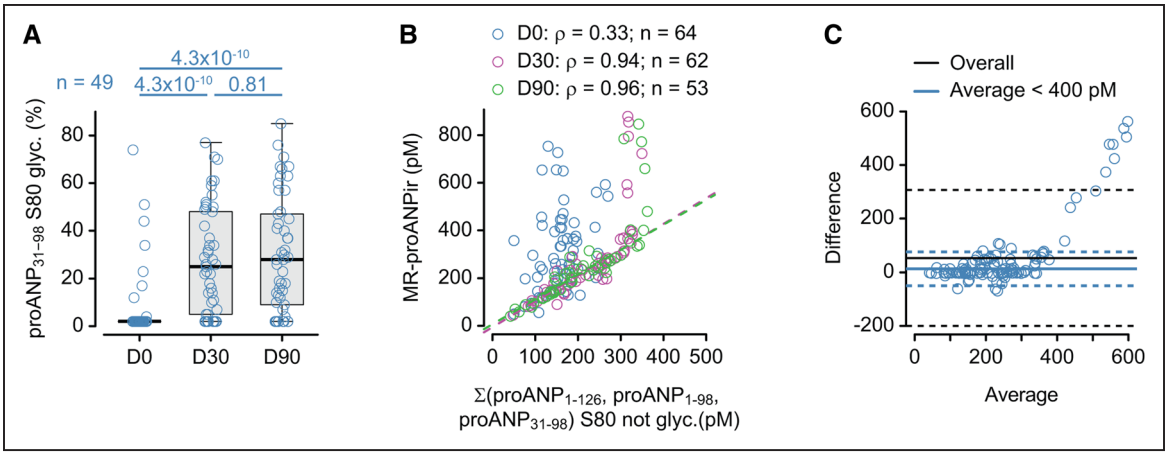

Figure 2. Impact of S80 (serine 80) glycosylation on midregional proANP immunoreactivity (MR-proANPir).
A, S80 glycosylation level (S80 glyc.) of $proANP_{31-98}$ quantified by mass spectrometry at baseline (D0) and D30 and D90 after the initiation of sacubitril/valsartan (S/V). **B**, Relationship between theoretical MR-proANPir not glycosylated at S80 and MR-proANPir at baseline and D30 and D90 after the initiation of S/V. The Spearman correlation coefficient (ρ) is indicated for each time point along with the number of samples. **C**, Bland-Altman comparison of theoretical MR-proANPir not glycosylated at S80 and measured MR-proANPir at D30 and D90 after the initiation of S/V. The black and blue lines indicate when the full samples or samples with measured MR-proANPir <400 nmol/L were considered, respectively. Solid and dashed lines indicate the mean and mean±1.96 SDs of the difference, respectively. Variables in **A** were analyzed using repeated-measures ANOVA on log-transformed data followed by the Tukey honestly significant difference (HSD) test (blue). The number of subjects included in the analyses is indicated on each panel.

known as CD13 [cluster of differentiation 13]) resulted in the decrease in $proANP_{68-98}$ and the mirrored increase in $proANP_{79-98}$ (Figure 3D). Finally, to confirm the strict sequential cleavage of $proANP_{1-126}$, we incubated 250 nmol/L $proANP_{1-126}$ with human recombinant corin, meprin B, ECE1, and ANPEP (Figure 3E). In the presence of the 4 enzymes, ≈80% of $proANP_{1-126}$ was eventually processed into $proANP_{79-98}$, while the removal of any of the enzymes from the mix dramatically impaired its production. Altogether, these data indicate that $proANP_{1-126}$ is processed by the strict sequential action of corin, meprin B, ECE, and ANPEP, which may be dictated by secondary structure present in $proANP_{1-126}$. These data were used to generate a mathematical model of the proteolytic cascade (Figure S4).

S/V Increases $proANP_{1-126}$ Production and Its Further Processing by Corin and Meprin B

The increase in $proANP_{31-98}$ could result from either an increase in the production/processing of the upstream molecular species, that is, $proANP_{1-126}$ and $proANP_{1-98}$, or a decrease in $proANP_{31-98}$ processing. To address the former hypothesis, we first measured the plasma level of the proANP signal peptide ($proANP_{SP}$) as a surrogate for $proANP_{1-126}$ production, which was confirmed by plotting the kinetic of $proANP_{SP}$ a posteriori onto the input of the proteolytic cascade modeled mathematically (Figure 4A; Figure S5A). Plasma levels of $proANP_{SP}$ were higher in controls when compared with HFrEF patients at baseline and increased at D30 after the initiation of S/V (Figure 4A). Plasma levels of miR-425, which negatively regulates the *NPPA* transcript,[20,21] showed an inverse kinetic when compared with that of the $proANP_{SP}$ (Figure 4B), and the 2 parameters were strongly negatively correlated (Figure 4C). There was no change in either $proANP_{SP}$ or miR-425 until D14 (Figure S5B through S5E). The increase in $proANP_{SP}$ contrasted with the marked decrease in circulating $proANP_{1-126}$, suggesting that $proANP_{1-126}$ was also processed more efficiently. Accordingly, the mathematical model predicted a rapid increase in corin activity after the initiation of S/V (Figure 4D). The kinetic of the ANP/$proANP_{1-126}$ ratio fitted robustly a posteriori onto the model-derived corin activity and could be used as an estimate for corin activity (Figure 4D). At baseline, estimated corin activity was lower in HFrEF patients when compared with controls and increased after the initiation of S/V (Figure 4E). In agreement with this finding, the 4.7-fold difference in $proANP_{1-126}$ between HFrEF at baseline and healthy subjects contrasted with the moderate 1.3-fold increase in plasma ANP (Figure S5F), confirming that corin is limiting in HFrEF. As *CORIN* transcript is negatively regulated by miR-1-3p,[22] we measured plasma miR-1-3p (Figure 4F) and found a strong negative correlation between miR-1-3p and estimated corin activity (Figure 4G). Of note, the impact of S/V on estimated corin activity and miR-1-3p was observed as soon as D7 (Figure S5G and S5H). Next, we studied the processing of $proANP_{1-98}$ by meprin B. We found that $proANP_{1-30}$ plasma levels were lower in HFrEF patients at baseline when compared with controls and increased at D30 and D90 (Figure 4H), and the mathematical model predicted an increase in meprin B activity after initiation of S/V (Figure 4I). As the kinetic of the

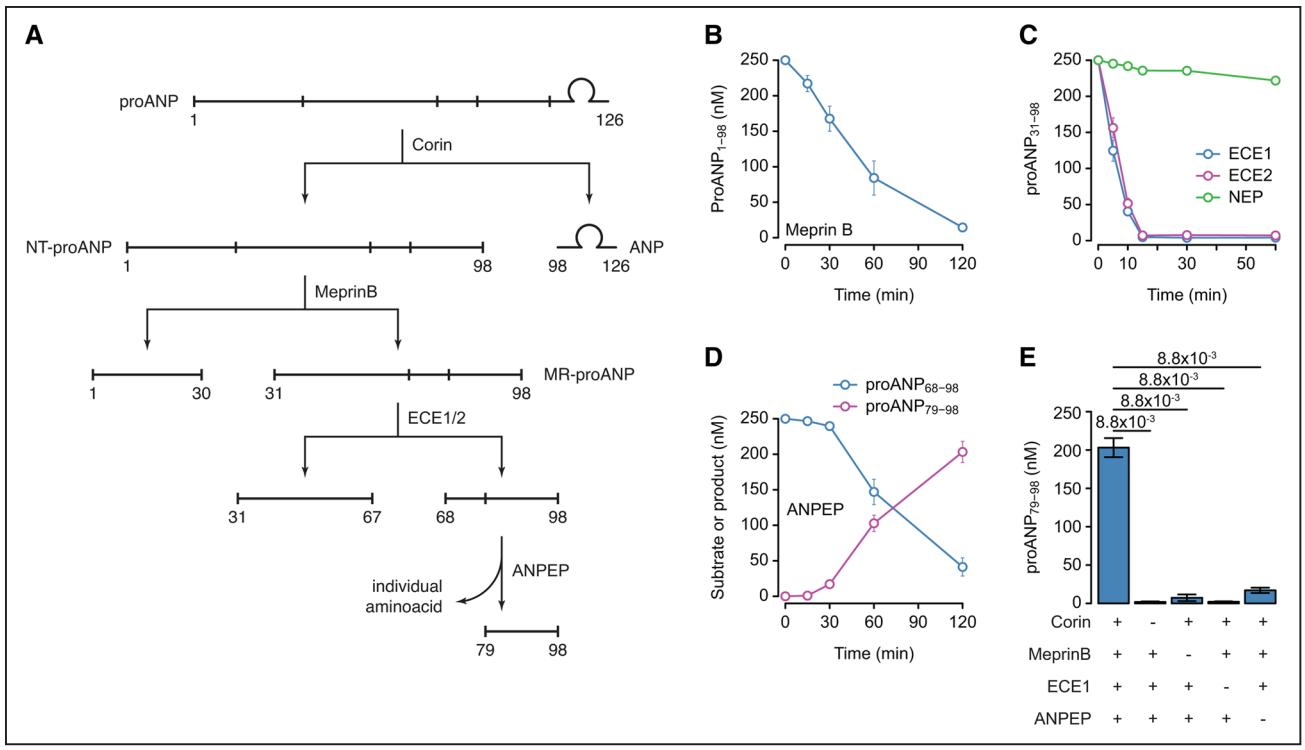

Figure 3. Characterization of the proANP proteolytic cascade.
A, Sequential proteolytic cascade of proANP$_{1-126}$ as deduced from the mass spectrometry data. **B**, Cleavage of synthetic proANP$_{1-98}$ by recombinant human meprin B in vitro. **C**, Cleavage of synthetic proANP$_{31-98}$ by recombinant human NEP (neprilysin), ECE (endothelin-converting enzyme) 1, and ECE2 in vitro. **D**, Cleavage of synthetic proANP$_{68-98}$ and appearance of the final product of the reaction proANP$_{79-98}$ by recombinant human ANPEP (aminopeptidase N) in vitro. **E**, Production of proANP$_{79-98}$, the end product of the proteolytic cascade, after incubating synthetic proANP$_{1-126}$ with human recombinant corin, meprin B, ECE1, and ANPEP in vitro. The same experiment was also performed removing 1 enzyme at the time. Variables in **B**–**E** are expressed as mean (n=5 for **B**–**D** and n=6 for **D**) and SD (whiskers). Variables in **E** were analyzed using the rank-sum Wilcoxon test corrected for multiple comparisons (holm). ANP indicates atrial natriuretic peptide; and NT-proANP, N-terminal proatrial natriuretic peptide.

proANP$_{1-30}$/proANP$_{1-98}$ ratio fitted robustly a posteriori onto the model-derived meprin B activity, it was used as an estimate for meprin B activity (Figure 4I). At baseline, estimated meprin B activity was found lower in HFrEF patients when compared with controls and increased after the initiation of S/V (Figure 4J). We also found a strong negative correlation between miR-1-3p and meprin B activity (Figure 4K), suggesting that the decrease in miR-1-3p could also be responsible for the increase in meprin B activity, although *MEP1B* is not a known miR-1-3p target. The impact of S/V on meprin B activity was also observed as soon as D7 (Figure S5I). While corin is expressed in cardiomyocytes,[8] little is known regarding meprin B expression. The strong positive correlation between corin and meprin B activities (Figure 4L) may indicate a cardiomyocyte origin for meprin B in this context. Altogether, these data indicate that HFrEF is characterized by a suboptimal production of ANP due to the posttranscriptional silencing of the *NPPA*, *CORIN*, and *MEP1B* transcripts by miR-425 and miR-1-3p, which is alleviated by S/V, resulting in an increase in bioactive ANP (Figure S5J). Overall, the increase in proANP$_{1-126}$ production and processing could be responsible for the increase in proANP$_{31-98}$.

S/V Prevents proANP$_{31-98}$ Processing by Inhibiting ECE-1

The increase in proANP$_{31-98}$ could also result from a decrease in its processing by ECE. Plasma levels of proANP$_{31-67}$ were lower in HFrEF patients at baseline when compared with controls and increased at D30 (Figure 5A); proANP$_{68-98}$ was short-lived and could only be detected in a few patients at D7. However, the difference in proANP$_{31-67}$ between baseline and D30 was smaller (6.0-folds [2.7–11.5]; Figure 5A) than that of proANP$_{1-30}$ (13.5-folds [8.7–17.1]; P=4.5×10^{-9}), suggesting that plasma ECE activity could be inhibited in vivo. As ECE2 could not be detected in the plasma, we, therefore, measured plasma ECE1 activity and concentration. ECE1 activity was markedly reduced at D30 (Figure 5B) and was mirrored by an increase in its concentration at D30 and D90 (Figure 5C). The impact of S/V on ECE1 activity and concentration was already observed at D7 (Figure S6A and S6B). ECE1 is primarily known for cleaving big-ET1 into ET1,[23] which is also an NEP substrate.[2] We, therefore, measured the plasma concentration of ET1 and big-ET1 and found that both were increased at D30 and D90 (Figure 5D

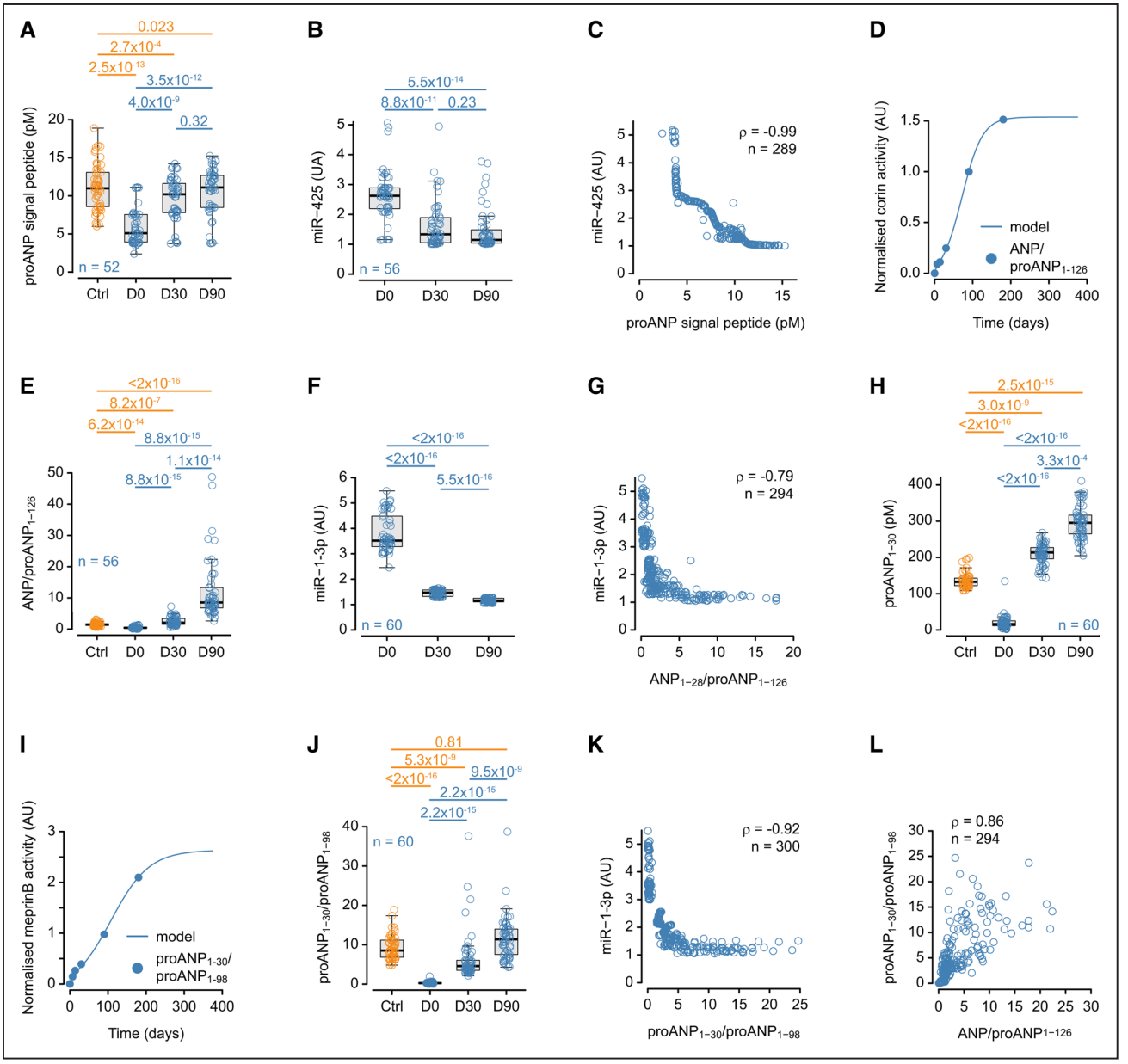

Figure 4. Impact of sacubitril/valsartan (S/V) on the proANP proteolytic cascade upstream of proANP$_{31-98}$.
A, Plasma levels of proANP signal peptide quantified by mass spectrometry (MS) in controls (Ctrl) and heart failure with reduced ejection fraction (HFrEF) patients at baseline (D0) and D30 and D90 after the initiation of S/V. **B**, Plasma levels of miR-425 at baseline and D30 and D90 after the initiation of S/V. **C**, Relationship between proANP signal peptide and miR-425. **D**, Kinetic evolution of corin activity predicted by the mathematical model (solid line). Points indicate the median values of the ANP (atrial natriuretic peptide)/proANP$_{1-126}$ ratio at each time point. The model and data values were normalized to one at D90 to fit within the same scale. **E**, Plasma levels of the ANP/proANP$_{1-126}$ ratio in controls and HFrEF patients at baseline and D30 and D90 after the initiation of S/V. **F**, Plasma levels of miR-1-3p at baseline and D30 and D90 after the initiation of S/V. **G**, Relationship between the ANP/proANP$_{1-126}$ ratio and plasma miR-1-3p levels. **H**, proANP$_{1-30}$ plasma levels quantified by MS in controls and HFrEF patients at baseline and D30 and D90 after the initiation of S/V. **I**, Kinetic evolution of meprin B activity predicted by the mathematical model (solid line). Points indicate the median values of the proANP$_{1-30}$/proANP$_{1-98}$ ratio at each time point. The model and data values were normalized to one at D90 to fit within the same scale. **J**, Plasma levels of the proANP$_{1-30}$/proANP$_{1-126}$ ratio in controls and HFrEF patients at baseline and D30 and D90 after the initiation of S/V. **K**, Relationship between the proANP$_{1-30}$/proANP$_{1-98}$ ratio and plasma miR-1-3p levels. **L**, Relationship between the ANP/proANP$_{1-126}$ and proANP$_{1-30}$/proANP$_{1-98}$ ratios as estimates of corin and meprin B activities. Variables in **A**, **B**, **F**–**H**, and **J** were analyzed using repeated-measures ANOVA on log-transformed data followed by the Tukey honestly significant difference (HSD) test (blue) or using the Wilcoxon rank-sum test corrected for multiple comparisons (holm, orange). Correlations between variables were estimated with Spearman rank correlation and expressed by the correlation coefficient (ρ). The number of subjects included in the analyses is indicated on each panel. In **G**, **K**, and **L**, samples at baseline, D7, D14, D30, and D90 were considered. In **D** and **I**, samples at baseline, D7, D14, D30, D90, and D180 were considered. The number of controls was 54.

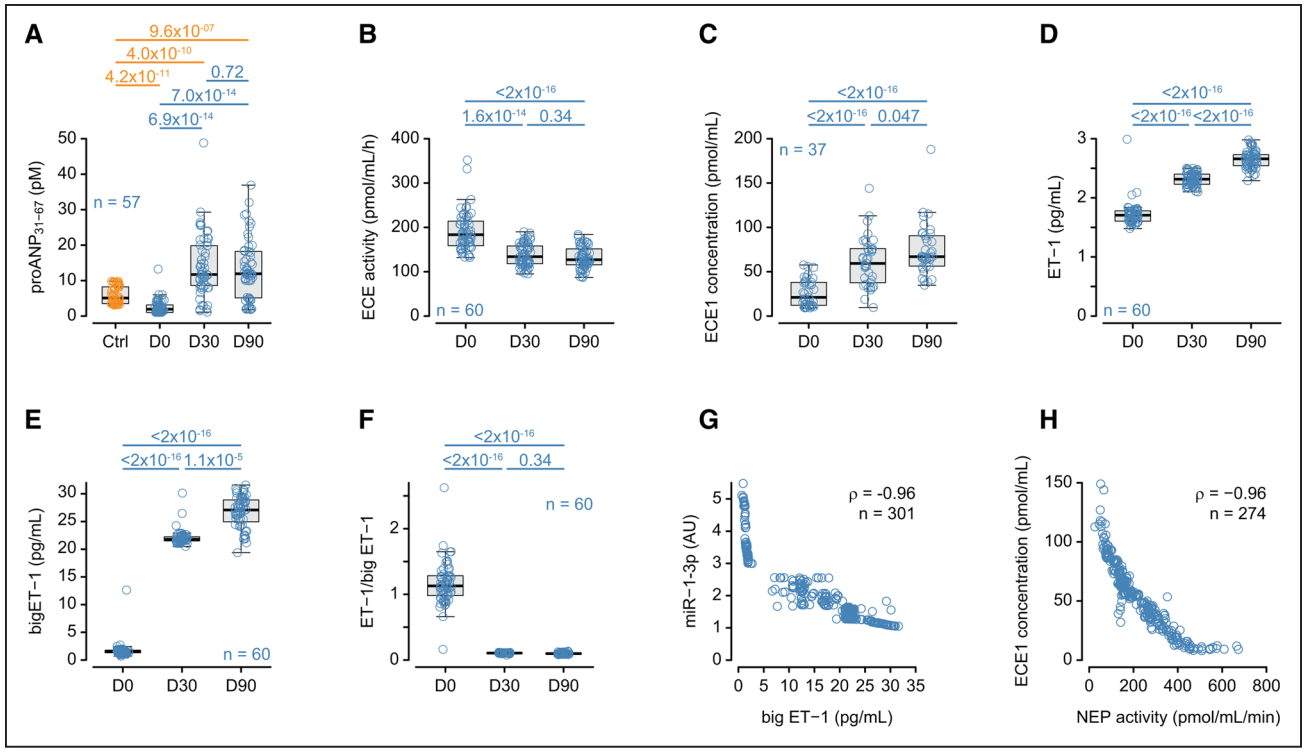

Figure 5. Impact of sacubitril/valsartan (S/V) on the proANP proteolytic cascade downstream of proANP$_{31-98}$.
A, proANP$_{31-67}$ plasma levels quantified by mass spectrometry in controls (Ctrl) and heart failure with reduced ejection fraction patients at baseline (D0) and D30 and D90 after the initiation of S/V. B, Plasma ECE (endothelin-converting enzyme) activity at baseline and D30 and D90 after the initiation of S/V. **C**, Plasma ECE1 concentration at baseline and D30 and D90 after the initiation of S/V. **D**, Plasma concentration of ET1 (endothelin 1) at baseline and D30 and D90 after the initiation of S/V. **E**, Plasma concentration of big-ET1 at baseline and D30 and D90 after the initiation of S/V. **F**, ET1/big-ET1 ratio at baseline and D30 and D90 after the initiation of S/V. **G**, Relationship between big-ET1 and plasma miR-1-3p levels. **H**, Relationship between plasma ECE1 concentration and NEP (neprilysin) activity. Variables in **A**–**F** were analyzed using repeated-measures ANOVA on log-transformed data followed by the Tukey honestly significant difference (HSD) test (blue) or using the Wilcoxon rank-sum test corrected for multiple comparisons (holm, orange). Correlations between variables were estimated with Spearman rank correlation and expressed by the correlation coefficient (ρ). The number of subjects included in the analyses is indicated on each panel. In **G** and **H**, samples at baseline, D7, D14, D30, and D90 were considered. The number of healthy subjects was 54.

and 5E), although big-ET1 increased far more between baseline and D30 (14.2-folds [12.6–16.4]) than ET1 (1.4-folds [1.3–1.5]; P=3.6×10^{-13}). Consequently, the ET1/big-ET1 ratio decreased (Figure 5F), indicating that big-ET1 was less cleaved into ET1 in vivo. ET1, big-ET1, and the ET1/big-ET1 ratio were modified as soon as D7 (Figure S6C through S6E). Besides regulating *CORIN*, miR-1-3p also regulates the big-ET1 encoding gene (*EDN1*),[24,25] and miR-1-3p and big-ET1 were strongly negatively correlated (Figure 5G). Of note, miR-1-3p plasma levels were also strongly negatively correlated to those of SP but less so to those of other NEP substrates we measured such as adrenomedullin, GLP-1 (glucagon-like peptide-1), or apelin-12 (Figure S6F through S6I). There was also a strong negative correlation between the NEP activity as a surrogate for sacubitril pharmacological action and ECE1 concentration (Figure 5H). Since ECE1 can be coreleased with big-ET1 and ET1,[26] this association suggests that the direct inhibition of ECE1 by sacubitril resulted in an increase in the secretion of big-ET1/ET1 to compensate for the high vasodilatory response. This mechanism of compensation extends to miR1-3p, whose reduction allows for a rapid increase in big-ET1 production. Altogether, these data suggest that the accumulation of proANP$_{31-98}$ also resulted from a decreased processing due to the partial inhibition of ECE1 by sacubitril.

S/V Directly and Indirectly Inhibits ANPEP

ANPEP, which sequentially cleaves proANP$_{68-98}$ into proANP$_{79-98}$, was previously found to be inhibited by sacubitril in vitro.[19] proANP$_{79-98}$ was lower in HFrEF patients at baseline when compared with controls and increased at D30 (Figure 6A). The amplitude of proANP$_{79-98}$ increase between D0 and D30 (6.1-folds [3.1–10.9]) was lower than that of proANP$_{1-30}$ (P=3.5×10^{-7}; Figure 6A). Plasma ANPEP activity decreased at D30 and D90 (Figure 6B) with no change in ANPEP concentration (Figure 6C). Since ANPEP can also be inhibited by endogenous SP,[27] which is increased after the initiation of S/V,[3] we tested the relationship between plasma ANPEP activity and SP concentration (Figure 6D). At D30 and D90, SP >55 pg/mL could be responsible for the decrease in ANPEP activity, which was confirmed in vitro (Figure 6E). However, there was already a decrease

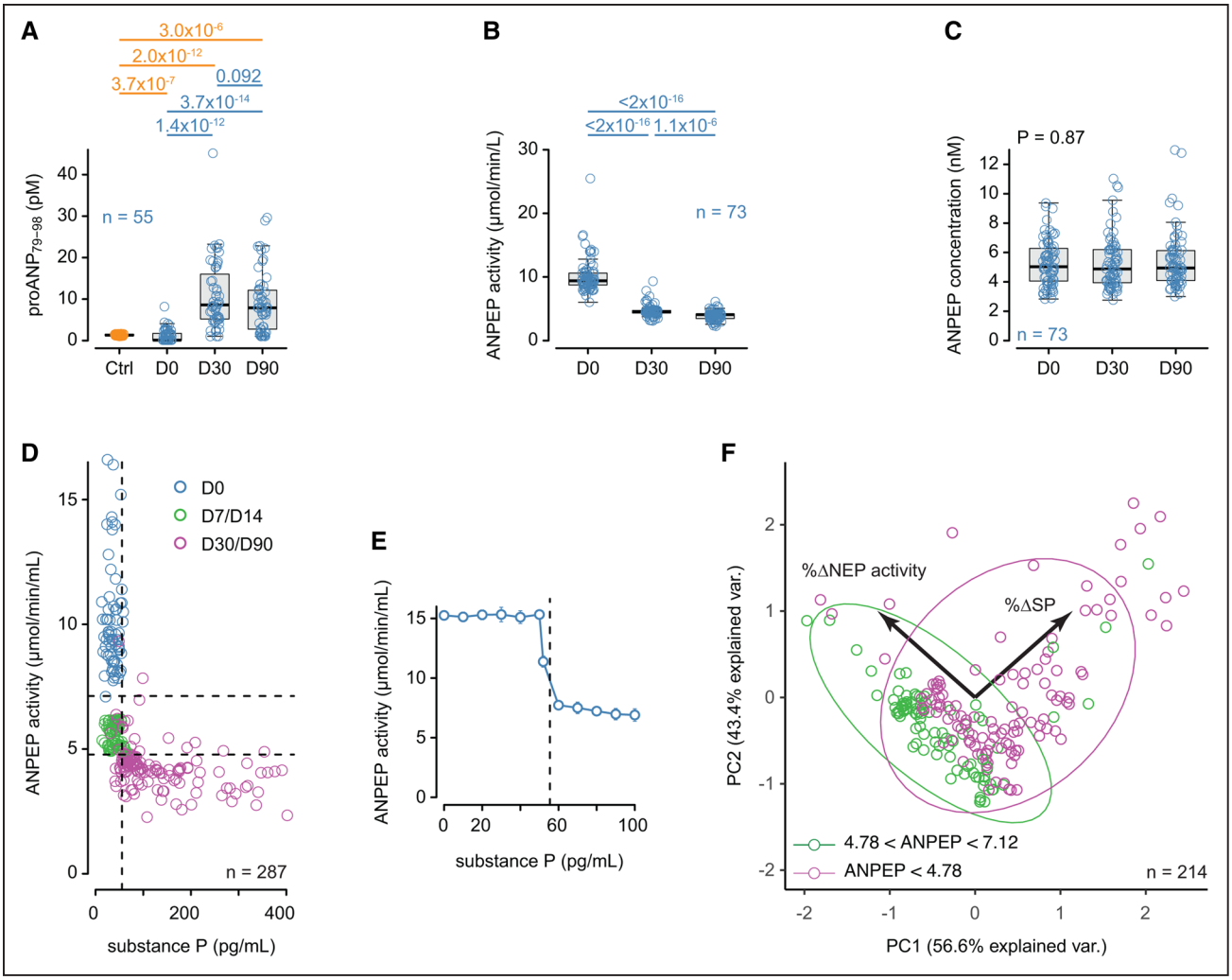

Figure 6. Impact of sacubitril/valsartan (S/V) on proANP$_{79-98}$ production.
A, proANP$_{79-98}$ plasma levels quantified by mass spectrometry in controls (Ctrl) and heart failure with reduced ejection fraction patients at baseline (D0) and D30 and D90 after the initiation of S/V. **B**, Plasma ANPEP (aminopeptidase N) activity at baseline and D30 and D90 after the initiation of S/V. **C**, Plasma ANPEP concentration at baseline and D30 and D90 after the initiation of S/V. **D**, Relationship between plasma ANPEP activity and substance P. **E**, Human recombinant ANPEP activity after incubation with increasing concentration of human synthetic substance P in vitro. **F**, Principal component (PC) analysis using ANPEP cutoffs as classifiers and the relative variation (%Δ) of NEP (neprilysin) between D7, D14, D30, or D90 and baseline of NEP activity and plasma SP (substance P) as predictors. Variables in **A**–**C** were analyzed using repeated-measures ANOVA on log-transformed data followed by the Tukey honestly significant difference (HSD) test (blue) or using the Wilcoxon rank-sum test corrected for multiple comparisons (holm, orange). Correlations between variables were estimated with the Spearman coefficient (ρ). The number of subjects included in the analyses is indicated on each panel. Variables in **E** are expressed as mean (n=4) and SD (whiskers). In **D** and **F**, samples at baseline, D7, D14, D30, and D90 were considered. The number of healthy subjects was 54.

in ANPEP activity at D7 and D14 while SP was unchanged (Figure S7), suggesting a possible bimodal inhibition of ANPEP by sacubitril and SP. Principal component analysis using thresholds of ANPEP activity as classifiers and SP plasma concentrations and variations of NEP activity as a surrogate for the pharmacological impact of sacubitril as predictors showed that at D7 and D14, the decrease in ANPEP activity was predominantly driven by sacubitril, while there was a clear effect of SP at D30 and D90 (Figure 6F). Altogether, these data indicate in vivo that ANPEP is a sacubitril off target and is also inhibited by ricochet by the increase in SP, which directly results from NEP inhibition.

Specificity of S/V

To test the specificity of S/V over the uptitration of Valsartan, we first estimated a dose equivalence to Valsartan for all patients treated with the ACE inhibitor at baseline (10 mg ramipril daily=320 mg valsartan daily) and for patients treated with S/V[6] at D30 (97 mg/103 mg S/V BID=320 mg valsartan daily). Patients were split into 2 groups based on Valsartan dose equivalence uptitration between baseline and D30. Comparison of the variations between baseline and D30 of all the parameters studied show that all but proANP$_{SP}$ were similar in the 2 groups. This result suggests that most of the effects observed are specific to S/V rather than the uptitration of Valsartan alone (Table).

Table. Comparisons of the Variations in Percentage of the Studied Parameters Between Baseline and D30 in Patients for Whom Valsartan-Equivalent Dose was Uptitrated or Not Between Baseline and D30

Variable	No uptitration	Uptitration	*P* value
$proANP_{SP}$	59 [−0.3 to 97.3] (n=36)	101.1 [54.4 to 146.6] (n=24)	0.04
$proANP_{1-126}$	−27.9 [−37.7 to −11.4] (n=43)	−35 [−48.4 to −23.3] (n=25)	0.11
ANP	330.8 [196.6 to 557.3] (n=40)	237.4 [87.4 to 542.8] (n=24)	0.43
$proANP_{1-98}$	−42 [−57 to −22.6] (n=43)	−37.1 [−46.7 to −3.3] (n=25)	0.11
$proANP_{1-30}$	1254.2 [773.1 to 1898.6] (n=43)	1278 [694.1 to 1536.4] (n=25)	0.92
$proANP_{31-98}$	1209.7 [776.3 to 2165.7] (n=43)	1440.7 [757.5 to 2103.3] (n=25)	0.58
$proANP_{31-67}$	481.8 [111.4 to 1070] (n=40)	620.8 [296.7 to 1030] (n=25)	0.66
$proANP_{79-98}$	632 [168.1 to 1134.1] (n=39)	473 [277.6 to 733.8] (n=24)	0.57
$proANP_{31-98}$ S80 glyc	525 [0 to 1525] (n=36)	446.4 [5.4 to 1225] (n=22)	0.63
big-ET1	1339.6 [1118.3 to 1564.4] (n=43)	1300 [1180.2 to 1496.4] (n=26)	0.82
ET1	40.4 [28.2 to 46.5] (n=43)	35.4 [26 to 39.3] (n=26)	0.37
miR-425	−39 [−53.3 to 1.8] (n=40)	−47 [−59.7 to −22.3] (n=24)	0.42
miR1-3p	−60.9 [−67.4 to −55.6] (n=43)	−58.5 [−67.8 to −54.9] (n=26)	0.71
ECE1 concentration	150.2 [40.5 to 291.4] (n=30)	255.4 [111 to 434.3] (n=13)	0.26
ECE1 activity	−23.1 [−36.5 to −13.5] (n=43)	−30.8 [−43.8 to −21.7] (n=25)	0.18
ANPEP concentration	−4.3 [−26.6 to 22.2] (n=44)	−10.1 [−27.4–17.9] (n=28)	0.54
ANPEP activity	−51.9 [−60.6 to −45.9] (n=44)	−50 [−55.8 to −48.5] (n=28)	0.61
$ANP/proANP_{1-126}$	478.4 [288 to 773.7] (n=40)	443.3 [159 to 1385.1] (n=24)	0.98
$proANP_{1-30}/proANP_{1-98}$	2126.8 [1317.1 to 5145.3] (n=43)	1462.4 [1093.8 to 2122.1] (n=25)	0.19

The number of patients per group is indicated in brackets. ANP indicates atrial natriuretic peptide; ANPEP, aminopeptidase N; ECE, endothelin-converting enzyme; ET1, endothelin 1; and S80 glyc, serine 80 glycosylation.

DISCUSSION

In this study, we identified the sequence of proteolytic events that produce $proANP_{79-98}$ from $proANP_{1-126}$. The results showed that S/V impacted the metabolism of proANP at multiple steps, via direct and indirect effects (Figure 7; Figure S8), providing new insights on the increase in ANP observed in patients treated with S/V and on the mechanism of action of S/V, along with bringing pathophysiological perspectives on HFrEF. Finally, our results also suggest that S/V not only has a direct impact on some of the NEP targets but also increases their plasma levels indirectly, possibly allowing for a more sustained response.

First, we identified the 3 enzymes that cleave $proANP_{1-98}$ into 3 bioactive peptides. To date, only corin was identified as involved in the cleavage of ANP and $proANP_{1-98}$ from $proANP_{1-126}$. Together with the measurement of all possible cleavage products, we found that $proANP_{1-126}$ is cleaved according to a precise sequence of proteolytic cleavages. Such sequential processing is unexpected as it involves 4 endopeptidases, but secondary structures present in $proANP_{1-126}$ could dictate this sequence. Such a secondary structure–driven sequence may also apply to other hormone precursors, whose cleavage is sequential despite being processed by similar enzymes like pro-opiomelanocortin.[28]

Our data also confirmed that stable chronic HFrEF is an ANP suboptimal state, as previously suggested for BNP.[29] In HFrEF, ANP production is curtailed by a reduced proANP production and cleavage by corin, when compared with healthy subjects. Both these mechanisms consequently limit the production of $proANP_{1-98}$ produced and together with a decrease in meprin B activity limit the production of the 3 bioactive peptides that originate from the cleavage of $proANP_{1-98}$ when compared with healthy subjects. Overall, in HFrEF, the upper part of the proANP metabolic cascade ($proANP_{1-126}$, ANP, $proANP_{1-98}$, $proANP_{1-30}$, and $proANP_{31-98}$) appears hampered by reduced proANP production, corin, and meprin B activities, while the lower part ($proANP_{31-67}$ and $proANP_{79-98}$) appears limited by the reduced amount of $proANP_{31-98}$ available. Of note, a decrease in corin has already been observed in acute decompensated HF[30] and animal model of dilated cardiomyopathy,[31] which may suggest a common trend toward a suboptimal proANP metabolism across HF, independently of any medication. After initiation of S/V treatment, our data strongly suggest a triple mechanism whereby ANP increased: (1) increase in $proANP_{1-126}$ production, (2) increase in corin activity, and (3) protection from NEP degradation. This increase in ANP is likely to be biologically relevant as cGMP plasma concentration paralleled that of ANP in the Prospective Study of Biomarkers, Symptom Improvement, and Ventricular Remodeling During Sacubitril/Valsartan Therapy for Heart Failure (PROVE-HF) study,[32] and in vitro cGMP production increased when HEK293 (human embryonic kidney) cells expressing NPRA (natriuretic peptide receptor A) were incubated with the plasma of these patients at D30. Furthermore, it

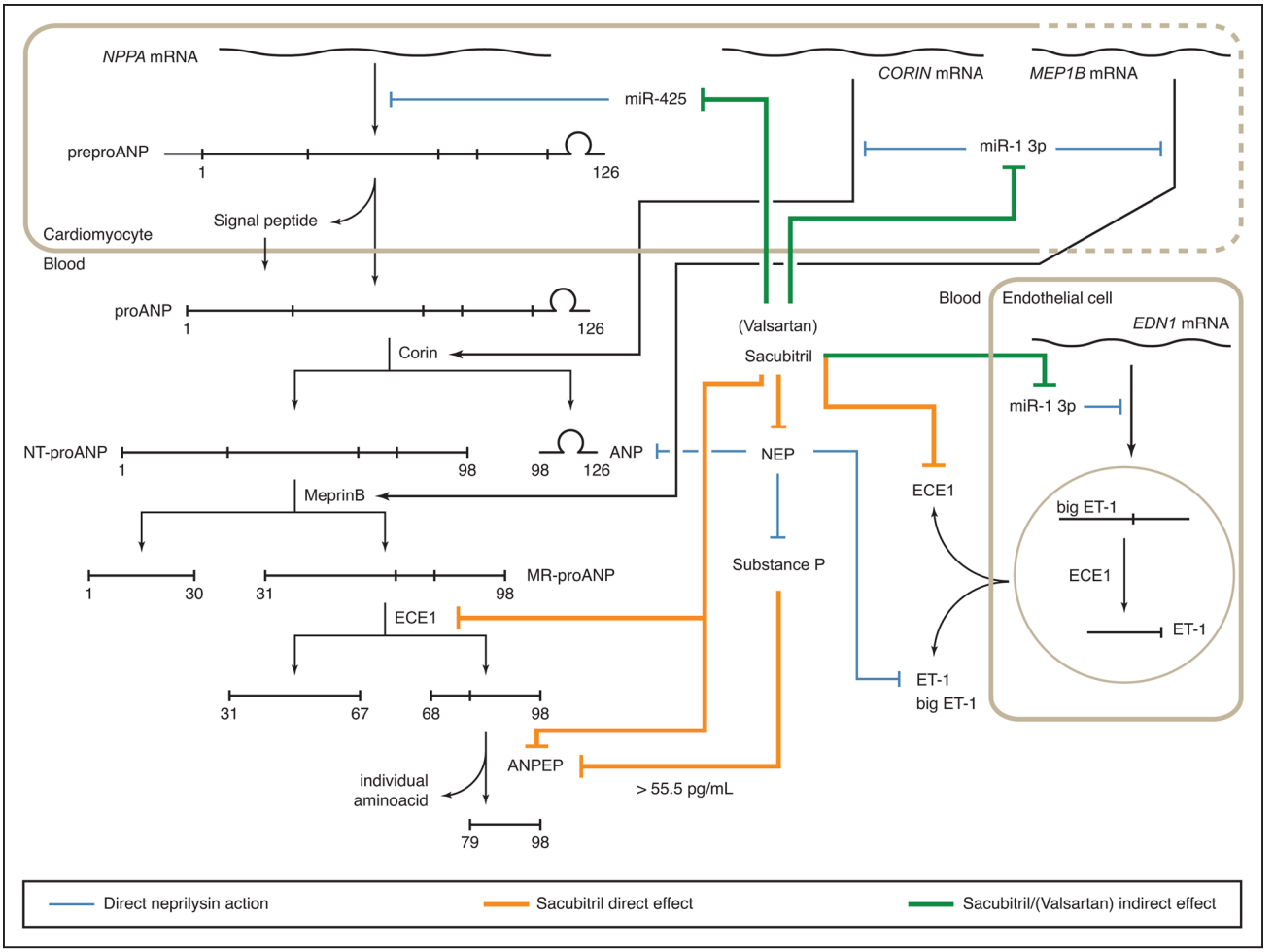

Figure 7. Schematic representation of the effect of sacubitril/valsartan (S/V) on the proANP proteolytic cascade.
Represented as a dashed line is the possible action of miR-1 3p on *MEP1B* in cardiomyocytes. Shown in blue is NEP (neprilysin)-related proteolysis, in orange are direct sacubitril effects, and in green are sacubitril or S/V indirect effects. ANPEP indicates aminopeptidase N; ECE, endothelin-converting enzyme; ET1, endothelin 1; MR-proANP, midregional proANP; and NT-proANP, N-terminal proatrial natriuretic peptide.

has been shown recently that reverse cardiac remodeling in patients treated with S/V was associated with an early and important increase in ANP.[32] The increase in corin and meprin B activity also resulted in an increase in the 3 biologically active peptides originating from proANP$_{1\text{-}98}$, although the increase in proANP$_{31\text{-}67}$ and proANP$_{79\text{-}98}$ was limited by the partial ECE-1 inhibition. The increase in the plasma levels of those peptides is likely to be biologically relevant as their administration in stable chronic HF patients resulted in increased vasodilation, renal filtration, diuresis, and natriuresis.[33,34] In particular, the increase in the kaliuric proANP$_{79\text{-}98}$ may explain the reduced number of hyperkalemia events in patients receiving S/V when compared with those receiving either the ACE inhibitor[1] or angiotensin receptor blocker.[35] Finally, the increase in the vasodilatory ANP, proANP$_{1\text{-}30}$, and proANP$_{31\text{-}67}$ as opposed to the limited increase in ET-1 production could be involved in the hypotensive effects of S/V observed in HF and healthy subjects.[1,6,32,33] Overall, S/V provoked a marked increase in the production of the 4 bioactive peptides that derive from proANP$_{1\text{-}126}$, to reach plasma levels much higher than in controls. It remains to be established whether the changes observed correspond to a restoration of an effective metabolism or a compensatory mechanism.

The impact of S/V on proANP metabolism involves indirect effects via the downregulation of 2 miRNAs. First, miR-425 regulates negatively the translation of the *NPPA* mRNA and was previously found to be positively regulated by NF-κB (nuclear factor kappa B) after glucose challenge in cardiomyocytes in vitro and in human.[20,21,34] Therefore, the decrease in miR-425 expression may reflect an overall better glucose management,[3,4] which would limit cardiomyocyte exposure to glucose or a decrease in cardiomyocyte inflammation, although we cannot exclude a mechanism whereby S/V downregulated miR-425 expression independently of these stressors. It remains to be determined whether miR-425 also mediates other effects of S/V as we did not find any association with any other NEP substrates that we measured. Second, miR-1-3p was found strongly negatively associated with the increase in corin and meprin B—2 enzymes that were limiting at baseline. miR-1-3p

appears to be a broader mediator of S/V effects since its decrease was also found strongly negatively associated with higher plasma levels of big-ET1 and SP. Whether the rapid and consistent decrease in miR-1-3p plasma levels reveals a corrective action of S/V on remodeling pathways or involves a compensatory mechanism remains to be determined. Overall, S/V decreased the expression of 2 miRNAs, which, in part, regulate the expression of NEP targets, providing a possible amplification of sacubitril effects. The extent of these miRNA-mediated effects is likely underestimated as miR-425 and miR-1-3p have other demonstrated and predicted targets.

From a pharmacological standpoint, we confirmed in vivo previous in vitro data[19] that sacubitril is also a partial ECE-1 and ANPEP inhibitor. Therefore, sacubitril is no exception to other NEP inhibitors, which show some lack of selectivity in vitro toward other metalloproteases.[19] Interestingly, the partial inhibitory effect of ANPEP was bimodal, resulting from the direct inhibition by sacubitril and the indirect inhibition by SP accumulation over 55 pg/mL. As NEP is involved in the degradation of >40 peptides that can also be cleaved by other proteases, the stabilization of NEP targets could also modify the activity of these proteases by modifying the relative abundance of their targets. While ECE1 partial inhibition had a direct impact on ET1 production and the cleavage of pro-ANP_{31-98}, the impact of the partial inhibition of ANPEP is less clear. Indeed, since intermediary products between $proANP_{68-98}$ and $proANP_{79-98}$ were only detected in a limited number of patients, predominantly at D7, the decrease in $proANP_{79-98}$ is likely to be associated with a decrease in $proANP_{68-98}$ rather than a decrease in pro-ANP_{68-98} cleavage. Another well-described ANPEP substrate is Ang_{1-7}, which can result from the cleavage of Ang I by NEP,[36] the cleavage of Ang_{1-9} by ACE, or the cleavage of Ang II (angiotensin II) by ACE2.[37] While NEP inhibition by sacubitril will inhibit the former, the latter is anticipated to be enhanced due to the overproduction of Ang II associated with sacubitril.[38] However, Ang_{1-7} was not detected in the plasma of patients treated with S/V.[38] The systemic impact of the partial inhibition of ANPEP by S/V remains to be established, although the dual NEP/ANPEP inhibition could qualify S/V as a dual enkephalinase inhibitor for the management of chronic pain.[39]

From a biomarker standpoint, our data indicate that glycosylation at S80 interferes with MR-proANPir measurements, and the changes in MR-proANPir observed in patients treated with S/V[7] resulted from an analytical interference. Importantly, the kinetic of proANP glycosylation at S80 paralleled that of proBNP glycosylation at T71 in the same patients.[3] Since the level of proBNP T71 glycosylation differs in acute[40] and chronic HF, one can anticipate similar variations in proANP glycosylation at S80 according to the clinical context. Furthermore, the contribution of the molecular species that constitute MR-proANPir was different in controls and HFrEF patients, and one can also anticipate differences according to the clinical context. While the diagnostic and prognostic values of MR-proANPir are not affected per se by these findings, one may be cautious of erroneous biological interpretations. Finally, our results may help the development of more precise and clinically relevant assays to follow patients with HF in the angiotensin receptor NEP inhibitor era.

Our study has some limitations that need to be acknowledged. First, the study population is rather small and not randomized, which may limit the statistical performances. Nevertheless, we could show robust, consistent, and highly significant changes in several biomarkers across the overall cohort. The use of healthy subjects as comparators only allowed the comparison with stable and fully medicated HFrEF patients, partly limiting pathophysiological interpretation. However, comparable HFrEF patients not receiving any relevant medication were not available. Second, the early clinical effects (first dose) were not assessed. Third, the uptitration of S/V was left at the discretion of the cardiologist according to the tolerance and patient clinical status, and, therefore, it is not possible to precisely assess the relationship between dose and time. Finally, the open design and the lack of a control arm may have affected the assessment of the clinical response even though the study is longitudinal.

In conclusion, the analysis of proANP processing clearly indicates that HFrEF is a natriuretic suboptimal state that is corrected or compensated by S/V treatment via direct and indirect mechanisms. These results provide new insights into the mechanism/mode of action of S/V involving both ECE-1 and ANPEP inhibition, which could participate in the hypotensive effects of this drug, although other mechanisms are most likely at play. This study also illustrates the limitation of the biological interpretation of MR-proANPir that could also be considered for other biomarkers.

ARTICLE INFORMATION

Received February 2, 2022; revision received April 6, 2022; accepted April 21, 2022.

Affiliations

Université Paris Cité and Inserm UMR-S 932, France (T.M., H.N., J.C., M.S., A.C.-S., D.L., J.-M.L., N.V.). Department of Anaesthesiology and Intensive Care Unit, Hôpital Lariboisière, Paris, France (H.N., J.C.). AP-HP, Hôpital Tenon, Biochemistry Department, Sorbonne Université, Paris, France (G.L.). Heart Failure Unit, Haut-Lévêque Hospital, Pessac, France (F.P.). Department of Cardiology, Lariboisière Hospital, Paris, France (A.C.-S., D.L.).

Acknowledgments

We thank the nurses from the Department of Cardiology of the Haut-Lévêque Hospital and Lariboisière Hospitals. We are grateful to Karine Coutant for advice regarding enzymatic studies. T. Michel, H. Nougué, J. Cartailler, M. Sadoune, A. Cohen-Solal, D. Logeart, J.-M. Launay, and N. Vodovar are members of the Institut des Sciences Cardiovasculaires de l'Université Paris Cité.

Sources of Funding

This work was supported by Inserm, Université Paris Cité, and a grant from the Fédération Française de Cardiologie.

Disclosures

Dr Picard received honorarium and nonfinancial support from Novartis, outside the scope of this study. Dr Cohen-Solal received grants, honorarium, and nonfinancial support from Novartis, Servier, Vifor, and MSD, outside the scope of this study. Dr Logeart had received consulting and conference fees for AstraZeneca, Bayer, Boehringer Ingelheim, Novartis, and Vifor, outside the scope of this study. Dr Vodovar has received speaker fees from Roche Diagnostics, Abbott, and Siemens, outside the scope of this study. The other authors report no conflicts.

Supplemental Material

Supplemental Materials & Methods
Tables S1–S5
Figures S1–S9
Major Resources Table
References 41–54

REFERENCES

1. McMurray JJ, Packer M, Desai AS, Gong J, Lefkowitz MP, Rizkala AR, Rouleau JL, Shi VC, Solomon SD, Swedberg K, Zile MR; PARADIGM-HF Investigators and Committees. Angiotensin-neprilysin inhibition versus enalapril in heart failure. *N Engl J Med.* 2014;371:993–1004. doi: 10.1056/NEJMoa1409077
2. Campbell DJ. Long-term neprilysin inhibition - implications for ARNIs. *Nat Rev Cardiol.* 2017;14:171–186. doi: 10.1038/nrcardio.2016.200
3. Nougué H, Pezel T, Picard F, Sadoune M, Arrigo M, Beauvais F, Launay JM, Cohen-Solal A, Vodovar N, Logeart D. Effects of sacubitril/valsartan on neprilysin targets and the metabolism of natriuretic peptides in chronic heart failure: a mechanistic clinical study. *Eur J Heart Fail.* 2019;21:598–605. doi: 10.1002/ejhf.1342
4. Seferovic JP, Claggett B, Seidelmann SB, Seely EW, Packer M, Zile MR, Rouleau JL, Swedberg K, Lefkowitz M, Shi VC, et al. Effect of sacubitril/valsartan versus enalapril on glycaemic control in patients with heart failure and diabetes: a post-hoc analysis from the PARADIGM-HF trial. *Lancet Diabetes Endocrinol.* 2017;5:333–340. doi: 10.1016/S2213-8587(17)30087-6
5. Kenny AJ, Bourne A, Ingram J. Hydrolysis of human and pig brain natriuretic peptides, urodilatin, C-type natriuretic peptide and some C-receptor ligands by endopeptidase-24.11. *Biochem J.* 1993;291(pt 1):83–88. doi: 10.1042/bj2910083
6. Gu J, Noe A, Chandra P, Al-Fayoumi S, Ligueros-Saylan M, Sarangapani R, Maahs S, Ksander G, Rigel DF, Jeng AY, et al. Pharmacokinetics and pharmacodynamics of LCZ696, a novel dual-acting angiotensin receptor-neprilysin inhibitor (ARNi). *J Clin Pharmacol.* 2010;50:401–414. doi: 10.1177/0091270009343932
7. Ibrahim NE, McCarthy CP, Shrestha S, Gaggin HK, Mukai R, Szymonifka J, Apple FS, Burnett JC Jr, Iyer S, Januzzi JL Jr. Effect of neprilysin inhibition on various natriuretic peptide assays. *J Am Coll Cardiol.* 2019;73:1273–1284. doi: 10.1016/j.jacc.2018.12.063
8. Yan W, Wu F, Morser J, Wu Q. Corin, a transmembrane cardiac serine protease, acts as a pro-atrial natriuretic peptide-converting enzyme. *Proc Natl Acad Sci USA.* 2000;97:8525–8529. doi: 10.1073/pnas.150149097
9. Gladysheva IP, Robinson BR, Houng AK, Kováts T, King SM. Corin is co-expressed with pro-ANP and localized on the cardiomyocyte surface in both zymogen and catalytically active forms. *J Mol Cell Cardiol.* 2008;44:131–142. doi: 10.1016/j.yjmcc.2007.10.002
10. Vesely DL. Atrial natriuretic hormones originating from the N-terminus of the atrial natriuretic factor prohormone. *Clin Exp Pharmacol Physiol.* 1995;22:108–114. doi: 10.1111/j.1440-1681.1995.tb01965.x
11. Dietz JR, Scott DY, Landon CS, Nazian SJ. Evidence supporting a physiological role for proANP-(1-30) in the regulation of renal excretion. *Am J Physiol Regul Integr Comp Physiol.* 2001;280:R1510–R1517. doi: 10.1152/ajpregu.2001.280.5.R1510
12. Gunning ME, Brady HR, Otuechere G, Brenner BM, Zeidel ML. Atrial natriuretic peptide(31-67) inhibits Na+ transport in rabbit inner medullary collecting duct cells. Role of prostaglandin E2. *J Clin Invest.* 1992;89:1411–1417. doi: 10.1172/JCI115730
13. Morgenthaler NG, Struck J, Thomas B, Bergmann A. Immunoluminometric assay for the midregion of pro-atrial natriuretic peptide in human plasma. *Clin Chem.* 2004;50:234–236. doi: 10.1373/clinchem.2003.021204
14. Maisel A, Mueller C, Nowak R, Peacock WF, Landsberg JW, Ponikowski P, Mockel M, Hogan C, Wu AH, Richards M, et al. Mid-region pro-hormone markers for diagnosis and prognosis in acute dyspnea: results from the BACH (Biomarkers in Acute Heart Failure) trial. *J Am Coll Cardiol.* 2010;55:2062–2076. doi: 10.1016/j.jacc.2010.02.025
15. Ponikowski P, Voors AA, Anker SD, Bueno H, Cleland JGF, Coats AJS, Falk V, González-Juanatey JR, Harjola VP, Jankowska EA, et al; ESC Scientific Document Group. 2016 ESC guidelines for the diagnosis and treatment of acute and chronic heart failure: the task force for the diagnosis and treatment of acute and chronic heart failure of the European Society of Cardiology (ESC)developed with the special contribution of the Heart Failure Association (HFA) of the ESC. *Eur Heart J.* 2016;37:2129–2200. doi: 10.1093/eurheartj/ehw128
16. Hunter I, Alehagen U, Dahlström U, Rehfeld JF, Crimmins DL, Goetze JP. N-terminal pro-atrial natriuretic peptide measurement in plasma suggests covalent modification. *Clin Chem.* 2011;57:1327–1330. doi: 10.1373/clinchem.2011.166330
17. Hansen LH, Madsen TD, Goth CK, Clausen H, Chen Y, Dzhoyashvili N, Iyer SR, Sangaralingham SJ, Burnett JC Jr, Rehfeld JF, et al. Discovery of O-glycans on Atrial Natriuretic Peptide (ANP) that affect both its proteolytic degradation and potency at its cognate receptor. *J Biol Chem.* 2019;294:12567–12578. doi: 10.1074/jbc.RA119.008102
18. Rawlings ND, Barrett AJ, Thomas PD, Huang X, Bateman A, Finn RD. The MEROPS database of proteolytic enzymes, their substrates and inhibitors in 2017 and a comparison with peptidases in the PANTHER database. *Nucleic Acids Res.* 2018;46(D1):D624–D632. doi: 10.1093/nar/gkx1134
19. Griggs DW, Prinsen MJ, Oliva J, Campbell MA, Arnett SD, Tajfirouz D, Ruminski PG, Yu Y, Bond BR, Ji Y, et al. Pharmacologic comparison of clinical neutral endopeptidase inhibitors in a rat model of acute secretory diarrhea. *J Pharmacol Exp Ther.* 2016;357:423–431. doi: 10.1124/jpet.115.231167
20. Arora P, Wu C, Hamid T, Arora G, Agha O, Allen K, Tainsh RET, Hu D, Ryan RA, Domian IJ, et al.Acute metabolic influences on the natriuretic peptide system in humans. *J Am Coll Cardiol.* 2016;67:804–812. doi: 10.1016/j.jacc.2015.11.049
21. Arora P, Wu C, Khan AM, Bloch DB, Davis-Dusenbery BN, Ghorbani A, Spagnolli E, Martinez A, Ryan A, Tainsh LT, et al. Atrial natriuretic peptide is negatively regulated by microRNA-425. *J Clin Invest.* 2013;123:3378–3382. doi: 10.1172/JCI67383
22. Celik S, Karbalaei-Sadegh M, Rådegran G, Smith JG, Gidlöf O. Functional screening identifies microRNA regulators of corin activity and atrial natriuretic peptide biogenesis. *Mol Cell Biol.* 2019;39:e00271–e00219. doi: 10.1128/MCB.00271-19
23. Xu D, Emoto N, Giaid A, Slaughter C, Kaw S, deWit D, Yanagisawa M. ECE-1: a membrane-bound metalloprotease that catalyzes the proteolytic activation of big endothelin-1. *Cell.* 1994;78:473–485. doi: 10.1016/0092-8674(94)90425-1
24. Wang S, Guo X, Long CL, Li C, Zhang YF, Wang J, Wang H. SUR2B/Kir6.1 channel openers correct endothelial dysfunction in chronic heart failure via the miR-1-3p/ET-1 pathway. *Biomed Pharmacother.* 2019;110:431–439. doi: 10.1016/j.biopha.2018.11.135
25. Li D, He B, Zhang H, Shan SF, Liang Q, Yuan WJ, Ren AJ. The inhibitory effect of miRNA-1 on ET-1 gene expression. *FEBS Lett.* 2012;586:1014–1021. doi: 10.1016/j.febslet.2012.02.044
26. Russell FD, Davenport AP. Secretory pathways in endothelin synthesis. *Br J Pharmacol.* 1999;126:391–398. doi: 10.1038/sj.bjp.0702315
27. Xu Y, Wellner D, Scheinberg DA. Substance P and bradykinin are natural inhibitors of CD13/aminopeptidase N. *Biochem Biophys Res Commun.* 1995;208:664–674. doi: 10.1006/bbrc.1995.1390
28. Harno E, Gali Ramamoorthy T, Coll AP, White A. POMC: the physiological power of hormone processing. *Physiol Rev.* 2018;98:2381–2430. doi: 10.1152/physrev.00024.2017
29. Ichiki T, Burnett JC Jr. Post-transcriptional modification of pro-BNP in heart failure: is glycosylation and circulating furin key for cardiovascular homeostasis? *Eur Heart J.* 2014;35:3001–3003. doi: 10.1093/eurheartj/ehu381
30. Ibebuogu UN, Gladysheva IP, Houng AK, Reed GL. Decompensated heart failure is associated with reduced corin levels and decreased cleavage of pro-atrial natriuretic peptide. *Circ Heart Fail.* 2011;4:114–120. doi: 10.1161/CIRCHEARTFAILURE.109.895581
31. Tripathi R, Wang D, Sullivan R, Fan TH, Gladysheva IP, Reed GL. Depressed corin levels indicate early systolic dysfunction before increases of atrial natriuretic peptide/B-type natriuretic peptide and heart failure development. *Hypertension.* 2016;67:362–367. doi: 10.1161/HYPERTENSIONAHA.115.06300
32. Murphy SP, Prescott MF, Camacho A, Iyer SR, Maisel AS, Felker GM, Butler J, Piña IL, Ibrahim NE, Abbas C, et al. Atrial natriuretic peptide and

treatment with sacubitril/valsartan in heart failure with reduced ejection fraction. *JACC Heart Fail*. 2021;9:127–136. doi: 10.1016/j.jchf.2020.09.013
33. Vesely DL, Perez-Lamboy GI, Schocken DD. Long-acting natriuretic peptide, vessel dilator, and kaliuretic peptide enhance urinary excretion rate of albumin, total protein, and beta(2)-microglobulin in patients with congestive heart failure. *J Card Fail*. 2001;7:55–63. doi: 10.1054/jcaf.2001.23109
34. Nasser A, Dietz JR, Siddique M, Patel H, Khan N, Antwi EK, San Miguel GI, McCormick MT, Schocken DD, Vesely DL. Effects of kaliuretic peptide on sodium and water excretion in persons with congestive heart failure. *Am J Cardiol*. 2001;88:23–29. doi: 10.1016/s0002-9149(01)01579-x
35. Solomon SD, McMurray JJV, Anand IS, Ge J, Lam CSP, Maggioni AP, Martinez F, Packer M, Pfeffer MA, Pieske B, et al; PARAGON-HF Investigators and Committees. Angiotensin-neprilysin inhibition in heart failure with preserved ejection fraction. *N Engl J Med*. 2019;381:1609–1620. doi: 10.1056/NEJMoa1908655
36. Domenig O, Manzel A, Grobe N, Königshausen E, Kaltenecker CC, Kovarik JJ, Stegbauer J, Gurley SB, van Oyen D, Antlanger M, et al. Neprilysin is a mediator of alternative renin-angiotensin-system activation in the murine and human kidney. *Sci Rep*. 2016;6:33678. doi: 10.1038/srep33678
37. Patel VB, Zhong JC, Grant MB, Oudit GY. Role of the ACE2/angiotensin 1-7 axis of the renin-angiotensin system in heart failure. *Circ Res*. 2016;118:1313–1326. doi: 10.1161/CIRCRESAHA.116.307708
38. Pavo N, Wurm R, Goliasch G, Novak JF, Strunk G, Gyöngyösi M, Poglitsch M, Säemann MD, Hülsmann M. Renin-angiotensin system fingerprints of heart failure with reduced ejection fraction. *J Am Coll Cardiol*. 2016;68:2912–2914. doi: 10.1016/j.jacc.2016.10.017
39. Bonnard E, Poras H, Fournié-Zaluski MC, Roques BP. Preventive and alleviative effects of the dual enkephalinase inhibitor (Denki) PL265 in a murine model of neuropathic pain. *Eur J Pharmacol*. 2016;788:176–182. doi: 10.1016/j.ejphar.2016.05.041
40. Vodovar N, Séronde MF, Laribi S, Gayat E, Lassus J, Boukef R, Nouira S, Manivet P, Samuel JL, Logeart D, et al; GREAT Network. Post-translational modifications enhance NT-proBNP and BNP production in acute decompensated heart failure. *Eur Heart J*. 2014;35:3434–3441. doi: 10.1093/eurheartj/ehu314
41. Chinkers M, Wilson EM. Ligand-independent oligomerization of natriuretic peptide receptors. Identification of heteromeric receptors and a dominant negative mutant. *J Biol Chem*. 1992;267:18589–18597.
42. Manivet P, Mouillet-Richard S, Callebert J, Nebigil CG, Maroteaux L, Hosoda S, Kellermann O, Launay JM. PDZ-dependent activation of nitric-oxide synthases by the serotonin 2B receptor. *J Biol Chem*. 2000;275:9324–9331. doi: 10.1074/jbc.275.13.9324
43. Liu HY, Grant H, Hsu HL, Sorkin R, Bošković F, Wuite G, Daniel S. Supported planar mammalian membranes as models of in vivo cell surface architectures. *ACS Appl Mater Interfaces*. 2017;9:35526–35538. doi: 10.1021/acsami.7b07500
44. Sinisalo J, Fyhrquist F, Syrjälä M, Nieminen MS. Stimulated release of endothelin-converting enzyme is simultaneous with tissue-type plasminogen activator and decrease in coronary heart disease. *Scand Cardiovasc J*. 2002;36:100–104. doi: 10.1080/140174302753675384
45. Yan X, Maixner DW, Yadav R, Gao M, Li P, Bartlett MG, Weng HR. Paclitaxel induces acute pain via directly activating toll like receptor 4. *Mol Pain*. 2015;11:10. doi: 10.1186/s12990-015-0005-6
46. Drozdetskiy A, Cole C, Procter J, Barton GJ. JPred4: a protein secondary structure prediction server. *Nucleic Acids Res*. 2015;43(W1):W389–W394. doi: 10.1093/nar/gkv332
47. Heffernan R, Paliwal K, Lyons J, Singh J, Yang Y, Zhou Y. Single-sequence-based prediction of protein secondary structures and solvent accessibility by deep whole-sequence learning. *J Comput Chem*. 2018;39:2210–2216. doi: 10.1002/jcc.25534
48. Yachdav G, Kloppmann E, Kajan L, Hecht M, Goldberg T, Hamp T, Hönigschmid P, Schafferhans A, Roos M, Bernhofer M, et al. PredictProtein–an open resource for online prediction of protein structural and functional features. *Nucleic Acids Res*. 2014;42(Web Server Issue):W337–W343. doi: 10.1093/nar/gku366
49. Buchan DWA, Jones DT. The PSIPRED protein analysis workbench: 20 years on. *Nucleic Acids Res*. 2019;47(W1):W402–W407. doi: 10.1093/nar/gkz297
50. Källberg M, Wang H, Wang S, Peng J, Wang Z, Lu H, Xu J. Template-based protein structure modeling using the RaptorX web server. *Nat Protoc*. 2012;7:1511–1522. doi: 10.1038/nprot.2012.085
51. Xu D, Zhang Y. Ab initio protein structure assembly using continuous structure fragments and optimized knowledge-based force field. *Proteins*. 2012;80:1715–1735. doi: 10.1002/prot.24065
52. Xu D, Zhang Y. Toward optimal fragment generations for ab initio protein structure assembly. *Proteins*. 2013;81:229–239. doi: 10.1002/prot.24179
53. R Core Team. R: a language and environment for statistical computing. R Foundation for Statistical Computing, Vienna, Austria; 2020. https://www.R-project.org/.
54. Vodovar N, Séronde MF, Laribi S, Gayat E, Lassus J, Januzzi JL Jr, Boukef R, Nouira S, Manivet P, Samuel JL, et al; GREAT Network. Elevated plasma b-type natriuretic peptide concentrations directly inhibit circulating neprilysin activity in heart failure. *JACC Heart Fail*. 2015;3:629–636. doi: 10.1016/j.jchf.2015.03.011

SUPPLEMENTARY MATERIALS

ProANP metabolism provides new insights into sacubitril/valsartan mode of action.

Thibault Michel, Hélène Nougué, Jérôme Cartailler, Guillaume Lefèvre, Malha Sadoune, François Picard, Alain Cohen-Solal, Damien Logeart, Jean-Marie Launay, and Nicolas Vodovar

Data Supplement

1- Supplementary methods

2- Tables S1-S5

3- Figures S1-S9

Methods

This study was approved by local ethic committees and written consent was obtained from patients or next of kin. This study was performed according to the current revision of the Helsinki Declaration and registered at clinicaltrials.gov under the NCT01374880 identifier.

Study population: The study population was previously described[3]. It consisted of 73 patients suffering from chronic stable HFrEF whose treatment by angiotensin receptor blocker (ARB) or ACE inhibitor (ACEi) was substituted by S/V as per European guidelines[15] (Table S1). Plasma samples were obtained from these patients at baseline – *i.e.* before the first S/V dose, and 30 and 90 days after initiation of S/V. Samples were available 7, 14, and 180 days after the initiation of S/V for some patients. In some instances, the number of patients is lower due to plasma samples exhaustion.

The control cohort consisted of 54 patients devoid of overt chronic heart failure or neurological diseases who were recruited in the orthopedic department during a follow-up visit (*e.g.* plaster removal). The characteristics of the patients are presented in Table S2.

Blood sampling: Venous blood samples were collected into tubes containing EDTA. Blood samples were immediately centrifuged at 2300 x *g* for 15 minutes at 4°C and plasma was aliquoted and frozen at -80°C until use. The maximum time between blood collection and freezing of aliquots was 30 minutes. All measurements were performed on samples that were subjected to a maximum of two freeze/thaw cycles: measurements of peptides by MS/MS were performed on samples not thawed before the experiment; some samples used to determine enzymatic concentration and activity were performed on samples that were thawed once before the measurement. All measurements were performed blinded from patient ID, time point, and clinical data.

Plasma concentration of biomarkers: MR-proANP was measured by an automated immunoassay on a Kryptor platform (B·R·A·H·M·S, Hennigsdorf, Germany). ANPEP (DY3815, R&D systems), ECE1 (EKU03892, Biomatik), ET1 (QET00B, R&D systems), and big-ET1 (BI-20082H, Biomedica Gruppe, Wien) plasma concentrations were measured by ELISA. Substance P, and GLP-1, Adrenomedullin plasma concentrations were previously published[3] and were determined by radioimmunoassay (Phoenix Pharmaceuticals, Belmont, California, and Cayman Chemical, respectively) or MS/MS, respectively. BNP and high-sensitivity cardiac troponin I (hsTnI) plasma concentrations were measured on an Abbott Architect system on an Architect i2000 (Abbott Laboratories, Abbott Park, IL, USA). NT-proBNP and fructosamine were measured on a Roche Cobas analyzer (Roche, Basel, Switzerland). All measurements were performed according to the manufacturer's instructions except for MS/MS determination (Adrenomedullin).

Plasma miRNA quantification: Total RNA was extracted from plasma samples using the mirVana PARIS kit (Ambion, Thermo Fisher Scientific, ref: AM1556, St-Quentin en Yvelines, France). Samples were spiked with synthetic *C. elegans* miRNA controls (cel-miR39, 54, and 238) to a final concentration of 2 pM for correction of extraction efficiency. After DNAse treatment, RNAs were reverse transcribed with the miScript reverse transcription kit (Qiagen). cDNA was diluted 10 folds before quantitative PCR using the miScript SYBR Green PCR kit (Qiagen). A control without reverse transcriptase and a control without RNA were added to each PCR plate to ensure the absence of contaminating DNA and to check for non-specific amplification, respectively. Cycling conditions for the amplification were an initial denaturation at 95°C for 1 min followed by 35-40 cycles [denaturation: 95°C for 15 sec, annealing: 58°C for 60 sec, and extension: 72°C for 20 sec]. Expression values were normalized using the mean Ct of the spiked-in controls and calculated with the $2^{-\Delta Ct}$ formula.

Apelin-12 was measured by MS/MS as follows: Immediately after thawing on ice, the plasma samples were mixed with an equal volume of water containing 2% TFA. SepPak cartridges (C18, 1 cc, Waters, Milford, MA, USA) were conditioned with 1 mL methanol, and further equilibrated with 2 mL of water containing 1% trifluoroacetic acid (TFA). Plasma samples (1 mL plasma previously diluted with a 2% TFA solution) were then passed through the solid-phase extraction (SPE) column, which was further washed with 1 mL of water containing 1% TFA and 2 mL of water. Elution was performed with 1 mL of 100% methanol and the resulting sample further evaporated to dryness. The samples were then reconstituted with an acidic solution (water/acetonitrile, 90:10 v/v, containing 1% formic acid).

LC/MS/MS experiments were performed using an HP 1100 HPLC system from Agilent (Palo Alto, CA, USA) coupled to a triple quadrupole TSQ Quantum Ultra mass spectrometer (Thermo Scientific, San Jose, CA, USA). Chromatographic separation was performed on a Polaris C18-A column (150 x 2 mm i.d., 3 mm particle size) from Varian (Palo Alto, CA, USA). The column was eluted at a flow rate of 0.2 mL/min using water as mobile phase A and acetonitrile as mobile phase B, both containing 0.1% formic acid. After 1 min at 5% B, a linear gradient was started to reach 35% B in 6 min. From 7 to 8.5 min, a linear gradient was set to reach 100% B and the column was washed for 10.5 min at this composition. The equilibration time before the next analysis was set at 6 min so that the time between two cycles was 25 min. The column temperature was maintained at 50°C and the injection volume was 30 µL. The column effluent was directly introduced into the electrospray source of the TSQ Quantum Ultra triple quadrupole mass spectrometer. Analyses were performed in the positive ion mode. The electrospray voltage and the capillary voltage were set at 3.9 kV and 35 V, respectively. An in-source potential of 8 V was used. The sheath, ion sweep, and auxiliary gas flow rates (nitrogen) were optimized at 30, 20, and 20 (arbitrary units), while the drying gas temperature was set at 3508C. During MS/MS experiments the protonated

molecules were fragmented by low-energy collision-induced dissociation (CID), using argon as the collision gas (at a pressure of 1.7 mTorr). Two MRM transitions were monitored for each apelin peptide to guarantee specific detection. Both the retention time of the two MRM peaks from a given apelin peptide and the MRM transition ratio must match the retention time and ratio obtained when analyzing standard apelin peptides under the same analytical conditions. The optimized tube lens and collision energy values for apelin 12 were:

Apelin	**Precursor ion (m/z)**	**Product ion (m/z)**	**Collision energy (eV)**	**Tube lens (V)**
Apelin 12	356.5 (4 +)	387.7 (b_{10}^{3+})	12	70
	356.5 (4 +)	371.6 (b_{10}^{3+} - CH_3SH)	12	
[(13C5,15N]Pro2,9)apelin-12	359.5 (4 +)	391.7 (b_{11}^{3+})	12	70
	359.5 (4 +)	375.6 (b_{11}^{3+} - CH_3SH)	12	

The limit of quantification was 30 pg/mL, coefficient of variation (CV) was 5.3%, reproducibility CV was 8.8%, and accuracy was 98-105% (n=15).

Peptide and proANP glycosylation quantification by mass spectrometry: These determinations were performed as previously described for BNP[40] with the modifications. After O-glycosidase and/or neuraminidase and trypsin digestions, separation of the proANP proteolytic fragments and characterization of the O-glycosylated sites were performed on an Agilent 1290 Infinity II LC system (Agilent Technologies, Santa Clara, US) connected to a

TripleTOF®5600 mass spectrometer (SCIEX, Framingham, MA) for all LC-MS analysis. Mobile phase A was H_2O with 0.1% formic acid and mobile phase B was acetonitrile with 0.1% formic acid. 10 µL of the sample was injected onto a C18 column (Waters Acquity UPLC, BEH C18; 2.1 mm x 100 mm, 1.7 µm) for each run at a flow rate of 400 µL/min. The chromatography started at a solvent composition of 2% B and 98% A for 2 min, and then increased to 45% B at 45 min, and reached 90% B at45.1 min and held until 47 min. Thereafter, the column was re-equilibrated back to the starting solvent conditions of 2% B and 98% A at 47.1 min and held to the end of the gradient (54 min).To maximize the information acquired on the mass spectrometer for each sample, a full MS scan (m/z 300-2000) was acquired, followed by top 20 information-dependent acquisition (IDA) MS/MS scans (m/z 100-1600) in positive ion mode. The parameters for curtain plate (CUR), declustering potential (DP), collision energy(CE), ion spray voltage (IS), Gas1, Gas2 in full MS scan mode were 30psi, 80V, 10V, 5500V, 55 psi, and 55 psi, respectively. Source temperature was set to 450°C and tray temperature was set to 22°C. The criteria for the IDA precursor selection were as follows: top 20 most intense peaks with charge states from 2 to 5 and intensities greater than 50 were selected. Previous candidates within the mass tolerance of 50 mDa were excluded for the duration of 3 s after 1 occurrence. Dynamic background subtraction was activated. Rolling collision energy for multiply charged peptides was enabled. Divert Valco valve was used to switch LC flow to MS between 2 and 50 min.

ANP activity assay: HEK293 cells stably transfected by the ANP and BNP receptor NPRA, were used as previously described[41]. Cells were incubated with the plasma samples of 30 patients at D0 and D30 for 20 minutes, before cGMP measurement by radioimmunoassay as previously described[42] using the cGMP RIA from IBL/TECAN (IBL/TECAN, ref: RE29071). In parallel, the plasma was depleted of ANP and proANP by immunocapture using 10µg/mL the monoclonal antibody (ANP-(F-2), Santa Cruz, ref: 515701) and assayed to provide ANP-

independent cGMP production. ANP-dependent cGMP production was calculated as the difference between the cGMP produced by the plasma and cGMP produced by the ANP/proANP-depleted plasma.

Ex vivo *enzymatic activities:* NEP activity (EC 3.4.24.11) was previously published[3] and measured as previously described[3]. Plasma ANPEP activity measurement derived from[43], was performed in triplicate by incubating 2 µL of sample in a 100 mM Tris pH 7.2, Brij 35 0.0002% w/v assay buffer with 0.1 µM APN and 100 µM H-Ala-AMC (fluorophore, Bachem/ Fischer scientific, ref: NC1747106) containing 0.1% BSA with or without the CD13 (ANPEP)-specific inhibitory antibody WM-15 (5 µg/mL; PharMingen, ref: 555393, Heerhugowaard, the Netherlands) at 37°C. BSA (0.1%) was added to exclude the effects of differences in protein concentration on ANPEP activity. Values were recorded by Infinite pro plate reader every 2 minutes for 30 minutes with laser parameters set for excitation at 355 nm and emission at 460 nm. The specific ANPEP activity was calculated from the slope of total aminopeptidase activity after subtraction of the slope of the aminopeptidase activity remaining in the presence of WM-15. Plasma ECE-activity was measured according to[44] with modifications. Plasma samples were diluted 1:50 with a buffer containing 30 mM HEPES, 350 mM NaCl, 50 mM $ZnCl_2$, pH 7.0, and pre-incubated on ice with thiorphan (Sigma, St Louis, Mo) to a final concentration of 1 mM for 30 min, as an inhibitor of serum neutral endopeptidase. The reaction was started by adding 300 nM big-ET1 (Peptide Institute, Barnet, United Kingdom), and carried out at 37°C for 60 min. The reaction was terminated by cooling on ice and adding Na_2 EDTA to a final concentration of 1 mM. The amount of ET1 generated was quantified by ELISA of ET1 (the polyclonal antiserum chosen showed 100% cross-reaction with human ET-2 and ET-3 and < 0.1% for pre-proEndothelin sequences (20 – 50, 74 – 91, 171 – 201) and human big-ET 1 – 38 and 22 – 38). Pooled plasma from healthy subjects was tested in each assay at dilution 1:50 and 1:20 as internal controls and to assess intra-assay

and inter-assay variations. The within and between assay coefficients of variation were 5.4% and 13.6%, respectively. The ECE activity was a measure of the formation of ET1, *i.e.* the difference between the concentration of ET1 after the addition of big-ET1 and the basal concentration of ET1. Plasma ECE activity remained stable despite freezing and thawing up to eight times.

In vitro *enzymatic assays*: Recombinant human ECE1, ECE2, meprin beta subunit/meprin1B, and ANPEP proteins were from R&D systems (refs 1784-ZN-010, 1645-ZN-010, 2895-ZN-010, and 3815-ZN-010, respectively). Recombinant human corin and NEP were from Origene (ref TP 312742) and Sigma (ref SRP6450) respectively. Artificial CSF (aCSF) was prepared according to[45] as follows: appropriate amounts of solid powders were dissolved in LC/MS grade water to the final concentration of 234 mM sucrose, 3.6 mM KCl, 1.2 mM $MgCl_2$, 2.5 mM $CaCl_2$, 1.2 mM NaH_2PO_4, 12.0 mM glucose and 25.0 mM $NaHCO_3$. The composition of the aCSF that was chosen is commonly used by many laboratories for behavioral and physiological studies. While there are many recipes for aCSF, they are all generally very similar in composition to the one used in this study. All solvents and reagents were of LC/MS grade or analytical grade and were purchased from Fluka. The chosen enzyme concentrations (1 nM for corin, 2.5 nM for meprinB, 5 nM for ANPEP, and 50 nM for ECE1) were close to those found in human plasma.

Secondary structure prediction: Secondary structure prediction of $proANP_{1-30}$ was performed using either model-based (JPRED4[46], SPIDER3[47], PredictProtein[48], PSIPRED[49], RaptorX[50]) or *ab initio* (Quark[51, 52]) algorithms available online using $proANP_{1-98}$ (NP_006163) as the input sequence. The predicted structure was ray-traced using pymol.

Mathematical modeling: The proANP proteolytic cascade was modeled using an 18 equations-based dynamical system. The ordinary system of equations was solved using a

Runge-Kutta 4 numerical solver. Prior parameters optimization, median values computed at D0, D7, D14, D30, D90, and D180 were used to construct a piecewise cubic Hermite interpolating polynomial with a point every 0.5 day. Parameter estimation was made using a nonlinear least-squares solver with a 10^{-10} step/function tolerance and iterations until convergence. The simulation was performed was on a 375-day scale to verify the stability of the model beyond the last time point at which data were obtained (D180). Methods were implemented in Matlab2018 using the *lsqcurvefit* function from the optimization toolbox. The full description of the model is presented in **Tables S2-S5**.

Statistics: All statistical analyses were performed using the R-statistical software[53]. Data normality was assessed using the Shapiro-Wilk test. Continuous variables are expressed as median [interquartile range (IQR)]. Comparisons between baseline and D7 or D14 using paired data were performed using the Wilcoxon signed-rank test. Comparisons between controls and HFrEF patients at baseline, D30, and D90 were performed using rank-sum Wilcoxon test corrected for multiple comparisons (holm). Longitudinal variables were analyzed using repeated measure ANOVA log-transformed data followed by Tukey test. Correlations between variables were estimated with Spearman rank correlation and expressed by the correlation coefficient (ρ). Principal component analysis was performed on standardized (scaled and centered) data. No experiment-wide/across-test multiple test correction was applied. A p-value < 0.05 was considered statistically significant. Exact P values are indicated unless $< 2x10^{-16}$ (R limit). Determination of cut-off for ANPEP was performed as previously described[54] (**Figure S9**).

Table S1: Baseline characteristics of the study population (n = 73) adapted from[3]. eGFR estimated glomerular filtration rate, NYHA New York Heart Association, ACEi: angiotensin-converting enzyme inhibitor, ARB: angiotensin receptor blocker, MRA mineralocorticoid receptor antagonist, hsTnI: high-sensitive troponin I, Variables are expressed as number (percentage) or median [interquartile range], as appropriate.

Patient characteristics	
Age – year	65 [56 – 72]
Men	61 (84%)
Body mass index– kg/m^2	25.1 [23.0 – 28.0]
Diabetes	16 (22%)
Atrial fibrillation	25 (34%)
Ischemic heart disease	40 (55%)
Last decompensation – months	6 [3 – 25]
Systolic blood pressure – mmHg	114 [102 – 125]
Diastolic blood pressure – mmHg	67 [60 – 77]
eGFR – ml/min/1.73m^2	62 [48 – 84]
NYHA classification	
I	2 (3%)
II	36 (49%)
III	33 (45%)
IV	2 (3%)
Medication	
Furosemide	62 (85%)
ACEi or ARB	72 (98%)

Beta-blocker	68 (73%)
MRA	58 (73%)
Plasma biomarkers	
Creatinine – µmol/l	103 [87 – 124]
BNP – ng/L	370 [193 – 702]
NT-proBNP – ng/L	1201 [571 – 1997]
hsTnI – ng/L	14.3 [9.4 – 20.7]

Table S2: **Baseline characteristics of the healthy subsects (n = 54)**

Characteristics	
Age – year	75 [71 – 82]
Men	16 (30%)
Body mass index– kg/m^2	26.1 [22.8 – 28.8]
Diabetes	8 (14%)
Atrial fibrillation	2 (4%)
Hypertension	27 (50%)
Chronic Kidney disease	2 (4%)
Medication	
Diuretics	6 (11%)
ACEi or ARB	14 (26%)
Beta-blocker	8 (15%)
MRA	6 (11%)

Table S3: Variables included in the mathematical model

	Measured	**Modelled**
Peptides	F (Peptide signal proxy) $proANP_{1-126}$ (proANP) ANP $proANP_{1-98}$ (NT-proANP) $proANP_{1-30}$ $proANP_{31-98}$ $proANP_{31-67}$ $proANP_{79-98}$	F (Peptide signal proxy) $proANP_{1-126}$ (proANP) ANP $proANP_{1-98}$ (NT-proANP) $proANP_{1-30}$ $proANP_{31-98}$ $proANP_{31-67}$ $proANP_{79-98}$ $proANP_{68-98}$
Enzyme concentrations	ECE ANPEP	ECE ANPEP
Enzyme activity	ECE ANPEP	Corin Meprin B ECE ANPEP

Table S4: List of the equations and initial conditions used to construct the mathematical model. d_t indicates derivative with respect to time, square brackets indicate concentrations, and "0" indicates initial conditions.

1- F: proxy for the input into the cascade
Simple exponential saturation starting at *F0*, reaching F_{lim} with a single τ_F time constant. $$\boldsymbol{d_t[F] = -\tau_F([F] - ([F_0] + [F_{lim}]))}$$ $[F]_0$ = 92.70 pM (obtained from proANP$_{1\text{-}126}$ data) Note: F is used to model an increase in proANP$_{1\text{-}126}$ based on the kinetics of the increase in signal peptide. Importantly, proANP signal peptide concentration was not used for optimization.
2- proANP$_{1\text{-}126}$
Compartmental: proANP$_{1\text{-}126}$ concentration increases with a similar dynamics as signal peptide, then is consumed proportionally to the amount of Corin. $$\boldsymbol{d_t[\mathbf{proANP_{1-126}}] = (-\tau_F([\mathbf{proANP_{1-126}}] - ([F_0] + [F_{lim}])) - [\mathbf{proANP_{1-126}}] \cdot Corin_{act})}$$ $[proANP_{1\text{-}126}]_0$ = 92.70 pM (obtained from data) Note: F and Corin are truly defined up to a constant-rate multiplicative factor as their initial conditions are unknown. $F = rateF * F_{real}$ $Corin_{act} = rateCor * Corin_{act-real}$
3- Corin
Exponential equilibrium with 2 successive steady states Corin equilibrates first to k_a then to k_b.

$$d_t S_{Cor} = k_{sC} S_{Cor}(1 - S_{Cor})$$

$$d_t Corin = -\tau_{Cor}(Corin_{act} - (k_a S_{Cor} + k_b(1 - S_{Cor})))$$

$S_{Cor\ 0}$ = 0.0759 and $Corin_{act\ 0}$ = 0.0081 (derived from optimisation)

Note: Changes in Corin activity are modeled with an exponential saturation to a time-dependent level shaped using a logistic equation.

4- ANP

Compartmental with linear flux:

$$d_t[ANP] = [\mathbf{proANP_{1-126}}] \cdot Corin_{act} - k_{ANP} \cdot [ANP]$$

$[ANP]_0$ = 40.75 pM (obtained from data)

5- Meprin B

Exponential equilibrium with 2 successive steady states:

$$d_t S_{Mep} = k_{sM} S_{Mep}(1 - S_{Mep})$$

$$d_t Meprin_{act} = -\tau_{Mep}(Meprin_{act} - (k_c S_{Mep} + k_d(1 - S_{Mep})))$$

$S_{Mep\ 0}$ = 0.1192 and $Meprin_{act\ 0}$ = 0.15 (derived from optimisation)

Note: Modelling of Meprin B activity follows the same rules as Corin.

6- proANP$_{1\text{-}98}$

Compartmental:

$$d_t[proANP_{1-98}] = [\mathbf{proANP_{1-126}}] \cdot Corin_{act} - [proANP_{1-98}] \cdot Meprin_{act}$$

$[proANP_{1\text{-}98}]_0$ = 65.5 pM (obtained from data)

Note: As for proANP$_{1\text{-}126}$, there are hidden constant-rate variables as neither Corin nor Meprin B initial conditions are known

$$Mep = rateMep * Mep_{real}$$

7- proANP$_{1\text{-}30}$

Compartmental with linear flux:

$$\boldsymbol{d_t[proANP_{1-30}] = [proANP_{1-98}] \cdot Meprin_{act} - k_{proANP_{1-30}} \cdot [proANP_{1-30}]}$$

[proANP$_{1\text{-}30}$]$_0$ = 16.03 pM (obtained from data)

8- proANP$_{31\text{-}98}$

Compartmental:

$$\boldsymbol{d_t[proANP_{31-98}] = [proANP_{1-98}] \cdot Meprin_{act} - [proANP_{31-98}] \cdot k_{ECE} \cdot [ECE]}$$

[proANP$_{31\text{-}98}$]$_0$ = 15.10 pM (obtained from data)

9- ECE

Exponential saturation for the concentration and double exponential modeling of the activity:

$$\boldsymbol{d_t[ECE] = -\tau_{ECE} \cdot ([ECE] - ([ECE_0] + [ECE_{lim}]))}$$

$$\boldsymbol{d_t{}^2 k_{ECE} = (k_{on_{ECE}} + k_{off_{ECE}}) \cdot d_t k_{ECE} - k_{on_{ECE}} . k_{off_{ECE}} . (k_{ECE} - g_{ECE})}$$

[ECE]$_0$ = 21.1 nM*; k$_{ECE}$(0)* = 8.768; *dk$_{ECE}$(0)* =;15.7 (obtained from data)

10- proANP$_{31\text{-}67}$

Compartmental with linear flux:

$$\boldsymbol{d_t[proANP_{31-67}] = [proANP_{31-98}] \cdot k_{ECE} \cdot [ECE] - k_{proANP_{31-98}} \cdot [proANP_{31-67}]}$$

[proANP$_{31-67}$]$_0$ = 1.55 pM (obtained from data)

11- proANP$_{68-98}$

Compartmental:

$$\boldsymbol{d_t[proANP_{68-98}] = 0}$$

[proANP$_{68-98}$]$_0$ = 1.515 pM (obtained from data)

12- ANPEP

Exponential saturation for the concentration and double exponential modeling of the activity:

$$\boldsymbol{d_t[\mathrm{ANPEP}] = -\tau_{\mathrm{ANPEP}} \cdot ([\mathrm{ANPEP}] - ([\mathrm{ANPEP_0}] - [\mathrm{ANPEP}_{lim}]))}$$

$$\boldsymbol{d_t{}^2 k_{\mathrm{PANPEP}} = (k_{on_{\mathrm{ANPEP}}} + k_{off_{\mathrm{ANPEP}}}) \cdot d_t k_{\mathrm{ANPEP}} - k_{on_{\mathrm{ANPEP}}} \cdot k_{off_{\mathrm{ANPEP}}} \cdot (k_{\mathrm{ANPEP}} - g_{\mathrm{ANPEP}})}$$

[ANPEP]$_0$ = 4.79 nM; *k$_{ANPEP\ 0}$* = 1.93; *dk$_{ANPEP\ 0}$* =;0.183 (obtained from data)

13- proANP$_{79-98}$

Compartmental with linear flux:

$$\boldsymbol{d_t[proANP_{79-98}] = d_t[proANP_{31-67}] - k_{proANP_{79-98}} \cdot [proANP_{79-98}]}$$

[proANP$_{79-98}$]$_0$ = 1 pM (obtained from data)

Table S5: List of parameters used in the model

Parameters	**Obtained**
τ_F	0.051 day^{-1}
$[F_{lim}]$	150.31 pM
k_{sC}	0.0375 day^{-1}
τ_{Cor}	0.2 day^{-1}
k_a	0.60 day^{-1}
k_b	0.132 day^{-1}
k_{ANP}	0.20 day^{-1}
k_{sM}	0.02 day^{-1}
τ_{Mep}	0.13 day^{-1}
k_c	0.80 day^{-1}
k_d	0.14 day^{-1}
$k_{proANP_{1-30}}$	0.0278 day^{-1}
τ_{ECE}	0.0556 day^{-1}
$[ECE_{lim}]$	47.63 nM
$k_{on_{ECE}}$	-0.069 day^{-1}
$k_{off_{ECE}}$	-3.575 day^{-1}
g_{ECE}	1.91 day^{-1}
$k_{proANP_{31-98}}$	25.1 day^{-1}
τ_{PEP}	0.01 day^{-1}
$[ANPEP_{lim}]$	1 nM
$k_{on_{PEP}}$	-0.013 day^{-1}
$k_{off_{PEP}}$	-0.212 day^{-1}
g_{PEP}	0.79 day^{-1}
$k_{proANP_{79-98}}$	14.02 day^{-1}

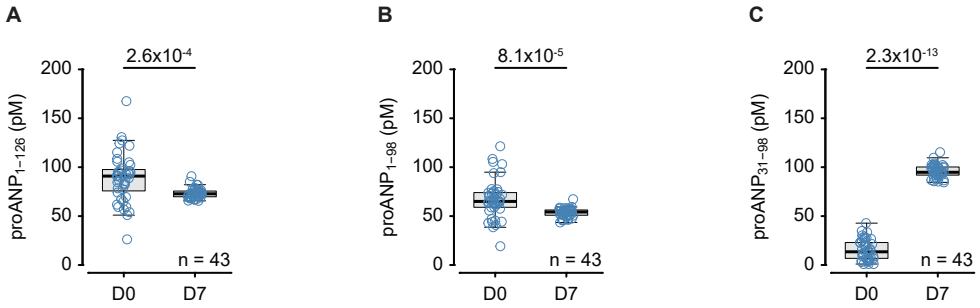

Figure S1: Plasma levels of proANP$_{1\text{-}126}$ (**A**), proANP$_{1\text{-}98}$ (**B**), and proANP$_{31\text{-}98}$ (**C**) quantified by MS at baseline (D0) and D7 after initiation of S/V. Variables were analyzed using the signed-rank Wilcoxon test. The numbers of subjects included in the analyses are indicated on each panel.

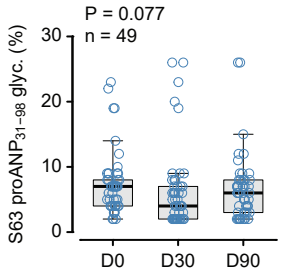

Figure S2: Plasma levels of proANP$_{31\text{-}98}$ glycosylated at S63 quantified by MS at baseline (D0), and D30 and D90 after initiation of S/V. Variables were analyzed by repeated-measure ANOVA on log-transformed data followed by the Tukey HSD test. The number of subjects included in the analysis is indicated in the panel.

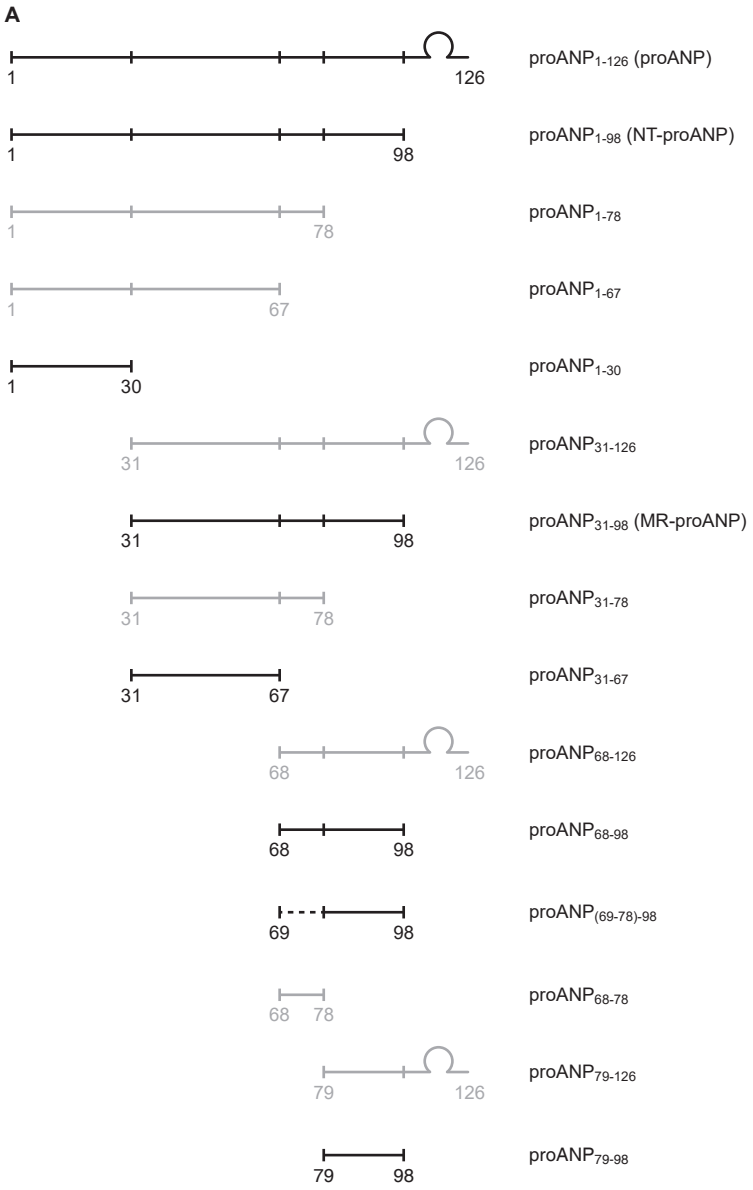

B

Algorithm	NPMYNAVSNADLMDFKNLLDHLEEKMPLED
JPRED4*	CCCCCCCCCCCHHHHHHHHHHHHHCCCCCC
SPIDER3*	CCCCCCCCHHHHHHHHHHHHHHHHHCCCCC
RaptorX*	CCCCCCCCCHHHHHHHHHHHHHHHHCCCCC
PsiPred*	CCCCCCCCHHHHHHHHHHHHHHHHHCCCCC
PredictProtein*	CCCCCCCCCHHHHHHHHHHHHHHHHCCCCC
Quark**	CCCCCCCCCHHHHHHHHHHHHHHHHCCCCC

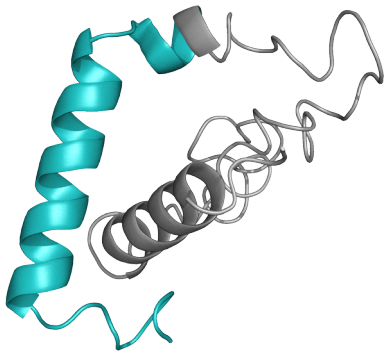

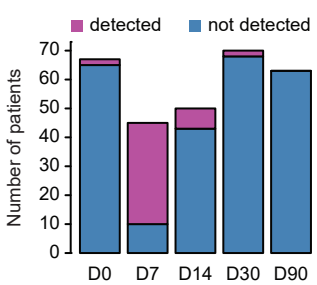

Figure S3: A) proANP molecular species searched by MS. Shown in black and grey are detected and not detected species, respectively. **B)** Results from the structure prediction of $proANP_{1\text{-}98}$ using model-based (*) and *ab initio* (**) structure prediction algorithms: C: coil, H: α-helix. **C)** Structure of $proANP_{1\text{-}98}$ predicted by Quark. Shown in teal is the $proANP_{1\text{-}30}$ fragment. **D)** Number of samples at which $proANP_{(69\text{-}78)\text{-}98}$ were detected at each time point.

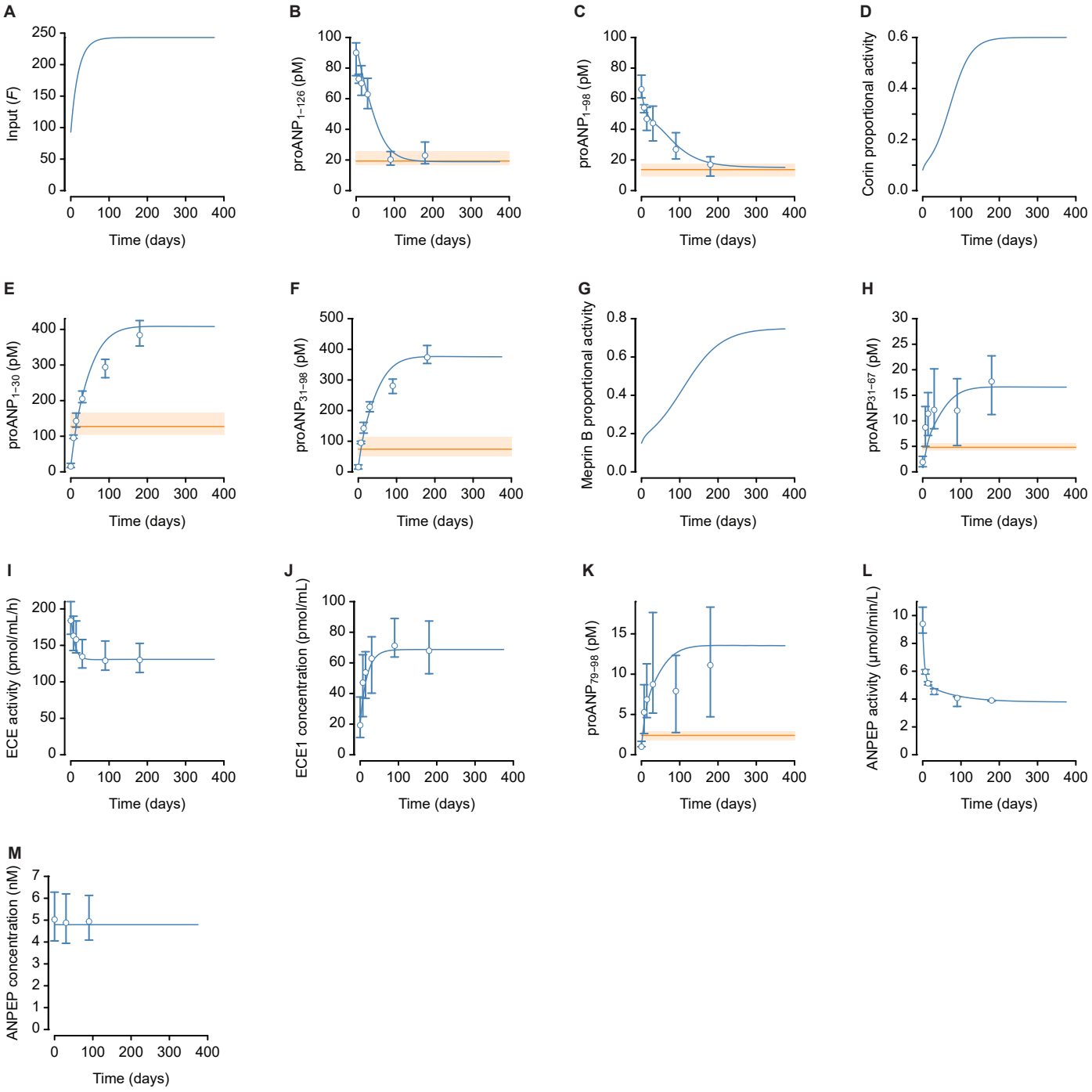

Figure S4: Numerical outputs from the model of the proANP cascade. Sown as blue line the direct output of the model after optimization, as circle and error bars the median and interquartile range from HFrEF patients at the different time points available, and as an orange line and a transparent rectangle the median and inter-quartile range observed in healthy individuals. The simulation was allowed to run over 375 days to ensure the stability of the system.

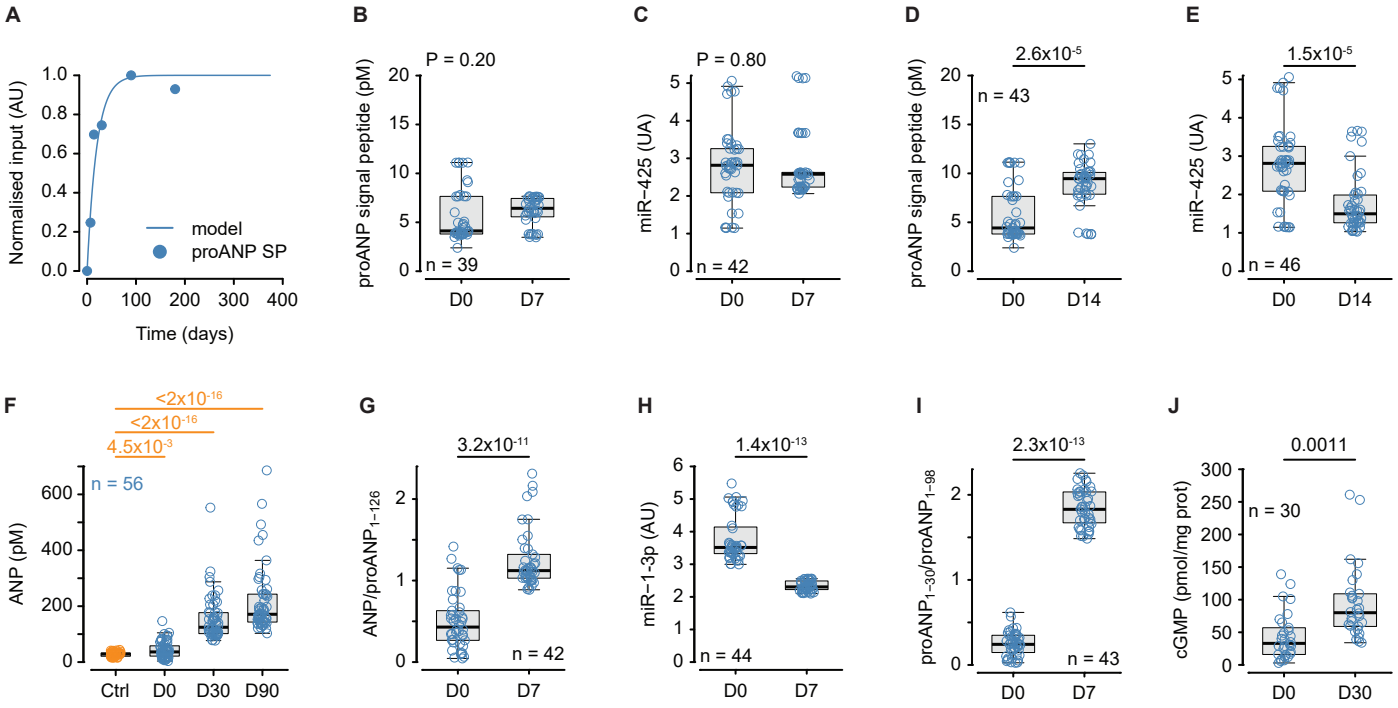

Figure S5: A) Kinetic evolution of the input of the cascade predicted by the mathematical model (solid line). Points indicate the median values of the proANP signal peptide at each time point. The model and data values were normalized to one at D90 to fit within the same scale. Plasma levels of proANP signal peptide (**B, D)** were quantified by MS and miR-425 (**C, E**) at baseline (D0) and D7 (**B, C**) or baseline and D14 (**D, E**) after initiation of S/V. **F)** ANP plasma levels in controls (Ctrl) and HFrEF patients at baseline, and D30 and D90 after initiation of S/V. The comparisons between baseline, D30, and D90 were already published[3] and are shown for reference. **G)** Plasma ANP/proANP$_{1-126}$ at baseline and D7 after initiation of S/V. **H)** miR-1-3p plasma levels at baseline and D7 after initiation of S/V. **I)** Plasma proANP$_{1-30}$/proANP$_{1-98}$ at baseline and D7 after initiation of S/V. **J)** cGMP production after incubating HEK293 cells transfected with NPRA with the plasma of 30 patients at baseline and D30 after initiation of S/V. All variables were analyzed using the signed-rank Wilcoxon test except for (**F**) in which data were analyzed by repeated-measure ANOVA on log-transformed data followed by the Tukey HSD test (blue) or using Wilcoxon rank-sum test corrected for multiple comparisons (holm, orange). The number of subjects included in the analyses is indicated on each panel. The number of healthy subjects was 54.

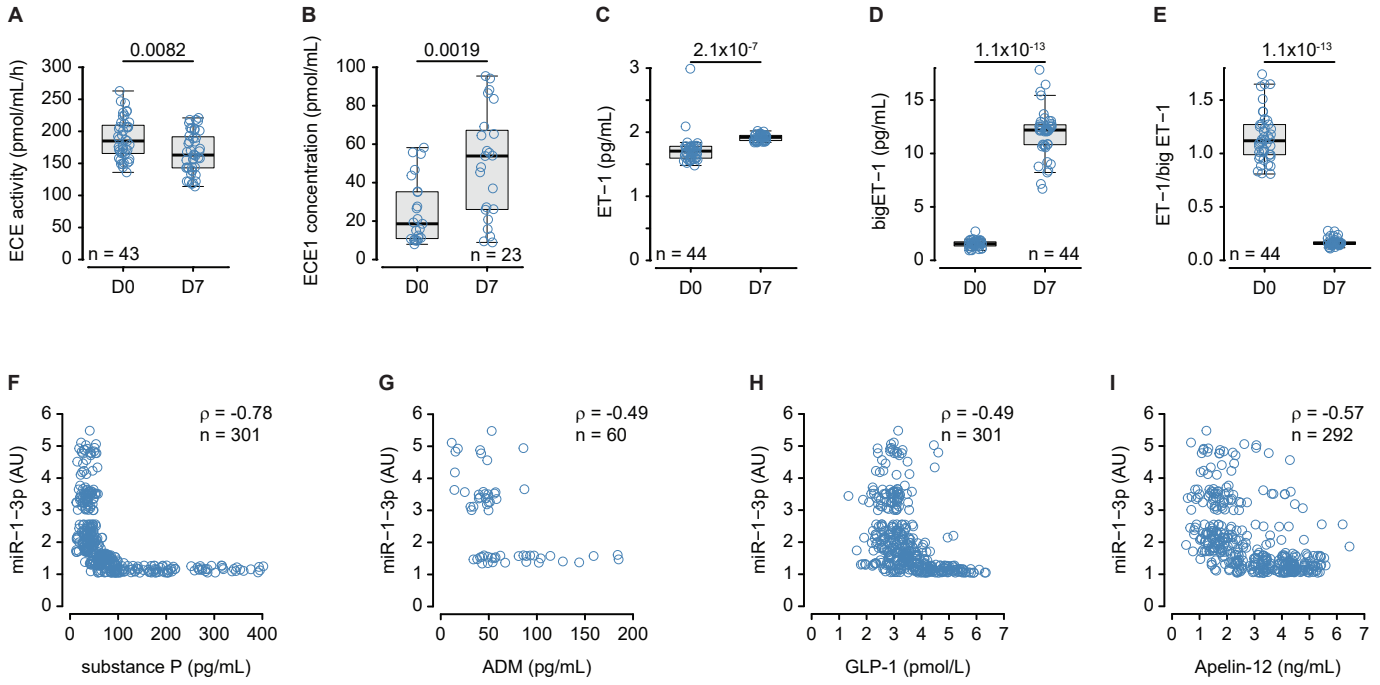

Figure S6: A) Plasma ECE activity at baseline and D7 after initiation of S/V. **B)** Plasma ECE1 concentration at baseline and D7 after initiation of S/V. **C)** Plasma ECE1 specific activity at baseline and D7 after initiation of S/V. **D)** Plasma ET-1 levels at baseline and D7 after initiation of S/V. **E)** Plasma ET-1/bigET-1 ratio at baseline and D7 after initiation of S/V. **F-I)** Relationship between plasma levels of miR-1-3p and plasma levels of substance P (**F**), ADM (**G**), GLP-1 (**H**), and apelin-12 (**I**). All variables were analyzed using the signed-rank Wilcoxon test. Correlations between variables were estimated with Spearman rank correlation and expressed by the correlation coefficient (ρ) (**F-G**). The number of subjects included in the analyses is indicated on each panel.

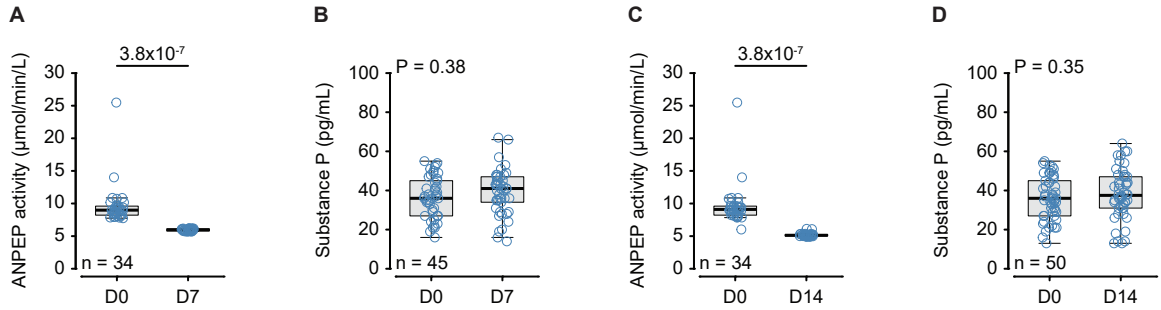

Figure S7: A) Plasma ANPEP activity at baseline (D0), and D30 and D90 after initiation of S/V. **B)** Plasma substance P (SP) levels at baseline and D7 after initiation of S/V. **C)** Plasma ANPEP activity at baseline and D14 after initiation of S/V. **D)** Plasma substance P (SP) levels at baseline and D14 after initiation of S/V. All variables were analyzed using the signed-rank Wilcoxon test. The number of subjects included in the analyses is indicated on each panel.

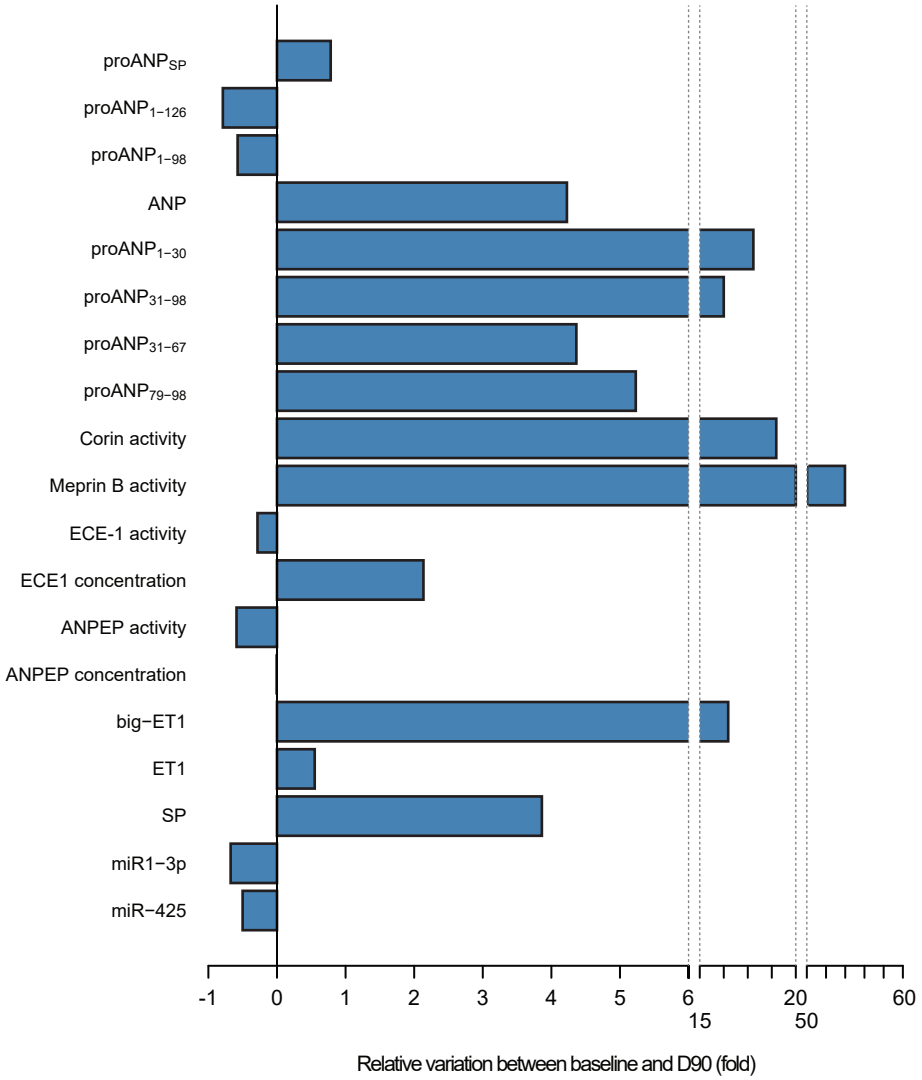

Figure S8: Summary of the relative variations of all the parameters measured between baseline (D0) and D90 after initiation of S/V in HFrEF patients. Each histogram represents the median of the relative variation. Corin and meprin B activities were estimated by the ANP/proANP$_{1-126}$ the proANP$_{1-30}$/proANP$_{1-98}$ ratios, respectively.

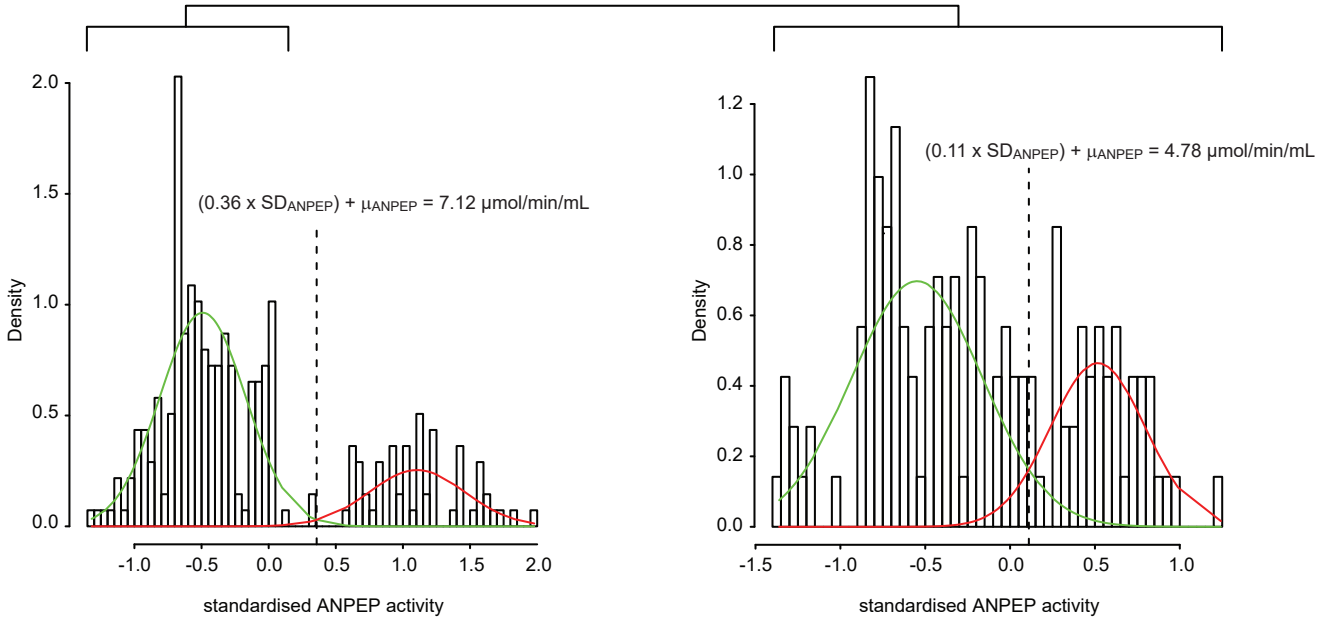

Figure S9: Determination of the two cut-offs of ANPEP activity. Each bimodal distribution was modeled as two independent normal distributions, and the cut-off was determined as the intersection of the two normal distributions. The data were standardized (scaled and centered) before fitting the normal models.

Major Resources Table

In order to allow validation and replication of experiments, all essential research materials listed in the Methods should be included in the Major Resources Table below. Authors are encouraged to use public repositories for protocols, data, code, and other materials and provide persistent identifiers and/or links to repositories when available. Authors may add or delete rows as needed.

Antibodies

Target antigen	Vendor or Source	Catalog #	Working concentration	Lot # (preferred but not required)	Persistent ID / URL
ANPEP	R&D systems	DY3815	ELISA		https://www.rndsystems.com/products/human-aminopeptidase-n-cd13-duoset-elisa_dy3815
ECE1	Biomatik	EKU03892	ELISA		https://www.biomatik.com/elisa-kits/human-endothelin-converting-enzyme-1-ece1-elisa-kit-cat-eku03892/
ET1	R&D systems	QET00B	ELISA		https://www.rndsystems.com/products/human-endothelin-1-quantiglo-elisa-kit_qet00b
Big-ET1	Biomedica Gruppe	BI-20082H	ELISA		https://www.bmgrp.com/product/cardiovascular/big-et1-elisa-kit-human-endothelin-1-biomedica/
Substance P	Phoenix Pharmaceutical	RK-061-05	RIA		https://www.phoenixpeptide.com/products/view/Assay-Kits/RK-061-05
GLP-1	Chemicon International/ Merck Millipore	AB3244			https://www.merckmillipore.com/FR/fr/product/Anti-GLP-1-7-36-Antibody-CT-amide-reactive,MM_NF-AB3244?ReferrerURL=https%3A%2F%2Fwww.google.com%2F
BNP ARCHITECT	Abbott Laboratories	08K28	Sandwich assay		NA
hsTnI ARCHITECT	Abbott Laboratories	G5-6634/RO1	Sandwich assay		NA
proBNP II	Roches Diagnostics	09315268190	Sandwich assay		NA
Kryptor MR-proANP	Thermo Fisher B.R.A.H.M.S	819.050	Sandwich assay		NA
cGMP	IBL/Tecan	RE29071	RIA		https://www.ibl-international.com/en/cgmp
ANP-(F-2)	Santa Cruz	515701	10 µg/mL		https://www.scbt.com/p/anp-antibody-f-2
CD13-specific inhibitory antibody WM-15	PharMingen	555393	5 µg/mL		https://www.bdbiosciences.com/en-us/products/reagents/flow-cytometry-reagents/research-reagents/single-color-antibodies-ruo/purified-mouse-anti-human-cd13.555393

DOI [to be added]

Cultured Cells

Name	Vendor or Source	Sex (F, M, or unknown)	Persistent ID / URL
HEK293	ATCC	unknown	https://www.atcc.org/products/crl-1573

Other

Description	Source / Repository	Persistent ID / URL
H-Ala-AMC	Bachem	https://www.fishersci.com/shop/products/h-ala-amc-50mg/NC1747106
Big-ET1 synthetic peptide	Peptide Institute	https://www.peptide.co.jp/en/catalog/f-cat?k_code=4208-s
Thiorphan	Sigma	https://www.sigmaaldrich.com/FR/fr/product/sigma/t6031
Recombinant human ECE1	R&D systems	https://www.rndsystems.com/products/recombinant-human-ece-1-protein-cf_1784-zn
Recombinant human ECE2	R&D systems	https://www.rndsystems.com/products/recombinant-human-ece-2-protein-cf_1645-zn
Recombinant human meprin B	R&D systems	https://www.rndsystems.com/products/recombinant-human-meprin-beta-subunit-mep1b-protein-cf_2895-zn
Recombinant human ANPEP	R&D systems	https://www.rndsystems.com/products/recombinant-human-aminopeptidase-n-cd13-protein-cf_3815-zn
Recombinant human corin	Origen	https://www.origene.com/catalog/proteins/recombinant-proteins/tp312742/corin-nm_006587-human-recombinant-protein
Recombinant human NEP	Sigma	https://www.sigmaaldrich.com/FR/fr/product/sigma/srp6450
synthetic GLP-17-36 amide	Cayman Chemical	https://www.caymanchem.com/product/15069
^{125}I-GLP1	Perkin Elmer	https://www.perkinelmer.com/uk/product/glp-1-7-36-125i-nex308010uc
mirVana PARIS kit	Ambion, Thermo Fisher Scientific	https://www.thermofisher.com/order/catalog/product/AM1556

DOI [to be added]

2 Article II. Deconvolution of BNP and NT-proBNP immunoreactivities by mass spectrometry in heart failure and sacubitril/valsartan treatment

Le BNP et NT-proBNP sont des biomarqueurs couramment mesurés pour le diagnostic, pronostic et le suivi des patients souffrant d'insuffisance cardiaque. Le proBNP est clivé en NT-proBNP et BNP_{1-32} par la furine, le BNP_{1-32} est lui-même clivé BNP_{3-32} par DPP4 ou BNP_{5-32} par la néprilysine (NEP). Chez les patients en insuffisance cardiaque chronique recevant du sacubitril/valsartan, une discordance d'évolution entre BNP et NT-proBNP a été observé. En effet, sous sacubitril/valsartan, le BNP restait stable ou augmentait modestement alors que le NT-proBNP diminuait. Nous avions fait l'hypothèse que la glycosylation du proBNP pouvait jouer un rôle dans l'évolution différentielle du BNP et NT-pro-BNP chez ces patients. De plus, les espèces moléculaires qui contribuent à chacun de ces dosages n'est que partiellement connue. Afin de tester cette hypothèse, nous avons comparé les dosages standards (BNPir et NT-proBNPir) avec les dosages par spectrométrie de masse des différentes espèces moléculaires contribuant aux deux biomarqueurs. Cette étude a été réalisée sur le spectre complet des patients chez lesquels le dosage du BNP ou NT-proBNP est pertinent : une cohorte de 73 patients en insuffisance cardiaque chronique avec fraction d'éjection du ventricule gauche réduite chez lesquels le sacubitril/valsartan a été introduit, une population de 49 souffrants d'insuffisance cardiaque aiguë, 51 patients souffrants de dyspnée aiguë d'origine non-cardiaque. Nous avons également mesuré ces peptides dans une population de sujet sain comme contrôle.

Les résultats de cette étude :

i) Confirment que le BNPir est la somme du proBNP, BNP_{1-32}, BNP_{3-32} et BNP_{5-32}, et que le proBNP est le contributeur majeur au signal, même si l'amplitude de cette contribution varie avec le contexte chimique.
ii) Confirme que la glycosylation du proBNP et NT-proBNP sur la serine 44 (S44) interfère avec le dosage de NT-proBNPir, et que le NT-proBNPir correspond à la somme du proBNP et NT-proBNP non-glycosylé en S44. La glycosylation en S44 varie en fonction du contexte clinique et explique la diminution du NT-proBNPir chez les patients traités par sacubitril/valsartan.
iii) Démontre que le BNPir et le NT-proBNPir sont de bons estimateurs de la production du proBNP, basé sur la mesure du peptide signal du proBNP comme marqueur indépendant du métabolisme du proBNP. Nos données montrent néanmoins que le NT-proBNPir est plus robuste et homogène.
iv) Contrairement à ce qui a été proposé, et contrairement à l'ANP, il ne semble pas y avoir de déficit de production de BNP dans l'insuffisance cardiaque.

Cette étude a donc permis de définir pour la première fois les espèces moléculaires qui contribuent aux dosages de BNPir et NT-proBNPir, et de mesurer leur contribution respective dans différents contextes physiologiques et pathologique. Cette étude montre également que le BNP n'est que peu associé avec les bénéfices observés chez les patients traités par le sacubitril/valsartan.

Deconvolution of BNP and NT-proBNP Immunoreactivities by Mass Spectrometry in Heart Failure and Sacubitril/Valsartan Treatment

Hélène Nougué,[a,b,†] Thibault Michel,[a,†] François Picard,[c] Johan Lassus,[d] Malha Sadoune,[a] Said Laribi,[e] Alain Cohen-Solal,[a,f] Damien Logeart,[a,f] Jean-Marie Launay,[a,*,‡] and Nicolas Vodovar[a,*,‡]

BACKGROUND: Elevated BNP and the N-terminal fragment of the proBNP (NT-proBNP) are hallmarks of heart failure (HF). Generally, both biomarkers parallel each other. In patients receiving sacubitril/valsartan, BNP remained stable while NT-proBNP decreased. As BNP and NT-proBNP assays have limited specificity due to cross-reactivity, we quantified by mass spectrometry (MS) the contributing molecular species.

METHODS: We included 356 healthy volunteers, 100 patients with acute dyspnoea (49 acute decompensated HF; 51 dyspnoea of non-cardiac origin), and 73 patients with chronic HF and reduced ejection fraction treated with sacubitril/valsartan. BNP and NT-proBNP immunoreactivities (BNPir and NT-proBNPir) were measured by immunoassays (Abbott ARCHITECT and Roche Diagnostics proBNPII) and proBNP-derived peptides and glycosylation at serine 44 by MS on plasma samples.

RESULTS: BNPir corresponded to the sum of $proBNP_{1–108}$, $BNP_{1–32}$, $BNP_{3–32}$, and $BNP_{5–32}$ ($R^2 = 0.9995$), while NT-proBNPir corresponded to $proBNP_{1–108}$ and $NT\text{-}proBNP_{1–76}$ not glycosylated at serine 44 ($R^2 = 0.992$). NT-proBNPir was better correlated ($R^2 = 0.9597$) than BNPir ($R^2 = 0.7643$) with proBNP signal peptide (a surrogate of proBNP production). In patients receiving sacubitril/valsartan, non-glycosylated $NT\text{-}proBNP_{1–76}$ remained constant ($P = 0.84$) despite an increase in $NT\text{-}proBNP_{1–76}$ and its glycosylation ($P < 0.0001$). $ProBNP_{1–108}$ remained constant ($P = 0.12$) while its glycosylation increased ($P < 0.0001$), resulting in a decrease in non-glycosylated $proBNP_{1–108}$ ($P < 0.0001$), and in NT-proBNPir.

CONCLUSIONS: Glycosylation interfered with NT-proBNPir measurement, explaining the discrepant evolution of these 2 biomarkers in patients receiving sacubitril/valsartan. Both BNPir and NT-proBNPir are surrogates of $proBNP_{1–108}$ production, NT-proBNPir being more robust in the clinical contexts studied.

Introduction

B-type natriuretic peptide (BNP) and the N-terminal fragment of the proBNP (NT-proBNP) are gold standard biomarkers for the diagnosis and prognosis of heart failure (HF) as implemented by international guidelines (1, 2). $BNP_{1–32}$ and $NT\text{-}proBNP_{1–76}$ are produced in a 1:1 ratio from the cleavage of $proBNP_{1–108}$ by the action of the convertases furin or corin between arginine 76 and serine 77 (3; Fig. 1). proBNP is *O*-glycosylated at 7 positions within its N-terminal fragment (4), and glycosylation at threonine 71 (T71) prevents the cleavage of proBNP by furin (5), thereby playing a major role in the bioavailability of bioactive $BNP_{1–32}$ both in vitro and in vivo (6, 7). While little is known regarding further processing or degradation of $NT\text{-}proBNP_{1–76}$ besides its renal elimination, $BNP_{1–32}$ has been shown to produce shorter peptides in humans as the result of proteolytic cleavage by various proteases including dipeptidyl peptidase 4 (DPP4) ($BNP_{3–32}$, 8) and neprilysin ($BNP_{5–32}$, 9) amongst others.

Sacubitril/valsartan is a first-in-class fixed dose angiotensin receptor–neprilysin inhibitor that combines a neprilysin inhibitor (sacubitril) and an angiotensin

[a]Université Paris Cité and Inserm UMR-S 942, Paris, France; [b]Department of Anesthesiology and Intensive Care, Saint-Louis and Lariboisière Hospital, Paris, France; [c]Heart Failure Unit, Haut-Lévêque Hospital, Pessac, France; [d]Heart and Lung Center, Helsinki University and Helsinki University Hospital, Helsinki, Finland; [e]Emergency Medicine Department, Tours University Hospital, Tours, France; [f]Department of Cardiology, Lariboisière Hospital, Paris, France.

*Address correspondence to: N.V. at Inserm UMR-S 942, 41 boulevard de la Chapelle, Paris Cedex 10 75475, France. Fax +33-1-53-21-67-39; E-mail nicolas.vodovar@inserm.fr. J-M.L. at Inserm UMR-S 942, 41 boulevard de la Chapelle, Paris Cedex 10 75475, France. Fax +33-1-53-21-67-39; E-mail jean-marie.launay@inserm.fr.
[†]H.N. and T.M. equally contributed to this work.
[‡]J-M.L. and N.V. share senior authorship.
Received September 19, 2022; accepted December 13, 2022.
https://doi.org/10.1093/clinchem/hvac225

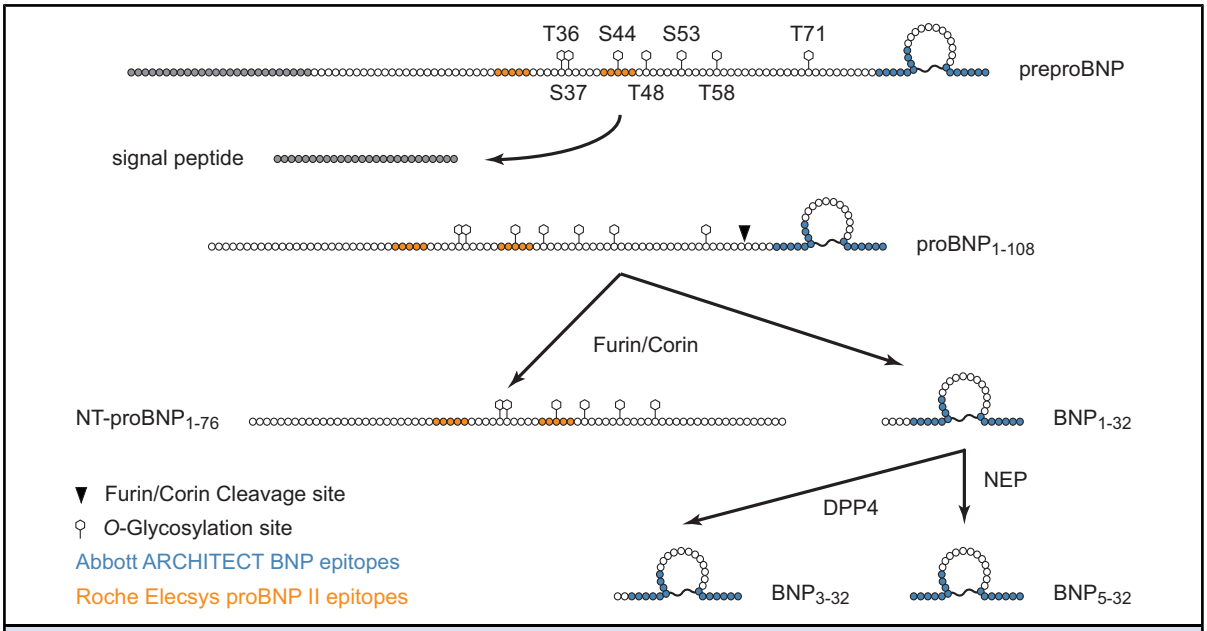

Fig. 1. Schematic representation of human pre-proBNP processing. The residues that are glycosylated are indicated; T71 when glycosylated prevents $proBNP_{1–108}$ cleavage and is not found in $NT\text{-}proBNP_{1–76}$. Shown in blue are the amino acids recognized by the antibodies of the ARCHITECT BNP assay; shown in orange are the amino acids recognized by the NT-proBNP II assay (Roche Diagnostics). The nomenclature of the molecular species considered is used for MS data throughout the manuscript. Abbreviations: NEP, neprilysin; DPP4, dipeptidyl peptidase 4.

receptor blocker (valsartan) (10). Sacubitril/valsartan was shown to be superior to enalapril for the treatment of heart failure with reduced ejection fraction (HFrEF), reducing mortality and hospital readmission by 20% (10). In various studies, sacubitril/valsartan treatment was shown to lead to a decrease in NT-proBNP while BNP remained unchanged or moderately increased (11, 12). However, patients whose NT-proBNP (13) or BNP (14) decreased the most benefited the most from the treatment and both biomarkers predicted the risk of major adverse events (14).

From an analytical standpoint, commercial assays for BNP and NT-proBNP have been shown to cross-react to various extents with $proBNP_{1–108}$ (Fig. 1). Indeed, BNP assays fully cross-react with $proBNP_{1–108}$, and the latter contributes most to BNP immunoreactivity in acute and chronic HF (15–20). NT-proBNP assays also cross-react with $proBNP_{1–108}$; however, several studies have shown that one epitope used in all commercial NT-proBNP assays overlaps serine 44 (S44) that can be glycosylated (21), thereby preventing the binding of the antibodies used. Consequently, NT-proBNP assays only detect the non-glycosylated fraction of $proBNP_{1–108}$ and $NT\text{-}proBNP_{1–76}$ (22–24). Although medical conditions and treatments may affect $proBNP_{1–108}$/$NT\text{-}proBNP_{1–76}$ glycosylation at the epitopes recognized by the assays, as we previously observed for T71 proBNP glycosylation (6), little is known about the impact of other glycosylations on NT-proBNP immunoreactivity, in particular at S44, in those contexts.

Materials and Methods

SUBJECTS

This study involving human subjects was performed according to the current revision of the Helsinki Declaration. First, we studied 73 patients with HFrEF who were switched from angiotensin receptor blocker or angiotensin-converting enzyme inhibitor to sacubitril/valsartan as per the current European guidelines (1). Plasma samples were collected at baseline—i.e., before the first dose of sacubitril/valsartan, 30 days (D30), and 3 months (D90) after the initiation of the treatment (11). Second, a subset of 100 patients admitted to the emergency department for acute dyspnoea and for which proBNP glycosylation at T71 was previously measured was also included (6). Amongst these patients, 49 patients had acute decompensated heart failure (ADHF) and 51 patients had acute non-cardiac dyspnoea (ANCD). The diagnosis of the cardiac or non-cardiac origin of the dyspnoea was first performed by the emergency physician and independently adjudicated by

a senior cardiologist and an intensivist, both heart failure experts based on patient files and BNP concentrations. Finally, we included 356 healthy controls (44% women; 56% men; median age 34 years [interquartile range {IQR}: 29–37]), free from cardiovascular disease, diabetes (glycated hemoglobin <6%), obesity (body mass index, BMI <25 kg/m^2), kidney disease (estimated glomerular filtration rate (eGFR) chronic kidney disease epidemiology (CKD-EPI) >60 mL/min/1.73 m^2), or any ongoing pharmacological treatment. In all the cohorts, plasma was obtained from venous blood collected in tubes containing EDTA (ethylenediaminetetraacetic acid) immediately centrifuged at 2200 × *g* for 15 min at 4 °C, and stored at −80 °C within 30 min after collection until further use. The samples used in this study were not subject to any freeze–thaw cycles before use. In some instances, the number of patients is lower due to plasma samples exhaustion and the use of repeated-measure ANOVA.

MEASUREMENT OF BNP AND NT-PROBNP BY SANDWICH ASSAYS

Immunoreactive NT-proBNP was measured using the Elecsys® proBNP II kit on a Roche Cobas analyzer e601 (Roche). Immunoreactive BNP was measured using the BNP ARCHITECT assay on an ARCHITECTi2000 (Abbott Diagnostics). Measurements obtained by the 2 immunoassays were converted into molar units using the molar mass of the calibrator used in each assay: synthetic $BNP_{1–32}$ (3464.04 g.mol^{-1}) and synthetic non-glycosylated NT-$proBNP_{1–76}$ (8457.49 g.mo/l−1) to allow comparisons with mass spectrometry (MS) data. The analytical characteristics of the sandwich assays are presented in online Supplemental Table 1.

proBNP AND DERIVATIVE QUANTIFICATION BY MASS SPECTROMETRY

NT-proBNP and proBNP glycosylation at S44 were determined by LC-MS/MS as previously described (6). Glycosylation expressed in % was calculated as the ratio between the amount of glycosylated peptide/the total amount of the peptide. Quantifications of $proBNP_{1–108}$, NT-$proBNP_{1–76}$, $BNP_{1–32}$, $BNP_{3–32}$, $BNP_{5–32}$, and proBNP signal peptide were performed by capillary electrophoresis (CE)-MS/MS as previously described (25). A detailed description of the MS/MS methodology used is presented in the online Supplemental Data. The analytical characteristics of the mass spectrometry quantifications are presented in Supplemental Table 1.

IN VITRO ASSAY

Human embryonic kidney 293 cell (HEK293) cells that were stably transfected with the human atrial natruretic peptide (ANP) and BNP receptor (NPRA) were incubated with 2.5 nM of synthetic human $proBNP_{1–108}$, NT-$proBNP_{1–76}$, $BNP_{1–32}$, $BNP_{3–32}$, or $BNP5_{–32}$ for 10 min at 37 °C. Maximal cGMP production was measured by radioimmunoassay (Tecan).

STATISTICAL ANALYSIS

All statistical analyses were performed using R statistical software (26). The normality of each variable was assessed using the Shapiro–Wilk normality test. Continuous variables are expressed as median [IQR]. Within-group ratios were calculated for each individual, and their median and IQR were reported. Continuous data were analyzed using the Wilcoxon rank-sum test, or the Kruskal–Wallis test followed by Wilcoxon rank-sum tests; *P*-values for multiple comparisons were corrected by the Holm–Bonferroni method. Longitudinal data were analyzed using repeated-measures ANOVA followed by the Tukey honest significant differences test on log-transformed values. In vitro data were analyzed by ANOVA followed by the Student *t*-test corrected for multiple comparisons. The correlation between variables was evaluated by a fitted linear model (R^2) or Spearman correlation coefficient (ρ). A *P*-value <0.05 was considered statistically significant.

Results

DECONVOLUTION OF BNP IMMUNOREACTIVITY BY MS

Based on the epitopes recognized by the ARCHITECT BNP assay (21), the assay can potentially detect $BNP_{1–32}$, $BNP_{3–32}$, and $BNP_{5–32}$ as well as $proBNP_{1–108}$ (Fig. 1). Hence, we hypothesized that BNP immunoreactivity (BNPir) measured by the assay was the sum of these 4 molecular species quantified by mass spectrometry (referred as to theoretical BNPir thereafter) in each of the 4 cohorts: patients with ADHF, patients with ANCD, patients with HFrEF before and after the initiation of sacubitril/valsartan, and controls. The plasma levels of the 4 molecular species in the 4 cohorts (HFrEF represent baseline values) are presented in Table 1. Theoretical and measured BNPir were very strongly correlated (Fig. 2, A), irrespectively of the health status and medication. The slope of the linear regression model indicated that mass spectrometry captured all the BNPir signal, which was confirmed by Bland–Altman plotting (online Supplemental Fig. 1, A).

Next, we looked at the contribution of the various molecular species that contribute to BNPir and show a variable composition of BNPir with regards to the health status (Fig. 2, B and Table 1): $proBNP_{1–108}$ constitutes more than 90% of BNPir in ADHF, ANCD, and HFrEF patients, while only contributing to approximately 50% of the signal in healthy volunteers. Conversely, the contribution of $BNP_{1–32}$, $BNP_{3–32,}$ and $BNP_{5–32}$ to BNPir was approximately 50% in controls, and <6% in ADHF, ANCD, and HFrEF patients.

Table 1. BNP and NT-proBNP immunoreactivities and $proBNP_{1–108}$ and derivatives measured by MS/MS in the 4 studied cohorts.

Variables (pM unless specified, with median and IQR)	Controls	HFrEF[a]	ADHF	ANCD	*P*
BNPir	1.62 [1.15–2.25]	107.5[b] [57.5–195.7]	394.91[c] [229.7–584.3]	12.41[c] [6.5–21.8]	<0.0001
NT-proBNPir	2.3 [1.6- 3.2]	151[b] [68.3–248]	1061.1[c] [518.2–1755.4]	25.4[c] [11.4–53.4]	<0.0001
$proBNP_{1–108}$	0.8 [0.5–1.2]	87.9 [47.6–182.2]	391.2 [219.5–575.7]	12.2 [6.2–20.7]	<0.0001
$BNP_{1–32}$	0.1 [0.1–0.1]	3.3 [1.8–4.7]	8.1 [6.3–9.7]	0.2 [0.1–0.3]	<0.0001
$BNP_{3–32}$	0.46 [0.34–0.68]	1.63 [1.15–2.16]	0.37 [0.09–0.67]	0.02 [0.02–0.02]	<0.0001
$BNP_{5–32}$	0.2 [0.13–0.31]	4.9 [2.7–7.5]	0.46 [0.15–0.8]	0.02 [0.02–0.02]	<0.0001
$NT\text{-}proBNP_{1–76}$	3 [1.9–4.8]	156 [108–257.3]	652.2 [180.7–1118.2]	18.23 [6.6–47.3]	<0.0001
$proBNP_{1–108}$ S44 glyc. (%)	47.5 [39–57]	58.1 [40.9–71.8]	7.7 [6.1–9.2]	8.2 [7–9.2]	<0.0001
$NT\text{-}proBNP_{1–76}$ S44 glyc. (%)	49 [39–59]	31.7 [24.7–41.4]	7.2 [6.1–8.3]	7.8 [6.6–8.6]	<0.0001
proBNP SP	3.41 [2.5–5.1]	122.8 [62.3–223.1]	665.6 [410.7–1064.3]	19.64 [9.2–42]	<0.0001
$proBNP_{1–108}$/BNPir	49.3% [43.7–53.3]	88.3% [84.2–93.1]	92.5% [84.8–96.0]	98.4% [95.6–98.9]	<0.0001
$BNP_{1–32}$/BNPir	5.5% [3.6–8.8]	2.8% [1.4–5.2]	3.3% [1.8–7.2]	1.5% [1.0–3.9]	<0.0001
$BNP_{3–32}$/BNPir	31.2% [25.6–36.0]	1.5% [0.9–3]	1.6% [0.8–3.5]	0.07% [0.03–0.14]	<0.0001
$BNP_{5–32}$/BNPir	12.8% [7.9–18.0]	4.8% [2.8–8.5]	0.29% [0.13–2.76]	0.11% [0.02–0.18]	<0.0001
$proBNP_{1–108}$ S44 not glyc./NT-proBNPir	20.7% [14.1–28.5]	24.3% [13.6–34.7]	13.9% [7.1–26.6]	36.1% [23.4–66.1]	<0.0001
$NT\text{-}proBNP_{1–76}$ S44 not glyc./NT-proBNPir	79.4% [71.5–85.9]	75.7% [65.3–86.4]	86.1% [73.5–92.9]	63.9% [33.9–76.6]	<0.0001

BNPir: BNP plasma levels measured with the Abbott ARCHITECT assay; NT-proBNPir: NT-proBNP levels measured with the Roche Diagnostics proBNP II assay.
Abbreviation: S44 glyc., glycosylation at serine 44.
[a]Baseline values before the initiation of sacubitril/valsartan.
[b]Published in (11).
[c]Published in (6).

DECONVOLUTION OF NT-PROBNP IMMUNOREACTIVITY BY MS

Based on the epitopes recognized by the Elecsys proBNP II assay (21), the assay can detect $proBNP_{1–108}$ and $NT\text{-}proBNP_{1–76}$. As glycosylation at S44 interferes with the binding of one of the antibodies (24), we hypothesized that NTproBNP immunoreactivity (NT-proBNPir) measured by the assay was the sum of $proBNP_{1–108}$ and $NT\text{-}proBNP_{1–76}$ not glycosylated at S44 (referred as to theoretical NT-proBNPir thereafter). We measured $proBNP_{1–108}$, $NT\text{-}proBNP_{1–76}$, and their

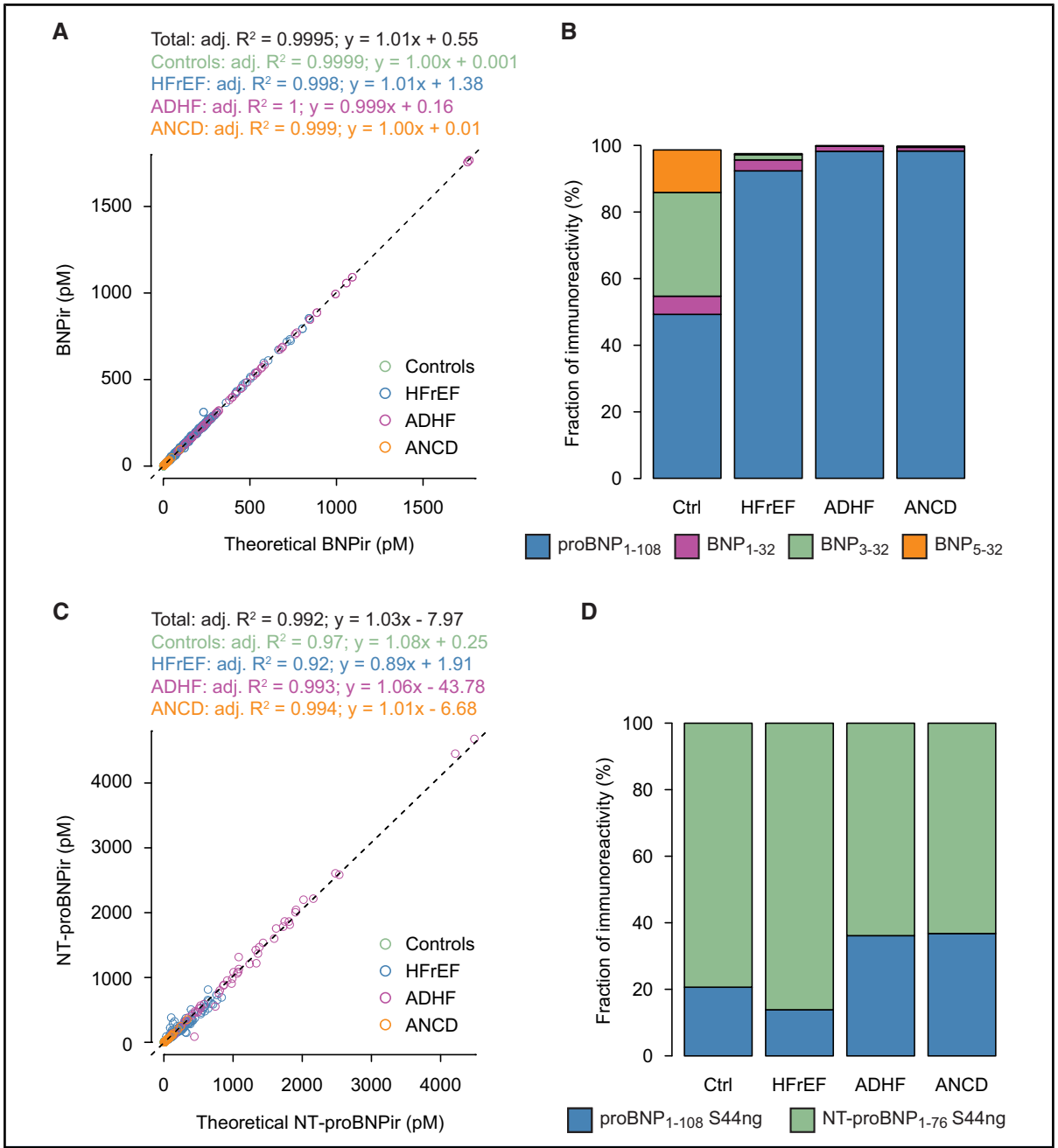

Fig. 2. Comparisons between BNP and NT-proBNP immunoreactivities and MS quantifications. (A), Correlation between measured (Abbott ARCHITECT, BNPir) and theoretical BNP immunoreactivity as the sum of $proBNP_{1–108}$, $BNP_{1–32}$, $BNP_{3–32}$, and $BNP_{5–32}$ as quantified by MS in the different cohorts; (B), Contribution of each of the molecular species to theoretical BNP immunoreactivity in the different cohorts; (C), Correlation between measured (Roche Diagnostics, proBNP II assay, NT-proBNPir) and theoretical BNP immunoreactivity as the sum of $proBNP_{1–108}$ and $NTproBNP_{1–76}$ not glycosylated at S44 as quantified by MS in the different cohorts; (D), Contribution of each of the molecular species to theoretical NT-proBNP immunoreactivity in the different cohorts. In (A) and (C), the correlations were calculated using linear regression models on all the subjects (black) and each cohort individually. Abbreviations: adj. R^2, adjusted R^2; S44ng, not glycosylated at S44.

S44-glycosylated forms (Table 1) and calculated theoretical NTproBNPir. Figure 2, C shows a strong correlation between theoretical and measured NT-proBNPir, indicating that mass spectrometry captured most of the NT-proBNPir signal, which was confirmed by Bland–Altman plotting (Supplemental Fig. 1, B). However, the agreement between measured and theoretical NT-proBNPir was lower than the agreement observed for BNPir. In patients with HFrEF, the slope of the linear regression strongly suggests another molecular species involved in the NT-proBNPir signal, which would increase linearly with NT-proBNPir (Fig. 2, C). Of note, NT-proBNPir is not a good estimator of either $proBNP_{1–108}$ (Supplemental Fig. 1, C) or $NT\text{-}proBNP_{1–76}$ (Supplemental Fig. 1, D) plasma levels, especially in controls and HFrEF patients. In ADHF and ANCD patients, NT-proBNPir is not a good estimator of $proBNP_{1–108}$ but a rather good estimator of $NT\text{-}proBNP_{1–76}$, probably reflecting overall metabolic differences between stable and acute conditions.

Next, we looked at the contribution of the 2 molecular species that contribute to the NT-proBNPir and show a variable composition of NT-proBNPir depending on the health status (Fig. 2, D and Table 1). In particular, both ADHF and ANCD patients exhibited similar profiles.

NATRIURETIC PEPTIDE IMMUNOREACTIVITY AND proBNP PRODUCTION

We previously showed that proANP signal peptide (SP) was a good surrogate of proANP production and independent of proANP metabolism (25). Applying the same reasoning, we measured the proBNP SP as a surrogate of proBNP production that is independent of proBNP metabolism. Overall, both BNPir (Fig. 3, A) and NT-proBNPir (Fig. 3, B) correlated strongly with proBNP SP. However, NT-proBNPir was a better and more consistent correlate than BNPir across the 4 cohorts. In particular, BNPir poorly correlated with proBNP SP in acute conditions, especially in ANCD patients. This may reflect overall metabolic differences between stable and acute conditions.

IMPACT OF SACUBITRIL/VALSARTAN TREATMENT ON BNP IMMUNOREACTIVITY

We previously showed that BNPir plasma levels did not change throughout the study in HFrEF patients treated with sacubitril/valsartan (11, online Supplemental Fig. 2, A). We next looked at the evolution of the molecular species that contribute to BNPir in these patients. Results show that $proBNP_{1–108}$ remained unchanged after the initiation of sacubitril/valsartan (Fig. 4, A) while proBNP SP decreased moderately at D30 (Fig. 4, B). In contrast, the sum of $BNP_{1–32}$, $BNP_{3–32}$, and $BNP_{5–32}$ remained unchanged at D30 (D0: 10.7 pM [7.5–14.4] vs D30: 9.3 pM [6.1–12.5]; $P = 0.45$) but decreased at D90 (3.1 pM [1.6–8.3]; $P < 0.0001$). Taking the molecular species individually, there was a transient increase in $BNP_{1–32}$ at D30 (Fig. 4, C) that resulted from the expected disappearance of $BNP_{5–32}$ (Fig. 4, E), the degradation product of $BNP_{1–32}$ by neprilysin that is inhibited by sacubitril. $BNP_{3–32}$ remained unchanged at D30 and decreased at D90 (Fig. 4, D).

To evaluate any potential functional impact of these variations in $BNP_{1–32}$, $BNP_{3–32}$, and $BNP_{5–32}$, we incubated HEK293 cells that stably express NPRA with 2.5 nM of each peptide and measured the resulting maximal cGMP production. Results show that $BNP_{1–32}$ was the best NPRA agonist, with $BNP_{3–32}$ and $BNP_{5–32}$ retaining 87% and 34% of $BNP_{1–32}$ activity, and $proBNP_{1–108}$ exhibiting only 6% of $BNP_{1–32}$ activity (Fig. 4, F). These results indicate that neprilysin inhibition provokes the disappearance of a weaker NPRA agonist ($BNP_{5–32}$) to the benefit of a more active one ($BNP_{1–32}$).

IMPACT OF SACUBITRIL/VALSARTAN TREATMENT ON NT-PROBNP IMMUNOREACTIVITY

Unlike NT-proBNPir, which decreased at D30 after initiation of sacubitril/valsartan (11, Supplemental Fig. 2, B), $NT\text{-}proBNP_{1–76}$ increased at D30 (Fig. 5, A) and $proBNP_{1–108}$ remained unchanged (Fig. 4, A). Consequently, the $NT\text{-}proBNP_{1–76}$/proBNP SP ratio increased as an indicator of $proBNP_{1–108}$ cleavage, hence $BNP_{1–32}$ production (Fig. 5, B). As glycosylation at S44 interferes with NT-proBNPir, we measured S44 glycosylation for $proBNP_{1–108}$ and $NT\text{-}proBNP_{1–76}$ at the 3 time points. Both $proBNP_{1–108}$ (Fig. 5, C) and $NT\text{-}proBNP_{1–76}$ (Fig. 5, D) S44 glycosylation markedly increased at D30. However, the decrease in $NT\text{-}proBNP_{1–76}$ compensated for the increase of its S44 glycosylation, resulting in stable S44 unglycosylated $NT\text{-}proBNP_{1–76}$ plasma levels (Fig. 5, E), while S44 glycosylated $proBNP_{1–108}$ plasma levels markedly decreased (Fig. 5, F). We next verified that the evolution in BNPir and NT-proBNPir still reflected the variation in $proBNP_{1–108}$ production using proBNP SP as a surrogate between baseline and 30 days after initiation of sacubitril/valsartan. Both BNPir ($\rho = 0.78$; $R^2 = 0.57$, online Supplemental Fig. 3, A) and NT-proBNPir ($\rho = 0.85$; $R^2 = 0.74$, Supplemental Fig. 3, B) strongly correlated (Spearman correlation, ρ) to proBNP SP changes, although the variation in NT-proBNPir correlated better when using linear regression (R^2). Finally, proBNP T71 glycosylation was reported to be different in obese (BMI > 30) and lean heart failure patients (27). However, in the HFrEF patients at baseline, neither $proBNP_{1–108}$ S44 glycosylation (BMI ≤ 30: 59%

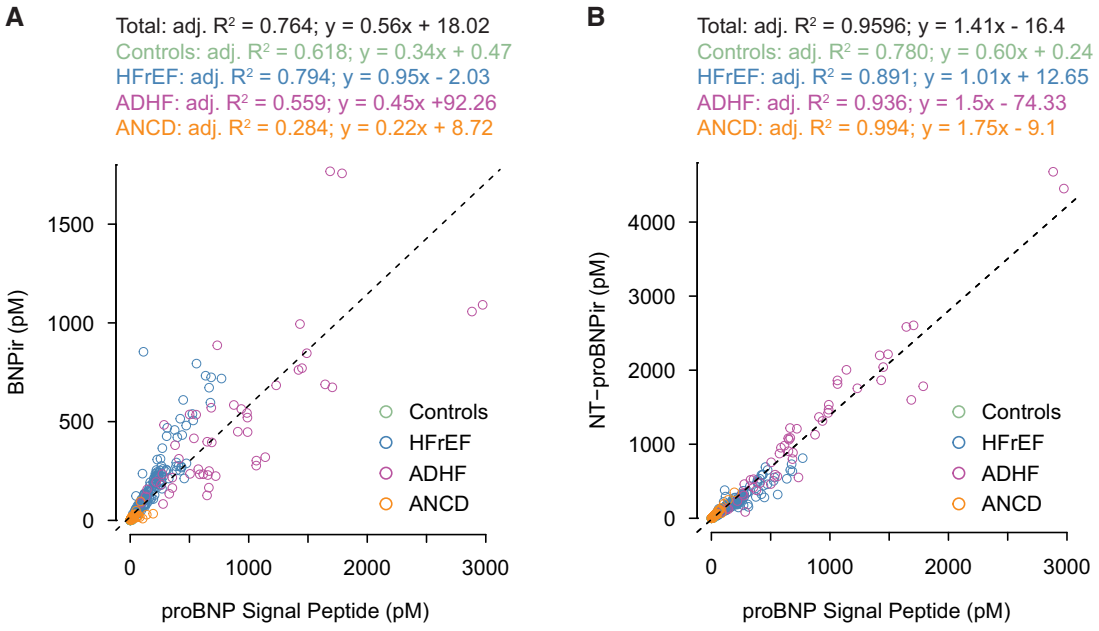

Fig. 3. Comparison between BNP and NT-proBNP immunoreactivities and proBNP signal peptide. Correlation between BNP (A) and NT-proBNP (B) immunoreactivities measured by sandwich assay and proBNP signal peptide as a surrogate for proBNP production. The correlations were calculated using linear regression models on all the subjects (black) and each cohort individually. Abbreviations: adj. R^2, adjusted R^2; S44ng, not glycosylated at S44.

[43.5–74.35]; n = 57; BMI > 30: 47.6% [37.7–60.5], n = 57; $P = 0.11$) nor NT-proBNP$_{1–76}$ S44 glycosylation (BMI ≤ 30: 31.5% [24.7–41]; BMI > 30: 36.7% [25.2–42.5]; $P = 0.73$) were different between the 2 BMI groups.

Discussion

The relative contribution of molecular species that contribute to BNP and NT-proBNP immunoreactivities has not previously been quantified in multiple cohorts. While BNP and NT-proBNP immunoreactivities are concordant in most contexts, the introduction of sacubitril/valsartan has challenged the use of BNPir which behaves conversely to NT-proBNPir. Although many explanations for this discrepant behavior have been proposed, the reason remains largely unknown.

From an analytical standpoint, we confirmed that BNPir corresponds mostly to proBNP$_{1–108}$ regardless of the pathophysiological or physiological context and therapeutics, including sacubitril/valsartan (15–19). We also confirmed and quantified that NT-proBNPir corresponds to proBNP$_{1–108}$ and NT-proBNP$_{1–76}$ species that are not glycosylated at S44 (24), regardless of the pathophysiological or physiological context and therapeutics, including sacubitril/valsartan.

These results, therefore, indicate that BNPir is a composite signal that should theoretically best reflect proBNP production, while NT-proBNPir is a more complex composite signal that should theoretically reflect both production and intracellular (glycosylation) and extracellular (cleavage) metabolism. However, considering proBNP SP as a metabolically independent surrogate of proBNP$_{1–108}$ production, we found that BNP and NT-proBNP immunoreactivities were both strongly correlated to proBNP SP, although surprisingly NT-proBNP immunoreactivity was a better correlate. In particular, NT-proBNPir correlated with proBNP SP more consistently in groups with different health status, while the correlation between BNPir and proBNP SP was weaker in acute conditions, especially in ANCD.

The fact that NT-proBNPir is better correlated to proBNP$_{1–108}$ production (signal peptide) can only result from serendipity since the proBNP II assay was developed before any knowledge of proBNP glycosylation, and independently from the estimation of proBNP$_{1–108}$ production (signal peptide). The reason for the lower correlation between BNPir and proBNP SP probably results from the higher consumption of the bioactive

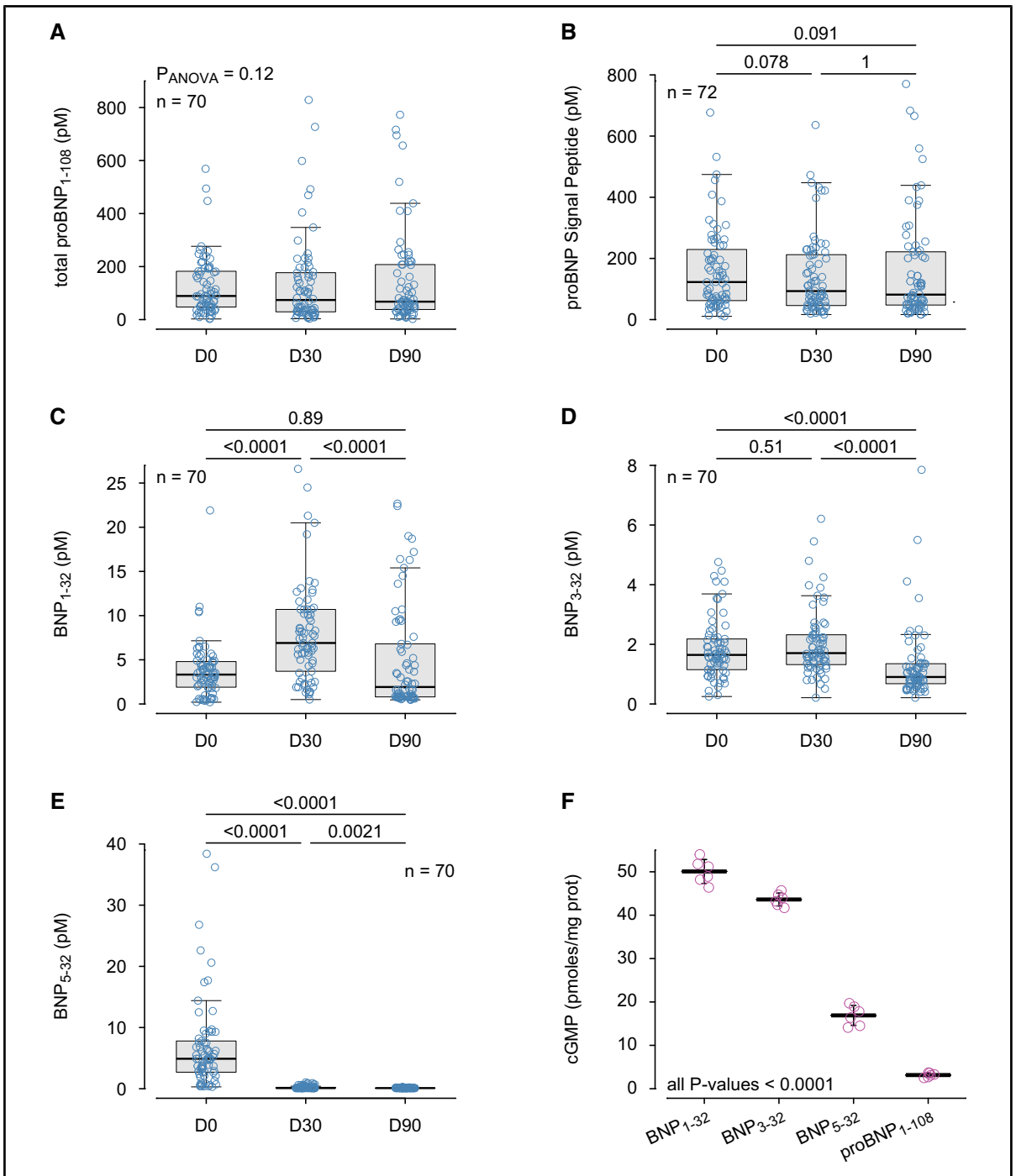

Fig. 4. Impact of sacubitril/valsartan on BNP immunoreactivity. Plasma levels of total proBNP$_{1–108}$ (A), proBNP signal peptide (B), BNP$_{1–32}$ (C), BNP$_{3–32}$ (D), and BNP$_{5–32}$ (E) in HFrEF patients at baseline (D0), 30, and 90 days after the initiation of sacubitril/valsartan. (F), Maximal cGMP production measured in NPRA-expressing HEK293 cells after a 10-min incubation with 2.5 nM of various peptides. The variables in (A)–(E) were analyzed using repeated-measures ANOVA on log-transformed data followed by the Tukey honestly significant difference test. In (F), the data were analyzed using the Kruskal–Wallis test followed by the rank-sum Wilcoxon test corrected for multiple comparisons. In (A), the *P*-value is that of the repeated-measure ANOVA.

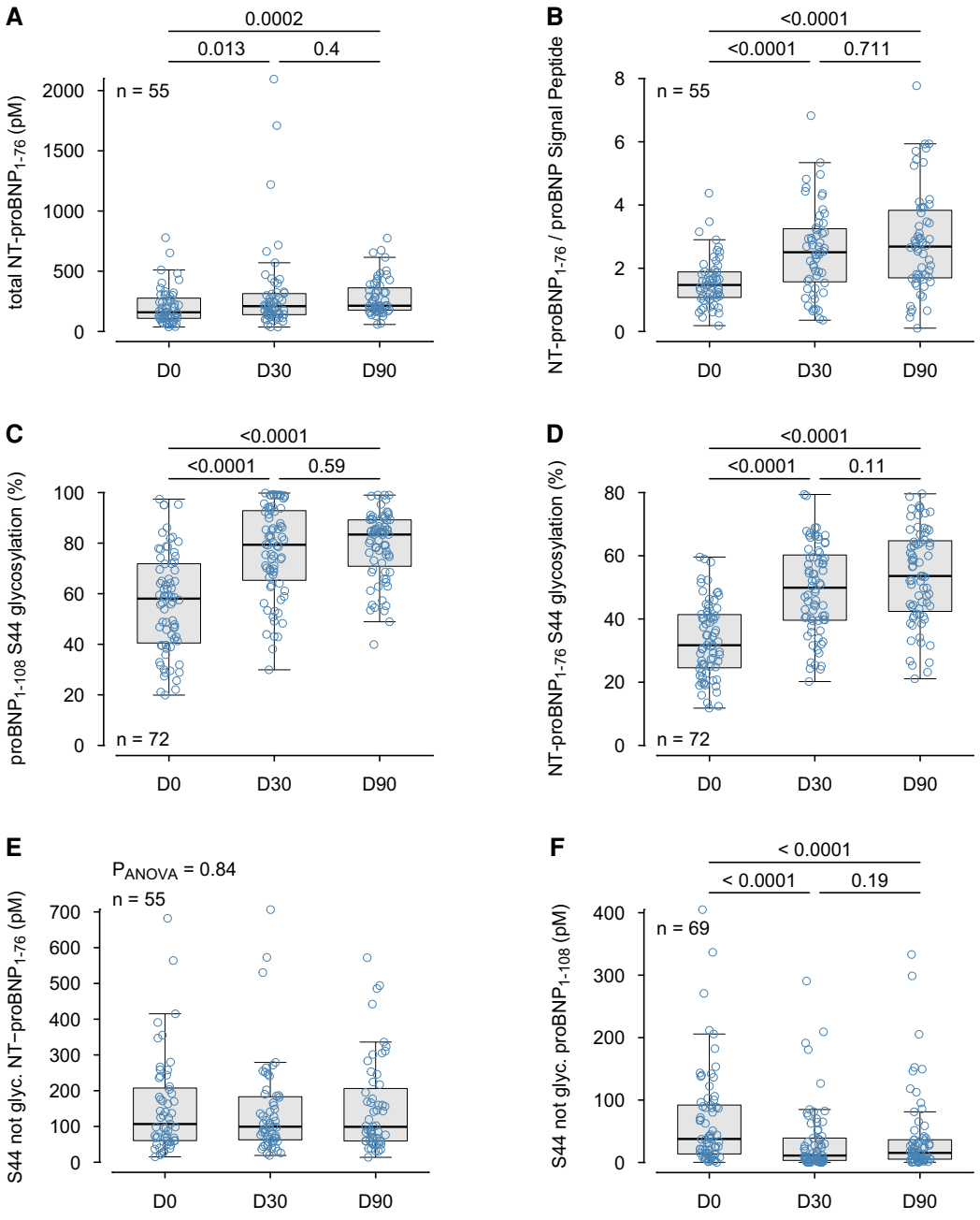

Fig. 5. Impact of sacubitril/valsartan on NT-proBNP immunoreactivity. (A), Plasma levels of total NT-proBNP$_{1–76}$ in HFrEF patients at baseline (D0), 30, and 90 days after the initiation of sacubitril/valsartan; (B), Ratio between NT-proBNP$_{1–76}$ and proBNP signal peptide as a surrogate for proBNP$_{1–108}$ processing in HFrEF patients at baseline, 30, and 90 days after the initiation of sacubitril/valsartan; (C, D), Relative proBNP$_{1–108}$ (C) and NT-proBNP$_{1–76}$ (D) glycosylation at S44 in HFrEF patients at baseline, 30, and 90 days after the initiation of sacubitril/valsartan; (E, F), Absolute quantification of proBNP$_{1–108}$ (E) and NT-proBNP$_{1–76}$ (F) not glycosylated at S44 in HFrEF patients at baseline, 30, and 90 days after the initiation of sacubitril/valsartan. The variables were analyzed using repeated-measures ANOVA on log-transformed data followed by the Tukey honestly significant difference test. In (E), the *P*-value is that of the repeated-measure ANOVA.

peptides $BNP_{1–32}$, $BNP_{3–32}$, and $BNP_{5–32}$, either by greater binding to their receptor NPRA, in vivo elimination (degradation or renal excretion), or lower in vitro stability.

There was no difference between ADHF and non-ADHF patients for S44 glycosylation and BNPir or NT-proBNPir signal composition. In patients admitted to the emergency department for acute dyspnoea, exclusion thresholds for the diagnosis of ADHF have been suggested (<100 pg/mL for BNPir and <300 pg/mL for NT-proBNPir) (1, 2, 28). However, in patients with BNPir or NT-proBNPir plasma levels moderately above these thresholds—formerly known as the grey zone—the cardiac or non-cardiac origin of the dyspnoea is often difficult to establish. In those instances, our data strongly suggest that no B-type natriuretic peptide-based biomarker could help discriminate the origin of the dyspnoea, specifically in those patients. Overall, these results indicate that the correlation between NT-proBNPir and $proBNP_{1–108}$ production (signal peptide) is more robust and independent of the health status (acute vs chronic HF), making its pathophysiological interpretation easier. Both BNPir and NT-proBNPir as biomarkers are equally effective for the diagnosis and prognosis of HF and either could be used. However, given the high variability of BNPir and NT-proBNPir across assays and platforms (29) (BNPir being more impacted) we would highly recommend, as does the International Federation of Clinical Chemistry (30), the use of the same biomarker with the same assay/platform when it comes to following the clinical course of these patients.

In HFrEF patients treated with sacubitril/valsartan, the dissociated evolution of BNPir and NT-proBNPir was initially attributed to the reduced degradation of $BNP_{1–32}$ by neprilysin inhibition. However, $BNP_{1–32}$ is a poor neprilysin substrate in humans (31) and its main cleavage product by neprilysin ($BNP_{5–32}$) can be detected by the Abbott BNP assay. Furthermore, at D30 after initiation of sacubitril/valsartan the expected disappearance of $BNP_{5–32}$ translated into an equal increase in $BNP_{1–32}$, overall not changing the contribution of the sum of these molecular species to BNPir. Instead, we proposed that proBNP glycosylation could be responsible for the decrease in NT-proBNPir (11, 32). Here, we confirm this hypothesis and show that the decrease in NT-proBNP immunoreactivity results from an analytical interference of $proBNP_{1–108}$ and $NT\text{-}proBNP_{1–76}$ glycosylation at S44 with the assay. While the increase in $NT\text{-}proBNP_{1–76}$ and $NT\text{-}proBNP_{1–76}$ S44 glycosylation cancelled each other and produced unchanged concentration of S44-unglycosyated $NT\text{-}proBNP_{1–76}$, S44-unglycosylated $proBNP_{1–108}$ markedly decreased, provoking the decrease in NT-proBNPir observed in those patients. However, the mechanism involved in the variations of $proBNP_{1–108}$ and $NT\text{-}proBNP_{1–76}$ S44 glycosylation observed in acute dyspnoea, HFrEF, and sacubitril/valsartan treatment remains to be established.

In patients treated with sacubitril/valsartan, ANP markedly increased in response to neprilysin inhibition (11, 33). This increase is multifactorial and involves the increase in proANP production and cleavage, and the protection of ANP from inactivation by cleavage (25). Regarding the production of $proBNP_{1–108}$ (signal peptide), sacubitril/valsartan has only a modest impact on proBNP production, which suggests that sacubitril/valsartan (*a*) has little impact on the stimuli that regulate $proBNP_{1–108}$ production and that (*b*) $proBNP_{1–108}$ production is not as hampered by HF as proANP production. However, in patients who respond the best to sacubitril/valsartan—i.e., those for whom either BNPir or NT-proBNPir decreased the most (13, 14)—our data suggest that the production of $proBNP_{1–108}$ (signal peptide) decreases. This is likely to be associated with a decrease in the stimuli that are responsible for $proBNP_{1–108}$ production, as $proBNP_{1–108}$ glycosylation is already very high despite a moderate decrease in NT-proBNPir. A similar scenario is also likely in patients with ADHF treated with sacubitril/valsartan at discharge (34) and patients with HF and preserved ejection fraction (35).

Importantly, while changes in both BNPir and NT-proBNPir between baseline and D30 after initiation of the sacubitril/valsartan remained unchanged or modest, a similar variation in either biomarker reflects changes in $proBNP_{1–108}$ production (signal peptide) similarly, suggesting that either biomarker can be used. Of note, NT-proBNPir varied more linearly with proBNP SP than BNPir did, rendering the interpretation more straightforward. From a pathophysiological standpoint, changes in ANP production are greater than those in $BNP_{1–32}$ and derivatives. Nevertheless, sacubitril/valsartan likely provokes an increase in BNP-mediated NPRA signaling via two mechanisms: (*a*) the increase in $BNP_{1–32}$ due to the inhibition of its cleavage into the less biologically active $BNP_{5–32}$ by neprilysin, and (*b*) by an increase in $proBNP_{1–108}$ processing, which consequently increases $BNP_{1–32}$ production. The decrease in all $BNP_{1–32}$ and derivatives at D90 despite an increase in $proBNP_{1–108}$ processing suggests that $BNP_{1–32}$ and $BNP_{3–32}$ are more consumed, possibly by an increase in binding to NPRA, although an increase in elimination cannot be excluded. Nevertheless, the impact of BNP on the improvement observed in HFrEF patients treated with sacubitril/valsartan remains probably marginal when compared to the amplitude of its impact on ANP (11, 25, 33, 36). This reinforces the pleiotropic effects of sacubitril/valsartan on HFrEF as NYHA improvement was not associated with variations in either BNPir or NT-proBNPir (11).

Based on the increase observed in ANP (11, 33), one could be tempted to use it as a biomarker to follow the evolution of patients treated with sacubitril/valsartan. However, while an increase in ANP may reflect the immediate pharmacological impact of sacubitril/valsartan and may help to prognosticate those patients (33), further changes in ANP levels in the event of a clinical deterioration cannot be fully predicted. Furthermore, the clinically available assays for BNPir and NT-proBNPir perform equally well in the context of long-term follow-up and estimation of prognosis (13, 14). However, as mentioned above, we strongly recommend using the same assay/platform when following an individual patient due to between assay differences.

STUDY LIMITATIONS

First, the number of patients per cohort is limited, which may limit the statistical power. However, the results are in the main robust, consistent, and highly significant across all the cohorts tested. Furthermore, the longitudinal analysis of HFrEF patients treated with sacubitril/valsartan also provided consistent results throughout the study. Second, the very early clinical effects (first dose) were not assessed. Third, the up-titration of sacubitril/valsartan was left at the discretion of the cardiologist according to clinical need, and therefore it is not possible to precisely assess the relationship between dose and time. Finally, we only used one assay for BNPir (Abbott) and NT-proBNPir (Roche Diagnostics), and other assays have given different results, in particular for BNP (14, 36), likely due to the use of antibodies targeting different epitopes in BNP or different calibrators.

In conclusion, the deconvolution of BNP and NT-proBNP immunoreactivities by MS/MS describes the molecular species that contribute to their measurements with the Abbot and Roche assays and shows that both biomarkers are equally useful for the estimation of $proBNP_{1–108}$ production in all the clinical contexts studied. Furthermore, $proBNP_{1–108}$ and $NT\text{-}proBNP_{1–76}$ glycosylation at S44 explain the discrepant evolution of BNP and NT-proBNP immunoreactivities in patients treated by sacubitril/valsartan.

Supplemental Material

Supplemental material is available at *Clinical Chemistry* online.

Nonstandard Abbreviations: BNP, B-type natriuretic peptide; NT-proBNP, N-terminal fragment of proBNP; HF, heart failure; BNPir, BNP immunoreactivity; NT-proBNPir, NT-proBNP immunoreactivity; MS, mass spectrometry; HFrEF, heart failure with reduced ejection fraction; ADHF, acute decompensated heart failure; ANCD, acute non-cardiac dyspnoea; IQR, interquartile range; BMI, body mass index; ANP, A-type natriuretic peptide, atrial natriuretic peptide; NPRA, ; SP, signal protein.

Author Contributions: *The corresponding author takes full responsibility that all authors on this publication have met the following required criteria of eligibility for authorship: (a) significant contributions to the conception and design, acquisition of data, or analysis and interpretation of data; (b) drafting or revising the article for intellectual content; (c) final approval of the published article; and (d) agreement to be accountable for all aspects of the article thus ensuring that questions related to the accuracy or integrity of any part of the article are appropriately investigated and resolved. Nobody who qualifies for authorship has been omitted from the list.*

Authors' Disclosures or Potential Conflicts of Interest: *Upon manuscript submission, all authors completed the author disclosure form. Disclosures and/or potential conflicts of interest:*

Employment or Leadership: None declared.
Consultant or Advisory Role: J. Lassus has received consulting honoraria from AstraZeneca, Bayer, Boehringer Ingelheim, and Roche Diagnostics, outside of the scope of this study. D. Logeart received consulting fees from Astra Zeneca, Bayer, Boehringer Ingelheim, Novartis, and Vifor, outside the scope of this study.
Stock Ownership: None declared.
Honoraria: F. Picard received honorarium from Novartis, outside the scope of this study. J. Lassus has received speaker's fees from AstraZeneca, Bayer, Boehringer Ingelheim, Pfizer, and ViforPharma, outside of the scope of this study. A. Cohen-Solal received honoraria from AstraZeneca, Novartis, Servier, Vifor, Bayer, Boehringer Ingelheim, Sanofi, and MSD, outside the scope of this study. N. Vodovar received speaker fees from Roche Diagnostics, Abbott Laboratories, and Siemens, outside the scope of this study.
Research Funding: This work was supported by Inserm, Université Paris Cité, and a grant from the Fédération Française de Cardiologie to Damien Logeart. A. Cohen-Solal received grants from Novartis, Servier, Vifor, Bayer, Boehringer Ingelheim, Sanofi, and MSD, outside the scope of this study.
Expert Testimony: None declared.
Patents: None declared.
Other Remuneration: F. Picard received non-financial support from Novartis, outside the scope of this study. A. Cohen-Solal received non-financial support from Novartis, Servier, Vifor, Bayer, Boehringer Ingelheim, Sanofi, and MSD, outside the scope of this study. D. Logeart received conference fees for Astra Zeneca, Bayer, Boehringer Ingelheim, Novartis, and Vifor, outside the scope of this study.

Role of Sponsor: The funding organizations played no role in the design of study, choice of enrolled patients, review and interpretation of data, preparation of manuscript, or final approval of manuscript.

Acknowledgments: We thank the nurses from the Department of Cardiology of the Haut-Lévêque Hospital and Lariboisière Hospitals. H. Nougué, T. Michel, M. Sadoune, A. Cohen-Solal, D. Logeart, J.-M. Launay, and N. Vodovar are members of the Institut des Sciences Cardiovasculaires de l'université Paris Cité. T. Michel and N. Vodovar are members of the INI-CRCT network.

References

1. Ponikowski P, Voors AA, Anker SD, Bueno H, Cleland JG, Coats AJ, et al. 2016 ESC guidelines for the diagnosis and treatment of acute and chronic heart failure: the task force for the diagnosis and treatment of acute and chronic heart failure of the European Society of Cardiology (ESC). Developed with the special contribution of the Heart Failure Association (HFA) of the ESC. Eur J Heart Fail 2016;18:891–975.
2. Yancy CW, Jessup M, Bozkurt B, Butler J, Casey DE Jr, Colvin MM, et al. 2017 ACC/AHA/HFSA focused update of the 2013 ACCF/AHA guideline for the management of heart failure: a report of the American College of Cardiology/American Heart Association task force on clinical practice guidelines and the Heart Failure Society of America. J Am Coll Cardiol 2017;70:776–803.
3. Semenov AG, Tamm NN, Seferian KR, Postnikov AB, Karpova NS, Serebryanaya DV, et al. Processing of pro-b-type natriuretic peptide: furin and corin as candidate convertases. Clin Chem 2010;56:1166–76.
4. Schellenberger U, O'Rear J, Guzzetta A, Jue RA, Protter AA, Pollitt NS. The precursor to b-type natriuretic peptide is an o-linked glycoprotein. Arch Biochem Biophys 2006;451:160–6.
5. Semenov AG, Postnikov AB, Tamm NN, Seferian KR, Karpova NS, Bloshchitsyna MN, et al. Processing of pro-brain natriuretic peptide is suppressed by O-glycosylation in the region close to the cleavage site. Clin Chem 2009;55:489–98.
6. Vodovar N, Seronde MF, Laribi S, Gayat E, Lassus J, Boukef R, et al. Post-translational modifications enhance NT-proBNP and BNP production in acute decompensated heart failure. Eur Heart J 2014;35:3434–41.
7. Tonne JM, Campbell JM, Cataliotti A, Ohmine S, Thatava T, Sakuma T, et al. Secretion of glycosylated pro-B-type natriuretic peptide from normal cardiomyocytes. Clin Chem 2011;57:864–73.
8. Brandt I, Lambeir AM, Ketelslegers JM, Vanderheyden M, Scharpe S, De Meester I. Dipeptidyl-peptidase IV converts intact B-type natriuretic peptide into its des-SerPro form. Clin Chem 2006;52:82–7.
9. Norman JA, Little D, Bolgar M, Di Donato G. Degradation of brain natriuretic peptide by neutral endopeptidase: species specific sites of proteolysis determined by mass spectrometry. Biochem Biophys Res Commun 1991;175:22–30.
10. McMurray JJ, Packer M, Desai AS, Gong J, Lefkowitz MP, Rizkala AR, et al. Angiotensin-neprilysin inhibition versus enalapril in heart failure. N Engl J Med 2014;371:993–1004.
11. Nougue H, Pezel T, Picard F, Sadoune M, Arrigo M, Beauvais F, et al. Effects of sacubitril/valsartan on neprilysin targets and the metabolism of natriuretic peptides in chronic heart failure: a mechanistic clinical study. Eur J Heart Fail 2019;21:598–605.
12. Packer M, McMurray JJ, Desai AS, Gong J, Lefkowitz MP, Rizkala AR, et al. Angiotensin receptor neprilysin inhibition compared with enalapril on the risk of clinical progression in surviving patients with heart failure. Circulation 2015;131:54–61.
13. Zile MR, Claggett BL, Prescott MF, McMurray JJ, Packer M, Rouleau JL, et al. Prognostic implications of changes in n-terminal pro-B-type natriuretic peptide in patients with heart failure. J Am Coll Cardiol 2016;68:2425–36.
14. Myhre PL, Vaduganathan M, Claggett B, Packer M, Desai AS, Rouleau JL, et al. B-type natriuretic peptide during treatment with sacubitril/valsartan: the PARADIGM-HF trial. J Am Coll Cardiol 2019;73:1264–72.
15. Hawkridge AM, Heublein DM, Bergen HR III, Cataliotti A, Burnett JC Jr, Muddiman DC. Quantitative mass spectral evidence for the absence of circulating brain natriuretic peptide (BNP-32) in severe human heart failure. Proc Natl Acad Sci U S A 2005;102:17442–7.
16. Luckenbill KN, Christenson RH, Jaffe AS, Mair J, Ordonez-Llanos J, Pagani F, et al. Cross-reactivity of BNP, NT-proBNP, and proBNP in commercial BNP and NT-proBNP assays: preliminary observations from the IFCC Committee for standardization of markers of cardiac damage. Clin Chem 2008;54:619–21.
17. Miller WL, Phelps MA, Wood CM, Schellenberger U, Van Le A, Perichon R, Jaffe AS. Comparison of mass spectrometry and clinical assay measurements of circulating fragments of B-type natriuretic peptide in patients with chronic heart failure. Circ Heart Fail 2011;4:355–60.
18. Roubille F, Delseny D, Cristol JP, Merle D, Salvetat N, Larue C, et al. Depletion of proBNP1-108 in patients with heart failure prevents cross-reactivity with natriuretic peptides. PLoS One 2013;8:e75174.
19. Seferian KR, Tamm NN, Semenov AG, Mukharyamova KS, Tolstaya AA, Koshkina EV, et al. The brain natriuretic peptide (BNP) precursor is the major immunoreactive form of BNP in patients with heart failure. Clin Chem 2007;53:866–73.
20. Dillon EM, Wei SD, Gupta DK, Nian H, Rodibaugh BS, Bachmann KN, et al. Active B-type natriuretic peptide measured by mass spectrometry and response to sacubitril/valsartan. J Card Fail 2021;27:1231–9.
21. IFCC. Analytical characteristics of commercial MR-proANP, BNP and NT-proBNP assays as per the manufacturer. http://www.ifcc.org/media/102208/NP%20Assay%20Table%20C%20SMCD%20vJuly_2011.pdf (Accessed November 2022).
22. Rosjo H, Dahl MB, Jorgensen M, Roysland R, Brynildsen J, Cataliotti A, et al. Influence of glycosylation on diagnostic and prognostic accuracy of N-terminal pro-B-type natriuretic peptide in acute dyspnea: data from the Akershus cardiac examination 2 study. Clin Chem 2015;61:1087–97.
23. Saenger AK, Rodriguez-Fraga O, Ler R, Ordonez-Llanos J, Jaffe AS, Goetze JP, Apple FS. Specificity of b-type natriuretic peptide assays: cross-reactivity with different BNP, NT-proBNP, and proBNP peptides. Clin Chem 2017;63:351–8.
24. Seferian KR, Tamm NN, Semenov AG, Tolstaya AA, Koshkina EV, Krasnoselsky MI, et al. Immunodetection of glycosylated NT-proBNP circulating in human blood. Clin Chem 2008;54:866–73.
25. Michel T, Nougue H, Cartailler J, Lefevre G, Sadoune M, Picard F, et al. ProANP metabolism provides new insights into sacubitril/valsartan mode of action. Circ Res 2022;130:e44–e57.
26. R Core Team. R: A language and environment for statistical computing. Vienna (Austria): R Foundation for Statistical Computing; 2020. https://www.R-project.org/ (Accessed January 2023).
27. Lewis LK, Raudsepp SD, Prickett TCR, Yandle TG, Doughty RN, Frampton CM, et al. ProBNP that is not glycosylated at threonine 71 is decreased with obesity in patients with heart failure. Clin Chem 2019;65:1115–24.
28. Vodovar N, Mebazaa A, Januzzi JL Jr, Murtagh G, Stough WG, Adams KF Jr, Zannad F. Evolution of natriuretic peptide biomarkers in heart failure: implications for clinical care and clinical trials. Int J Cardiol 2018;254:215–21.
29. Collin-Chavagnac D, Dehoux M, Schellenberg F, Cauliez B, Maupas-Schwalm F, Lefevre G; Societe Francaise de Biologie Clinique Cardiac Markers Working Group. Head-to-head comparison of 10 natriuretic peptide assays. Clin Chem Lab Med 2015;53:1825–37.
30. Kavsak PA, Lam CSP, Saenger AK, Jaffe AS, Collinson P, Pulkki K, et al. Educational recommendations on selected analytical and clinical aspects of natriuretic peptides with a focus on heart failure: a report from the IFCC Committee on clinical applications of cardiac bio-markers. Clin Chem 2019;65:1221–7.
31. Kenny AJ, Bourne A, Ingram J. Hydrolysis of human and pig brain natriuretic peptides, urodilatin, C-type natriuretic peptide and some C-receptor ligands by endopeptidase-24.11. Biochem J 1993;291:83–8.
32. Jaffe AS, Apple FS, Mebazaa A, Vodovar N. Unraveling N-terminal pro-B-type natriuretic peptide: another piece to a very complex puzzle in heart failure patients. Clin Chem 2015;61:1016–8.
33. Murphy SP, Prescott MF, Camacho A, Iyer SR, Maisel AS, Felker GM, et al. Atrial natriuretic peptide and treatment with sacubitril/valsartan in heart failure with reduced ejection fraction. JACC Heart Fail 2021;9:127–36.

34. Velazquez EJ, Morrow DA, DeVore AD, Duffy CI, Ambrosy AP, McCague K, et al. Angiotensin-neprilysin inhibition in acute decompensated heart failure. N Engl J Med 2019;380:539–48.

35. Cunningham JW, Vaduganathan M, Claggett BL, Zile MR, Anand IS, Packer M, et al. Effects of sacubitril/valsartan on N-terminal pro-B-type natriuretic peptide in heart failure with preserved ejection fraction. JACC Heart Fail 2020;8:372–81.

36. Ibrahim NE, McCarthy CP, Shrestha S, Gaggin HK, Mukai R, Szymonifka J, et al. Effect of neprilysin inhibition on various natriuretic peptide assays. J Am Coll Cardiol 2019;73:1273–84.

SUPPLEMENTARY DATA

Deconvolution of BNP and NT-proBNP immunoreactivity by mass spectrometry in heart failure and sacubitril/valsartan treatment.

Hélène Nougué, MD, PhD[a, b], Thibault Michel, MD, MSc[a], François Picard, MD[c], Johan Lassus, MD, PhD[d], Malha Sadoune, MSc[a], Said Laribi, MD, PhD[e], Alain Cohen-Solal, MD, PhD[a,f], Damien Logeart, MD, PhD[a,f], Jean-Marie Launay, PharmD, PhD[a*], and Nicolas Vodovar, PhD [a*].

Supplementary Methods

Quantification of BNP after tryptic digestion was performed by isotope dilution CE-MS using isotopically labeled peptides as internal standards [for instance the 32 amino acid BNP was from Sigma-Aldrich and the isotopically labeled BNP (SPKMV($^{13}C_5$,^{15}N)Q-G($^{13}C_2$,^{15}N)S-G($^{13}C_2$,^{15}N)-CF-G($^{13}C_2$,^{15}N)-RKMDR-I($^{13}C_6$,^{15}N)-SSSSGLGC-K($^{13}C_6$,$^{15}N_2$)-VLRRH) from CPC Scientific (Sunnydale, CA, USA); the lyophilized peptides were dissolved in water:acetonitrile (90:10 v/v) containing 0.1% formic acid (v/v) and further dilutions were carried out in water containing 500 μg/g BSA and 0.5% formic acid (v/v). Before tryptic mapping, each plasma sample was digested with either neuraminidase (NANase III) and O-glycosidase (both from Sigma-Aldrich) in 250 mM sodium phosphate buffer, pH 6 at 37°C. A concentrated buffer was added to achieve a final concentration of 50 mM Tris – HCl, pH 8, and 1 mg trypsin (modified sequencing grade trypsin from Roche Applied Science, Penzberg, Germany) was added. Digestion was allowed to proceed overnight at room temperature. All plasma samples were centrifuged through a 0.22 μm spin filter (E&K Scientific, Amsterdam) for 15 min at 16100g. The filtered plasmas were lyophilized and stored at 4°C until use. Before analysis, lyophilized samples were resuspended in appropriate volumes of HPLC grade H_2O allowing the measurement of the considered peptide within the limits of detection, and kept on ice. A neutral-coated capillary electrophoresis-electrospray ionization (CESI) separation system coupled online to a microTOF MS (Bruker Daltonic, Bremen, Germany) was used. CE was carried out with a CESI 8000 High-Performance Separation-ESI Module (Sciex Separations, Brea, CA). The capillary temperatures were maintained at 25 °C. The capillary used in this study was the OptiMS Neutral Surface Cartridge (Sciex Separations, Brea, CA). Before use, the capillary was first washed by 0.1 M hydrochloric acid (Sigma-Aldrich), then rinsed with background electrolyte (BGE) consisting of 10% acetic acid (Fisher Scientific), and finally rinsed with

deionized water for 30 min at 100 psi and stored overnight filled with water. Before each run, the capillary was rinsed with 0.1 M HCl and flushed with fresh BGE for 10 min at 100 psi. Unless otherwise stated, samples were injected by 10 kV voltage for 5 s, and the BGE spacer was added between samples by hydrodynamic injection. A separation voltage of 30 kV was applied across the capillary with a supplemental forward pressure of 1.5 psi. Data acquisition and MS acquisition methods were automatically controlled by the CE via contact–close– relays. Spectra were accumulated every 3 s, over a range of m/z 350 to 3000. Samples from CE-MS were also analyzed on a Dionex Ultimate 3000 RSLS nano-flow system (Dionex, Camberly, UK). The samples (5 μL) were loaded onto a Dionex 100 μm × 2 cm 5 μmC18 nano trap column at a flowrate of 5 μL/min by an Ultimate 3000 RS autosampler (Dionex). Loading solution comprised 0.1% formic acid and acetonitrile (98:2). Once loaded onto the trap column, the sample was then washed off into an Acclaim PepMap C18 nano-column 75 μm × 15 cm, 2 μm 100 A° at a flow rate of 0.3 μL/min. The trap and nano-flow column were maintained at 35°C in a column oven in the Ultimate 3000 RSLC. Samples were eluted with a gradient of solvent A: 0.1% formic acid versus solvent B: acetonitrile starting at 5% B rising to 50% B over 100 min. The column was washed using 90% B before being equilibrated before the next sample was loaded. The eluant from the column was directed to a Proxeon nano-spray ESI source (Thermo Fisher, Hemel, UK) operating in positive-ion mode and then into an Orbitrap Velos FTMS. The ionization voltage was 2.5 kV and the capillary temperature was 200°C. The mass spectrometer was operated in MS–MS mode scanning from 380 to 2000 amu. The fragmentation method was HCD at 35% collision energy. The ions were selected for MS2 using a data-dependent method with a repeat count of 1 and repeat and exclusion times of 15 sec. Precursor ions with a charge state of 1 were rejected. The resolution of ions in MS1 was 60000 and 7500 for HCD MS2. Data files were searched using SEQUEST (by using Thermo Proteome Discoverer), without any enzyme specificity.

No fixed modification was selected, and oxidation of methionine and proline were set as variable modifications. Mass error windows of 10 ppm and 0.05 Da were allowed for MS and MS/MS, respectively. Peptide data were extracted using high peptide confidence and top-one peptide rank filters. Validation of identified peptides was achieved by the correlation between peptide charge at the working pH of 2 and CE-migration time. CE migration time deviations lower than ± 2 min corresponding to the CE-MS measurement were accepted.

Characterization of O-glycosylated sites was performed by online nano-liquid chromatography coupled to electrospray ionization-linear ion trap-Fourier transform mass spectrometry in an LTQ-Orbitrap XL hybrid spectrometer (Thermo Scientific) equipped for electron transfer dissociation for peptide sequence analysis by MS/MS with retention of glycan site-specific fragments. Samples were dissolved in methanol/ water (1:1) containing 1% formic acid and introduced by direct infusion via a TriVersa NanoMate ESI-Chip interface (Advion BioSystems, Ithaca, NY, USA) at a flow rate of 100 nL/min and 1.4 kV spray voltage. Mass spectra were acquired in a positive ion FT mode using parameters similar to previous studies (1) except at a nominal resolving power of either 30 000 or 60 000. Electron transfer dissociation-MS/MS spectra were analyzed by comparison with theoretical c and z. Fragment m/z values were calculated for all positional combinations of one HexNAc residue distributed on all the potential S and T glycosylation sites in the sequence. Calculations were performed using the web-based Protein Prospector MS-Product software routine.

1. Semenov AG, Postnikov AB, Tamm NN, Seferian KR, Karpova NS, Bloshchitsyna MN, et al. Processing of pro-brain natriuretic peptide is suppressed by o-glycosylation in the region close to the cleavage site. *Clin Chem* 2009;55:489-98.

Supplementary Table 1: Analytical parameters for all the assays used*.

Assay	Intra-assay CV	Inter-assay CV	Limit of detection	Linearity range
BNPir	1.8 %	3.5 %	3.2 pM	7 – 1377 pM
NT-proBNPir	1.5 %	3.1 %	2.1 pM	5 – 4130 pM
$proBNP_{1-108}$	3.3 %	6.7 %	7.3 pM	15 – 156 pM
BNP_{1-32}	4.6 %	7.9 %	1.6 pM	3 – 167 pM
BNP_{3-32}	4.8 %	8.4 %	1.6 pM	3 – 167 pM
BNP_{5-32}	5.3 %	8.1 %	1.6 pM	3 – 167 pM
$NT\text{-}proBNP_{1-76}$	3.7 %	7.6 %	5.8 pM	12 – 147 pM
NT-proBNPsp	4.9 %	8.5 %	4.3 pM	9 – 128 pM
$proBNP_{1-108}$ S44 glyc.	7.8 %	11.3 %	8.6 pM	17 – 88 pM
$NT\text{-}proBNP_{1-76}$ S44 glyc.	7.1 %	10.5 %	7.5 pM	15 – 93 pM
cGMP	6.4 %	11.2 %	5 pM	8 – 225 pM

* Precision was determined using pooled human plasmas and controls in a protocol (EP5-A) of the CLSI (Clinical and Laboratory Standards Institute): 2 runs per day in sextuplicate each for 10 days. Concentrations were twice the limits of detection.

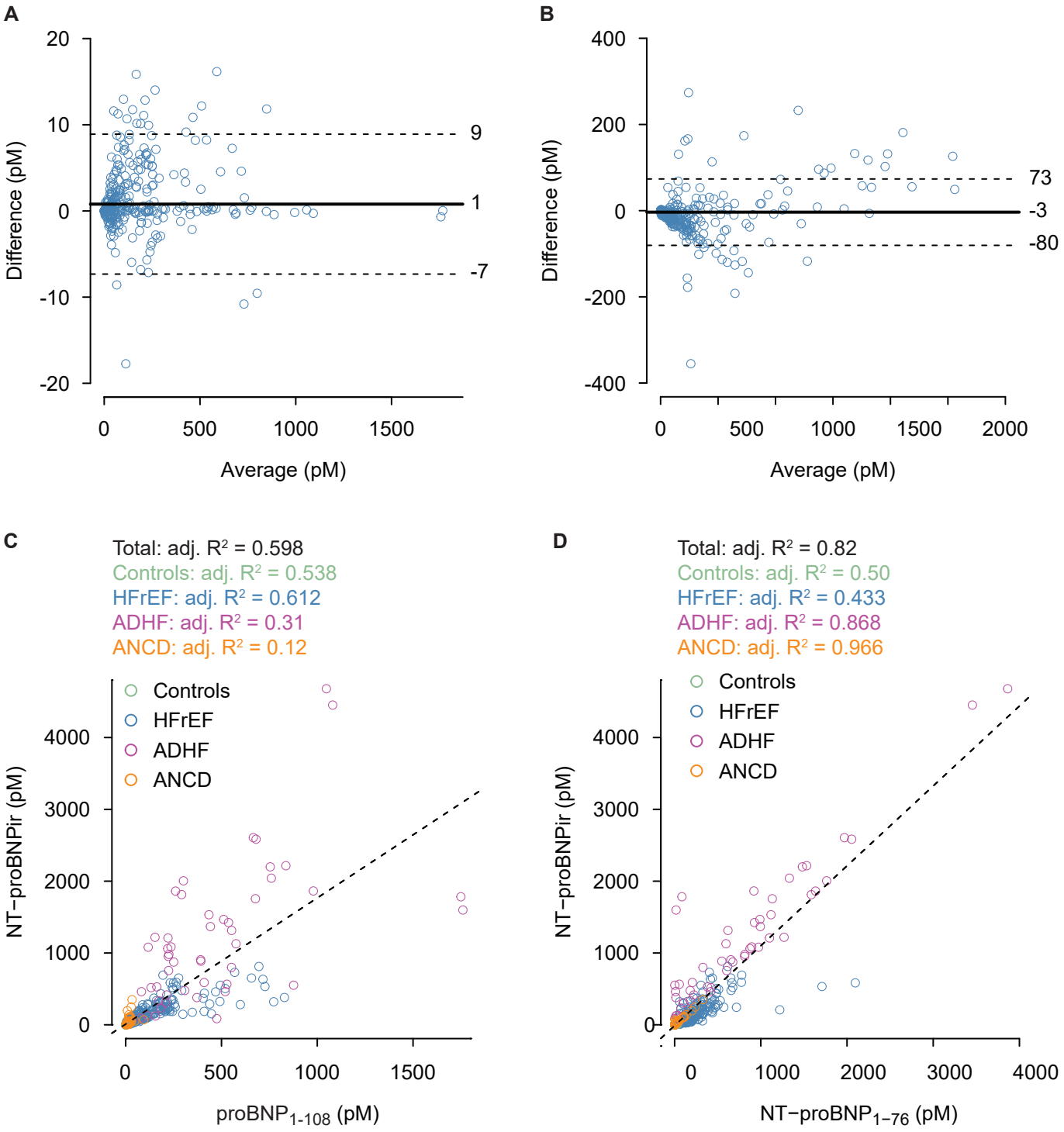

Supplementary Figure 1: Comparison between BNP and NT-proBNP immunoreactivities and mass spectrometry quantification. A) Bland-Altman plot comparing measured and theoretical BNPir. **B)** Bland-Altman plot comparing measured and theoretical NT-proBNPir. **C)** Correlation between NT-proBNPir and $proBNP_{1\text{-}108}$ measured by mass spectrometry in the different cohorts. **D)** Correlation between NT-proBNPir and $NT\text{-}proBNP_{1\text{-}76}$ measured by mass spectrometry in the different cohorts. In C and D, the correlations were calculated using linear regression models on all the subjects (black) and each cohort individually. HFrEF: Heart Failure with reduced ejection fraction, ADHF: Acute Decompensated Heart Failure, ANCD: Acute Non-Cardiac Dyspnoea, adj. R^2: adjusted R^2.

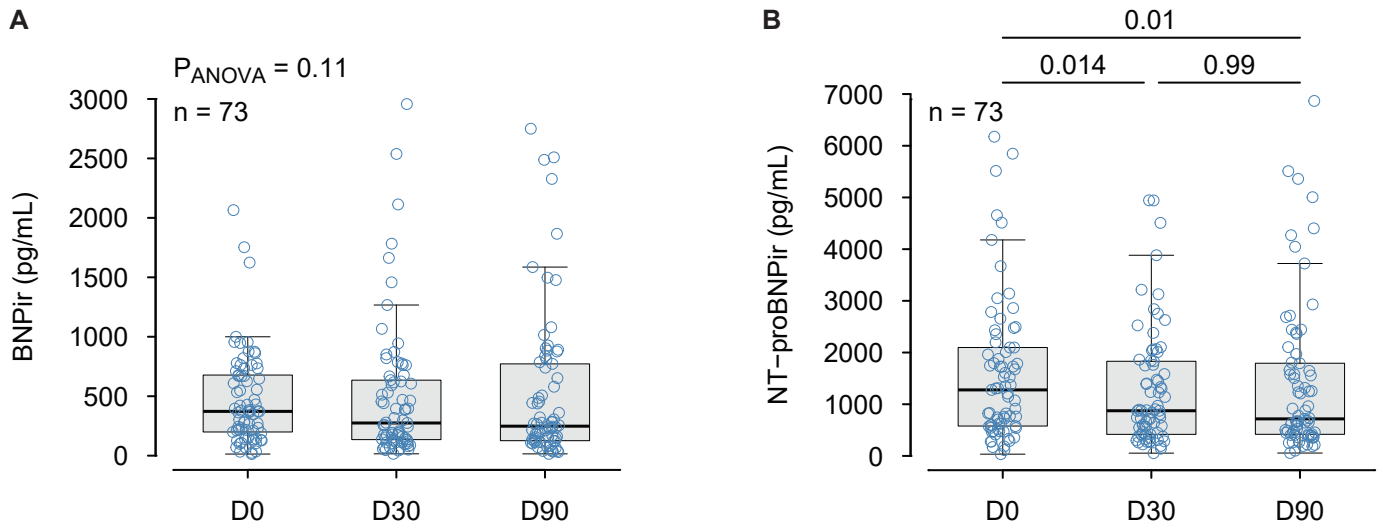

Supplementary Figure 2: Evolution of BNPir (A) and NT-proBNPir (B) in HFrEF patients at baseline (D0), 30 and 90 days after the initiation of sacubitril/valsartan as described in (11). The variables were analyzed using repeated-measures ANOVA on log-transformed data followed by the Tukey honestly significant difference (HSD). In A, the p-value is that of the repeated-measure ANOVA. HFrEF: Heart Failure with reduced ejection fraction.

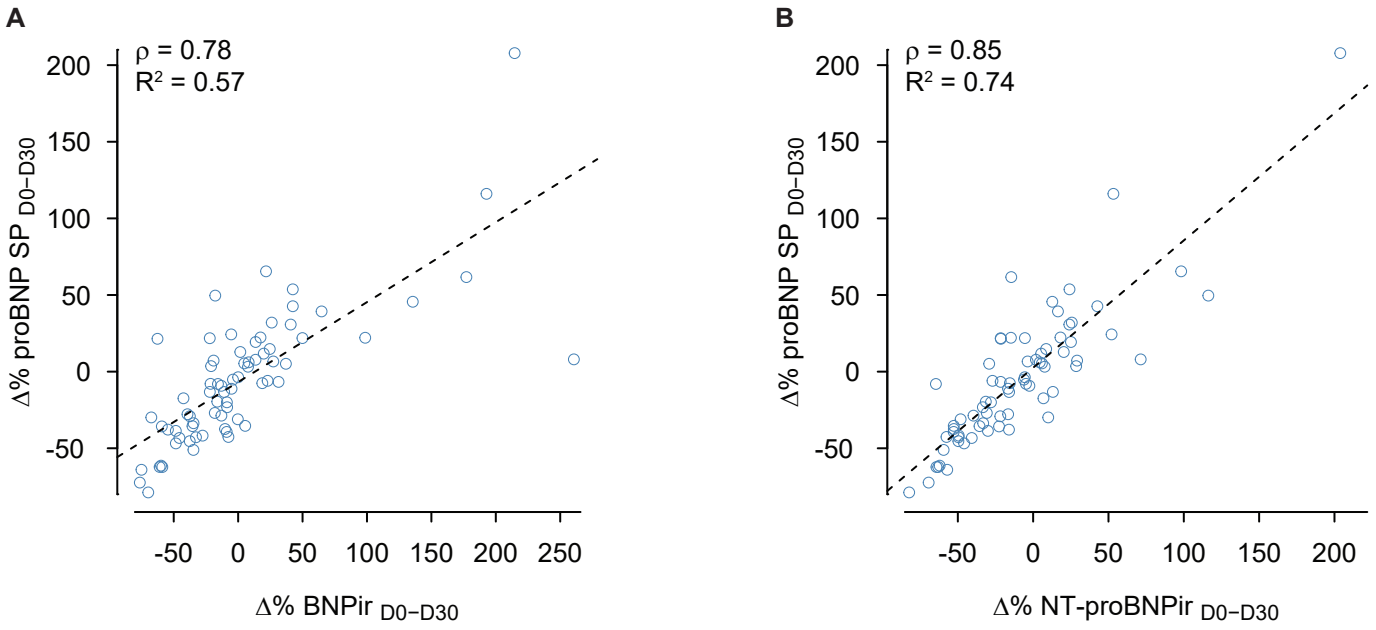

Supplementary Figure 3: Relationship between variations in proBNP signal peptide and BNPir or NT-proBNPir in patients receiving sacubitril/valsartan. A) Correlation between the variations between baseline (D0) and 30 days after the initiation of sacubitril/valsartan proBNP SP and BNPir in HFrEF patients. **B)** Correlation between the variations between baseline (D0) and 30 days after the initiation of sacubitril/valsartan proBNP SP and NT-proBNPir in HFrEF patients. The correlations were calculated using Spearman's correlation (ρ) and linear regression models (R^2). HFrEF: Heart Failure with reduced ejection fraction, Δ%: relative variation.

3 Article III. Neprilysin and the renin-angiotensin-aldosterone system in acute kidney injury after cardiac surgery

La néprilysine (NEP) a récemment été étudié comme biomarqueur de l'insuffisance rénale aigue (IRA) chez les patients en réanimation. De plus la NEP joue un rôle majeur dans le système rénine-angiotensine-aldostérone (SRAA) en convertissant l'angiotensine 1 en angiotensine 1-7, SRAA dont le rôle dans le processus physiopathologique de l'insuffisance rénale aigue reste débattu. Afin de valider la NEP comme biomarqueur et acteur potentiel dans l'IRA, dans une cohorte helvétique de 40 patients admis en réanimation dans les suites d'une chirurgie cardiaque élective avec circulation extracorporelle, nous avons mesurer la NEP plasmatique et urinaire comme biomarqueur précoce de l'IRA. Les résultats obtenus nous ont conduit étendre cette étude au SRAA pour tester l'implication de la NEP dans ce contexte.

Les résultats obtenus dans cette étude montrent que :

i) Le NEP plasmatique est un biomarqueur précoce (admission en réanimation) de l'insuffisance rénale aigue dans les suites d'une chirurgie cardiaque. Il présente des performances similaires au NephroCheck, mais est capable de distinguer les IRA infraclinique et clinique.

ii) La NEP urinaire est bien un biomarqueur de l'IRA mais avec une cinétique plus longue que la NEP plasmatique, puisqu'elle n'est capable d'identifier les patients avec une IRA que 6 heures après l'admission en réanimation.

iii) La présence d'une IRA est associée à une activation complète et non biaisé du SRAA, alors que chez les patients présentant une IRA infraclinique, l'activation du SRAA n'est que transitoire et n'implique pas tous les éléments du SRAA.

iv) Que même si l'activité NEP plasmatique augmente au cours de l'IRA, cette augmentation n'a pas d'impact sur le SRAA.

L'ensemble de ces résultats confirment la NEP urinaire comme biomarqueur de l'IRA, mais surtout positionne la NEP plasmatique comme un biomarqueur plus précoce de l'IRA. Cette augmentation de la NEP plasmatique reflète possiblement les agressions vasculaires subies lors d'une chirurgie cardiaque, dont l'IRA est secondaire. Ce travail clarifie également l'association du SRAA dans l'IRA clinique et infraclinique, et permet d'envisager des perspectives thérapeutiques pour la prévention/traitement précoce de l'IRA post-chirurgie cardiaque.

Neprilysin and the renin-angiotensin-aldosterone system in acute kidney injury after cardiac surgery: an exploratory study

Thibault Michel, MD[1,2], Marco Altarelli, MD[1,3], Adrien Picod, MD[2], Mathias Kirsch, MD, PhD[3,4], Matthieu Legrand, MD, PhD[5], Jean-Marie Launay, PharmD, PhD[2], Antoine Schneider, MAD, PhD[1,3,*], and Nicolas Vodovar, PhD[2,*]

[1] Adult Intensive Care Unit, Centre Hospitalier Universitaire Vaudois (CHUV), Lausanne, Switzerland.

[2] Université Paris Cité and Inserm UMR-S 942 MASCOT, Paris, France

[3] Faculty of Biology and Medicine, University of Lausanne, Lausanne, Switzerland

[4] Department of Cardiovascular Surgery, Centre Hospitalier Universitaire Vaudois (CHUV), Lausanne, Switzerland

[5] Department of Anesthesia and Perioperative Care, Division of Critical Care Medicine, UCSF, San Francisco, USA

* Correspondence should be addressed to Antoine Schneider: Service de Médecine Intensive Adulte (SMIA), Centre Hospitalier Universitaire Vaudois (CHUV), 46 avenue du Bugnon, 1011 Lausanne Switzerland; Tel : +41 21 314 16 32; email: Antoine.Schneider@chuv.ch) or Nicolas Vodovar: Inserm UMR-S 942, Hôpital Lariboisière, 2 rue Ambroise Paré, 75010 Paris, France; Tel : +33 1 53 21 67 90; email: nicolas.vodovar@inserm.fr.

Abstract word count: 287

Text word count: 2996

Figures: 4

Table: 1

Abstract

Background: Cardiac surgery-associated acute kidney injury (CSA-AKI) is associated with increased morbidity and mortality. Better predicting CSA-AKI and understanding its pathophysiology are needed.

Objective: To evaluate neprilysin (NEP) as a predictive biomarker for CSA-AKI and its impact on the renin-angiotensin-aldosterone system (RAAS).

Methods: We enrolled 40 patients who underwent cardiac surgery, of whom 25 developed CSA-AKI. Plasma was collected before surgery, at ICU admission, and 24h and 48h after. We measured NEP concentration and activity by mass spectrometry and a fluorogenic assay, respectively. We also measured renin, prorenin, and aldosterone by radioimmunoassay and angiotensins I, II and (1-7) by mass spectrometry. Within-group longitudinal variables were analyzed using repeated-measure ANOVA on log-transformed data followed by the Tukey HSD test, or using the signed rank Wilcoxon test. Intergroup comparisons were performed using the Kruskal-Wallis test followed by the sum rank Wilcoxon test corrected for multiple comparisons.

Results: NEP plasma concentration and activity increased in all patients at ICU admission, with a greater increase in patients who developed CSA-AKI. Given NEP involvement in the RAAS, we compared RAAS components in patients who developed or did not CSA-AKI. Compared to preoperative values, patients who did not develop CSA-AKI only exhibited a moderate and transient increase in renin concentration and angiotensin (1-7) plasma levels at ICU admission. In marked contrast, patients with AKI exhibited increases in renin concentration and activity, angiotensins, and aldosterone, and a decrease in prorenin concentration at ICU admission. Preoperative angiotensin I was higher in patients who developed CSA-AKI, with an AUC of 0.93.

Conclusions: Plasma NEP appears as a potential early biomarker for the prediction of CSA-AKI. Patients who developed CSA-AKI exhibited full and unbiased RAAS activation, with preoperative angiotensin I as a potential predictive biomarker of CSA-AKI.

Keywords: Cardiac Surgical, Acute Kidney Injury, neprilysin, Renin-Angiotensin System, Aldosterone

Introduction

Cardiac surgery is often complicated by acute kidney injury (AKI), which is associated with increased morbidity, hospital length of stay and mortality.[1-3] The incidence of cardiac surgery-associated AKI (CSA-AKI) is ~20%, but mostly moderate in severity.[3, 4] Until now, AKI has been defined by an increase in serum creatinine relative to baseline and a decrease in urinary output.[5-7] However, the slow kinetics of creatinine elevation has prompted the identification of new urinary or plasma biomarkers to predict and diagnose AKI.[8] Consideration of these biomarkers led to defining a new class of AKI, based solely on renal biomarkers elevation (AKI 1S) without any change in KDIGO criteria.[9] he association of IGFBP7 and TIMP-2 (Nephrocheck) has been validated to predict CSA-AKI.[10] Predicting CSA-AKI is important as preventive measures can be effectively set in place for patients at risk of developing CSA-AKI.[11]

CSA-AKI pathophysiology is not fully understood but involves the renin-angiotensin-aldosterone system (RAAS). The RAAS (**Figure 1A**) is initiated by renin that cleaves angiotensinogen into angiotensin I (AngI), which is further cleaved into the vasoconstrictive angiotensin II (AngII) by angiotensin-converting enzyme (ACE) or the vasodilatory angiotensin 1-7 [Ang(1-7)] by neprilysin (NEP, CD10 or neutral endopeptidase). NEP is a protease involved in the inactivation of numerous vasoactive peptides,[12] and its activity markedly impacts vascular tone. Of note, urinary NEP has recently been identified as a potential biomarker of CSA-AKI.[13] An increase in plasma renin concentration was associated with AKI, and hypothesized to reflect a response to insufficient AngII concentration, leading to intrarenal vasodilatation, loss of glomerular filtration pressure, eventually causing a decrease in glomerular filtration rate (GFR). Additionally, a relative excess of Ang(1-7) could also contribute to excessive intra-renal vasodilatation.[14] Alternatively, increased renin could

reflect the complete activation of RAAS, implicating renal vasoconstriction as a main pathophysiological drive in AKI.[15]

We conducted a prospective observational study in patients undergoing cardiac surgery to investigate plasma neprilysin as a biomarker of AKI. Changes observed in NEP activity led us to investigate the impact of these changes on RAAS.

Methods

Study design and patients

This study using human samples was carried out per the current revision of the Declaration of Helsinki. This study was approved by the cantonal commission for Ethics in Research on Humans (CER-VD 2018-01442). All patients included provided informed consent.

We included 40 adult patients admitted to the intensive care unit (ICU) after elective cardiac surgery with a high risk of perioperative AKI: > 80 years, diabetes mellitus, hypertension, peripheral artery disease, chronic obstructive pulmonary disease, stage 2-3 chronic kidney disease (GFR 30-60 mL/min), intervention with expected pulmonary bypass > 120 min. Exclusion criteria were: severe systolic heart failure (LVEF < 35%), GFR < 30 mL/min or chronic dependence on dialysis or renal transplantation, preoperative shock, inability to provide informed consent, enrolment in another study in progress. After the procedure, all patients were admitted to the ICU. Clinical and standard biological data were obtained from patient electronic medical records. AKI was defined as either a urinary Nephrocheck > 0.3 (AKI 1S) on ICU admission, an increase in serum creatinine and/or a decrease in urinary output in the first seven days of ICU admission according to KDIGO criteria (AKI ≥1A) [9].

Blood and urine sampling

Blood samples were collected in EDTA-containing vacutainer tubes before surgery, on ICU admission, and 24 and 48h after. Blood samples were immediately centrifuged at 2000 *g* for 10 min at 4°C, and plasma was immediately stored at -80°C until use. Urine samples were collected via the urinary catheter and immediately stored at -80°C. Urine samples were obtained for all patients at admission to ICU and only in 10 patients 6h after admission to ICU after protocol amendment.

Biomarker measurements

IGFBP7 and TIMP-2 were measured using the Nephrocheck assay (bioMérieux) on urine samples. Neprilysin concentration and activities were measured in both plasma and urine samples by mass spectrometry and using a fluorogenic substrate, respectively as previously described.[16] Aldosterone was measured by radioimmunoassay (ref R-CW-100, Diasource, Louvain-la-Neuve, Belgium). Active renin (AR) and total renin were measured by an AR immunoradiometric assay (IRMA, ref: KIR 1531, IBL, Minneapolis, MN). To measure total renin, 200 µL of plasma were mixed with 25 µL of the renin inhibitor VTP-27999 TFA (ref S2488, Selleck Chemicals, Houston, TX) and incubated at 4°C for 24 hours. The renin inhibitor caused the conformational change of the prorenin molecule, exposing the antigenic binding site to the monoclonal antibody specific to AR. Prorenin concentrations were calculated by subtracting the amount of AR from the total renin. Plasma renin activity (PRA) was measured using a commercial chemiluminescent assay (IB 57101, IBL, Minneapolis, MN). AngI, AngII, and Ang(1-7) were measured by LC/ESI-SRM/MS as previously described.[17] Other biological measurements were performed by the Department of Biochemistry at the CHUV, Lausanne.

Statistical analysis

All statistical analyses were performed using R 4.2.1.[18, 19] Variables are expressed as median [interquartile range] or number (percentage). Normality was assessed using the Shapiro-Wilk test. Within-group longitudinal data were analyzed by repeated measure ANOVA on log-transformed data followed by the Tukey HSD test, or by the signed rank Wilcoxon test. Intergroup data were analyzed with the sum rank Wilcoxon test, or by the Kruskal-Wallis test followed by the sum rank Wilcoxon test corrected for multiple comparisons (Holm). Correlations were measured using linear regression. Receiver-Operator Characteristic (ROC) analysis was performed with the pROC package, and the 95% confidence interval (95CI) was calculated by the DeLong method.[19] A p-value < 0.05 was considered significant.

Results

Study population

We included 40 patients between May 2018 and May 2019 who underwent elective cardiac surgery. Patient characteristics are described in **Table 1**. Overall, the population consisted mainly of women with a median age of 69 years. 15 (37.5%) patients did not develop AKI (noAKI). Among the 35 patients with AKI ≥1S referred as to AKI thereafter, 16 (40%) had AKI stage 1S, and 9 (22.5%) had AKI ≥1A (8 stage 1A, 1 stage 1B). On postoperative day 7, most (37/40, 92.5%) patients had recovered preoperative renal function. No patient required renal replacement therapy. Patients in the noAKI and AKI groups were similar in terms of preoperative, intraoperative, and postoperative characteristics, except for a higher age and a trend towards lower renal function in the AKI group.

NEP levels after cardiac surgery

Patients in the AKI group had higher preoperative plasma NEP concentrations compared to the noAKI group (**Figure 1B**) while both groups had similar circulating NEP activity (**Supplemental Figure 1A**). Higher NEP concentration in AKI patients was moderately predictive of AKI (AUC = 0.79 [0.63-0.94]). Compared to preoperative values, both groups exhibited an increase in NEP concentration at ICU admission (noAKI: +6.8% [3.4 – 15], P = 0.031; AKI: (+69% [46 – 88], P < 0.0001) with a return to preoperative values at 48h (**Figure 1B** and **Supplemental Table 1**). The increase in NEP concentration at ICU admission was markedly higher in AKI patients (P < 0.0001), and there was no overlap between the two groups at ICU admission. Baseline NEP activity was similar in both groups at baseline, and only AKI patients exhibited an increase in NEP activity at ICU admission (+53% [38 – 80], P < 0.0001). In all patients, NEP activity decreased lower than preoperative values at 48h (**Supplemental Figure 1A** and **Supplemental Table 2**). In a sensitivity analysis, we compared patients with AKI 1S and AKI ≥1A. The results show that NEP concentration and activity followed the same kinetic in the two groups, although increases were more pronounced in the AKI ≥1A group (**Figure 1C**, **Supplemental Figure 1** and **Supplemental Table 3-4**).

Finally, we collected urine samples from 10 patients at admission to the ICU and 6 hours after. At ICU admission, both NEP concentration and activity were lower in patients with AKI (n = 6) when compared to noAKI patients (n = 4; **Supplemental Figure 2**). While there was no change in urinary NEP concentration or activity in noAKI patients, both markedly increased in the urine of AKI patients (**Supplemental Figure 2**).

Renin in CSA-AKI

As NEP is involved in RAAS, we evaluated the impact of variations in plasma NEP concentration and activity on RAAS components. As NEP concentration and activity were markedly higher in AKI ≥1A patients than AKI 1S patients, we compared RAAS components in the three groups noAKI, AKI 1S, and AKI ≥1A.

First, renin concentration (**Figure 2A**), plasma renin activity (PRA, **Figure 2B**) and prorenin (**Figure 2C**) concentrations were similar across the three groups at baseline. Renin concentration increased more in AKI ≥1A than in AKI 1S patients at ICU admission and remained elevated afterwards (**Figure 2A** and **Supplemental Table 5**). This increase in renin concentration only translated into an increase in PRA in the AKI 1S and AKI ≥1A groups (noAKI: $P_{ANOVA} = 0.9$) that followed the same kinetic as renin concentration, the AKI ≥1A group showing the greatest increase (**Figure 2B** and **Supplemental Table 6**). Renin increase was associated with a decrease in plasma prorenin concentration only in the AKI 1S and AKI ≥1A groups (noAKI: $P_{ANOVA} = 0.2$), with a kinetic that mirrored that of renin. In the AKI 1S group, the decrease in prorenin was intermediary and transient, and prorenin plasma concentration reached preoperative values at 48h (**Figure 2C** and **Supplemental Table 7**). Finally, the sum of renin and prorenin concentration was similar in the three groups before surgery, increased in the three groups at ICU admission, with noAKI > AKI 1S > AKI ≥1A, and remained elevated afterwards with a trend toward a decrease at 48h (**Supplemental Figure 3** and **Supplemental Table 8**).

Angiotensins in CSA-AKI

Next, we measured plasma concentrations of AngI, Ang(1-7) and AngII. Unlike AngII and Ang(1-7) whose levels were similar in the three groups before surgery, AngI plasma levels were the highest in the noAKI group and the lowest in the AKI group (**Figure 3**).

Consequently, preoperative AngI levels were highly predictive of the occurrence of AKI with an AUC of 93% (95 DI: 86 -100). Plasma levels of AngI did not change in the noAKI group (P_{ANOVA} = 0.44), while increased at admission to the ICU and remained elevated in the AKI 1S and AKI ≥1A groups, with the greatest increase in the AKI ≥1A group (**Figure 3A** and **Supplemental Table 9**). Similarly, plasma levels of AngII increased in the AKI 1S and AKI ≥1A groups at admission to the ICU until 24h and decreased at 48h without reaching preoperative levels (**Figure 3B** and **Supplemental Table 10**). Ang(1-7), increased in the three groups at ICU admission, with noAKI > AKI 1S > AKI ≥1A, and with a gradual decrease at 48h, although Ang(1-7) plasma levels remained higher than preoperative levels in the AKI 1S and AKI ≥1A groups and return to pre-operative values in the no AKI group at 24h (**Figure 3C** and **Supplemental Table 11**). Importantly, the AngII / Ang(1-7) ratio was similar between the three groups at all time points and did not change throughout the study (**Figure 3D** and **Supplemental Table 12**).

Aldosterone in CSA-AKI

Finally, we measured plasma aldosterone concentration, as a measure of AngII biological activity. Before surgery, aldosterone levels were similar in the three groups (**Figure 4A**). Aldosterone levels remained unchanged in the noAKI group throughout the study, while increased more in AKI ≥1A patients than AKI 1S patients without returning to preoperative values at 48h. (**Supplemental Table 13**). Importantly, despite an increase in aldosterone in the AKI 1S group (**Figure 4B** and **Supplemental Table 13**), aldosterone levels were similar between the noAKI and AKI 1S groups at all time points (Figure 4A). There was also a strong positive correlation between relative variations of AngII and aldosterone between preoperative and ICU admission values, only in the AKI 1S and AKI ≥1A groups (**Figure 4C**). Finally, there were no differences in the renin/aldosterone ratio between the three groups

throughout the study (**Figure 4D**), although the ratio increased only in the noAKI group upon admission to the ICU and remained elevated afterwards (**Supplemental Table 14**).

Discussion

In this study, we tested the association between NEP and RAAS component with AKI after cardiac surgery. We confirmed plasma NEP as a potential predictive biomarker for CSA-AKI, and that RAAS activation was incremental with the severity of CSA-AKI. Furthermore, we found preoperative AngI as a potential predictive biomarker of CSA-AKI.

Firstly, we found that cardiac surgery was associated with a rapid increase in NEP plasma levels in all patients at ICU admission after cardiac surgery, ~24-48h before serum creatinine elevation. NEP increase was markedly greater in those with AKI, and was greater in patients with AKI ≥1A than those with AKI 1S. Although plasma NEP could predict AKI at admission to the ICU as Nephrocheck, it could discriminate patients at risk of AKI 1S and AKI ≥1A. The kinetics of plasma NEP levels strongly suggest that its elevation is associated with operative stress since plasma NEP was the highest at admission to the ICU and normalized at 48h. Since NEP is highly present at the surface of endothelial cells, its rapid plasma release could result from the vascular stress secondary to cardiopulmonary bypass and aortic clamping, although plasma NEP could also originate from other tissue and organs. Urinary NEP concentration and activity also increased in AKI patients as previously reported,[13] with a slower kinetic than plasma NEP. While NEP is highly expressed in the kidney, it is mostly expressed in the brush border of the proximal tubular cells and does not contribute to plasma NEP. Whether urinary NEP elevation is due to plasma NEP filtration or to its release from the membrane of proximal tubular cells remains to be determined. However, since plasma NEP is not impaired by renal function,[20] the latter is more likely. Taken together, these data show plasma NEP as an early plasma biomarker of CSA-AKI and

could reflect the hemodynamic challenges on the kidney and other organs during cardiac surgery.

Secondly, our data also indicate that CSA-AKI is accompanied by a full and unbiased RAAS activation, which is incremental with the severity (1S vs ≥1A) of CSA-AKI. We found an increase in renin concentration and activity, as previously observed,[14] which relied on prorenin activation and an increase in production/release, which was also incremental with the severity of the AKI. Renin increase was accompanied by a consistent increase in AngI, AngII, and Ang(1-7). Importantly, baseline AngI levels differed markedly between the groups and were predictive of the development of AKI. The mechanism underlying this difference is unclear, but a low preoperative AngI level could be a susceptibility factor for the development of AKI and could predict AKI post-surgery. RAAS activation was not biased toward vasodilation or vasoconstriction, as AngII and Ang(1-7) increased similarly and their ratio remained unchanged throughout the study, although the impact of these variations on renal microcirculation remains unknown. Of note, the unchanged AngII/Ang(1-7) ratio indicates that the increase in plasma NEP observed in AKI patients had no impact on RAAS. Finally, RAAS activation translated into a linear increase in aldosterone levels in patients with AKI ≥1S. However, while in patients with AKI ≥ 1A, aldosterone plasma levels markedly increased and remained elevated from admission to the ICU onward, aldosterone levels were similar in noAKI and AKI 1S patients. Importantly, AKI 1S is associated with poor outcomes both after cardiac surgery[21] and in ICU patients.[22] In our AKI 1S patients, since the RAAS was activated but aldosterone levels were similar to the noAKI group, one may speculate that in that context angiotensins rather than aldosterone participate in the pathophysiology of AKI 1S. In contrast, in AKI ≥1A patients, aldosterone elevation could be another layer in the pathophysiology of AKI and suggest that aldosterone elevation is associated with the transition from AKI 1S to ≥1A. However, our study design does not allow us to test whether

RAAS activation is a cause or a consequence of AKI. Interestingly, spironolactone administered before and after cardiac surgery did not prevent CSA-AKI.[23] Similarly, a meta-analysis found that continuation of chronic ACEi or ARB treatment before surgery was associated with a poorer outcome,[24] although no randomized trials were included in this study. Although the STOP-OR-NOT trial does not include patients after cardiac surgery, it may provide insights into the role of the upstream RAAS component in AKI.[25] Overall, this does not exclude a possible role of RAAS in the pathophysiology of CSA-AKI and RAASi may need fine adjustment only to limit the consequences of the operative stress.

Finally, it has been proposed that in severe CSA-AKI, the reduced renin/aldosterone ratio resulted from an increase in renin due to a deficit in AngII production.[14] Although we did not include patients with severe AKI, our data indicate that this may not be the case: i) RAAS activation was complete and unbiased; ii) the renin/aldosterone ratio was constant over time, as described in the less severe patients in the aforementioned study[14]; iii) there was an incremental increase in prorenin/renin production with the severity of the AKI that was not associated with a deficit in AngII, even in absence of AKI. Alternatively, one may speculate that in severe CSA-AKI the low aldosterone output result from either the depletion of aldosterone storage, aldosterone release relying on rate limiting aldosterone *de novo* synthesis or from the inhibition of aldosterone release and synthesis by increasing ANP concentration.[26]

Our study has some limitations that need to be acknowledged. First, this is a monocentric study with a limited population which may limit the statistical performances. However, the patients included were well-phenotyped and the variations in biomarkers were homogeneous between the groups considered. Second, the samples were not collected specifically for RAAS measurements. However, the results obtained are consistent across all the RAAS components measured, suggesting it had a minimal impact on the conclusions.

In conclusion, plasma NEP appears as a promising biomarker to differentially predict CSA-AKI 1S and CSA-AKI ≥1A. Similarly, preoperative AngI plasma levels could predict CSA-AKI. More studies are warranted to test those potential biomarkers as a general predictor of AKI as suggested for urinary NEP.[27] Finally, CSA-AKI is associated with fully unbiased RAAS activation, whose pathophysiological role needs clarification.

Disclosures

AP received a grant from 4TEEN4 Pharmaceutical GmbH outside the scope of this study. AS received a grant from B Braun Avitum and Edwards Lifescience, consulting fees from Biomerieux, and honoraria from Fresenius Medical Care, Jafron Medical, and Cytosorbent SA, all outside the scope of this study. ML received consulting fees from Sphingotech, La Jolla, and Alexion outside the scope of this study. TM, JML, and NV have no competing interests to declare.

Funding

This work was funded by the Institut national de la santé et de la recherche médicale and Université Paris Cité and the Intensive Care Unit Research Fund of the Centre Hospitalier Universitaire Vaudois.

Acknowledgements

The authors thank the nurses and clinical research assistants of the ICU department and the department of biochemistry at CHUV Lausanne for their assistance. We thank Walter Fischli for his technical advice. TM, ML, and NV are member of the F-CRIN INI-CRCT Network Nancy, France. TM, AP, JML and NV are member of the Institute for Cardiovascular Sciences, Université Paris Cité, France.

Authors' contributions

Substantial contributions to the conception or design of the work: TM, ML, MK, AS, and NV; acquisition, analysis, or interpretation of data for the work: TM, MA, AP, JML, and NV; Drafting the work: TM, JML, and NV; revising it critically for important intellectual content: MA, AP, MK, ML, and AS. All the authors approved the final version of the manuscript and agree to be accountable for all aspects of the work.

Data sharing statement

Datasets used and/or analyzed during the current study are available from the corresponding author upon reasonable request.

References

1. Hobson CE, Yavas S, Segal MS, Schold JD, Tribble CG, Layon AJ, Bihorac A: Acute kidney injury is associated with increased long-term mortality after cardiothoracic surgery. *Circulation,* 119**:** 2444-2453, 2009 10.1161/CIRCULATIONAHA.108.800011

2. Ferreiro A, Lombardi R: Acute kidney injury after cardiac surgery is associated with mid-term but not long-term mortality: A cohort-based study. *PLoS One,* 12**:** e0181158, 2017 10.1371/journal.pone.0181158

3. Hu J, Chen R, Liu S, Yu X, Zou J, Ding X: Global Incidence and Outcomes of Adult Patients With Acute Kidney Injury After Cardiac Surgery: A Systematic Review and Meta-Analysis. *J Cardiothorac Vasc Anesth,* 30**:** 82-89, 2016 10.1053/j.jvca.2015.06.017

4. Vandenberghe W, Gevaert S, Kellum JA, Bagshaw SM, Peperstraete H, Herck I, Decruyenaere J, Hoste EA: Acute Kidney Injury in Cardiorenal Syndrome Type 1

Patients: A Systematic Review and Meta-Analysis. *Cardiorenal Med,* 6**:** 116-128, 2016 10.1159/000442300

5. Bellomo R, Ronco C, Kellum JA, Mehta RL, Palevsky P, Acute Dialysis Quality Initiative w: Acute renal failure - definition, outcome measures, animal models, fluid therapy and information technology needs: the Second International Consensus Conference of the Acute Dialysis Quality Initiative (ADQI) Group. *Crit Care,* 8**:** R204-212, 2004 10.1186/cc2872
6. Khwaja A: KDIGO clinical practice guidelines for acute kidney injury. *Nephron Clin Pract,* 120**:** c179-184, 2012 10.1159/000339789
7. Mehta RL, Kellum JA, Shah SV, Molitoris BA, Ronco C, Warnock DG, Levin A, Acute Kidney Injury N: Acute Kidney Injury Network: report of an initiative to improve outcomes in acute kidney injury. *Crit Care,* 11**:** R31, 2007 10.1186/cc5713
8. Legrand M, Darmon M: Biomarkers for AKI improve clinical practice: yes. *Intensive Care Med,* 41**:** 615-617, 2015 10.1007/s00134-014-3530-2
9. Ostermann M, Zarbock A, Goldstein S, Kashani K, Macedo E, Murugan R, Bell M, Forni L, Guzzi L, Joannidis M, Kane-Gill SL, Legrand M, Mehta R, Murray PT, Pickkers P, Plebani M, Prowle J, Ricci Z, Rimmele T, Rosner M, Shaw AD, Kellum JA, Ronco C: Recommendations on Acute Kidney Injury Biomarkers From the Acute Disease Quality Initiative Consensus Conference: A Consensus Statement. *JAMA Netw Open,* 3**:** e2019209, 2020 10.1001/jamanetworkopen.2020.19209
10. Su LJ, Li YM, Kellum JA, Peng ZY: Predictive value of cell cycle arrest biomarkers for cardiac surgery-associated acute kidney injury: a meta-analysis. *Br J Anaesth,* 121**:** 350-357, 2018 10.1016/j.bja.2018.02.069
11. Meersch M, Schmidt C, Hoffmeier A, Van Aken H, Wempe C, Gerss J, Zarbock A: Prevention of cardiac surgery-associated AKI by implementing the KDIGO guidelines

in high risk patients identified by biomarkers: the PrevAKI randomized controlled trial. *Intensive Care Med,* 43**:** 1551-1561, 2017 10.1007/s00134-016-4670-3

12. Campbell DJ: Long-term neprilysin inhibition - implications for ARNIs. *Nat Rev Cardiol,* 14**:** 171-186, 2017 10.1038/nrcardio.2016.200
13. Bernardi MH, Wagner L, Ryz S, Puchinger J, Nixdorf L, Edlinger-Stanger M, Geilen J, Kainz M, Hiesmayr MJ, Lassnigg A: Urinary neprilysin for early detection of acute kidney injury after cardiac surgery: A prospective observational study. *Eur J Anaesthesiol,* 38**:** 13-21, 2021 10.1097/EJA.0000000000001321
14. Kullmar M, Saadat-Gilani K, Weiss R, Massoth C, Lagan A, Cortes MN, Gerss J, Chawla LS, Fliser D, Meersch M, Zarbock A: Kinetic Changes of Plasma Renin Concentrations Predict Acute Kidney Injury in Cardiac Surgery Patients. *Am J Respir Crit Care Med,* 203**:** 1119-1126, 2021 10.1164/rccm.202005-2050OC
15. Legrand M, Bokoch MP: The Yin and Yang of the Renin-Angiotensin-Aldosterone System in Acute Kidney Injury. *Am J Respir Crit Care Med,* 203**:** 1053-1055, 2021 10.1164/rccm.202012-4419ED
16. Nougue H, Pezel T, Picard F, Sadoune M, Arrigo M, Beauvais F, Launay JM, Cohen-Solal A, Vodovar N, Logeart D: Effects of sacubitril/valsartan on neprilysin targets and the metabolism of natriuretic peptides in chronic heart failure: a mechanistic clinical study. *Eur J Heart Fail,* 21**:** 598-605, 2019 10.1002/ejhf.1342
17. Suzuki S, Goto T, Lee SH, Oe T: Robust analysis of angiotensin peptides in human plasma: Column switching-parallel LC/ESI-SRM/MS without adsorption or enzymatic decomposition. *Anal Biochem,* 630**:** 114327, 2021 10.1016/j.ab.2021.114327
18. R Core Team: R: A Language and Environment for Statistical Computing. 4.0.3 Ed. Vienna, Austria, R Foundation for Statistical Computing, 2020

19. Robin X, Turck N, Hainard A, Tiberti N, Lisacek F, Sanchez JC, Muller M: pROC: an open-source package for R and S+ to analyze and compare ROC curves. *BMC Bioinformatics,* 12**:** 77, 2011 10.1186/1471-2105-12-77

20. Bayes-Genis A, Barallat J, Galan A, de Antonio M, Domingo M, Zamora E, Gastelurrutia P, Vila J, Penafiel J, Galvez-Monton C, Lupon J: Multimarker Strategy for Heart Failure Prognostication. Value of Neurohormonal Biomarkers: Neprilysin vs NT-proBNP. *Rev Esp Cardiol (Engl Ed),* 68**:** 1075-1084, 2015 10.1016/j.rec.2015.07.001

21. Albert C, Albert A, Kube J, Bellomo R, Wettersten N, Kuppe H, Westphal S, Haase M, Haase-Fielitz A: Urinary biomarkers may provide prognostic information for subclinical acute kidney injury after cardiac surgery. *J Thorac Cardiovasc Surg,* 155**:** 2441-2452 e2413, 2018 10.1016/j.jtcvs.2017.12.056

22. Depret F, Hollinger A, Cariou A, Deye N, Vieillard-Baron A, Fournier MC, Jaber S, Damoisel C, Lu Q, Monnet X, Rennuit I, Darmon M, Leone M, Guidet B, Sonneville R, Montravers P, Pili-Floury S, Lefrant JY, Duranteau J, Laterre PF, Brechot N, Oueslati H, Cholley B, Struck J, Hartmann O, Mebazaa A, Gayat E, Legrand M: Incidence and Outcome of Subclinical Acute Kidney Injury Using penKid in Critically Ill Patients. *Am J Respir Crit Care Med,* 202**:** 822-829, 2020 10.1164/rccm.201910-1950OC

23. Barba-Navarro R, Tapia-Silva M, Garza-Garcia C, Lopez-Giacoman S, Melgoza-Toral I, Vazquez-Rangel A, Bazua-Valenti S, Bobadilla N, Wasung de Lay M, Baranda F, Chawla LS, Gamba G, Madero M: The Effect of Spironolactone on Acute Kidney Injury After Cardiac Surgery: A Randomized, Placebo-Controlled Trial. *Am J Kidney Dis,* 69**:** 192-199, 2017 10.1053/j.ajkd.2016.06.013

24. Yacoub R, Patel N, Lohr JW, Rajagopalan S, Nader N, Arora P: Acute kidney injury and death associated with renin angiotensin system blockade in cardiothoracic surgery: a

meta-analysis of observational studies. *Am J Kidney Dis*, 62**:** 1077-1086, 2013 10.1053/j.ajkd.2013.04.018

25. Legrand M, Futier E, Leone M, Deniau B, Mebazaa A, Plaud B, Coriat P, Rossignol P, Vicaut E, Gayat E, investigators S-O-Ns: Impact of renin-angiotensin system inhibitors continuation versus discontinuation on outcome after major surgery: protocol of a multicenter randomized, controlled trial (STOP-or-NOT trial). *Trials*, 20**:** 160, 2019 10.1186/s13063-019-3247-1
26. Chartier L, Schiffrin EL: Role of calcium in effects of atrial natriuretic peptide on aldosterone production in adrenal glomerulosa cells. *Am J Physiol*, 252**:** E485-491, 1987 10.1152/ajpendo.1987.252.4.E485
27. Pajenda S, Mechtler K, Wagner L: Urinary neprilysin in the critically ill patient. *BMC Nephrol*, 18**:** 172, 2017 10.1186/s12882-017-0587-5

Figure legends

Figure 1: Neprilysin in CSA-AKI. A) Schematic representation of the Renin-Angiotensin-Aldosterone system. **B)** Plasma NEP concentration in noAKI and AKI patients before cardiac surgery (pre-op), at admission to the ICU (ICU adm.), and 24 and 48 hours after the admission to the ICU. **C)** Plasma NEP concentration in AKI 1S and AKI ≥1A patients before cardiac surgery (pre-op), at admission to the ICU (ICU adm.), and 24 and 48 hours after the admission to the ICU. Variables in A and C were analyzed using repeated measure ANOVA followed by the HSD Tukey test **(Supplemental Table *1* and *3*)**, and intergroup comparisons were performed using the Wilcoxon sum rank test. Filled and open circles represent patients that do and do not receive chronic angiotensin receptor blockers/angiotensin converting enzyme inhibitor treatment.

Figure 2: Renin in CSA-AKI. A) Plasma renin concentration in noAKI, AKI 1S and AKI≥1A patients before cardiac surgery (pre-op), at admission to the ICU (ICU adm.), and 24 and 48 hours after the admission to the ICU. **B)** Plasma renin activity (PRA) in noAKI, AKI 1S and AKI≥1A patients before cardiac surgery (pre-op), at admission to the ICU (ICU adm.), and 24 and 48 hours after the admission to the ICU. **C)** Plasma prorenin concentration in noAKI, AKI 1S and AKI≥1A patients before cardiac surgery (pre-op), at admission to the ICU (ICU adm.), and 24 and 48 hours after the admission to the ICU. Variables were analyzed using repeated measure ANOVA followed by the HSD Tukey test (**Supplemental Table *5*-*7***), and intergroup comparisons were performed using the Kruskal Wallis test followed by the Wilcoxon sum rank test corrected for multiple comparisons. Filled and open circles represent patients that do and do not receive chronic angiotensin receptor blockers/angiotensin converting enzyme inhibitor treatment.

Figure 3: Angiotensins in CSA-AKI. A) Plasma angiotensin I (AngI) concentration in noAKI, AKI 1S and AKI ≥1A patients before cardiac surgery (pre-op), at admission to the ICU (ICU adm.), and 24 and 48 hours after the admission to the ICU. **B)** Plasma angiotensin II (AngII) concentration in noAKI, AKI 1S and AKI ≥1A patients before cardiac surgery (pre-op), at admission to the ICU (ICU adm.), and 24 and 48 hours after the admission to the ICU. **C)** Plasma angiotensin (1-7) [Ang(1-7)] concentration in noAKI, AKI 1S and AKI ≥1A patients before cardiac surgery (pre-op), at admission to the ICU (ICU adm.), and 24 and 48 hours after the admission to the ICU. **D)** AngII/Ang(1-7) in noAKI, AKI 1S and AKI ≥1A patients before cardiac surgery (pre-op), at admission to the ICU (ICU adm.), and 24 and 48 hours after the admission to the ICU. Variables were analyzed using repeated measure ANOVA followed by the HSD Tukey test (**Supplemental Table *9-12***), and intergroup comparisons were performed using the Kruskal Wallis test followed by the Wilcoxon sum rank test corrected for multiple comparisons. Filled and open circles represent patients that do and do not receive chronic angiotensin receptor blockers/angiotensin converting enzyme inhibitor treatment.

Figure 4: Aldosterone in CSA-AKI. A) Plasma aldosterone concentration in noAKI, AKI 1S and AKI ≥1A patients before cardiac surgery (pre-op), at admission to the ICU (ICU adm.), and 24 and 48 hours after the admission to the ICU. B) Comparisons of the relative variation between before surgery (pre-op) and at admission to the ICU of plasma aldosterone in noAKI, AKI 1S and AKI ≥1A patients. C) Relationship between the relative variation between before surgery (pre-op) and at admission to the ICU of the angiotensin II (AngII) and aldosterone in noAKI, AKI 1S and AKI ≥1A patients. E) Renin/aldosterone ratio in noAKI, AKI 1S and AKI ≥1A patients before cardiac surgery (pre-op), at admission to the ICU (ICU adm.), and 24 and 48 hours after the admission to the ICU. Variables in A and D were analyzed using

repeated measure ANOVA followed by the HSD Tukey test **(Supplemental Table *13*-*E14***), and intergroup comparisons were performed using the Kruskal Wallis test followed by the Wilcoxon sum rank test corrected for multiple comparisons. Variables in B were analyzed using the Kruskal Wallis test followed by the Wilcoxon sum rank test corrected for multiple comparisons. In C, correlations were calculated using linear regression. Filled and open circles represent patients that do and do not receive chronic angiotensin receptor blockers/angiotensin converting enzyme inhibitor treatment.

Table 1: Characteristics of the study population. CKD: chronic kidney disease; GFR: glomerular filtration rate; LVEF: left ventricular ejection fraction; COPD: chronic obstructive pulmonary disease; ACEi: angiotensin-converting enzyme inhibitor; ARB: angiotensin receptor blocker; CABG: coronary artery bypass grafting; SOFA: sequential organ failure assessment; Hb: haemoglobin. Intergroup comparisons were performed using the Wilcoxon sum rank test.

	No AKI (N=15)	AKI ≥1S (N=25)	Overall (N=40)	P value
Preoperative Characteristics				
Age – years	64.0 [54.0, 69.0]	71.0 [65.0, 77.0]	69.0 [60.0, 75.5]	0.027
Female sex - no. (%)	13 (86.7)	18 (72.0)	31 (77.5)	0.494
CKD - no. (%)	9 (60.0)	21 (84.0)	30 (75.0)	0.135
GFR (mL/min)	85.0 [67.0, 90.0]	69.0 [55.0, 81.0]	74.0 [61.2, 88.5]	0.065
Heart Failure - no. (%)	4 (26.7)	6 (25.0)	10 (25.6)	1.00
LVEF (%)	67.0 [60.0, 69.5]	62.5 [56.5, 65.0]	65.0 [56.0, 68.0]	0.125
Diabetes - no.(%)	4 (26.7)	6 (24.0)	10 (25.0)	1.00
Hypertension - no. (%)	12 (80.0)	17 (68.0)	29 (72.5)	0.648
Tobacco users - no. (%)	5 (33.3)	5 (20.0)	10 (25.0)	0.572
Peripheral Vascular Disease - no.(%)	1 (6.7)	2 (8.0)	3 (7.5)	1.00
COPD - no.(%)	0 (0)	0 (0)	0 (0)	NA
Iodine-based contrast - no.(%)	3 (20.0)	7 (28.0)	10 (25.0)	0.85
ACEi - no.(%)	7 (46.7)	14 (56.0)	21 (52.5)	0.806
ARBs - no.(%)	1 (6.7)	2 (8.0)	3 (7.5)	1.00
Intraoperative Characteristic				
Types of heart surgery: CABG Aortic valve surgery	 6 (40.0) 1 (6.7)	 10 (40.0) 3 (12.0)	 16 (40.0) 4 (10.0)	0.926

Mitral valve surgery Aortic surgery Multiple heart surgery	4 (26.7) 2 (13.3) 2 (13.3)	4 (16.0) 4 (16.0) 4 (16.0)	8 (20.0) 6 (15.0) 6 (15.0)	
Cardiopulmonary bypass (min)	80.0 [56.0, 94.0]	78.0 [64.0, 101.0]	78.0 [62.5, 100.5]	0.747
Aortic Cross-clamping (min)	49.0 [40.7, 81.2]	58.0 [41.0, 75.0]	58.0 [40.5, 78.0]	0.703
Urinary Output (mL/h)	300.0 [217.5, 470.0]	250.0 [190.0, 380.0]	260.0 [190.0, 445.0]	0.4
Postoperative Characteristics				
SOFA at ICU admission	5.0 [3.2, 6.0]	5.0 [4.0, 5.0]	5.0 [4.0, 5.5]	0.74
Mechanical Ventilation - no.(%)	9 (60.0)	10 (40.0)	19 (47.5)	0.369
Dobutamine (μg /min)	0.0 [0.0, 50.0]	0.0 [0.0, 100.0]	0.0 [0.0, 100.0]	0.567
Norepinephrine (μg /min)	5.0 [0.5, 5.5]	5.0 [2.0, 8.0]	5.0 [2.0, 8.0]	0.535
Epinephrine (μg/min)	0.0 [0.0, 0.0]	0.0 [0.0, 0.0]	0.0 [0.0, 0.0]	0.711
Systolic Arterial Pressure(mmHg)	109.0 [105.5, 114.5]	105.0 [94.0, 112.0]	107.5 [97.0, 114.0]	0.269
Diastolic Arterial Pressure (mmHg)	59.0 [55.0, 67.5]	55.0 [44.0, 62.0]	57.0 [48.75, 65.5]	0.162
Mean Arterial Pressure (mmHg)	77.0 [69.5, 85.5]	73.0 [63.0, 80.0]	74.5 [63.75, 83.0]	0.175
Lactate (mmol/l)	1.5 [1.30, 1.70]	2.0 [1.40, 2.10]	1.70 [1.30, 2.10]	0.117
Hb (g/l)	118.0 [107.5, 130.5]	121.0 [103.0, 132.0]	120.0 [105.5, 132.0]	0.889
Urea (mmol/l)	5.45 [3.70, 6.2]	5.0 [4.6, 5.7]	5.1 [4.3, 6.0]	0.884
Serum creatinine (μmol/l)	78.0 [74.0, 83.0]	79.0 [71.0, 101.0]	78.0 [71.0, 90.2]	0.52

Abbreviations

CSA-AKI: Cardiac Surgery-Associated Acute Kidney Injury

NEP: Neprilysin

RAAS: Renin-Angiotensin-Aldosterone System

AngII: Angiotensin II

AngI: Angiotensin I

Ang(1-7): Angiotensin (1-7)

ICU: Intensive Care Unit

RAASi: Renin-Angiotensin-Aldosterone System inhibitor

AKI: Acute Kidney Injury

ANOVA: Analysis of Variance

AR: Active Renin

KDIGO: Kidney Disease Improving Global Outcomes

GFR: Glomerular Filtration Rate

LVEF: Left Ventricular Ejection Fraction

IGFBP-7: Insulin Growth Factor Binding Protein 7

TIMP-2: Tissue inhibitor of metalloproteinases 2

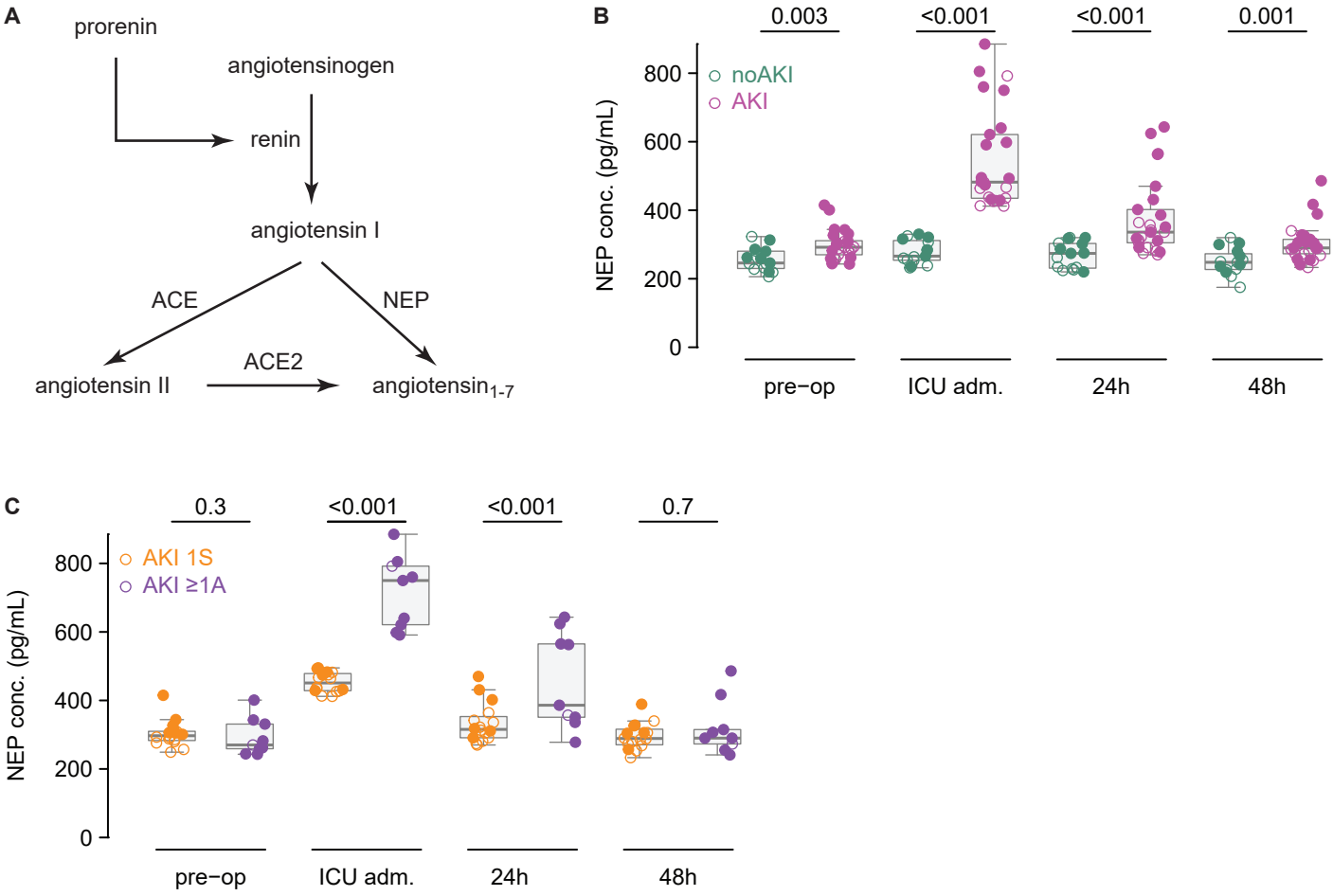
A
prorenin
angiotensinogen
renin
angiotensin I
ACE
NEP
ACE2
angiotensin II
angiotensin1-7
B
0.003
<0.001
<0.001
0.001
noAKI
AKI
NEP conc. (pg/mL)
800
600
400
200
0
pre−op
ICU adm.
24h
48h
C
0.3
<0.001
<0.001
0.7
AKI 1S
AKI ≥1A
NEP conc. (pg/mL)
800
600
400
200
0
pre−op
ICU adm.
24h
48h

Figure 1

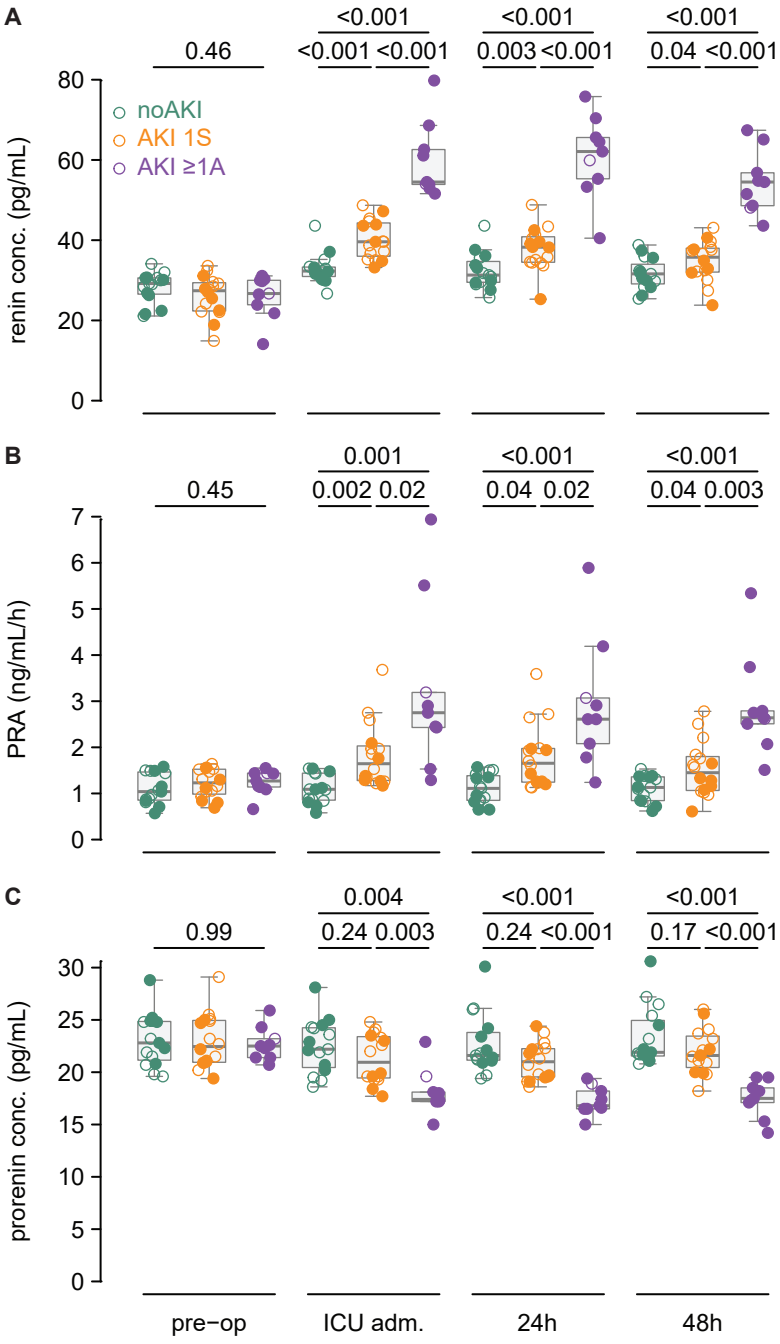
A
B
C
noAKI
AKI 1S
AKI ≥1A
renin conc. (pg/mL)
PRA (ng/mL/h)
prorenin conc. (pg/mL)
0.46
<0.001
<0.001 <0.001
<0.001
0.003 <0.001
<0.001
0.04 <0.001
0.45
0.001
0.002 0.02
<0.001
0.04 0.02
<0.001
0.04 0.003
0.99
0.004
0.24 0.003
<0.001
0.24 <0.001
<0.001
0.17 <0.001
pre−op
ICU adm.
24h
48h

Figure 2

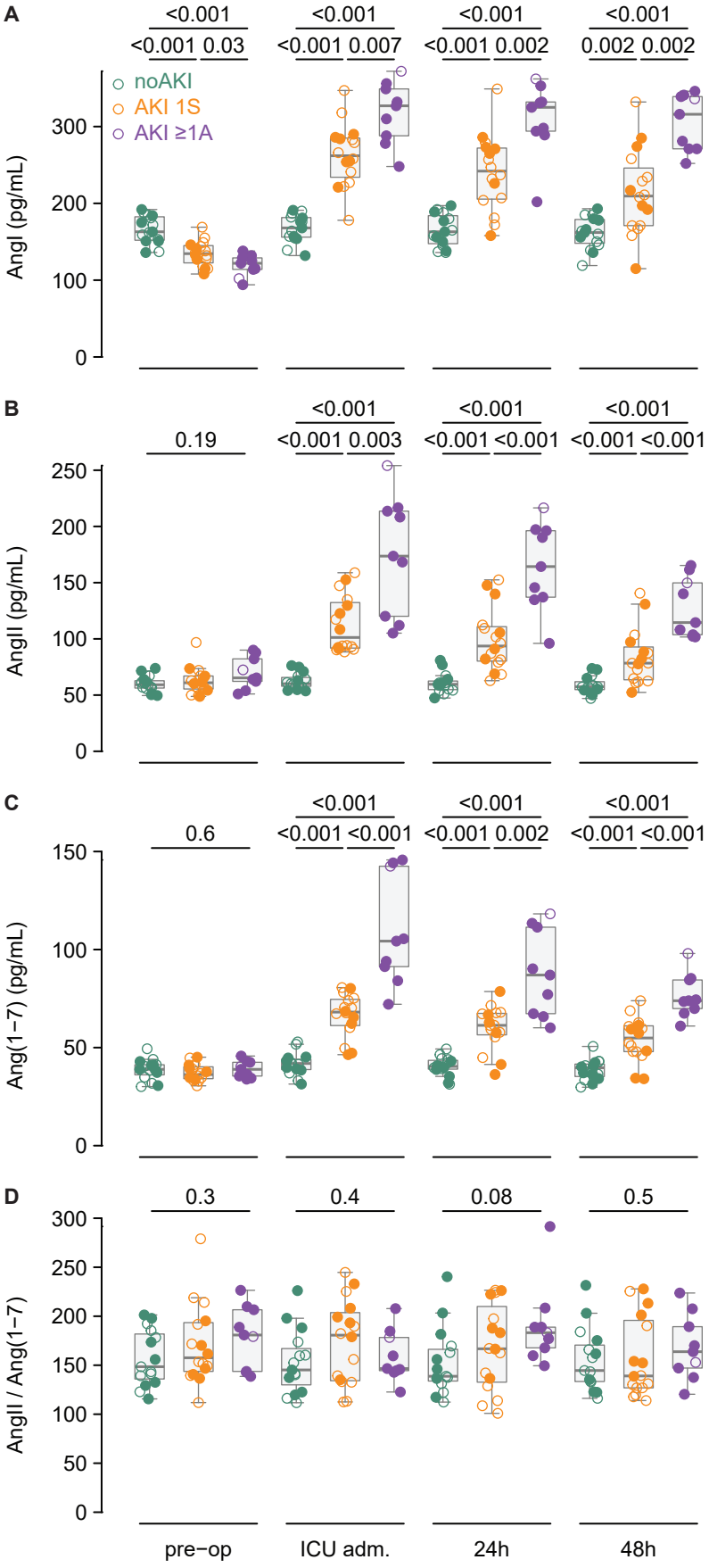
A
<0.001
<0.001 0.03
<0.001
<0.001 0.007
<0.001
<0.001 0.002
<0.001
0.002 0.002
noAKI
AKI 1S
AKI ≥1A
AngI (pg/mL)
300
200
100
0
B
0.19
<0.001
<0.001 0.003
<0.001
<0.001 <0.001
<0.001
<0.001 <0.001
AngII (pg/mL)
250
200
150
100
50
0
C
0.6
<0.001
<0.001 <0.001
<0.001
<0.001 0.002
<0.001
<0.001 <0.001
Ang(1−7) (pg/mL)
150
100
50
0
D
0.3
0.4
0.08
0.5
AngII / Ang(1−7)
300
250
200
150
100
50
0
pre−op
ICU adm.
24h
48h

Figure 3

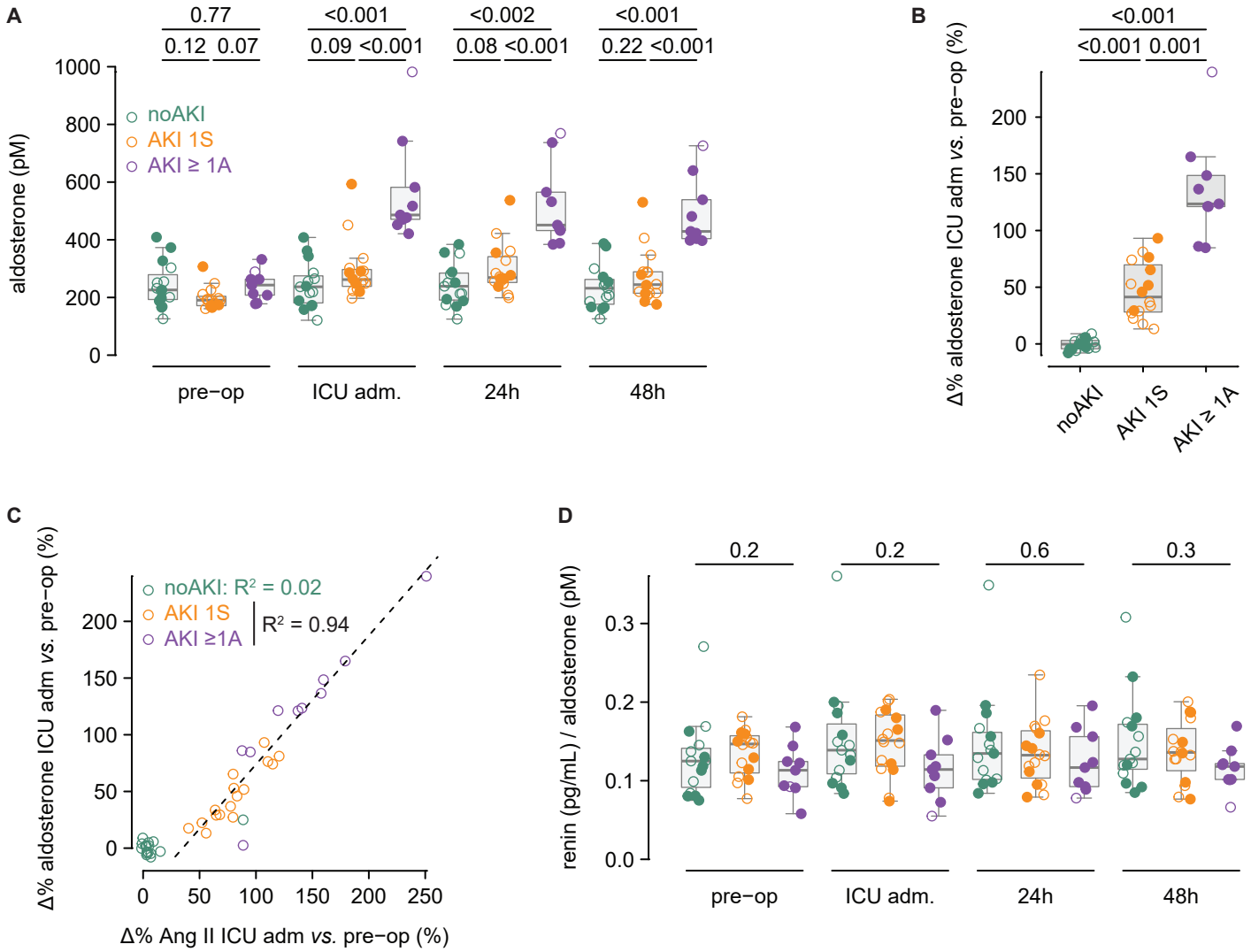
A
0.77
<0.001
<0.002
<0.001
0.12 0.07
0.09 <0.001
0.08 <0.001
0.22 <0.001
aldosterone (pM)
noAKI
AKI 1S
AKI ≥ 1A
pre−op
ICU adm.
24h
48h
B
<0.001
<0.001 0.001
Δ% aldosterone ICU adm vs. pre−op (%)
noAKI
AKI 1S
AKI ≥ 1A
C
noAKI: R² = 0.02
AKI 1S
AKI ≥1A
R² = 0.94
Δ% aldosterone ICU adm vs. pre−op (%)
Δ% Ang II ICU adm vs. pre−op (%)
D
0.2
0.2
0.6
0.3
renin (pg/mL) / aldosterone (pM)
pre−op
ICU adm.
24h
48h

Figure 4

Neprilysin and the renin-angiotensin-aldosterone system in acute kidney injury after cardiac surgery: an exploratory study

Thibault Michel, Marco Altareli, Adrien Picod, Mathias Kirch, Matthieu Legrand, Jean-Marie Launay, Antoine Schneider, Nicolas Vodovar

Online Data Supplement

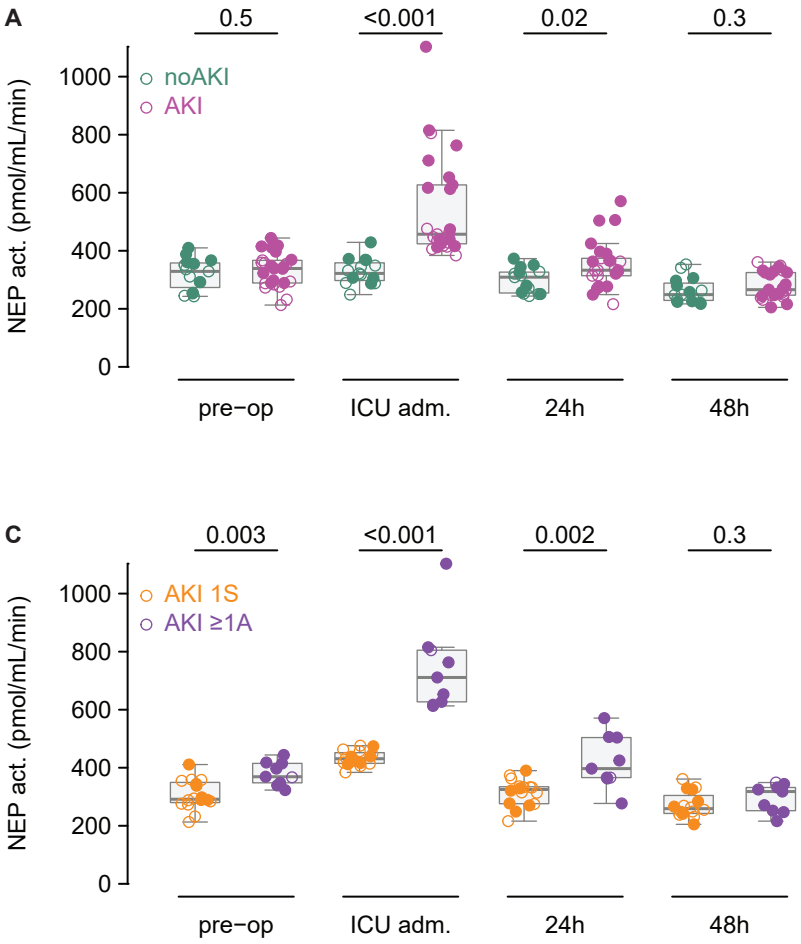

Supplemental Figure 1: Neprilysin activity in CSA-AKI. A) Plasma NEP activity in noAKI and AKI patients before cardiac surgery (pre-op), at admission to the ICU (ICU adm.), and 24 and 48 hours after the admission to the ICU. **B)** Plasma NEP activity in AKI 1S and AKI ≥1A patients before cardiac surgery (pre-op), at admission to the ICU (ICU adm.), and 24 and 48 hours after the admission to the ICU. Variables were analyzed using repeated measure ANOVA followed by the HSD Tukey test (***Supplemental Tables 2 and 4***), and intergroup comparisons were performed using the Wilcoxon sum rank test. Filled and open circles represent patients that do and do not receive chronic angiotensin receptor blockers/angiotensin converting enzyme inhibitor treatment.

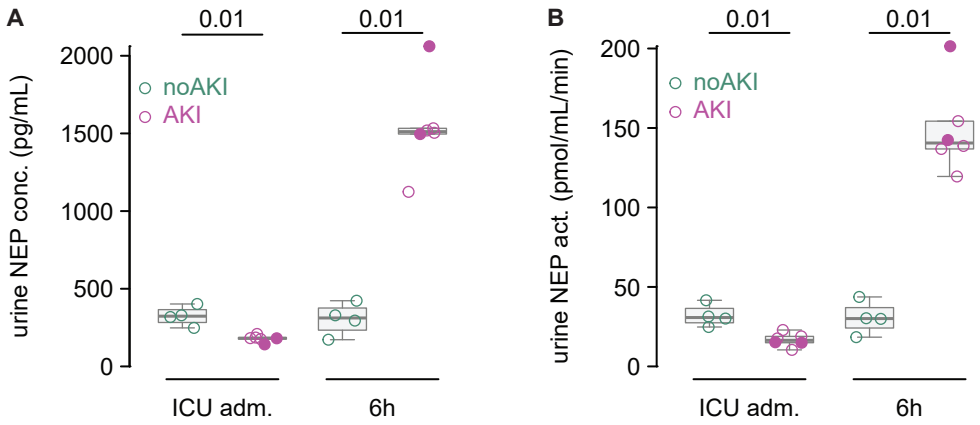

Supplemental Figure 2: Urine neprilysin in CSA-AKI. A-B) Urine NEP concentration (**A**) and activity (**B**) in noAKI and AKI patients at admission to the ICU (ICU adm.) and 6 hours after the admission to the ICU in patients with urine samples at both time points. Variables were analyzed using the Wilcoxon sum rank test and Wilcoxon signed rank test for intergroup and within group comparisons, respectively. Filled and open circles represent patients that do and do not receive chronic angiotensin receptor blockers/angiotensin converting enzyme inhibitor treatment.

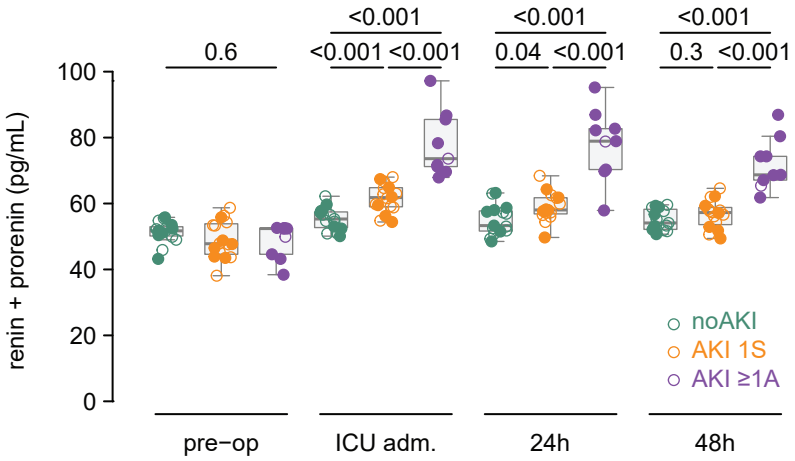

Supplemental Figure 3: Renin and prorenin in CSA-AKI. Sum of plasma renin and prorenin concentrations in noAKI, AKI 1S, and AKI ≥1A patients before cardiac surgery (pre-op), at admission to the ICU (ICU adm.), and 24 and 48 hours after the admission to the ICU. Variables were analyzed using repeated measure ANOVA followed by the HSD Tukey test (***Supplemental Table 8***). Filled and open circles represent patients that do and do not receive chronic angiotensin receptor blockers/angiotensin converting enzyme inhibitor treatment.

Supplemental Table 1: Longitudinal analysis of NEP concentration (pg/mL) in the noAKI and AKI ≥ 1S groups by repeated-measure ANOVA on log-transformed data followed by the Tukey HSD test.

Comparison	Time1	Time2	P-value
noAKI group (P_{ANOVA} = 0.0024)			
Pre-op vs. ICU adm.	246 [230 - 280.5]	266 [254 - 311.5]	**0.031**
Pre-op vs. 24h	246 [230 - 280.5]	274 [231 - 303]	0.39
Pre-op vs. 48h	246 [230 - 280.5]	248 [227 - 273]	0.8
ICU adm. vs. 24h	266 [254 - 311.5]	274 [231 - 303]	0.58
ICU adm. vs. 48h	266 [254 - 311.5]	248 [227 - 273]	**0.003**
24h vs. 48h	274 [231 - 303]	248 [227 - 273]	0.07
AKI ≥ 1S group (P_{ANOVA} < 0.0001)			
Pre-op vs. ICU adm.	292 [270 - 311]	482 [435 - 621]	< **0.0001**
Pre-op vs. 24h	292 [270 - 311]	336 [305 - 402]	**0.0004**
Pre-op vs. 48h	292 [270 - 311]	290 [273 - 315]	0.99
ICU adm. vs. 24h	482 [435 - 621]	336 [305 - 402]	< **0.0001**
ICU adm. vs. 48h	482 [435 - 621]	290 [273 - 315]	< **0.0001**
24h vs. 48h	336 [305 - 402]	290 [273 - 315]	**0.0009**

Supplemental Table 2: Longitudinal analysis of NEP activity (pmol/mL/min) in the no AKI and AKI ≥ 1S groups by repeated-measure ANOVA on log-transformed data followed by the Tukey HSD test.

Comparison	Time1	Time2	P-value
noAKI group ($P_{ANOVA} < 0.0001$)			
Pre-op vs. ICU adm.	329 [273.5 - 358]	322 [297.5 - 358.5]	0.75
Pre-op vs. 24h	329 [273.5 - 358]	309 [254.5 - 326.5]	0.26
Pre-op vs. 48h	329 [273.5 - 358]	249 [229 - 288.5]	**< 0.0001**
ICU adm. vs. 24h	322 [297.5 - 358.5]	309 [254.5 - 326.5]	**0.033**
ICU adm. vs. 48h	322 [297.5 - 358.5]	249 [229 - 288.5]	**< 0.0001**
24h vs. 48h	309 [254.5 - 326.5]	249 [229 - 288.5]	**0.004**
AKI ≥ 1S group ($P_{ANOVA} < 0.0001$)			
Pre-op vs. ICU adm.	339 [289 - 367]	457 [424 - 627]	**< 0.0001**
Pre-op vs. 24h	339 [289 - 367]	333 [314 - 374]	0.71
Pre-op vs. 48h	339 [289 - 367]	266 [247 - 325]	**0.001**
ICU adm. vs. 24h	457 [424 - 627]	333 [314 - 374]	**< 0.0001**
ICU adm. vs. 48h	457 [424 - 627]	266 [247 - 325]	**< 0.0001**
24h vs. 48h	333 [314 - 374]	266 [247 - 325]	**< 0.0001**

Supplemental Table 3: Longitudinal analysis of NEP concentration (pg/mL) in the AKI 1S and AKI ≥ 1A groups by repeated-measure ANOVA on log-transformed data followed by the Tukey HSD test.

Comparison	Time1	Time2	P-value
noAKI group ($P_{ANOVA} < 0.0001$)			
Pre-op vs. ICU adm.	297 [284.5 - 309.5]	451 [428.75 - 476.75]	**<0.0001**
Pre-op vs. 24h	297 [284.5 - 309.5]	315.5 [291 - 347.5]	**0.046**
Pre-op vs. 48h	297 [284.5 - 309.5]	289 [271.75 - 311]	0.88
ICU adm. vs. 24h	451 [428.75 - 476.75]	315.5 [291 - 347.5]	**<0.0001**
ICU adm. vs. 48h	451 [428.75 - 476.75]	289 [271.75 - 311]	**<0.0001**
24h vs. 48h	315.5 [291 - 347.5]	289 [271.75 - 311]	**0.007**
AKI ≥ 1S group ($P_{ANOVA} < 0.0001$)			
Pre-op vs. ICU adm.	270 [259 - 331]	750 [621 - 792]	**<0.0001**
Pre-op vs. 24h	270 [259 - 331]	386 [351 - 565]	**0.0008**
Pre-op vs. 48h	270 [259 - 331]	290 [273 - 315]	0.84
ICU adm. vs. 24h	750 [621 - 792]	386 [351 - 565]	**0.0001**
ICU adm. vs. 48h	750 [621 - 792]	290 [273 - 315]	**<0.0001**
24h vs. 48h	386 [351 - 565]	290 [273 - 315]	**0.006**

Supplemental Table 4: Longitudinal analysis of NEP activity (pmol/mL/min) in the no AKI 1S and AKI ≥ 1A groups by repeated-measure ANOVA on log-transformed data followed by the Tukey HSD test.

Comparison	Time1	Time2	P-value
noAKI group ($P_{ANOVA} < 0.0001$)			
Pre-op vs. ICU adm.	291.5 [282 - 346.75]	431 [415.5 - 449.5]	**<0.0001**
Pre-op vs. 24h	291.5 [282 - 346.75]	325 [276.5 - 333.75]	0.93
Pre-op vs. 48h	291.5 [282 - 346.75]	259 [243.25 - 294.25]	**0.06**
ICU adm. vs. 24h	431 [415.5 - 449.5]	325 [276.5 - 333.75]	**<0.0001**
ICU adm. vs. 48h	431 [415.5 - 449.5]	259 [243.25 - 294.25]	**<0.0001**
24h vs. 48h	325 [276.5 - 333.75]	259 [243.25 - 294.25]	**0.014**
AKI ≥ 1S group ($P_{ANOVA} < 0.0001$)			
Pre-op vs. ICU adm.	369 [348 - 415]	711 [627 - 805]	**<0.0001**
Pre-op vs. 24h	369 [348 - 415]	397 [366 - 504]	0.54
Pre-op vs. 48h	369 [348 - 415]	318 [252 - 332]	**0.001**
ICU adm. vs. 24h	711 [627 - 805]	397 [366 - 504]	**<0.0001**
ICU adm. vs. 48h	711 [627 - 805]	318 [252 - 332]	**<0.0001**
24h vs. 48h	397 [366 - 504]	318 [252 - 332]	**<0.0001**

Supplemental Table 5: Longitudinal analysis of renin plasma concentration (pg/mL) in the noAKI, AKI 1S and AKI ≥ 1A groups by repeated-measure ANOVA on log-transformed data followed by the Tukey HSD test.

Comparison	Time1	Time2	P-value
noAKI group (P_{ANOVA} < 0.0001)			
Pre-op vs. ICU adm.	29.2 [26.6 - 30.6]	32.3 [31 - 33.3]	**<0.0001**
Pre-op vs. 24h	29.2 [26.6 - 30.6]	31.3 [29.5 - 34.7]	**<0.0001**
Pre-op vs. 48h	29.2 [26.6 - 30.6]	31.6 [29.1 - 34]	**0.0002**
ICU adm. vs. 24h	32.3 [31 - 33.3]	31.3 [29.5 - 34.7]	0.88
ICU adm. vs. 48h	32.3 [31 - 33.3]	31.6 [29.1 - 34]	0.4
24h vs. 48h	31.3 [29.5 - 34.7]	31.6 [29.1 - 34]	0.83
AKI 1S group (P_{ANOVA} < 0.0001)			
Pre-op vs. ICU adm.	27.4 [22.4 - 29.3]	39.6 [36.4 - 44.1]	**<0.0001**
Pre-op vs. 24h	27.4 [22.4 - 29.3]	38.25 [34.6 - 40.6]	**<0.0001**
Pre-op vs. 48h	27.4 [22.4 - 29.3]	35.75 [32.1 - 37.9]	**<0.0001**
ICU adm. vs. 24h	39.6 [36.4 - 44.1]	38.25 [34.6 - 40.6]	0.26
ICU adm. vs. 48h	39.6 [36.4 - 44.1]	35.75 [32.1 - 37.9]	**0.0006**
24h vs. 48h	38.25 [34.6 - 40.6]	35.75 [32.1 - 37.9]	0.09
AKI ≥ 1A (P_{ANOVA} < 0.0001)			
Pre-op vs. ICU adm.	26.7 [23.9 - 30]	54.5 [53.9 - 62.6]	**<0.0001**
Pre-op vs. 24h	26.7 [23.9 - 30]	62.1 [55.3 - 65.6]	**<0.0001**
Pre-op vs. 48h	26.7 [23.9 - 30]	54.5 [48.6 - 56.8]	**<0.0001**
ICU adm. vs. 24h	54.5 [53.9 - 62.6]	62.1 [55.3 - 65.6]	1
ICU adm. vs. 48h	54.5 [53.9 - 62.6]	54.5 [48.6 - 56.8]	0.67
24h vs. 48h	62.1 [55.3 - 65.6]	54.5 [48.6 - 56.8]	0.59

Supplemental Table 6: Longitudinal analysis of plasma renin activity (PRA, ng/mL/h) in the noAKI, AKI 1S and AKI ≥ 1A groups by repeated-measure ANOVA on log-transformed data followed by the Tukey HSD test, when appropriate.

Comparison	Time1	Time2	P-value
noAKI group (P_{ANOVA} = 0.9)			
Pre-op vs. ICU adm.	1.04 [0.855 - 1.465]	1.09 [0.855 - 1.44]	na
Pre-op vs. 24h	1.04 [0.855 - 1.465]	1.11 [0.85 - 1.385]	na
Pre-op vs. 48h	1.04 [0.855 - 1.465]	1.13 [0.845 - 1.36]	na
ICU adm. vs. 24h	1.09 [0.855 - 1.44]	1.11 [0.85 - 1.385]	na
ICU adm. vs. 48h	1.09 [0.855 - 1.44]	1.13 [0.845 - 1.36]	na
24h vs. 48h	1.11 [0.85 - 1.385]	1.13 [0.845 - 1.36]	na
AKI 1S group (P_{ANOVA} < 0.0001)			
Pre-op vs. ICU adm.	1.23 [1.0125 - 1.5225]	1.645 [1.285 - 2]	**<0.0001**
Pre-op vs. 24h	1.23 [1.0125 - 1.5225]	1.655 [1.2525 - 1.9725]	**<0.0001**
Pre-op vs. 48h	1.23 [1.0125 - 1.5225]	1.45 [1.0725 - 1.78]	**0.0007**
ICU adm. vs. 24h	1.645 [1.285 - 2]	1.655 [1.2525 - 1.9725]	0.98
ICU adm. vs. 48h	1.645 [1.285 - 2]	1.45 [1.0725 - 1.78]	**0.0005**
24h vs. 48h	1.655 [1.2525 - 1.9725]	1.45 [1.0725 - 1.78]	**0.002**
AKI ≥ 1A (P_{ANOVA} < 0.0001)			
Pre-op vs. ICU adm.	1.27 [1.14 - 1.44]	2.75 [2.43 - 3.19]	**<0.0001**
Pre-op vs. 24h	1.27 [1.14 - 1.44]	2.61 [2.08 - 3.07]	**<0.0001**
Pre-op vs. 48h	1.27 [1.14 - 1.44]	2.64 [2.51 - 2.79]	**<0.0001**
ICU adm. vs. 24h	2.75 [2.43 - 3.19]	2.61 [2.08 - 3.07]	0.94
ICU adm. vs. 48h	2.75 [2.43 - 3.19]	2.64 [2.51 - 2.79]	0.98
24h vs. 48h	2.61 [2.08 - 3.07]	2.64 [2.51 - 2.79]	1

Supplemental Table 7: Longitudinal analysis of prorenin plasma concentration (pg/mL) in the noAKI, AKI 1S and AKI ≥ 1A groups by repeated-measure ANOVA on log-transformed data followed by the Tukey HSD test, when appropriate.

Comparison	Time1	Time2	P-value
noAKI group (P_{ANOVA} = 0.2)			
Pre-op vs. ICU adm.	22.8 [21.15 - 24.85]	22.2 [20.45 - 24.25]	na
Pre-op vs. 24h	22.8 [21.15 - 24.85]	21.6 [21.15 - 23.8]	na
Pre-op vs. 48h	22.8 [21.15 - 24.85]	21.9 [21.55 - 24.95]	na
ICU adm. vs. 24h	22.2 [20.45 - 24.25]	21.6 [21.15 - 23.8]	na
ICU adm. vs. 48h	22.2 [20.45 - 24.25]	21.9 [21.55 - 24.95]	na
24h vs. 48h	21.6 [21.15 - 23.8]	21.9 [21.55 - 24.95]	na
AKI 1S group (P_{ANOVA} = 0.0004)			
Pre-op vs. ICU adm.	22.45 [20.975 - 24.925]	20.95 [19.525 - 23.35]	**0.002**
Pre-op vs. 24h	22.45 [20.975 - 24.925]	21 [19.575 - 22.225]	**0.0007**
Pre-op vs. 48h	22.45 [20.975 - 24.925]	21.6 [20.675 - 23.325]	0.16
ICU adm. vs. 24h	20.95 [19.525 - 23.35]	21 [19.575 - 22.225]	0.97
ICU adm. vs. 48h	20.95 [19.525 - 23.35]	21.6 [20.675 - 23.325]	0.36
24h vs. 48h	21 [19.575 - 22.225]	21.6 [20.675 - 23.325]	0.18
AKI ≥ 1A (P_{ANOVA} < 0.0001)			
Pre-op vs. ICU adm.	22.5 [21.4 - 23.2]	17.4 [17.2 - 18.1]	**<0.0001**
Pre-op vs. 24h	22.5 [21.4 - 23.2]	16.8 [16.5 - 18.2]	**<0.0001**
Pre-op vs. 48h	22.5 [21.4 - 23.2]	17.5 [17.1 - 18.5]	**<0.0001**
ICU adm. vs. 24h	17.4 [17.2 - 18.1]	16.8 [16.5 - 18.2]	0.5
ICU adm. vs. 48h	17.4 [17.2 - 18.1]	17.5 [17.1 - 18.5]	0.69
24h vs. 48h	16.8 [16.5 - 18.2]	17.5 [17.1 - 18.5]	0.99

Supplemental Table 8: Longitudinal analysis of the sum of plasma renin and prorenin concentration (pg/mL) in the noAKI, AKI 1S and AKI ≥ 1A groups by repeated-measure ANOVA on log-transformed data followed by the Tukey HSD test.

Comparison	Time1	Time2	P-value
noAKI group ($P_{ANOVA} < 0.0001$)			
Pre-op vs. ICU adm.	51.7 [50.2 - 53]	55.3 [52.7 - 57.5]	**<0.0001**
Pre-op vs. 24h	51.7 [50.2 - 53]	53.3 [51.7 - 57.8]	**<0.0001**
Pre-op vs. 48h	51.7 [50.2 - 53]	54.1 [52.2 - 58.3]	**<0.0001**
ICU adm. vs. 24h	55.3 [52.7 - 57.5]	53.3 [51.7 - 57.8]	0.96
ICU adm. vs. 48h	55.3 [52.7 - 57.5]	54.1 [52.2 - 58.3]	0.98
24h vs. 48h	53.3 [51.7 - 57.8]	54.1 [52.2 - 58.3]	1
AKI 1S group ($P_{ANOVA} < 0.0001$)			
Pre-op vs. ICU adm.	47.8 [45 - 53.6]	61.8 [59.1 - 64.8]	**<0.0001**
Pre-op vs. 24h	47.8 [45 - 53.6]	58.1 [57.025 - 61.7]	**<0.0001**
Pre-op vs. 48h	47.8 [45 - 53.6]	57.3 [54 - 58.6]	**<0.0001**
ICU adm. vs. 24h	61.8 [59.1 - 64.8]	58.1 [57 - 61.7]	0.16
ICU adm. vs. 48h	61.8 [59.1 - 64.8]	57.3 [54 - 58.6]	**0.002**
24h vs. 48h	58.1 [57 - 61.7]	57.3 [54 - 58.6]	0.31
AKI ≥ 1A ($P_{ANOVA} < 0.0001$)			
Pre-op vs. ICU adm.	52.4 [44.6 - 52.5]	73.6 [71.2 - 85.5]	**<0.0001**
Pre-op vs. 24h	52.4 [44.6 - 52.5]	78.9 [70.3 - 82.7]	**<0.0001**
Pre-op vs. 48h	52.4 [44.6 - 52.5]	68.7 [67.1 - 74.3]	**<0.0001**
ICU adm. vs. 24h	73.6 [71.2 - 85.5]	78.9 [70.3 - 82.7]	1
ICU adm. vs. 48h	73.6 [71.2 - 85.5]	68.7 [67.1 - 74.3]	0.41
24h vs. 48h	78.9 [70.3 - 82.7]	68.7 [67.1 - 74.3]	0.42

Supplemental Table 9: Longitudinal analysis of plasma angiotensin I concentration (pg/mL) in the noAKI, AKI 1S and AKI ≥ 1A groups by repeated-measure ANOVA on log-transformed data followed by the Tukey HSD test, when appropriate.

Comparison	Time1	Time2	P-value
noAKI group (P_{ANOVA} = 0.4)			
Pre-op vs. ICU adm.	163 [152 - 182.5]	168 [156 - 181.5]	na
Pre-op vs. 24h	163 [152 - 182.5]	163 [147.5 - 184]	na
Pre-op vs. 48h	163 [152 - 182.5]	162 [148 - 179]	na
ICU adm. vs. 24h	168 [156 - 181.5]	163 [147.5 - 184]	na
ICU adm. vs. 48h	168 [156 - 181.5]	162 [148 - 179]	na
24h vs. 48h	163 [147.5 - 184]	162 [148 - 179]	na
AKI 1S group (P_{ANOVA} < 0.0001)			
Pre-op vs. ICU adm.	134.5 [124.75 - 144.5]	262 [237.5 - 284.5]	**<0.0001**
Pre-op vs. 24h	134.5 [124.75 - 144.5]	242 [206.3 - 271.5]	**<0.0001**
Pre-op vs. 48h	134.5 [124.75 - 144.5]	209.5 [171 - 240]	**<0.0001**
ICU adm. vs. 24h	262 [237.5 - 284.5]	242 [206.3 - 271.5]	0.17
ICU adm. vs. 48h	262 [237.5 - 284.5]	209.5 [171 - 240]	**0.0001**
24h vs. 48h	242 [206.3 - 271.5]	209.5 [171 - 240]	**0.045**
AKI ≥ 1A (P_{ANOVA} < 0.0001)			
Pre-op vs. ICU adm.	122 [114 - 129]	327 [288 - 349]	**<0.0001**
Pre-op vs. 24h	122 [114 - 129]	325 [294 - 332]	**<0.0001**
Pre-op vs. 48h	122 [114 - 129]	316 [271 - 339]	**<0.0001**
ICU adm. vs. 24h	327 [288 - 349]	325 [294 - 332]	0.95
ICU adm. vs. 48h	327 [288 - 349]	316 [271 - 339]	0.92
24h vs. 48h	325 [294 - 332]	316 [271 - 339]	1

Supplemental Table 10: Longitudinal analysis of plasma angiotensin II concentration (pg/mL) in the noAKI, AKI 1S and AKI ≥ 1A groups by repeated-measure ANOVA on log-transformed data followed by the Tukey HSD test.

Comparison	Time1	Time2	P-value
noAKI group (P_{ANOVA} = 0.04)			
Pre-op vs. ICU adm.	59.2 [56.3 - 62.8]	60.1 [57.9 - 65.7]	0.19
Pre-op vs. 24h	59.2 [56.3 - 62.8]	59.6 [54.9 - 62.5]	0.94
Pre-op vs. 48h	59.2 [56.3 - 62.8]	57.4 [54.9 - 61.9]	0.81
ICU adm. vs. 24h	60.1 [57.9 - 65.7]	59.6 [54.9 - 62.5]	0.46
ICU adm. vs. 48h	60.1 [57.9 - 65.7]	57.4 [54.9 - 61.9]	**0.027**
24h vs. 48h	59.6 [54.9 - 62.5]	57.4 [54.9 - 61.9]	0.47
AKI 1S group (P_{ANOVA} < 0.0001)			
Pre-op vs. ICU adm.	61 [56 - 67]	101.3 [92.1 - 131]	**<0.0001**
Pre-op vs. 24h	61 [56 - 67]	93.65 [80.8 - 110.1]	**<0.0001**
Pre-op vs. 48h	61 [56 - 67]	78.4 [64.2 - 90.6]	**<0.0001**
ICU adm. vs. 24h	101.3 [92.1 - 131]	93.7 [80.8 - 110.1]	0.05
ICU adm. vs. 48h	101.3 [92.1 - 131]	78.4 [64.2 - 90.6]	**<0.0001**
24h vs. 48h	93.7 [80.8 - 110.1]	78.4 [64.2 - 90.6]	**0.015**
AKI ≥ 1A (P_{ANOVA} < 0.0001)			
Pre-op vs. ICU adm.	65.3 [62.2 - 82.2]	173.6 [120.1 - 213.6]	**<0.0001**
Pre-op vs. 24h	65.3 [62.2 - 82.2]	164.3 [137.1 - 196.2]	**<0.0001**
Pre-op vs. 48h	65.3 [62.2 - 82.2]	114.5 [103.7 - 149.8]	**<0.0001**
ICU adm. vs. 24h	173.6 [120.1 - 213.6]	164.3 [137.1 - 196.2]	0.89
ICU adm. vs. 48h	173.6 [120.1 - 213.6]	114.5 [103.7 - 149.8]	**0.0006**
24h vs. 48h	164.3 [137.1 - 196.2]	114.5 [103.7 - 149.8]	**0.004**

Supplemental Table 11: Longitudinal analysis of plasma angiotensin (1-7) concentration (pg/mL) in the noAKI, AKI 1S and AKI ≥ 1A groups by repeated-measure ANOVA on log-transformed data followed by the Tukey HSD test.

Comparison	Time1	Time2	P-value
noAKI group (P_{ANOVA} = 0.0003)			
Pre-op vs. ICU adm.	38.9 [36.1 - 41.25]	41.9 [38.8 - 44.05]	**0.002**
Pre-op vs. 24h	38.9 [36.1 - 41.25]	40.4 [39 - 43.5]	0.1
Pre-op vs. 48h	38.9 [36.1 - 41.25]	39.7 [35.25 - 41.6]	1
ICU adm. vs. 24h	41.9 [38.8 - 44.05]	40.4 [39 - 43.5]	0.41
ICU adm. vs. 48h	41.9 [38.8 - 44.05]	39.7 [35.25 - 41.6]	**0.001**
24h vs. 48h	40.4 [39 - 43.5]	39.7 [35.25 - 41.6]	0.07
AKI 1S group (P_{ANOVA} < 0.0001)			
Pre-op vs. ICU adm.	36.25 [34.425 - 39.75]	68.1 [61.775 - 74.3]	**<0.0001**
Pre-op vs. 24h	36.25 [34.425 - 39.75]	61.35 [57.05 - 67.325]	**<0.0001**
Pre-op vs. 48h	36.25 [34.425 - 39.75]	54.9 [47.975 - 60.95]	**<0.0001**
ICU adm. vs. 24h	68.1 [61.775 - 74.3]	61.35 [57.05 - 67.325]	0.11
ICU adm. vs. 48h	68.1 [61.775 - 74.3]	54.9 [47.975 - 60.95]	**0.0003**
24h vs. 48h	61.35 [57.05 - 67.325]	54.9 [47.975 - 60.95]	0.15
AKI ≥ 1A (P_{ANOVA} < 0.0001)			
Pre-op vs. ICU adm.	38.9 [35.5 - 42.5]	104.3 [91.3 - 142.5]	**<0.0001**
Pre-op vs. 24h	38.9 [35.5 - 42.5]	87 [67.3 - 111.4]	**<0.0001**
Pre-op vs. 48h	38.9 [35.5 - 42.5]	73.9 [69.9 - 84.5]	**<0.0001**
ICU adm. vs. 24h	104.3 [91.3 - 142.5]	87 [67.3 - 111.4]	**0.022**
ICU adm. vs. 48h	104.3 [91.3 - 142.5]	73.9 [69.9 - 84.5]	**0.0003**
24h vs. 48h	87 [67.3 - 111.4]	73.9 [69.9 - 84.5]	0.34

Supplemental Table 12: Longitudinal analysis of the angiotensin II/angiotensin (1-7) ratio in the noAKI, AKI 1S and AKI ≥ 1A groups by repeated-measure ANOVA on log-transformed data followed by the Tukey HSD test, when appropriate.

Comparison	Time1	Time2	P-value
noAKI group (P_{ANOVA} = 0.59)			
Pre-op vs. ICU adm.	148.4[135.9 - 181.8]	145.2 [130 - 167]	na
Pre-op vs. 24h	148.44 [135.9 - 181.8]	138.7 [133.8 - 166.2]	na
Pre-op vs. 48h	148.44 [135.9 - 181.8]	144.6 [133.4 - 170.5]	na
ICU adm. vs. 24h	145.16 [1230 - 167]	138.7 [133.8 - 166.2]	na
ICU adm. vs. 48h	145.16 [130 - 167]	144.6 [133.4 - 170.5]	na
24h vs. 48h	138.72 [133.8 - 166.2]	144.6 [133.4 - 170.5]	na
AKI 1S group (P_{ANOVA} = 0.32)			
Pre-op vs. ICU adm.	157.6 [145.2 - 192.6]	180.6 [134.7 - 201.4]	na
Pre-op vs. 24h	157.6 [145.2 - 192.6]	166.8 [134.7 - 203.7]	na
Pre-op vs. 48h	157.6 [145.2 - 192.6]	139.1 [126.9 - 193]	na
ICU adm. vs. 24h	180.6 [134.7 - 201.4]	166.8 [134.6 - 203.7]	na
ICU adm. vs. 48h	180.6 [134.7 - 201.4]	139.1 [126.9 - 193.0]	na
24h vs. 48h	166.8 [134.6 - 203.7]	139.1 [126.9 - 193.0]	na
AKI ≥ 1A (P_{ANOVA} = 0.054)			
Pre-op vs. ICU adm.	180.8 [143.7 - 206.6]	146.6 [144.5 - 178.3]	na
Pre-op vs. 24h	180.8 [143.7 - 206.6]	183.2 [167.7 - 188.9]	na
Pre-op vs. 48h	180.8 [143.7 - 206.6]	163.8 [147.1 - 189.3]	na
ICU adm. vs. 24h	146.6 [144.5 - 178.3]	183.2 [167.7 - 188.9]	na
ICU adm. vs. 48h	146.6 [144.5 - 178.3]	163.8 [147.1 - 189.3]	na
24h vs. 48h	183.2 [167.7 - 188.9]	163.8 [147.1 - 189.3]	na

Supplemental Table 13: Longitudinal analysis of plasma aldosterone concentration (pM) in the noAKI, AKI 1S and AKI ≥ 1A groups by repeated-measure ANOVA on log-transformed data followed by the Tukey HSD test, when appropriate.

Comparison	Time1	Time2	P-value
noAKI group (P_{ANOVA} = 0.4)			
Pre-op vs. ICU adm.	226 [193 - 279]	237 [181 - 275]	na
Pre-op vs. 24h	226 [193 - 279]	239 [191 - 284.5]	na
Pre-op vs. 48h	226 [193 - 279]	232 [176.5 - 262.5]	na
ICU adm. vs. 24h	237 [181 - 275]	239 [191 - 284.5]	na
ICU adm. vs. 48h	237 [181 - 275]	232 [176.5 - 262.5]	na
24h vs. 48h	239 [191 - 284.5]	232 [176.5 - 262.5]	na
AKI 1S group (P_{ANOVA} < 0.0001)			
Pre-op vs. ICU adm.	190.5 [172.25 - 200.5]	262 [243.25 - 294.5]	**<0.0001**
Pre-op vs. 24h	190.5 [172.25 - 200.5]	269 [254 - 334.75]	**<0.0001**
Pre-op vs. 48h	190.5 [172.25 - 200.5]	244.5 [214.75 - 289]	**<0.0001**
ICU adm. vs. 24h	262 [243.25 - 294.5]	269 [254 - 334.75]	0.91
ICU adm. vs. 48h	262 [243.25 - 294.5]	244.5 [214.75 - 289]	0.19
24h vs. 48h	269 [254 - 334.75]	244.5 [214.75 - 289]	0.046
AKI ≥ 1A (P_{ANOVA} < 0.0001)			
Pre-op vs. ICU adm.	243 [208 - 263]	486 [471 - 582]	**<0.0001**
Pre-op vs. 24h	243 [208 - 263]	451 [432 - 565]	**<0.0001**
Pre-op vs. 48h	243 [208 - 263]	429 [404 - 539]	**<0.0001**
ICU adm. vs. 24h	486 [471 - 582]	451 [432 - 565]	0.25
ICU adm. vs. 48h	486 [471 - 582]	429 [404 - 539]	0.028
24h vs. 48h	451 [432 - 565]	429 [404 - 539]	0.68

Supplemental Table 14: Longitudinal analysis of the renin/aldosterone ratio in the noAKI, AKI 1S and AKI ≥ 1A groups by repeated-measure ANOVA on log-transformed data followed by the Tukey HSD test, when appropriate.

Comparison	Time1	Time2	P-value
noAKI group (P_{ANOVA} = 0.0006)			
Pre-op vs. ICU adm.	0.13 [0.09 - 0.14]	0.14 [0.11 - 0.17]	<0.0001
Pre-op vs. 24h	0.13 [0.09 - 0.14]	0.13 [0.1 - 0.16]	0.01
Pre-op vs. 48h	0.13 [0.09 - 0.14]	0.13 [0.11 - 0.17]	<0.0001
ICU adm. vs. 24h	0.14 [0.11 - 0.17]	0.13 [0.1 - 0.16]	0.81
ICU adm. vs. 48h	0.14 [0.11 - 0.17]	0.13 [0.11 - 0.17]	0.99
24h vs. 48h	0.1 [0.1 - 0.16]	0.13 [0.11 - 0.17]	0.94
AKI 1S group (P_{ANOVA} = 0.32)			
Pre-op vs. ICU adm.	0.15 [0.11 - 0.16]	0.15 [0.12 - 0.18]	na
Pre-op vs. 24h	0.15 [0.11 - 0.16]	0.13 [0.11 - 0.16]	na
Pre-op vs. 48h	0.15 [0.11 - 0.16]	0.14 [0.12 - 0.16]	na
ICU adm. vs. 24h	0.15 [0.12 - 0.18]	0.13 [0.11 - 0.16]	na
ICU adm. vs. 48h	0.15 [0.12 - 0.18]	0.14 [0.12 - 0.16]	na
24h vs. 48h	0.13 [0.11 - 0.16]	0.14 [0.12 - 0.16]	na
AKI ≥ 1A (P_{ANOVA} = 0.76)			
Pre-op vs. ICU adm.	0.11 [0.09 - 0.12]	0.11 [0.09 - 0.13]	na
Pre-op vs. 24h	0.11 [0.09 - 0.12]	0.12 [0.09 - 0.16]	na
Pre-op vs. 48h	0.11 [0.09 - 0.12]	0.12 [0.10 - 0.12]	na
ICU adm. vs. 24h	0.11 [0.09 - 0.13]	0.12 [0.09 - 0.16]	na
ICU adm. vs. 48h	0.11 [0.09 - 0.13]	0.12 [0.1 - 0.12]	na
24h vs. 48h	0.12 [0.09 - 0.16]	0.12 [0.1 - 0.12]	na

4 Article IV. Neprilysin inhibition is a major pathophysiological driver in severe septic shock: a preliminary (partial) proof-of-concept study

Chez les patients en choc septique, il existe une élévation du BNP indépendante de la dysfonction cardiaque. Chez des patients en insuffisance cardiaque, l'élévation du BNP au-delà d'un seuil de 916 pg/ml induit une inhibition de la néprilysine (NEP), qui a été confirmée in vitro. L'inhibition de la NEP est responsable d'une vasodilatation et d'une baisse de la pression artérielle qui peut participer à la physiopathologie et à la gravité de la défaillance hémodynamique des chocs septiques les plus sévères ou chocs septiques dits réfractaires aux amines. Afin de répondre à cette hypothèse selon laquelle les chocs septiques réfractaires sont secondaires à une inhibition de la NEP par l'élévation du BNP, nous avons dans un premier temps confirmer l'inhibition de la NEP dans une cohorte de patients en choc septique puis dans un second temps, dans un modèle de choc septique par ligature et ponction caecale chez le rat, testé l'administration de BNP humain sur la NEP et l'hémodynamique systémique.

Les résultats obtenus dans cette étude montrent :

i) Une association entre l'inhibition de la NEP et la survie au décours d'un choc septique.

ii) Dans le modèle de choc septique chez le rat, l'administration de BNP humain aggrave la défaillance hémodynamique systémique et diminue la survie.

iii) La molécule X.Y.U. prévient et réverse partiellement l'inhibition du BNP par la NEP in vitro.

iv) Dans le modèle de choc septique chez le rat, la molécule X.Y.U., prévient l'aggravation hémodynamique induit par l'administration de BNP.

Au total, ce travail a permis de montrer dans un premier temps que l'inhibition de la NEP par l'élévation au-delà du seuil de 916 pg/ml du BNP participe très probablement à l'aggravation de l'hémodynamique systémique dans le choc septique. Dans un second temps, ce travail démontre que la prévention de l'inhibition de la NEP par l'élévation du BNP grâce à la molécule X.Y.U. permet de prévenir la dégradation de la défaillance hémodynamique. Finalement, ce travail montre également que les modèles animaux classiquement utilisés pour étudier le choc septique ne récapitule que partiellement les cas les plus sévères observés en pratique clinique.

Neprilysin inhibition is a major pathophysiological driver in severe septic shock: a preliminary (partial) proof-of-concept study

Thibault Michel[1], François Phillipart, Florence Riché[2], Jean-Marie Launay[1], Hélène Nougué[1], Nicolas Vodovar[1]

Introduction

Sepsis is a life-threatening condition that is caused by an inadequate and excessive inflammatory response to infection, leading to organ dysfunction. Sepsis can worsen into septic shock that is define by a drop in mean arterial pressure (MAP) < 65 mmHg, lactate elevation > 2 mmol/L despite adequate fluid resuscitation, and the need for vasopressor support.[1] Septic shock is associated with an increased mortality, and is the leading cause of death in intensive care units. The so-called refractory shock is the most severe form of septic shock in which the pharmacokinetic of vasopressor is lost to maintain appropriate MAP, the coherence between macro and microcirculation is lost, resulting in even more reduced organ perfusion. Refractory shock is associated with increase organ dysfunction and is associated with a greater death rate.

Neprilysin (NEP, also known as CD10, membrane metallo-endopeptidase, neutral endopeptidase, or CALLA) is a transmembrane metalloprotease encoded by the *MME* gene, which is involved in the inactivation of > 40 peptides[2], amongst which numerous have vasoactive properties (e.g., natriuretic peptides, bradykinins, adrenomedullin, substance P, endothelin-1). Several lines of evidence suggest an important role for NEP in septic shock. *Mme* knockout mice exhibit lower blood pressure and increased vascular permeability[3], which are two hallmarks of sepsis and septic shock. *Mme* knockout mice[4] or rats treated with NEP inhibitor[5] also exhibit enhanced sensitivity to endotoxin challenge, supporting a possible role for NEP in sepsis and septic shock. Furthermore, numerous vasoactive peptides that can be inactivated by NEP were found relevant in sepsis/septic shock. Indeed, mice knockout for the natriuretic peptide receptor *Npr1* did not exhibit a drop in blood pressure after endotoxin challenge,[6] while mice administered with a BNP neutralising antibody exhibited an intermediate decrease[7]. Likewise, the blocking of CRCR1/2 improved the outcome mice subjected to LPS challenge mice via the down-regulation of substance P.[8] Finally, plasma

levels of adrenomedullin were recently found to be associated with short-term mortality and vasopressor requirement in patients admitted for sepsis,[9] and partial inactivation of adrenomedullin improved responsiveness to catecholamine in a resuscitated model of sepsis in rat.[10]

In humans, NEP activity was found to be low in a small cohort of patients with septic shock,[11] which was interpreted as the reason for BNP elevation in septic shock patients. However, we since found that human BNP acted as an endogenous NEP inhibitor *in vivo* when plasma levels > 916 pg/mL,[12] providing a possible pathophysiological mechanism for low NEP activity in septic shock. Of note, BNP-mediated NEP inhibition is not immediate *in vitro*, and require two hours of NEP exposure to inhibitory concentration of human BNP.[12] Importantly, BNP elevation is common in septic shock despite being associated the severity of the critical illness rather than septic cardiomyopathy.[13] Moreover, BNP elevation is associated with a poorer outcome in septic shock, and BNP > 800 pg/mL predicted mortality, a cut-off not far from the NEP-inhibitory threshold.[13]

We therefore hypothesised that BNP-mediated NEP inhibition could be responsible for the increased vasoplegia observed in the most severe patients with septic shock, and that preventing or reversing BNP-mediated NEP inhibition could offer new therapeutic options

Methods

Patients

This study was performed according to the current revision of the Helsinki Declaration, approved by the Institutional Review Board (IRB 00006477), and written consent was obtained for each patient or next of kin. The study population has already been described.[14] Briefly, it consisted in 86 patients admitted in intensive care for septic shock after abdominal surgery. Blood samples were collected at ICU admission using EDTA as anticoagulant,

immediately centrifuged at 2000g for 10 minutes at 4°C. Plasma were aliquoted and immediately stored at -80°C until use.

Animals

All experiments involving animals have been approved by the local ethic committee. As we were looking for a very strong effect, size calculation was performed using $\alpha = 0.05$, power $(1-\beta) = 0.90$, and a size effect of 0.9. Male Wistar rats aged 2-3 months and weighting 400-600 gr were obtained from Janvier Lab, and housed in light- (on from 0800 - 2000 h) and temperature (21–24 °C)-controlled testing rooms, with food and water available *ad libitum*. Septic shock was provoked by the caecal ligation and puncture (CLP) method.[15] Briefly, rats were anaesthetised with 100 mg/kg ketamine and 10 mg/kg xylazine intraperitoneally, while analgesia was managed by administering 75 µg/kg Buprenorphine. After a laparotomy, the caecum was exposed, ligatured around an 18-gauge catheter to maximise reproducibility, and puncture with an 18-gauge needle. The rats were sutured until further experimentation. Sham-operated animal had a laparotomy and caecal exposure without ligation or puncture. Sixteen hours after CLP, rats were anaesthetised with the same ketamine/xylazine mixture and ventilated. A catheter was set in place in the carotid artery for invasive blood pressure measurement, and a second catheter was set in place in the jugular vein for fluid resuscitation (1 ml saline/hour), drug administration and blood collection, as previously described.[16] Rats were enrolled when mean arterial blood pressure was < 65 mmHg, and randomised to receive the various interventions. Anaesthesia was maintained by injecting intraperitoneally 50 mg/kg ketamine and 5 mg/kg xylazine every 45 minutes. Human BNP variant was administered in 300 µL saline as a bolus to target 500 pg/mL or 2000 pg/mL final concentration based on 60 ml of blood per kg of body weight. Molecule X.Y.U. was administered at a target concentration of 500 ng/mL in saline. After four hours of monitoring, the rats were euthanised

using a lethal dose of pentobarbital, and their organs harvested. Some rats were euthanised prior the expected end of protocol if mean arterial blood pressure < 20 mm Hg.

Blood samples (250µL) were obtained every hour in precooled tube containing heparin (ref), immediately centrifuged at 2,000 *g*, at 4°C for 10 minutes. Plasma samples were stored at -80°C until use. Organs were harvested, snap frozen in liquid nitrogen and stored at -80°C.

Peptides and proteins

All the peptides used were obtained at purity > 95% as endotoxin-free lyophilizates from Genscript (Rijswijk, Netherlands), which were resuspended at appropriate concentrations in intravenous-compatible 0.09% saline solution. Human recombinant NEP was obtained from Sigma-Aldrich (SRP6450).

Neprilysin activity

Neprilysin activity was measured by fluorimetry as previously described.[12]

Statistical analysis

All statistical analyses were performed with statistical software R (version 4.2.1). For non-human studies, variables were analysed using repeated-measure ANOVA on log-transformed data, followed by the Tukey honest difference test. Intergroup comparisons were performed using the Kruskal-Wallis test followed by the sum rank Wilcoxon test corrected for multiple comparisons, or the sum rank Wilcoxon test. For human data, normality was assessed using the Shapiro-Wilk test. Data were analysed using the sum rank Wilcoxon test. Survival curve were performed using Kaplan-Meier analysis. A P-value < 0.05 was considered statistically different.

Results

NEP activity in septic shock patients

First, we measured NEP activity and concentration in a cohort of septic shock patients, and found that NEP activity was markedly lower in those who died in-hospital (137 pmol/mL/min [110 – 170]), than those who survived (378 pmol/mL/min [279 – 532], $P < 0.0001$, ***Figure 1A***). To evaluate a possible decrease in NEP activity due to NEP extravasation, we measured NEP plasma concentration, which was not different in the two groups (***Figure 1B***).

BNP-mediated NEP inhibition in a rat model of septic shock

In order to test potential intervention that would prevent or reverse BNP-mediated NEP inhibition, we needed to establish an animal model of septic shock that would recapitulate the vent. Administration of human BNP is vasodilatory, irrespectively of its inhibitory effect on NEP. However, as BNP requires it disulphide bond to be active, we designed two human BNP derivatives in which each cysteine (at position 10: hBNP* and 26: hBNP**) involved in the disulphide bond were changed to its steric equivalent serine (***Figure 2A***). Human recombinant NEP was then incubated with inhibitory (1600 pg/mL) concentration of native human BNP or the derivatives for two hours. Results showed that the ~mean decrease in NEP activity was ~93%, ~80%, and ~63% when incubated for two hours with hBNP, hBNP*, and hBNP**, respectively (***Figure 2B***). As hBNP* exhibited the strongest inhibitory effect amongst the variants tested, it was selected for the *in vivo* experiments.

Next, we tested hBNP* in a rat model of septic shock induced by caecum ligature-puncture. As expected, CLP provoked a decrease in MAP, which gradually decreased over the four hours of invasive monitoring. Similar results were obtained when CLP rats received a single bolus of hBNP* at non-inhibitor concentration (500 pg/mL final concentration). In

animals that received a single bolus of hBNP* at inhibitory concentration (2000 pg/mL), MAP remained stable for ~two hours, and abruptly dropped in three animals out of the five tested. As this model did not involve the administration of vasopressor, the animals died within the hour that succeeded the initial drop in MAP.

X.Y.U. prevent and partially reverse BNP-mediated NEP inhibition

We identified a molecule, referred to as X.Y.U. hereafter for reason of confidentiality, as a potential candidate for the prevention and reversion of BNP-mediated NEP inhibition. First, we preincubated 250 pg/mL human recombinant NEP with 500 ng/mL of X.Y.U. for one hour, and added hBNP at inhibitory concentration (1600 pg/mL). Results show that X.Y.U. itself had no effect on NEP activity (between -1 and 0 hours) and prevented but prevented BNP-mediated NEP inhibition for 24 hours after the addition of BNP (***Figure 3A***). At 48 hours, molecule X started to lose efficacy as NEP activity decrease by ~22%. Next, we tested the ability of X.Y.U. to reverse BNP-mediated NEP inhibition. We first incubated 250 pg/mL human recombinant NEP with 1600 pg/mL hBNP for two hours to reach maximal inhibition, and added X.Y.U. at 500 ng/mL final concentration. Results show that X.Y.U. was capable of restoring NEP activity to ~40% of baseline value, as soon as one hour after its addition (***Figure 3B***).

Next, we tested the ability of X.Y.U. to prevent BNP-mediated NEP inhibition in the rat model of CLP that received inhibitory concentration of hBNP*. To parallel in vitro experiments, X.Y.U. was administered as a single intravenous bolus (500 ng/mL target concentration), and a single bolus of hBNP* at inhibitory concentration was administered one hour later. Results show that in CLP animals that received a single bolus of hBNP* at inhibitory concentration, X.Y.U. prevented the drop in MAP observed in CLP that only received a single bolus of hBNP* at inhibitory concentration (***Figure 3C***). Furthermore,

X.Y.U. also prevented the mortality observed in CLP rats that received inhibitory hBNP* concentrations.

Discussion

The present study indicate that BNP-mediated NEP inhibition is a possible major driver in the pathophysiology of severe septic shock, and can be leveraged pharmacologically at least to prevent the transition to the most severe forms of septic shock.

First, we show that BNP elevation > 916 pg/mL could be a major driver of septic shock physiopathology as all patients who died in ICU had very low plasma NEP activity. Furthermore, we were capable of replicating BNP-mediated NEP inhibition in a rat model of septic shock, which provoked a marked and abrupt drop in MAP as observed in the most severe cases of septic shock in human. Importantly, BNP-mediated NEP inhibition is only present in simians, and therefore absent from most animal models commonly used. This indicates that all those preclinical models only recapitulate a part of the pathophysiology of septic shock, and in particular lack the mechanism involved in the abrupt exacerbation of shock.

From a pathophysiological standpoint, multiple preclinical studies have shown the importance of peptides that are neprilysin targets in sepsis and septic shock;[6-10] the elevation of some of those peptides being the consequence of dysregulated inflammation.[8] Altogether, these data and ours suggest that the low blood pressure observed in septic shock is likely to be due to an increased production of vasoactive peptides, which activities lead to increased vasodilation and vascular leakage. This increase in activity of vasodilatory peptides is likely accompanied by a deficit in endogenous vasopressor, such as endothelin-1, angiotensin-II, or endogenous catecholamines. However, when BNP reaches NEP inhibitory concentration NEP, we anticipate a second elevation of those vasoactive peptides, resulting from their

reduced degradation. Altogether, these data allow us to propose a model whereby; i) the first stage of septic shock, which responds to limited concentrations of vasopressor, is associated with an increase in production of vasodilatory and vasopermeant factor; and ii) the second step, which is associated with extreme vasoplegia and the most severe forms of septic shock, a double penalty occurs as not only those vasoplegia factor are overproduced, but they are also less eliminated, leading to their rapid accumulation.

From a therapeutic standpoint, we have identified a molecule, X.Y.U., which is capable of preventing BNP-mediated NEP inhibition both *in vitro* and *in vivo*, and capable of its partial reversion in vitro. Importantly, both prevention and reversion occur rapidly *in vitro*, which is important when dealing with such an unstable clinical situation. Most of the recent therapeutic attempts in septic shock have failed because the population of interest could not be identified. Here, as BNP is the cause of NEP inhibition and is a routine biomarker used worldwide, we anticipate that the patients that would benefit from either of the prevention or reversion of BNP-mediated NEP inhibition could be readily identified, as long as serial BNP measurements are performed. We therefore anticipate that molecule X.Y.U. could help manage blood pressure in septic shock patients by reducing the doses of vasopressor used. Therefore, the impact of molecule X.Y.U. in septic shock is likely to go beyond its sole hemodynamic benefit, and may help reduce immune paralysis that is often observed after the chronic dose of high doses of noradrenaline. However, only clinical trials performed in human will allow to explore extended benefits of molecule X.Y.U..

Our study has some limitations that needs to be acknowledged. First, the study population is rather small and not randomized which may limit the statistical performance. Furthermore, we did not have access to vasopressor or BNP data.

In conclusion, BNP-mediated NEP inhibition appears as a critical factor in the pathophysiology of severe septic shock, and X.Y.U. offers a promising avenue to prevent the occurrence of extreme vasoplegia, and possibly reverse it.

Acknowledgments

The authors would like to thank…

References

1. Singer, M., *et al.* The Third International Consensus Definitions for Sepsis and Septic Shock (Sepsis-3). *JAMA* **315**, 801-810 (2016).
2. Campbell, D.J. Long-term neprilysin inhibition - implications for ARNIs. *Nat Rev Cardiol* **14**, 171-186 (2017).
3. Lu, B., *et al.* The control of microvascular permeability and blood pressure by neutral endopeptidase. *Nat Med* **3**, 904-907 (1997).
4. Lu, B., *et al.* Neutral endopeptidase modulation of septic shock. *J Exp Med* **181**, 2271-2275 (1995).
5. Pham, D., Jeng, A.Y., Escher, E., Sirois, P. & Battistini, B. Effects of a selective neutral endopeptidase and a nonselective neutral endopeptidase/endothelin-converting enzyme inhibitor on lipopolysaccharide-induced endotoxaemia in anaesthetized Sprague-Dawley rats. *J Cardiovasc Pharmacol* **36**, S362-366 (2000).
6. Panayiotou, C.M., *et al.* Resistance to endotoxic shock in mice lacking natriuretic peptide receptor-A. *Br J Pharmacol* **160**, 2045-2054 (2010).
7. Hoffman, M., *et al.* B-type natriuretic peptide is upregulated by c-Jun N-terminal kinase and contributes to septic hypotension. *JCI Insight* **5**(2020).
8. Wang, M., Zhong, D., Dong, P. & Song, Y. Blocking CXCR1/2 contributes to amelioration of lipopolysaccharide-induced sepsis by downregulating substance P. *J Cell Biochem* **120**, 2007-2014 (2019).
9. Marino, R., *et al.* Plasma adrenomedullin is associated with short-term mortality and vasopressor requirement in patients admitted with sepsis. *Crit Care* **18**, R34 (2014).
10. Wagner, K., *et al.* Adrenomedullin binding improves catecholamine responsiveness and kidney function in resuscitated murine septic shock. *Intensive Care Med Exp* **1**, 21 (2013).
11. Pirracchio, R., *et al.* Impaired plasma B-type natriuretic peptide clearance in human septic shock. *Crit Care Med* **36**, 2542-2546 (2008).
12. Vodovar, N., *et al.* Elevated Plasma B-Type Natriuretic Peptide Concentrations Directly Inhibit Circulating Neprilysin Activity in Heart Failure. *JACC Heart Fail* **3**, 629-636 (2015).
13. Papanikolaou, J., *et al.* New insights into the mechanisms involved in B-type natriuretic peptide elevation and its prognostic value in septic patients. *Crit Care* **18**, R94 (2014).
14. Riche, F., *et al.* Protracted immune disorders at one year after ICU discharge in patients with septic shock. *Crit Care* **22**, 42 (2018).
15. Rittirsch, D., Huber-Lang, M.S., Flierl, M.A. & Ward, P.A. Immunodesign of experimental sepsis by cecal ligation and puncture. *Nat Protoc* **4**, 31-36 (2009).

16. Deniau, B., *et al.* Inhibition of circulating dipeptidyl-peptidase 3 restores cardiac function in a sepsis-induced model in rats: A proof of concept study. *PLoS One* **15**, e0238039 (2020).

Legends to the Figures

Figure 1: NEP in septic shock. Plasma NEP activity (**A**) and concentration (**B**) measured in septic shock patients who survived (Surv) or not (non-Surv) in the intensive care unit. Variable were compared using the sum rank Wilcoxon test.

Figure 2: BNP-mediated NEP inhibition. A) Schematic illustrating the structure of human BNP and the sequence corresponding of the derivative tested. **B)** NEP activity measured *in vitro* after incubation with inhibitory concentration of human BNP and derivatives. **C)** Effect of hBNP* on mean arterial blood pressure (MAP) in rat model of septic shock (CLP). The time at which hBNP* was administered is indicated by an arrow. Variables in **B** were analysed using repeated-measure ANOVA on log-transformed data followed by the Tukey HSD test for within-group comparisons, and by the Kruskal-Wallis test followed by the sum rank Wilcoxon test corrected for multiple comparisons (holm's method) for inter-group comparisons.

Figure 3: X.Y.U. as a modulator or BNP-mediated NEP inhibition. A) NEP activity after preincubation with X.Y.U. prior to the administration of hBNP* at inhibitory concentration. **B)** NEP activity after its initial inhibition by hBNP* and a secondary incubation with X.Y.U.. C) Mean arterial blood pressure in rats that received 500 ng/mL of X.Y.U. and hBNP* at 2000 pg/mL one hour later. The data from CLP rats that only received hBNP* is from **Figure 2C** for illustration.

Figure 4: Model for the transition from septic shock to severe septic shock. Below 916 pg/mL BNP, NEP is fully active and capable of eliminating vasoactive peptides. Consequently, blood pressure can be maintained using low doses of vasopressors. Once BNP > 916 pg/mL, the marked decrease in NEP activity provokes a rapid and abrupt accumulation

of vasoactive peptides, which in turn provoke a rapid and abrupt decrease in blood pressure and a consequent increase in vasopressor.

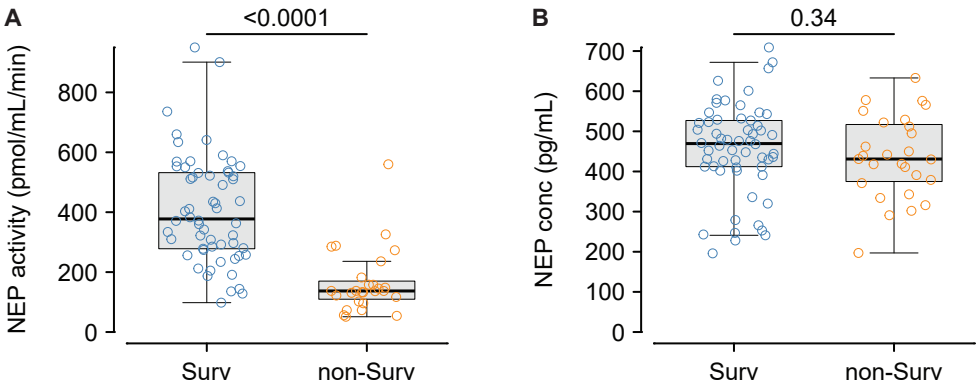
A
<0.0001
NEP activity (pmol/mL/min)
800
600
400
200
0
Surv
non-Surv
B
0.34
NEP conc (pg/mL)
700
600
500
400
300
200
100
0
Surv
non-Surv

Figure 1

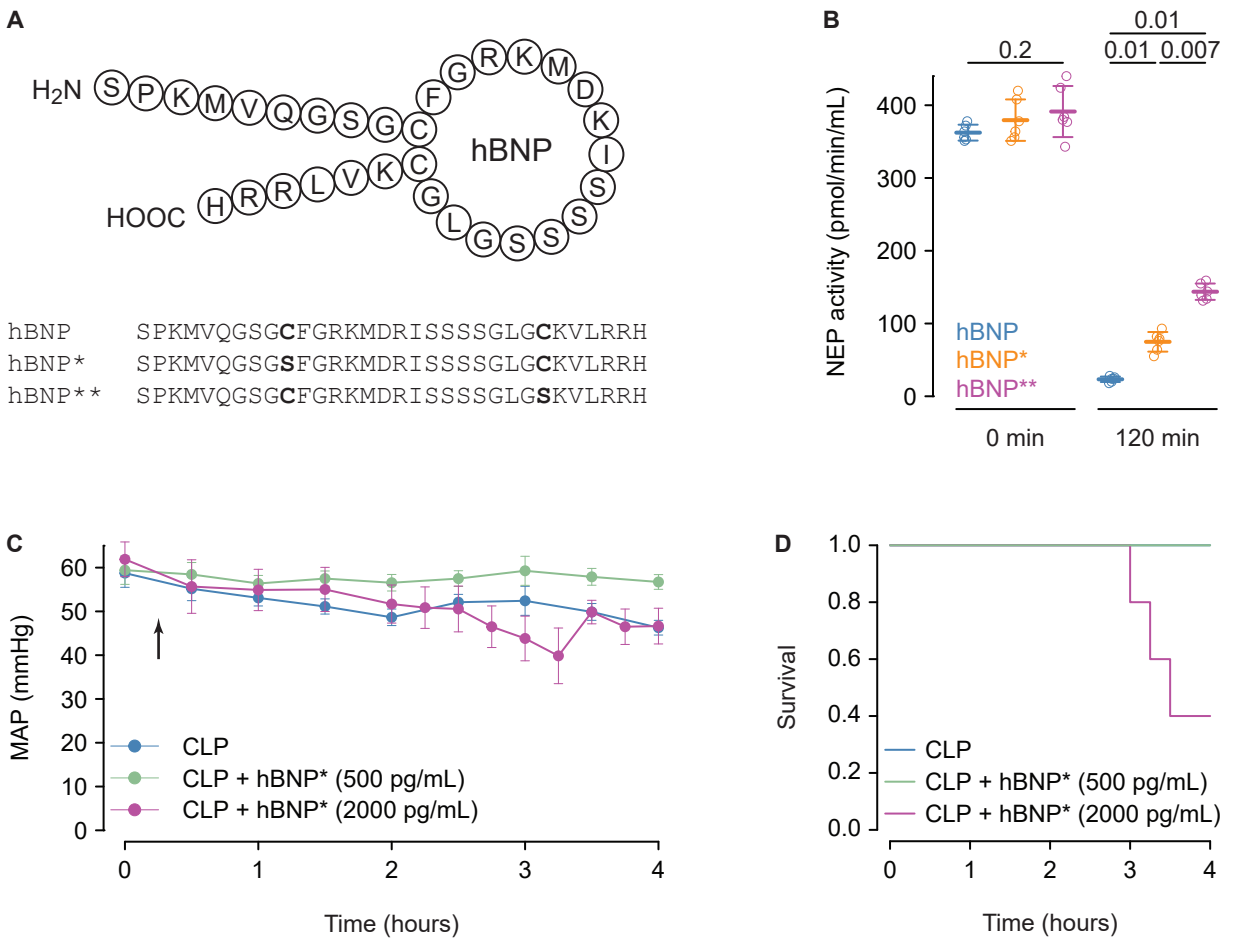
A
H2N
HOOC
hBNP
hBNP SPKMVQGSGCFGRKMDRISSSSGLGCKVLRRH
hBNP* SPKMVQGSGSFGRKMDRISSSSGLGCKVLRRH
hBNP** SPKMVQGSGCFGRKMDRISSSSGLGSKVLRRH
B
0.2
0.01
0.01 0.007
NEP activity (pmol/min/mL)
hBNP
hBNP*
hBNP**
0 min
120 min
C
MAP (mmHg)
CLP
CLP + hBNP* (500 pg/mL)
CLP + hBNP* (2000 pg/mL)
Time (hours)
D
Survival
CLP
CLP + hBNP* (500 pg/mL)
CLP + hBNP* (2000 pg/mL)
Time (hours)

Figure 2

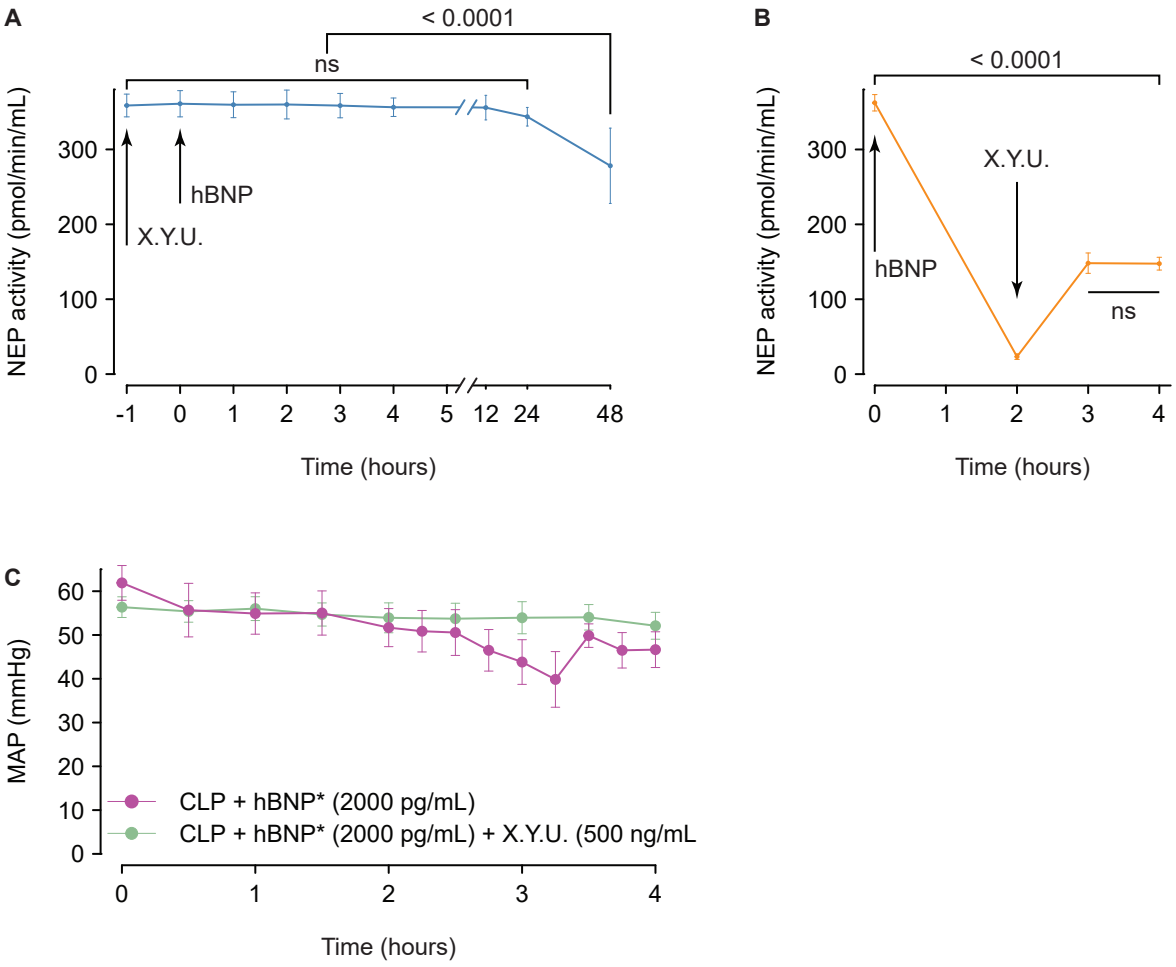
A
< 0.0001
ns
NEP activity (pmol/min/mL)
300
200
100
0
hBNP
X.Y.U.
-1
0
1
2
3
4
5
12
24
48
Time (hours)
B
< 0.0001
X.Y.U.
hBNP
ns
NEP activity (pmol/min/mL)
300
200
100
0
0
1
2
3
4
Time (hours)
C
MAP (mmHg)
60
50
40
30
20
10
0
CLP + hBNP* (2000 pg/mL)
CLP + hBNP* (2000 pg/mL) + X.Y.U. (500 ng/mL
0
1
2
3
4
Time (hours)

Figure 3

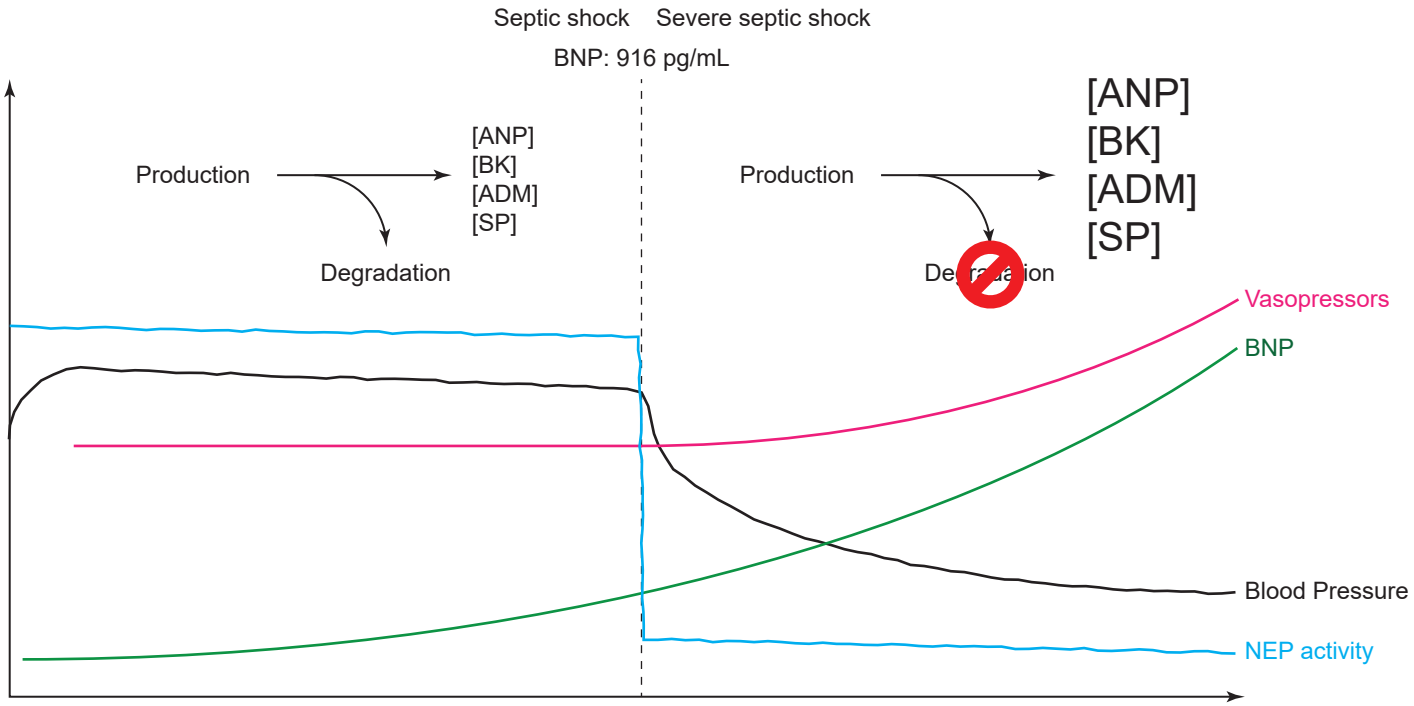
Septic shock
Severe septic shock
BNP: 916 pg/mL
Production
[ANP]
[BK]
[ADM]
[SP]
Degradation
Production
[ANP]
[BK]
[ADM]
[SP]
Vasopressors
BNP
Blood Pressure
NEP activity

Figure 4

DISCUSSION

1 Sacubitril/valsartan : effets pléiotropes et non spécifiques de la NEP

1.1 Effets vasoactifs

L'une des voies métaboliques impactée par l'inhibition de la NEP par le sacubitril/valsartan sont les peptides natriurétiques. En effet, chez les patients traités par sacubitril/valsartan, il existe une augmentation forte augmentation de l'ANP [55, 123] alors que le BNP reste stable [55, 124]. Parmi les peptides natriurétique, l'ANP semble donc être l'effecteur de l'augmentation du GMPc observé chez ces patients [54]. Il est à noter que le CNP doit également être stabilisé par le sacubitril/valsartan mais son dosage est extrêmement compliqué en raison de sa très courte demi-vie [125] et du manque de spécificité de son dosage [126] .

Mes travaux montrent que l'insuffisance cardiaque à FEVG réduite est un état suboptimal de production d'ANP. En effet, chez les patients avant l'introduction du sacubitril/valsartan, les taux d'ANP sont relativement faibles par rapport aux concentrations de proANP, alors que chez le sujet sain, malgré des taux de proANP plus faibles, l'ANP est plus produit [127]. En revanche, l'insuffisance cardiaque à FEVG réduite ne semble pas être un état suboptimal en BNP, puisque l'administration de sacubitril/valsartan ne modifie que très peu la quantité de BNP, en particulier rapidement après l'introduction du sacubitril/valsartan [128]. L'introduction du sacubitril/valsartan permet chez ces patients de restaurer et de potentialiser les taux circulants d'ANP et de proANP, ainsi que des peptides dérivants du NT-proANP (proANP$_{1-30,}$ proANP$_{31-67}$ et proANP$_{79-98}$) qui deviennent supérieurs à ceux observés

chez les sujets sains. De ce fait, le sacubitril/valsartan n'est pas limité à une augmentation de l'ANP mais également des peptides dérivants du NT-proANP, dont les actions sont bénéfiques dans l'insuffisance cardiaque chronique. Par ailleurs, l'augmentation rapide et forte de l'ANP ne s'explique pas uniquement par sa simple protection contre la dégradation par la NEP. En effet, deux autres facteurs entrent en jeu : l'augmentation de la production de proANP par la diminution de miR-425, et l'augmentation de l'activité corine par la diminution de miR-1-3p. Cette augmentation massive d'ANP est également accompagnée de l'augmentation d'autres peptides vasodilatateurs comme l'adrenomédulline [55, 129] et de la substance P [55] amplifiant l'effet vasodilatateur de ce traitement.

L'effet vasodilatateur et hypotenseur du sacubitril/valsartan reste néanmoins difficile à expliquer étant donné que la NEP dégrade aussi des peptides vasoconstricteurs (angiotensine, endothéline 1), dont les concentrations devraient augmenter quand la NEP est inhibée. Cependant, les effets vasoconstricteurs de l'angiotensine II sont bloqués par l'administration concomitante d'un antagoniste du récepteur à l'angiotensine II (valsartan). De plus, mes travaux ont montré que le sacubitril était également un inhibiteur partiel d'ECE-1 qui procède à la maturation de la big-endothéline 1 en endothéline 1. De ce fait, même si la concentration plasmatique d'endothéline 1 augmente chez les patients traités par sacubitril/valsartan, elle n'augmente pas autant qu'elle ne devrait pour maintenir une balance vasoactive neutre. Il faut aussi ajouter que tous ces patients sont traités par bétabloquant qui limite les effets presseurs des catécholamines. En conséquence, la résultante vasoactive nette du sacubitril/valsartan est en faveur d'une plus grande vasodilatation, en raison de la potentialisation de peptides vasodilatateurs et d'un blocage total ou partiel de la réponse vasoconstrictrice, permettant de mieux comprendre le mode d'action du sacubitril/valsartan.

1.2 Autres Effets du sacubitril/valsartan

Un des effets décrit après l'introduction du sacubitril/valsartan est l'amélioration du contrôle glycémique [55, 130] qui est accompagnée par une diminution de l'HbA_{1C} [130] ou de la fructosamine [55], et d'un moindre recours à l'insuline chez les patients diabétiques [130]. Cette amélioration métabolique s'explique en partie par une augmentation de GLP-1 qui est substrat de la NEP [130, 131]. Au même titre que l'ANP, l'augmentation de GLP-1 est probablement bimodale, avec une protection contre la dégradation via l'inhibition de la NEP, et un effet métabolique lié à la diminution d'indole [132], qui limite la libération de GLP-1. L'ANP pourrait également jouer un rôle métabolique dans ce contexte via son action lipolytique [133]. Finalement, cette trace d'un meilleur contrôle glycémique est observé vi la régulation de la production de proANP par miR-425 [127]. En effet, miR-425 est régulé positivement par le glucose, et la diminution que nous avons observé chez les patients traités par le sacubitril/valsartan pourrait refléter une diminution de l'utilisation du glucose par les cardiomyocytes.

Une des particularités du sacubitril/valsartan est que les patients rapportent se sentir mieux dans les jours qui suivent son introduction, et bien avant que des effets cardiovasculaires ou métaboliques puissent être observés. Cette amélioration subjective est associée à une baisse des symptômes dépressifs et d'anxiété [134, 135] et une meilleure tolérance à l'exercice [136]. Ces modifications semblent être associées à la potentialisation du système opioïde endogène (endorphine et enképhalines). L'inhibition centrale de la NEP semble être au cœur de ces observations car elle est associée à des effets antidépresseurs, analgésiques et antinociceptifs [137]. L'effet analgésique pourrait participer à la meilleure

tolérance à l'effort. Il est à noter qu'une faible fraction du sacubitril traverse la barrière hémato encéphalique et pourrait être responsable de cet effet du sacubitril/valsartan.

1.3 Un médicament non spécifique de la NEP

Le sacubitril est décrit comme un inhibiteur spécifique de la NEP. Cependant, de nombreux inhibiteur de la NEP ne sont pas aussi spécifique et peuvent avoir un effet inhibiteur partiel sur d'autres enzymes de la même famille [138]. Mes travaux confirment l'inhibition partielle d'ECE1 par le sacubitril et montre également son effet inhibiteur partiel sur l'ANPEP. Alors que l'inhibition partielle d'ECE1 se traduit par une diminution de la production d'ET1, l'inhibition partielle d'ANPEP ne semble pas avoir d'effet majeur. Cependant, ANPEP a de très nombreux substrats et nous n'en avons examiné qu'un seul.

Au-delà du manque de spécificité pharmacologique, le sacubitril/valsartan a également permis de mettre en évidence des effets indirectes sur d'autres protéases. En effet, l'ANPEP est initialement inhibée partiellement directement par le sacubitril, puis indirectement par la substance P. Cette inhibition ricochet est un facteur majeur qui est souvent négligé dans l'utilisation d'inhibiteur de protéase, sans pour autant que cela se traduise par une inhibition indirecte. En effet, la plupart des peptides clivés par la NEP peuvent également être clivés par d'autres protéases qui elle-même ont plusieurs substrats. Ainsi, l'augmentation des substrats de la NEP lors de son inhibition va modifier les concentrations relatives de ces substrats, et potentiellement affecter l'activité des autres protéases. De fait, l'inhibition de la NEP pourrait changer le profil de substrat d'autres protéases, ce qui pourrait également jouer un rôle dans les effets du sacubitril/valsartan. Nous anticipons que cet effet puisse être d'autant plus important que la NEP est probablement la protéase qui a le spectre de substrat le plus large (> 40 peptides). De fait, la compréhension exhaustive des effets de

l'inhibition de la NEP risque d'être inatteignable étant donné la complexité des mécanismes indirectes potentiellement mis en jeu.

1.4 Impact sur le dosage des biomarqueurs

L'inhibition de la NEP par le sacubitril/valsartan a également permis d'étudier plus en détail l'impact de la glycosylation sur les dosages des peptides natriurétiques utilisés en contexte clinique. Cette étude a été facilité par le fait qu'il s'agit d'une cohorte longitudinale et que l'évolution de la glycosylation du proANP et du proBNP est rapide après initiation du sacubitril/valsartan [55, 127, 128]. Mes travaux ont permis montrer que la diminution observée du MR-proANP, initialement imaginé comme un biomarqueur reflétant la production de proANP ou d'ANP, était due à une interférence analytique de la glycosylation du proANP sur le dosage du MR-proANP. Cela signifie que l'interprétation des dosages de MR-proANP ne sont pas interprétable en termes de métabolisme du proANP ou de l'ANP. En revanche, le MR-proANP conserve sa propriété de biomarqueur, à savoir sa capacité à discriminer des populations différentes de patients. De même, la glycosylation du proBNP en S44 impacte le dosage du NT-proBNP. Néanmoins, le BNP et le NT-proBNP restent de bons estimateurs de la production de proBNP. Cela était attendu pour le proBNP étant donné les espèces moléculaires qui constituent le signal, mais surprenant pour le NT-proBNP qui a été développé avant la découverte de site de glycosylation dans le proBNP. Cependant, le NT-proBNP a été développé comme compétiteur du BNP, probablement en comparant ses taux plasmatiques à ceux du BNP.

D'une manière plus générale, ce travail révèle la problématique de la glycosylation dans le dosage des biomarqueurs en général. Ce problème va viser principalement les protéines utilisées comme biomarqueurs et qui sont naturellement sécrétées. En effet, seules les

protéines sécrétées sont glycosylées lors de leur passage via le réticulum endoplasmique et l'appareil de Golgi les protéines intracellulaires libérées via des exosomes ou la mort cellulaire (e.g. troponines) ne sont pas glycosylées. D'une manière générale, la glycosylation des biomarqueurs pourrait ne pas poser de problème, si tenté que la glycosylation reste constante. Par exemple, si un biomarqueur est toujours glycosylé à 30% au niveau d'un des épitopes détectés par le dosage, l'impact restera négligeable. Le résultat ne sera qu'une sous-estimation constante de la quantité du biomarqueur. Cependant, mes travaux sur le proANP et le proBNP ont montré que la glycosylation de ces deux protéines n'est pas constante et évolue en fonction du contexte clinique. La glycosylation est maximale chez le sujet sains, minimale en condition aigue, intermédiaire en condition chronique, et peut évoluer par les traitements. De fait, une analyse précise des espèces moléculaires contribuant aux dosages des biomarqueurs, ainsi que l'impact potentiel de leur glycosylation sur le dosage deviennent impératif pour mieux tirer parti de ces dosages.

2 Néprilysine et SRAA : biomarqueur et déterminant de l'IRA associée à la chirurgie cardiaque

2.1 La NEP un nouveau biomarqueur de l'IRA

L'insuffisance rénale aigue est un continuum physiopathologique qui débute de l'agression rénale et qui aboutit à l'insuffisance rénale aigue [75]. Les biomarqueurs actuels de l'IRA retenus par la classification KDIGO [80] sont largement imparfaits. En effet, l'oligurie est un critère diagnostic précoce et qui marque la gravité de l'atteinte rénale [139] mais qui est largement inconstant. De plus la créatinine plasmatique est un marqueur retardé après l'agression rénale et peu sensible [139]. De nouveaux biomarqueurs sont donc indispensables à notre pratique clinique future afin de dépister précocement les patients avec une agression

rénale en cours afin de pouvoir appliquer une prise en charge spécifique permettant de prévenir la survenue de l'insuffisance rénale aigue [140]. Dans le cadre de l'insuffisance rénale aigue associée à la chirurgie cardiaque, seul le NEPHROCHECK est recommandé par les sociétés savantes.

Ce travail de thèse montre que la NEP plasmatique est un biomarqueur précoce de l'agression rénale dans le cadre de la chirurgie cardiaque. L'origine de l'élévation de la NEP plasmatique dans le contexte de la chirurgie cardiaque avec CEC reste à ce stade incertain. L'hypothèse principale est l'origine vasculaire de la NEP. En effet les effets hémodynamiques de la CEC [141] et du clampage aortique (CA) [141] peuvent expliquer une élévation brutale de la NEP plasmatique, via la dysfonction endothéliale qu'ils engendrent. La NEP plasmatique serait dans ce cas un reflet de la dysfonction endothéliale et des effets hémodynamique induits par la chirurgie cardiaque et assez peu spécifique de la fonction rénale. Cette hypothèse est cohérente avec les données que nous avons obtenus sur l'activation du SRAA. La chirurgie cardiaque avec CEC et CA induirait des anomalies hémodynamiques et vasculaires expliquant l'élévation de la NEP plasmatique et l'activation du SRAA. Cela confirme l'hypothèse selon laquelle le NEP plasmatique n'est dans ce cas qu'un biomarqueur et non pas un effecteur physiopathologique, d'autant plus qu'elle ne semble pas jouer sur la balance du SRAA.

Concernant la NEP urinaire nos données tendent à confirmer sa valeur diagnostique à H6 post opératoire. En effet la NEP urinaire post opératoire immédiate semble trop précoce afin de dépister l'agression rénale en cours. Cependant sur un nombre restreint de patients (n=10), la NEP urinaire dans notre étude semble confirmer les données publiées récemment [96]. A l'inverse de la NEP plasmatique, la NEP urinaire semble être spécifique de l'atteinte

rénale. En effet les cellules tubulaires rénales sont riches en NEP [142], la NEP urinaire semble être le reflet de l'agression tubulaire et du relargage dans le compartiment urinaire de la NEP cellulaire [96, 142].

La NEP plasmatique et urinaire sont deux biomarqueurs distincts impliquant des processus physiopathologiques distincts mais qui semblent tous deux avoir leur place dans la gestion de l'IRA en post opératoire de chirurgie cardiaque.

2.2 La NEP une cible thérapeutique dans l'IRA

Dans les études ancillaires de PARADIGM HF [143, 144], les auteurs ont démontré que l'un des effets du sacubitril/valsartan indépendant de son action hémodynamique, est un effet bénéfique sur la fonction rénale avec un ralentissement de la détérioration de la fonction rénale chez les patients diabétiques. De plus dans un modèle animal de néphropathies diabétiques [145], les auteurs ont démontré que le sacubitril/valsartan améliore la dysfonction glomérulaire, diminue l'agression tubulaire, diminue la fibrose tubulo-interstitielle et péri-artérielle. Les auteurs précisent que le sacubitril/valsartan est plus efficace sur la fonction rénale que le valsartan seul et que son action est indépendante de la pression artérielle. L'inhibition de la NEP dans l'insuffisance rénale chronique semble donc avoir un intérêt thérapeutique majeur.

Même si la NEP ne semble pas être un effecteur de l'insuffisance rénale aigue via le SRAA dans ce travail de thèse, nous ne pouvons exclure sa participation par d'autres voies physiopathologiques. Par conséquent il semble licite de réfléchir au potentiel de l'inhibition de la NEP dans l'arsenal thérapeutique de l'IRA.

2.3 Modulation du SRAA dans l'IRA

Dans les suites des travaux de Kullmar *et al* [98] montrant l'élévation de l'activité rénine chez les patients développant une IRA dans les suites d'une chirurgie cardiaque deux scénarios étaient possibles : le premier selon lequel l'élévation de la rénine serait la conséquence d'un déficit en angiotensine II responsable d'une vasodilatation excessive et d'une hypoperfusion rénale, le second selon lequel l'élévation de la rénine serait le reflet d'une activation complète du SRAA responsable d'une élévation de l'angiotensine II et d'une vasoconstriction excessive intra rénale. Nous démontrons dans cette thèse l'implication de l'activation complète du SRAA dans le processus physiopathologique de l'IRA secondaire à la chirurgie cardiaque (scénario 2). La chirurgie cardiaque via la CEC et le clampage aortique induit une stimulation de la sécrétion de rénine par les cellules de la macula densa, responsable d'une élévation de l'angiotensine II et de l'aldostérone.

L'inhibition du SRAA dans ce contexte apparaît donc comme une voie thérapeutique. Deux stratégies sont possibles : dans un premier temps la prévention de l'IRA avec le maintien des IEC ou ARA II chez les patients bénéficiant d'un traitement au long cours. Les résultats de l'étude STOP or NOT [146] qui évaluent l'arrêt ou la poursuite des bloqueurs du SRAA dans le cadre d'une chirurgie réglée seront une première évaluation de cette hypothèse. Dans un second temps il est possible d'imaginer une stratégie thérapeutique introduisant un bloqueur du SRAA lors de la documentation de l'activation de ce dernier, nous pourrions utiliser la NEP comme marqueur précoce. Les résultats de l'étude START or NOT qui évaluent l'intérêt de l'introduction d'un bloqueur du SRAA après un épisode d'IRA pourrait être un premier élément d'évaluation.

3 Modulation de la NEP dans le choc septique

3.1 Contrôle de l'inhibition de la NEP

Il est connu depuis longtemps que l'inhibition de la NEP (ablation génétique ou inhibition pharmacologique) dans le choc endotoxinique (LPS) est associée à une très forte mortalité dans des modèles précliniques [117, 120]. Cependant, cette observation n'a de sens que si cette diminution de l'activité NEP existe *in vivo*. De fait, il avait été montré dans le laboratoire un activité basse chez quelques patients souffrant de choc septique sévère [114] et que l'augmentation du BNP > 916 pg/mL pouvait être responsable de cette inhibition [44]. L'administration d'une forme de BNP humain inactif mais toujours capable d'inhiber la NEP (hBNP*) a des rats en choc septique, entraîne une diminution brusque de la pression artérielle dans les deux heures suivant son administration, ce qui est compatible avec le mécanisme d'inhibition lente de la NEP par le BNP [44]. Ce résultat est essentiel car il montre que l'augmentation du BNP dans le choc septique pourrait avoir comme conséquence directe l'inhibition de la NEP, dont la conséquence directe est une instabilité hémodynamique brutale (**Figure 16**). Ce travail montre également que les modèles précliniques couramment utilisés et chez lesquels l'inhibition de la NEP par le BNP n'existe pas, ne reflètent que partiellement la physiopathologie du choc septique, et en particulier ne permettent pas de modéliser les formes les plus graves qui sont associées à une forte mortalité. Cela pourrait expliquer en partie les échecs récents des thérapeutiques testés dans le choc septique.

L'implication de la NEP dans la physiopathologie du choc septique sévère a permis d'identifier un processus à cibler pour améliorer potentiellement la survie des patients en choc septiques. Pendant ma thèse, j'ai tenté de restaurer l'activité NEP inhiber par le hBNP* en administrant de la NEP humaine recombinante ou en perfusant les rats avec du sérum qui

contient de grande quantité de NEP. Ces approches n'ont pas été couronnées de succès, probablement car la NEP circulante ne représente qu'une fraction de la NEP totale. Cependant, nous avons identifié une molécule, X.Y.U., qui a la capacité in vitro de prévenir l'inhibition de la NEP par le BNP humain, et de partiellement reverser cette inhibition. Chez le rat, l'administration préalable d'X.Y.U. à celle de hBNP* prévient l'inhibition de la NEP par hBNP*. Il reste à tester l'impact de la réversion partielle de l'inhibition de la NEP par X.Y.U. *in vivo*.

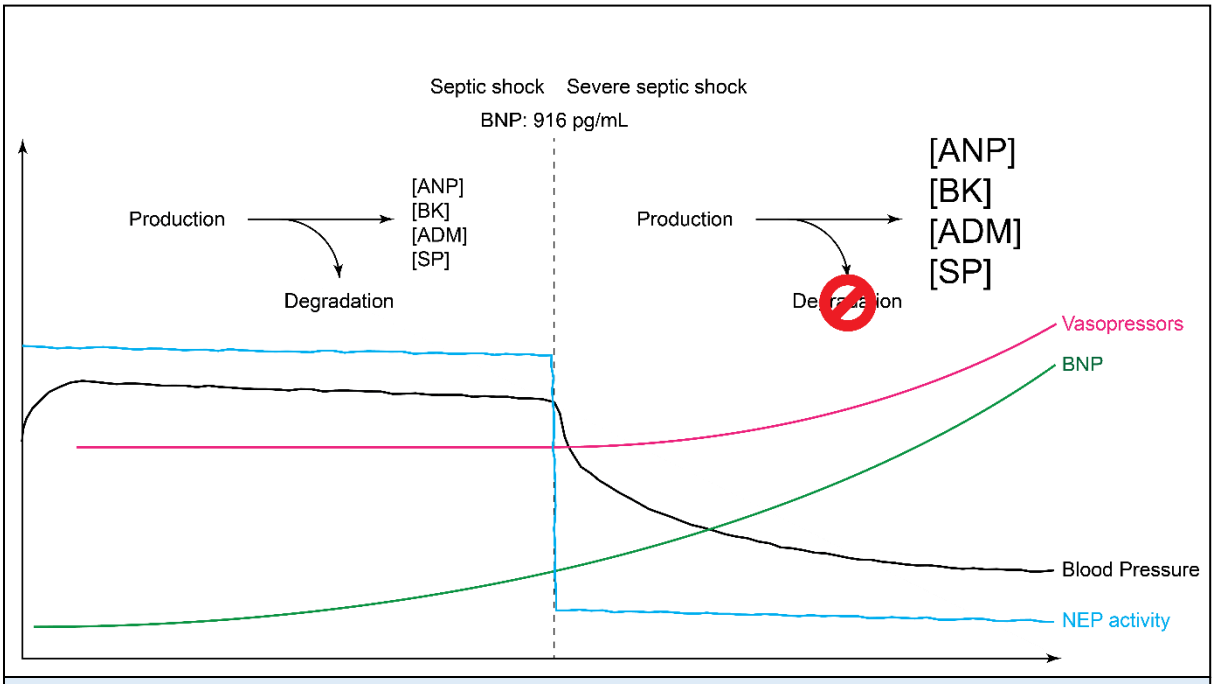

Figure 16 : Mécanismes impliquant l'inhibition de la NEP dans le choc septique. ANP : peptide natriurétique de type A, BK : bradykinine, ADM : adrenomédulline, SP : substance P.

D'un point de vue clinique, une stratégie de prévention de l'inhibition de la NEP n'est pas toujours compatible avec la réalité clinique, car au moment de l'admission en service de réanimation, le processus physiopathologique est bien avancé et l'inhibition de la NEP peut déjà être en cours. En revanche, si la réversion partielle de la NEP par X.Y.U. est confirmée in vivo, cela apporterait une nouvelle approche thérapeutique dans le choc septique. Que l'on

considère la prévention ou la réversion de l'inhibition de la NEP par le BNP humain, nous anticipons des bénéfices au-delà d'une plus grande stabilité hémodynamique. En effet, la prévention ou la réversion de l'inhibition de la NEP devrait permettre de limiter l'utilisation de doses massives de vasopresseurs, et ainsi diminuer les effets secondaires associés tel que la paralysie immunitaire. Des études dans ce sens devront être menée pour vérifier cette hypothèse.

Finalement, l'une des raisons de l'échec de nombreuses thérapeutiques, en particulier dans le choc septique, est l'incapacité d'identifier les patients à même de bénéficier de l'intervention. Le dosage de l'activité NEP (le dosage de la concentration NEP n'a pas de sens ici) n'est pas fait en routine, mais pourrait être adapté sur des automates de dosages déjà existant ou des point-of-care. Cependant, étant donné que l'augmentation de BNP est directement responsable de l'inhibition de la NEP, un simple dosage de BNP devrait permettre d'identifier les patients chez lesquels la NEP est active ou non, et ainsi sélectionner les patients qui bénéficieraient le plus de l'action de X.Y.U.. Une telle étude est en train d'être designer.

3.2 Inhibition de la Néprilysine en réanimation

Ce travail sur le rôle de la NEP dans le choc septique s'étend au-delà de cette pathologie et soulève plusieurs questions. Les données issues des grands essais thérapeutiques testant le sacubitril/valsartan dans le cadre de l'insuffisance cardiaque ont tous décrit l'hypotension artérielle comme effet secondaire principal **(Figure 8)**, et mes travaux ont mis en lumière des mécanismes qui peuvent expliquer en partie cette action hypotensive du sacubitril/valsartan. Dans les années à venir de plus en plus de patients vont se voir prescrire un traitement au long cours par sacubitril/valsartan compte tenu des recommandations actuelles de la prise en charge de l'insuffisance cardiaque chronique [50].

Il va donc être nécessaire d'évaluer l'impact d'un traitement par sacubitril/valsartan sur la gestion hémodynamique de ces patients qui ont une FEVG réduite et une vasoréactivité régulée par des molécules exogènes.

Cette problématique peut également survenir dans le cadre de patients sous sacubitril/valsartan qui seraient amenés à développer un choc distributif (septique ou anaphylactique). Ajouter de la vasodilatation pharmacologique à la vasodilatation induite par le sepsis ou la réaction allergique pourrait rendre la gestion hémodynamique difficile. De même la survenue d'un choc cardiogénique est une complication attendue dans la population cible du sacubitril/valsartan. Dans cette population spécifique de patients sous sacubitril/valsartan il faut s'inquiéter de l'absence de compensation possible en cas de choc cardiogénique. La baisse du débit cardiaque associée à une vasodilatation serait responsable d'une diminution importante de la perfusion des organes. Mais il n'y a pas aujourd'hui de données dans la littérature de description hémodynamique des patients sous sacubitril/valsartan qui souffrent d'une décompensation cardiaque aigue voire d'un choc cardiogénique. Les effets pléiotrope du sacubitril/valsartan et le rôle central de la NEP au sein de la vasoréactivité ne permettent pas de privilégier une hypothèse physiopathologique.

4 Conclusion

En conclusion, ce travail positionne la NEP et son inhibition comme des facteurs physiopathologique majeur dans plusieurs contextes cliniques. Cependant, comme tout processus biologique, l'inhibition de la NEP est à double tranchant puisqu'elle est bénéfique dans l'insuffisance cardiaque à FEVG réduite mais délétère dans le choc septique. Néanmoins, l'importance de la NEP dans la régulation de peptides impliqués dans de nombreux processus biologique en font une cible thérapeutique de choix que ce soit dans

l'insuffisance cardiaque à FEVG réduite (sacubitril/valsartan) ou le choc septique (X.Y.U.), même si dans ces deux contextes des effets opposés sont recherchés. Ce travail, permettra je l'espère d'offrir un nouvel axe thérapeutique dans la prise en charge du choc septique sévère.

BIBLIOGRAPHIE

1. Barr, C. S., Rhodes, P. & Struthers, A. D. (1996) C-type natriuretic peptide, *Peptides.* **17**, 1243-51.

2. Tamura, N., Ogawa, Y., Chusho, H., Nakamura, K., Nakao, K., Suda, M., Kasahara, M., Hashimoto, R., Katsuura, G., Mukoyama, M., Itoh, H., Saito, Y., Tanaka, I., Otani, H. & Katsuki, M. (2000) Cardiac fibrosis in mice lacking brain natriuretic peptide, *Proc Natl Acad Sci U S A.* **97**, 4239-44.

3. Silberbach, M. & Roberts, C. T., Jr. (2001) Natriuretic peptide signalling: molecular and cellular pathways to growth regulation, *Cell Signal.* **13**, 221-31.

4. Rubattu, S., Sciarretta, S., Valenti, V., Stanzione, R. & Volpe, M. (2008) Natriuretic peptides: an update on bioactivity, potential therapeutic use, and implication in cardiovascular diseases, *Am J Hypertens.* **21**, 733-41.

5. Kuhn, M., Volker, K., Schwarz, K., Carbajo-Lozoya, J., Flogel, U., Jacoby, C., Stypmann, J., van Eickels, M., Gambaryan, S., Hartmann, M., Werner, M., Wieland, T., Schrader, J. & Baba, H. A. (2009) The natriuretic peptide/guanylyl cyclase--a system functions as a stress-responsive regulator of angiogenesis in mice, *J Clin Invest.* **119**, 2019-30.

6. Brunner-La Rocca, H. P., Kaye, D. M., Woods, R. L., Hastings, J. & Esler, M. D. (2001) Effects of intravenous brain natriuretic peptide on regional sympathetic activity in patients with chronic heart failure as compared with healthy control subjects, *J Am Coll Cardiol.* **37**, 1221-7.

7. Richards, A. M., Wittert, G. A., Espiner, E. A., Yandle, T. G., Ikram, H. & Frampton, C. (1992) Effect of inhibition of endopeptidase 24.11 on responses to angiotensin II in human volunteers, *Circ Res.* **71**, 1501-7.

8. Hansen, L. H., Madsen, T. D., Goth, C. K., Clausen, H., Chen, Y., Dzhoyashvili, N., Iyer, S. R., Sangaralingham, S. J., Burnett, J. C., Jr., Rehfeld, J. F., Vakhrushev, S. Y., Schjoldager, K. T. & Goetze, J. P. (2019) Discovery of O-glycans on atrial natriuretic peptide (ANP) that affect both its proteolytic degradation and potency at its cognate receptor, *J Biol Chem.* **294**, 12567-12578.

9. Schellenberger, U., O'Rear, J., Guzzetta, A., Jue, R. A., Protter, A. A. & Pollitt, N. S. (2006) The precursor to B-type natriuretic peptide is an O-linked glycoprotein, *Arch Biochem Biophys.* **451**, 160-6.

10. Jamieson, J. D. & Palade, G. E. (1964) Specific Granules in Atrial Muscle Cells, *J Cell Biol.* **23**, 151-72.

11. Arrigo, M., Vodovar, N., Nougue, H., Sadoune, M., Pemberton, C. J., Ballan, P., Ludes, P. O., Gendron, N., Carpentier, A., Cholley, B., Bizouarn, P., Cohen-Solal, A., Singh, J. P., Szymonifka, J., Latremouille, C., Samuel, J. L., Launay, J. M., Pottecher, J., Richards, A. M., Truong, Q. A., Smadja, D. M. & Mebazaa, A. (2018) The heart regulates the endocrine response to heart failure: cardiac contribution to circulating neprilysin, *Eur Heart J.* **39**, 1794-1798.

12. Yan, W., Sheng, N., Seto, M., Morser, J. & Wu, Q. (1999) Corin, a mosaic transmembrane serine protease encoded by a novel cDNA from human heart, *J Biol Chem.* **274**, 14926-35.

13. Gladysheva, I. P., Robinson, B. R., Houng, A. K., Kovats, T. & King, S. M. (2008) Corin is co-expressed with pro-ANP and localized on the cardiomyocyte surface in both zymogen and catalytically active forms, *J Mol Cell Cardiol.* **44**, 131-42.

14. Ichiki, T. & Burnett, J. C., Jr. (2017) Atrial Natriuretic Peptide - Old But New Therapeutic in Cardiovascular Diseases, *Circ J.* **81**, 913-919.

15. Vesely, D. L. (1995) Atrial natriuretic hormones originating from the N-terminus of the atrial natriuretic factor prohormone, *Clin Exp Pharmacol Physiol.* **22**, 108-14.

16. Morgenthaler, N. G., Struck, J., Thomas, B. & Bergmann, A. (2004) Immunoluminometric assay for the midregion of pro-atrial natriuretic peptide in human plasma, *Clin Chem.* **50**, 234-6.

17. Hunter, I., Alehagen, U., Dahlstrom, U., Rehfeld, J. F., Crimmins, D. L. & Goetze, J. P. (2011) N-terminal pro-atrial natriuretic peptide measurement in plasma suggests covalent modification, *Clin Chem.* **57**, 1327-30.

18. Hosoda, K., Nakao, K., Mukoyama, M., Saito, Y., Jougasaki, M., Shirakami, G., Suga, S., Ogawa, Y., Yasue, H. & Imura, H. (1991) Expression of brain natriuretic peptide gene in human heart. Production in the ventricle, *Hypertension.* **17**, 1152-5.

19. Yasue, H., Yoshimura, M., Sumida, H., Kikuta, K., Kugiyama, K., Jougasaki, M., Ogawa, H., Okumura, K., Mukoyama, M. & Nakao, K. (1994) Localization and mechanism of secretion of B-type natriuretic peptide in comparison with those of A-type natriuretic peptide in normal subjects and patients with heart failure, *Circulation.* **90**, 195-203.

20. Hall, C. (2004) Essential biochemistry and physiology of (NT-pro)BNP, *Eur J Heart Fail.* **6**, 257-60.

21. Semenov, A. G., Tamm, N. N., Seferian, K. R., Postnikov, A. B., Karpova, N. S., Serebryanaya, D. V., Koshkina, E. V., Krasnoselsky, M. I. & Katrukha, A. G. (2010) Processing of pro-B-type natriuretic peptide: furin and corin as candidate convertases, *Clin Chem.* **56**, 1166-76.

22. Semenov, A. G., Postnikov, A. B., Tamm, N. N., Seferian, K. R., Karpova, N. S., Bloshchitsyna, M. N., Koshkina, E. V., Krasnoselsky, M. I., Serebryanaya, D. V. & Katrukha, A. G. (2009) Processing of pro-brain natriuretic peptide is suppressed by O-glycosylation in the region close to the cleavage site, *Clin Chem.* **55**, 489-98.

23. Nakagawa, O., Ogawa, Y., Itoh, H., Suga, S., Komatsu, Y., Kishimoto, I., Nishino, K., Yoshimasa, T. & Nakao, K. (1995) Rapid transcriptional activation and early mRNA turnover of brain natriuretic peptide in cardiocyte hypertrophy. Evidence for brain natriuretic peptide as an "emergency" cardiac hormone against ventricular overload, *J Clin Invest.* **96**, 1280-7.

24. Sudoh, T., Minamino, N., Kangawa, K. & Matsuo, H. (1990) C-type natriuretic peptide (CNP): a new member of natriuretic peptide family identified in porcine brain, *Biochem Biophys Res Commun.* **168**, 863-70.

25. Vodovar, N., Seronde, M. F., Laribi, S., Gayat, E., Lassus, J., Boukef, R., Nouira, S., Manivet, P., Samuel, J. L., Logeart, D., Ishihara, S., Cohen Solal, A., Januzzi, J. L., Jr., Richards, A. M., Launay, J. M., Mebazaa, A. & Network, G. (2014) Post-translational modifications enhance NT-proBNP and BNP production in acute decompensated heart failure, *Eur Heart J.* **35**, 3434-41.

26. Chang, M. S., Lowe, D. G., Lewis, M., Hellmiss, R., Chen, E. & Goeddel, D. V. (1989) Differential activation by atrial and brain natriuretic peptides of two different receptor guanylate cyclases, *Nature.* **341**, 68-72.

27. Ichiki, T., Dzhoyashvili, N. & Burnett, J. C., Jr. (2019) Natriuretic peptide based therapeutics for heart failure: Cenderitide: A novel first-in-class designer natriuretic peptide, *Int J Cardiol.* **281**, 166-171.

28. Bennett, B. D., Bennett, G. L., Vitangcol, R. V., Jewett, J. R., Burnier, J., Henzel, W. & Lowe, D. G. (1991) Extracellular domain-IgG fusion proteins for three human natriuretic peptide receptors. Hormone pharmacology and application to solid phase screening of synthetic peptide antisera, *J Biol Chem.* **266**, 23060-7.

29. Lopez, M. J., Garbers, D. L. & Kuhn, M. (1997) The guanylyl cyclase-deficient mouse defines differential pathways of natriuretic peptide signaling, *J Biol Chem.* **272**, 23064-8.

30. Pejchalova, K., Krejci, P. & Wilcox, W. R. (2007) C-natriuretic peptide: an important regulator of cartilage, *Mol Genet Metab.* **92**, 210-5.

31. Suga, S., Nakao, K., Mukoyama, M., Arai, H., Hosoda, K., Ogawa, Y. & Imura, H. (1992) Characterization of natriuretic peptide receptors in cultured cells, *Hypertension.* **19**, 762-5.

32. Suga, S., Nakao, K., Hosoda, K., Mukoyama, M., Ogawa, Y., Shirakami, G., Arai, H., Saito, Y., Kambayashi, Y., Inouye, K. & et al. (1992) Receptor selectivity of natriuretic peptide family, atrial natriuretic peptide, brain natriuretic peptide, and C-type natriuretic peptide, *Endocrinology.* **130**, 229-39.

33. Kuhn, M. (2016) Molecular Physiology of Membrane Guanylyl Cyclase Receptors, *Physiol Rev.* **96**, 751-804.

34. Vallee, B. L. & Auld, D. S. (1990) Zinc coordination, function, and structure of zinc enzymes and other proteins, *Biochemistry.* **29**, 5647-59.

35. Turner, A. J. & Tanzawa, K. (1997) Mammalian membrane metallopeptidases: NEP, ECE, KELL, and PEX, *FASEB J.* **11**, 355-64.

36. Bayes-Genis, A., Barallat, J. & Richards, A. M. (2016) A Test in Context: Neprilysin: Function, Inhibition, and Biomarker, *J Am Coll Cardiol.* **68**, 639-653.

37. Lafrance, M. H., Vezina, C., Wang, Q., Boileau, G., Crine, P. & Lemay, G. (1994) Role of glycosylation in transport and enzymic activity of neutral endopeptidase-24.11, *Biochem J.* **302 (Pt 2)**, 451-4.

38. Kakiya, N., Saito, T., Nilsson, P., Matsuba, Y., Tsubuki, S., Takei, N., Nawa, H. & Saido, T. C. (2012) Cell surface expression of the major amyloid-beta peptide (Abeta)-degrading enzyme, neprilysin, depends on phosphorylation by mitogen-activated protein kinase/extracellular signal-regulated kinase kinase (MEK) and dephosphorylation by protein phosphatase 1a, *J Biol Chem.* **287**, 29362-72.

39. Kawakubo, T., Mori, R., Shirotani, K., Iwata, N. & Asai, M. (2017) Neprilysin Is Suppressed by Dual-Specificity Tyrosine-Phosphorylation Regulated Kinase 1A (DYRK1A) in Down-Syndrome-Derived Fibroblasts, *Biol Pharm Bull.* **40**, 327-333.

40. Campbell, D. J. (2017) Long-term neprilysin inhibition - implications for ARNIs, *Nat Rev Cardiol.* **14**, 171-186.

41. Dickey, D. M. & Potter, L. R. (2010) Human B-type natriuretic peptide is not degraded by meprin A, *Biochem Pharmacol.* **80**, 1007-11.

42. Kenny, A. J., Bourne, A. & Ingram, J. (1993) Hydrolysis of human and pig brain natriuretic peptides, urodilatin, C-type natriuretic peptide and some C-receptor ligands by endopeptidase-24.11, *Biochem J.* **291 (Pt 1)**, 83-8.

43. Smith, M. W., Espiner, E. A., Yandle, T. G., Charles, C. J. & Richards, A. M. (2000) Delayed metabolism of human brain natriuretic peptide reflects resistance to neutral endopeptidase, *J Endocrinol.* **167**, 239-46.

44. Vodovar, N., Seronde, M. F., Laribi, S., Gayat, E., Lassus, J., Januzzi, J. L., Jr., Boukef, R., Nouira, S., Manivet, P., Samuel, J. L., Logeart, D., Cohen-Solal, A., Richards, A. M., Launay, J. M., Mebazaa, A. & Network, G. (2015) Elevated Plasma B-Type Natriuretic Peptide Concentrations Directly Inhibit Circulating Neprilysin Activity in Heart Failure, *JACC Heart Fail.* **3**, 629-36.

45. Domenig, O., Manzel, A., Grobe, N., Konigshausen, E., Kaltenecker, C. C., Kovarik, J. J., Stegbauer, J., Gurley, S. B., van Oyen, D., Antlanger, M., Bader, M., Motta-Santos, D., Santos, R. A., Elased, K. M., Saemann, M. D., Linker, R. A. & Poglitsch, M. (2016) Neprilysin is a

Mediator of Alternative Renin-Angiotensin-System Activation in the Murine and Human Kidney, *Sci Rep.* **6**, 33678.

46. Mangiafico, S., Costello-Boerrigter, L. C., Andersen, I. A., Cataliotti, A. & Burnett, J. C., Jr. (2013) Neutral endopeptidase inhibition and the natriuretic peptide system: an evolving strategy in cardiovascular therapeutics, *Eur Heart J.* **34**, 886-893c.

47. Lam, C. S., Donal, E., Kraigher-Krainer, E. & Vasan, R. S. (2011) Epidemiology and clinical course of heart failure with preserved ejection fraction, *Eur J Heart Fail.* **13**, 18-28.

48. Tuppin, P., Ricci-Renaud, P., de Peretti, C., Fagot-Campagna, A., Alla, F., Danchin, N. & Allemand, H. (2014) Frequency of cardiovascular diseases and risk factors treated in France according to social deprivation and residence in an overseas territory, *Int J Cardiol.* **173**, 430-5.

49. Mosterd, A. & Hoes, A. W. (2007) Clinical epidemiology of heart failure, *Heart.* **93**, 1137-46.

50. Heidenreich, P. A., Bozkurt, B., Aguilar, D., Allen, L. A., Byun, J. J., Colvin, M. M., Deswal, A., Drazner, M. H., Dunlay, S. M., Evers, L. R., Fang, J. C., Fedson, S. E., Fonarow, G. C., Hayek, S. S., Hernandez, A. F., Khazanie, P., Kittleson, M. M., Lee, C. S., Link, M. S., Milano, C. A., Nnacheta, L. C., Sandhu, A. T., Stevenson, L. W., Vardeny, O., Vest, A. R. & Yancy, C. W. (2022) 2022 AHA/ACC/HFSA Guideline for the Management of Heart Failure: A Report of the American College of Cardiology/American Heart Association Joint Committee on Clinical Practice Guidelines, *Circulation.* **145**, e895-e1032.

51. Ponikowski, P., Voors, A. A., Anker, S. D., Bueno, H., Cleland, J. G. F., Coats, A. J. S., Falk, V., Gonzalez-Juanatey, J. R., Harjola, V. P., Jankowska, E. A., Jessup, M., Linde, C., Nihoyannopoulos, P., Parissis, J. T., Pieske, B., Riley, J. P., Rosano, G. M. C., Ruilope, L. M., Ruschitzka, F., Rutten, F. H., van der Meer, P. & Group, E. S. C. S. D. (2016) 2016 ESC Guidelines for the diagnosis and treatment of acute and chronic heart failure: The Task Force for the diagnosis and treatment of acute and chronic heart failure of the European Society of Cardiology (ESC)Developed with the special contribution of the Heart Failure Association (HFA) of the ESC, *Eur Heart J.* **37**, 2129-2200.

52. McDonagh, T. A., Metra, M., Adamo, M., Gardner, R. S., Baumbach, A., Bohm, M., Burri, H., Butler, J., Celutkiene, J., Chioncel, O., Cleland, J. G. F., Coats, A. J. S., Crespo-Leiro, M. G., Farmakis, D., Gilard, M., Heymans, S., Hoes, A. W., Jaarsma, T., Jankowska, E. A., Lainscak, M., Lam, C. S. P., Lyon, A. R., McMurray, J. J. V., Mebazaa, A., Mindham, R., Muneretto, C., Francesco Piepoli, M., Price, S., Rosano, G. M. C., Ruschitzka, F., Kathrine Skibelund, A. & Group, E. S. C. S. D. (2021) 2021 ESC Guidelines for the diagnosis and treatment of acute and chronic heart failure, *Eur Heart J.* **42**, 3599-3726.

53. Vodovar, N., Mebazaa, A., Januzzi, J. L., Jr., Murtagh, G., Stough, W. G., Adams, K. F., Jr. & Zannad, F. (2018) Evolution of natriuretic peptide biomarkers in heart failure: Implications for clinical care and clinical trials, *Int J Cardiol.* **254**, 215-221.

54. Packer, M., McMurray, J. J., Desai, A. S., Gong, J., Lefkowitz, M. P., Rizkala, A. R., Rouleau, J. L., Shi, V. C., Solomon, S. D., Swedberg, K., Zile, M., Andersen, K., Arango, J. L., Arnold, J. M., Belohlavek, J., Bohm, M., Boytsov, S., Burgess, L. J., Cabrera, W., Calvo, C., Chen, C. H., Dukat, A., Duarte, Y. C., Erglis, A., Fu, M., Gomez, E., Gonzalez-Medina, A., Hagege, A. A., Huang, J., Katova, T., Kiatchoosakun, S., Kim, K. S., Kozan, O., Llamas, E. B., Martinez, F., Merkely, B., Mendoza, I., Mosterd, A., Negrusz-Kawecka, M., Peuhkurinen, K., Ramires, F. J., Refsgaard, J., Rosenthal, A., Senni, M., Sibulo, A. S., Jr., Silva-Cardoso, J., Squire, I. B., Starling, R. C., Teerlink, J. R., Vanhaecke, J., Vinereanu, D., Wong, R. C., Investigators, P.-H. & Coordinators (2015) Angiotensin receptor neprilysin inhibition compared with enalapril on the risk of clinical progression in surviving patients with heart failure, *Circulation.* **131**, 54-61.

55. Nougue, H., Pezel, T., Picard, F., Sadoune, M., Arrigo, M., Beauvais, F., Launay, J. M., Cohen-Solal, A., Vodovar, N. & Logeart, D. (2019) Effects of sacubitril/valsartan on neprilysin targets and the metabolism of natriuretic peptides in chronic heart failure: a mechanistic clinical study, *Eur J Heart Fail.* **21**, 598-605.

56. Jaffe, A. S., Apple, F. S., Mebazaa, A. & Vodovar, N. (2015) Unraveling N-terminal pro-B-type natriuretic peptide: another piece to a very complex puzzle in heart failure patients, *Clin Chem.* **61**, 1016-8.

57. Suwa, M., Seino, Y., Nomachi, Y., Matsuki, S. & Funahashi, K. (2005) Multicenter prospective investigation on efficacy and safety of carperitide for acute heart failure in the 'real world' of therapy, *Circ J.* **69**, 283-90.

58. Packer, M., O'Connor, C., McMurray, J. J. V., Wittes, J., Abraham, W. T., Anker, S. D., Dickstein, K., Filippatos, G., Holcomb, R., Krum, H., Maggioni, A. P., Mebazaa, A., Peacock, W. F., Petrie, M. C., Ponikowski, P., Ruschitzka, F., van Veldhuisen, D. J., Kowarski, L. S., Schactman, M., Holzmeister, J. & Investigators, T.-A. (2017) Effect of Ularitide on Cardiovascular Mortality in Acute Heart Failure, *N Engl J Med.* **376**, 1956-1964.

59. O'Connor, C. M., Starling, R. C., Hernandez, A. F., Armstrong, P. W., Dickstein, K., Hasselblad, V., Heizer, G. M., Komajda, M., Massie, B. M., McMurray, J. J., Nieminen, M. S., Reist, C. J., Rouleau, J. L., Swedberg, K., Adams, K. F., Jr., Anker, S. D., Atar, D., Battler, A., Botero, R., Bohidar, N. R., Butler, J., Clausell, N., Corbalan, R., Costanzo, M. R., Dahlstrom, U., Deckelbaum, L. I., Diaz, R., Dunlap, M. E., Ezekowitz, J. A., Feldman, D., Felker, G. M., Fonarow, G. C., Gennevois, D., Gottlieb, S. S., Hill, J. A., Hollander, J. E., Howlett, J. G., Hudson, M. P., Kociol, R. D., Krum, H., Laucevicius, A., Levy, W. C., Mendez, G. F., Metra, M., Mittal, S., Oh, B. H., Pereira, N. L., Ponikowski, P., Tang, W. H., Tanomsup, S., Teerlink, J. R., Triposkiadis, F., Troughton, R. W., Voors, A. A., Whellan, D. J., Zannad, F. & Califf, R. M. (2011) Effect of nesiritide in patients with acute decompensated heart failure, *N Engl J Med.* **365**, 32-43.

60. Lisy, O., Huntley, B. K., McCormick, D. J., Kurlansky, P. A. & Burnett, J. C., Jr. (2008) Design, synthesis, and actions of a novel chimeric natriuretic peptide: CD-NP, *J Am Coll Cardiol.* **52**, 60-8.

61. Wei, C. M., Kim, C. H., Miller, V. M. & Burnett, J. C., Jr. (1993) Vasonatrin peptide: a unique synthetic natriuretic and vasorelaxing peptide, *J Clin Invest.* **92**, 2048-52.

62. McKie, P. M., Schirger, J. A., Benike, S. L., Harstad, L. K., Slusser, J. P., Hodge, D. O., Redfield, M. M., Burnett, J. C., Jr. & Chen, H. H. (2016) Chronic subcutaneous brain natriuretic peptide therapy in asymptomatic systolic heart failure, *Eur J Heart Fail.* **18**, 433-41.

63. Chen, H. H., Glockner, J. F., Schirger, J. A., Cataliotti, A., Redfield, M. M. & Burnett, J. C., Jr. (2012) Novel protein therapeutics for systolic heart failure: chronic subcutaneous B-type natriuretic peptide, *J Am Coll Cardiol.* **60**, 2305-12.

64. Bevan, E. G., Connell, J. M., Doyle, J., Carmichael, H. A., Davies, D. L., Lorimer, A. R. & McInnes, G. T. (1992) Candoxatril, a neutral endopeptidase inhibitor: efficacy and tolerability in essential hypertension, *J Hypertens.* **10**, 607-13.

65. Packer, M., Lee, W. H., Yushak, M. & Medina, N. (1986) Comparison of captopril and enalapril in patients with severe chronic heart failure, *N Engl J Med.* **315**, 847-53.

66. Kostis, J. B., Packer, M., Black, H. R., Schmieder, R., Henry, D. & Levy, E. (2004) Omapatrilat and enalapril in patients with hypertension: the Omapatrilat Cardiovascular Treatment vs. Enalapril (OCTAVE) trial, *Am J Hypertens.* **17**, 103-11.

67. Gu, J., Noe, A., Chandra, P., Al-Fayoumi, S., Ligueros-Saylan, M., Sarangapani, R., Maahs, S., Ksander, G., Rigel, D. F., Jeng, A. Y., Lin, T. H., Zheng, W. & Dole, W. P. (2010) Pharmacokinetics and pharmacodynamics of LCZ696, a novel dual-acting angiotensin receptor-neprilysin inhibitor (ARNi), *J Clin Pharmacol.* **50**, 401-14.

68. McMurray, J. J., Packer, M., Desai, A. S., Gong, J., Lefkowitz, M. P., Rizkala, A. R., Rouleau, J. L., Shi, V. C., Solomon, S. D., Swedberg, K., Zile, M. R., Investigators, P.-H. & Committees (2014) Angiotensin-neprilysin inhibition versus enalapril in heart failure, *N Engl J Med.* **371**, 993-1004.

69. Solomon, S. D., McMurray, J. J. V., Anand, I. S., Ge, J., Lam, C. S. P., Maggioni, A. P., Martinez, F., Packer, M., Pfeffer, M. A., Pieske, B., Redfield, M. M., Rouleau, J. L., van Veldhuisen, D. J., Zannad, F., Zile, M. R., Desai, A. S., Claggett, B., Jhund, P. S., Boytsov, S. A., Comin-Colet, J., Cleland, J., Dungen, H. D., Goncalvesova, E., Katova, T., Kerr Saraiva, J. F., Lelonek, M., Merkely, B., Senni, M., Shah, S. J., Zhou, J., Rizkala, A. R., Gong, J., Shi, V. C., Lefkowitz, M. P., Investigators, P.-H. & Committees (2019) Angiotensin-Neprilysin Inhibition in Heart Failure with Preserved Ejection Fraction, *N Engl J Med.* **381**, 1609-1620.

70. Velazquez, E. J., Morrow, D. A., DeVore, A. D., Duffy, C. I., Ambrosy, A. P., McCague, K., Rocha, R., Braunwald, E. & Investigators, P.-H. (2019) Angiotensin-Neprilysin Inhibition in Acute Decompensated Heart Failure, *N Engl J Med.* **380**, 539-548.

71. Mann, D. L., Givertz, M. M., Vader, J. M., Starling, R. C., Shah, P., McNulty, S. E., Anstrom, K. J., Margulies, K. B., Kiernan, M. S., Mahr, C., Gupta, D., Redfield, M. M., Lala, A., Lewis, G. D., DeVore, A. D., Desvigne-Nickens, P., Hernandez, A. F., Braunwald, E. & Investigators, L. (2022) Effect of Treatment With Sacubitril/Valsartan in Patients With Advanced Heart Failure and Reduced Ejection Fraction: A Randomized Clinical Trial, *JAMA Cardiol.* **7**, 17-25.

72. Vodovar, N., Cohen-Solal, A. & Logeart, D. (2022) Could Neprilysin Be Already Inhibited by BNP in the LIFE Trial?, *JAMA Cardiol.* **7**, 656-657.

73. Hoste, E. A. J., Kellum, J. A., Selby, N. M., Zarbock, A., Palevsky, P. M., Bagshaw, S. M., Goldstein, S. L., Cerda, J. & Chawla, L. S. (2018) Global epidemiology and outcomes of acute kidney injury, *Nat Rev Nephrol.* **14**, 607-625.

74. Li, P. K., Burdmann, E. A., Mehta, R. L. & World Kidney Day Steering, C. (2013) Acute kidney injury: global health alert, *Transplantation.* **95**, 653-7.

75. Ichai, C., Vinsonneau, C., Souweine, B., Armando, F., Canet, E., Clec'h, C., Constantin, J. M., Darmon, M., Duranteau, J., Gaillot, T., Garnier, A., Jacob, L., Joannes-Boyau, O., Juillard, L., Journois, D., Lautrette, A., Muller, L., Legrand, M., Lerolle, N., Rimmele, T., Rondeau, E., Tamion, F., Walrave, Y., Velly, L., Societe francaise d'anesthesie et de, r., Societe de reanimation de langue, f., Groupe francophone de reanimation et urgences, p. & Societe francaise de, n. (2016) Acute kidney injury in the perioperative period and in intensive care units (excluding renal replacement therapies), *Ann Intensive Care.* **6**, 48.

76. Koyner, J. L. (2020) Subclinical Acute Kidney Injury Is Acute Kidney Injury and Should Not Be Ignored, *Am J Respir Crit Care Med.* **202**, 786-787.

77. Hoste, E. A. J. & Vandenberghe, W. (2017) Epidemiology of cardiac surgery-associated acute kidney injury, *Best Pract Res Clin Anaesthesiol.* **31**, 299-303.

78. Bellomo, R., Ronco, C., Kellum, J. A., Mehta, R. L., Palevsky, P. & Acute Dialysis Quality Initiative, w. (2004) Acute renal failure - definition, outcome measures, animal models, fluid therapy and information technology needs: the Second International Consensus Conference of the Acute Dialysis Quality Initiative (ADQI) Group, *Crit Care.* **8**, R204-12.

79. Mehta, R. L., Kellum, J. A., Shah, S. V., Molitoris, B. A., Ronco, C., Warnock, D. G., Levin, A. & Acute Kidney Injury, N. (2007) Acute Kidney Injury Network: report of an initiative to improve outcomes in acute kidney injury, *Crit Care.* **11**, R31.

80. Khwaja, A. (2012) KDIGO clinical practice guidelines for acute kidney injury, *Nephron Clin Pract.* **120**, c179-84.

81. Ostermann, M., Zarbock, A., Goldstein, S., Kashani, K., Macedo, E., Murugan, R., Bell, M., Forni, L., Guzzi, L., Joannidis, M., Kane-Gill, S. L., Legrand, M., Mehta, R., Murray, P. T., Pickkers, P., Plebani, M., Prowle, J., Ricci, Z., Rimmele, T., Rosner, M., Shaw, A. D., Kellum, J. A. & Ronco, C. (2020) Recommendations on Acute Kidney Injury Biomarkers From the Acute Disease Quality Initiative Consensus Conference: A Consensus Statement, *JAMA Netw Open.* **3**, e2019209.

82. Ponte, B. & Saudan, P. (2008) [Acute renal failure in 2008], *Rev Med Suisse.* **4**, 568, 570-2, 574-5.

83. Hoste, E. A., Damen, J., Vanholder, R. C., Lameire, N. H., Delanghe, J. R., Van den Hauwe, K. & Colardyn, F. A. (2005) Assessment of renal function in recently admitted critically ill patients with normal serum creatinine, *Nephrol Dial Transplant.* **20**, 747-53.

84. Ilaria, G., Kianoush, K., Ruxandra, B., Francesca, M., Mariarosa, C., Davide, G. & Claudio, R. (2021) Clinical adoption of Nephrocheck(R) in the early detection of acute kidney injury, *Ann Clin Biochem.* **58**, 6-15.

85. Meersch, M., Schmidt, C., Hoffmeier, A., Van Aken, H., Wempe, C., Gerss, J. & Zarbock, A. (2017) Prevention of cardiac surgery-associated AKI by implementing the KDIGO guidelines in high risk patients identified by biomarkers: the PrevAKI randomized controlled trial, *Intensive Care Med.* **43**, 1551-1561.

86. Nadim, M. K., Forni, L. G., Bihorac, A., Hobson, C., Koyner, J. L., Shaw, A., Arnaoutakis, G. J., Ding, X., Engelman, D. T., Gasparovic, H., Gasparovic, V., Herzog, C. A., Kashani, K., Katz, N., Liu, K. D., Mehta, R. L., Ostermann, M., Pannu, N., Pickkers, P., Price, S., Ricci, Z., Rich, J. B., Sajja, L. R., Weaver, F. A., Zarbock, A., Ronco, C. & Kellum, J. A. (2018) Cardiac and Vascular Surgery-Associated Acute Kidney Injury: The 20th International Consensus Conference of the ADQI (Acute Disease Quality Initiative) Group, *J Am Heart Assoc.* **7**.

87. Rabb, H., Griffin, M. D., McKay, D. B., Swaminathan, S., Pickkers, P., Rosner, M. H., Kellum, J. A., Ronco, C. & Acute Dialysis Quality Initiative Consensus, X. W. G. (2016) Inflammation in AKI: Current Understanding, Key Questions, and Knowledge Gaps, *J Am Soc Nephrol.* **27**, 371-9.

88. Jang, H. R. & Rabb, H. (2015) Immune cells in experimental acute kidney injury, *Nat Rev Nephrol.* **11**, 88-101.

89. Oh, J. & Rabb, H. (2013) Adiponectin: an enlarging role in acute kidney injury, *Kidney Int.* **83**, 546-8.

90. Kurts, C., Panzer, U., Anders, H. J. & Rees, A. J. (2013) The immune system and kidney disease: basic concepts and clinical implications, *Nat Rev Immunol.* **13**, 738-53.

91. Anders, H. J. & Schaefer, L. (2014) Beyond tissue injury-damage-associated molecular patterns, toll-like receptors, and inflammasomes also drive regeneration and fibrosis, *J Am Soc Nephrol.* **25**, 1387-400.

92. Hu, J., Chen, R., Liu, S., Yu, X., Zou, J. & Ding, X. (2016) Global Incidence and Outcomes of Adult Patients With Acute Kidney Injury After Cardiac Surgery: A Systematic Review and Meta-Analysis, *J Cardiothorac Vasc Anesth.* **30**, 82-9.

93. Vandenberghe, W., Gevaert, S., Kellum, J. A., Bagshaw, S. M., Peperstraete, H., Herck, I., Decruyenaere, J. & Hoste, E. A. (2016) Acute Kidney Injury in Cardiorenal Syndrome Type 1 Patients: A Systematic Review and Meta-Analysis, *Cardiorenal Med.* **6**, 116-28.

94. Hobson, C. E., Yavas, S., Segal, M. S., Schold, J. D., Tribble, C. G., Layon, A. J. & Bihorac, A. (2009) Acute kidney injury is associated with increased long-term mortality after cardiothoracic surgery, *Circulation.* **119**, 2444-53.

95. Ferreiro, A. & Lombardi, R. (2017) Acute kidney injury after cardiac surgery is associated with mid-term but not long-term mortality: A cohort-based study, *PLoS One.* **12**, e0181158.

96. Bernardi, M. H., Wagner, L., Ryz, S., Puchinger, J., Nixdorf, L., Edlinger-Stanger, M., Geilen, J., Kainz, M., Hiesmayr, M. J. & Lassnigg, A. (2021) Urinary neprilysin for early detection of acute kidney injury after cardiac surgery: A prospective observational study, *Eur J Anaesthesiol.* **38**, 13-21.

97. Pajenda, S., Mechtler, K. & Wagner, L. (2017) Urinary neprilysin in the critically ill patient, *BMC Nephrol.* **18**, 172.

98. Kullmar, M., Saadat-Gilani, K., Weiss, R., Massoth, C., Lagan, A., Cortes, M. N., Gerss, J., Chawla, L. S., Fliser, D., Meersch, M. & Zarbock, A. (2021) Kinetic Changes of Plasma Renin Concentrations Predict Acute Kidney Injury in Cardiac Surgery Patients, *Am J Respir Crit Care Med.* **203**, 1119-1126.

99. Legrand, M. & Bokoch, M. P. (2021) The Yin and Yang of the Renin-Angiotensin-Aldosterone System in Acute Kidney Injury, *Am J Respir Crit Care Med.* **203**, 1053-1055.

100. Bone, R. C., Balk, R. A., Cerra, F. B., Dellinger, R. P., Fein, A. M., Knaus, W. A., Schein, R. M. & Sibbald, W. J. (1992) Definitions for sepsis and organ failure and guidelines for the use of innovative therapies in sepsis. The ACCP/SCCM Consensus Conference Committee. American College of Chest Physicians/Society of Critical Care Medicine, *Chest.* **101**, 1644-55.

101. Levy, M. M., Fink, M. P., Marshall, J. C., Abraham, E., Angus, D., Cook, D., Cohen, J., Opal, S. M., Vincent, J. L., Ramsay, G. & International Sepsis Definitions, C. (2003) 2001 SCCM/ESICM/ACCP/ATS/SIS International Sepsis Definitions Conference, *Intensive Care Med.* **29**, 530-8.

102. Singer, M., Deutschman, C. S., Seymour, C. W., Shankar-Hari, M., Annane, D., Bauer, M., Bellomo, R., Bernard, G. R., Chiche, J. D., Coopersmith, C. M., Hotchkiss, R. S., Levy, M. M., Marshall, J. C., Martin, G. S., Opal, S. M., Rubenfeld, G. D., van der Poll, T., Vincent, J. L. & Angus, D. C. (2016) The Third International Consensus Definitions for Sepsis and Septic Shock (Sepsis-3), *JAMA.* **315**, 801-10.

103. Gotts, J. E. & Matthay, M. A. (2016) Sepsis: pathophysiology and clinical management, *BMJ.* **353**, i1585.

104. Angus, D. C. & van der Poll, T. (2013) Severe sepsis and septic shock, *N Engl J Med.* **369**, 840-51.

105. Arina, P. & Singer, M. (2021) Pathophysiology of sepsis, *Curr Opin Anaesthesiol.* **34**, 77-84.

106. Horiguchi, H., Loftus, T. J., Hawkins, R. B., Raymond, S. L., Stortz, J. A., Hollen, M. K., Weiss, B. P., Miller, E. S., Bihorac, A., Larson, S. D., Mohr, A. M., Brakenridge, S. C., Tsujimoto, H., Ueno, H., Moore, F. A., Moldawer, L. L., Efron, P. A., Sepsis & Critical Illness Research Center, I. (2018) Innate Immunity in the Persistent Inflammation, Immunosuppression, and Catabolism Syndrome and Its Implications for Therapy, *Front Immunol.* **9**, 595.

107. Hawkins, R. B., Raymond, S. L., Stortz, J. A., Horiguchi, H., Brakenridge, S. C., Gardner, A., Efron, P. A., Bihorac, A., Segal, M., Moore, F. A. & Moldawer, L. L. (2018) Chronic Critical Illness and the Persistent Inflammation, Immunosuppression, and Catabolism Syndrome, *Front Immunol.* **9**, 1511.

108. Villalba, N., Baby, S. & Yuan, S. Y. (2021) The Endothelial Glycocalyx as a Double-Edged Sword in Microvascular Homeostasis and Pathogenesis, *Front Cell Dev Biol.* **9**, 711003.

109. Landry, D. W. & Oliver, J. A. (2001) The pathogenesis of vasodilatory shock, *N Engl J Med.* **345**, 588-95.

110. Wang, M., Zhong, D., Dong, P. & Song, Y. (2019) Blocking CXCR1/2 contributes to amelioration of lipopolysaccharide-induced sepsis by downregulating substance P, *J Cell Biochem.* **120**, 2007-2014.

111. Monti, G., Terzi, V., Calini, A., Di Marco, F., Cruz, D., Pulici, M., Brioschi, P., Vesconi, S., Fumagalli, R. & Casella, G. (2015) Rescue therapy with polymyxin B hemoperfusion in high-dose vasopressor therapy refractory septic shock, *Minerva Anestesiol.* **81**, 516-25.

112. Leone, M., Albanese, J., Delmas, A., Chaabane, W., Garnier, F. & Martin, C. (2004) Terlipressin in catecholamine-resistant septic shock patients, *Shock.* **22**, 314-9.

113. Auchet, T., Regnier, M. A., Girerd, N. & Levy, B. (2017) Outcome of patients with septic shock and high-dose vasopressor therapy, *Ann Intensive Care.* **7**, 43.

114. Pirracchio, R., Deye, N., Lukaszewicz, A. C., Mebazaa, A., Cholley, B., Mateo, J., Megarbane, B., Launay, J. M., Peynet, J., Baud, F. & Payen, D. (2008) Impaired plasma B-type natriuretic peptide clearance in human septic shock, *Crit Care Med.* **36**, 2542-6.

115. Wagner, K., Wachter, U., Vogt, J. A., Scheuerle, A., McCook, O., Weber, S., Groger, M., Stahl, B., Georgieff, M., Moller, P., Bergmann, A., Hein, F., Calzia, E., Radermacher, P. &

Wagner, F. (2013) Adrenomedullin binding improves catecholamine responsiveness and kidney function in resuscitated murine septic shock, *Intensive Care Med Exp.* **1**, 21.

116. Sipka, A., Langner, K., Seyfert, H. M. & Schuberth, H. J. (2010) Substance P alters the in vitro LPS responsiveness of bovine monocytes and blood-derived macrophages, *Vet Immunol Immunopathol.* **136**, 219-26.

117. Pham, D., Jeng, A. Y., Escher, E., Sirois, P. & Battistini, B. (2000) Effects of a selective neutral endopeptidase and a nonselective neutral endopeptidase/endothelin-converting enzyme inhibitor on lipopolysaccharide-induced endotoxaemia in anaesthetized Sprague-Dawley rats, *J Cardiovasc Pharmacol.* **36**, S362-6.

118. Panayiotou, C. M., Baliga, R., Stidwill, R., Taylor, V., Singer, M. & Hobbs, A. J. (2010) Resistance to endotoxic shock in mice lacking natriuretic peptide receptor-A, *Br J Pharmacol.* **160**, 2045-54.

119. Marino, R., Struck, J., Maisel, A. S., Magrini, L., Bergmann, A. & Di Somma, S. (2014) Plasma adrenomedullin is associated with short-term mortality and vasopressor requirement in patients admitted with sepsis, *Crit Care.* **18**, R34.

120. Lu, B., Gerard, N. P., Kolakowski, L. F., Jr., Bozza, M., Zurakowski, D., Finco, O., Carroll, M. C. & Gerard, C. (1995) Neutral endopeptidase modulation of septic shock, *J Exp Med.* **181**, 2271-5.

121. Lu, B., Figini, M., Emanueli, C., Geppetti, P., Grady, E. F., Gerard, N. P., Ansell, J., Payan, D. G., Gerard, C. & Bunnett, N. (1997) The control of microvascular permeability and blood pressure by neutral endopeptidase, *Nat Med.* **3**, 904-7.

122. Hoffman, M., Kyriazis, I. D., Dimitriou, A., Mishra, S. K., Koch, W. J. & Drosatos, K. (2020) B-type natriuretic peptide is upregulated by c-Jun N-terminal kinase and contributes to septic hypotension, *JCI Insight.* **5**.

123. Murphy, S. P., Prescott, M. F., Camacho, A., Iyer, S. R., Maisel, A. S., Felker, G. M., Butler, J., Pina, I. L., Ibrahim, N. E., Abbas, C., Burnett, J. C., Jr., Solomon, S. D. & Januzzi, J. L. (2021) Atrial Natriuretic Peptide and Treatment With Sacubitril/Valsartan in Heart Failure With Reduced Ejection Fraction, *JACC Heart Fail.* **9**, 127-136.

124. Ibrahim, N. E., McCarthy, C. P., Shrestha, S., Gaggin, H. K., Mukai, R., Szymonifka, J., Apple, F. S., Burnett, J. C., Jr., Iyer, S. & Januzzi, J. L., Jr. (2019) Effect of Neprilysin Inhibition on Various Natriuretic Peptide Assays, *J Am Coll Cardiol.* **73**, 1273-1284.

125. Charles, C. J., Espiner, E. A., Richards, A. M., Nicholls, M. G. & Yandle, T. G. (1995) Biological actions and pharmacokinetics of C-type natriuretic peptide in conscious sheep, *Am J Physiol.* **268**, R201-7.

126. Nielsen, S. J., Rehfeld, J. F. & Goetze, J. P. (2008) Mismeasure of C-type natriuretic peptide, *Clin Chem.* **54**, 225-7.

127. Michel, T., Nougue, H., Cartailler, J., Lefevre, G., Sadoune, M., Picard, F., Cohen-Solal, A., Logeart, D., Launay, J. M. & Vodovar, N. (2022) proANP Metabolism Provides New Insights Into Sacubitril/Valsartan Mode of Action, *Circ Res.* **130**, e44-e57.

128. Nougue, H., Michel, T., Picard, F., Lassus, J., Sadoune, M., Laribi, S., Cohen-Solal, A., Logeart, D., Launay, J. M. & Vodovar, N. (2023) Deconvolution of BNP and NT-proBNP Immunoreactivities by Mass Spectrometry in Heart Failure and Sacubitril/Valsartan Treatment, *Clin Chem.* **69**, 350-362.

129. Arfsten, H., Goliasch, G., Bartko, P. E., Prausmuller, S., Spinka, G., Cho, A., Novak, J., Haslacher, H., Strunk, G., Struck, J., Hulsmann, M. & Pavo, N. (2021) Increased concentrations of bioactive adrenomedullin subsequently to angiotensin-receptor/neprilysin-inhibitor treatment in chronic systolic heart failure, *Br J Clin Pharmacol.* **87**, 916-924.

130. Seferovic, J. P., Claggett, B., Seidelmann, S. B., Seely, E. W., Packer, M., Zile, M. R., Rouleau, J. L., Swedberg, K., Lefkowitz, M., Shi, V. C., Desai, A. S., McMurray, J. J. V. & Solomon, S. D. (2017) Effect of sacubitril/valsartan versus enalapril on glycaemic control in patients with heart failure and diabetes: a post-hoc analysis from the PARADIGM-HF trial, *Lancet Diabetes Endocrinol.* **5**, 333-340.

131. Vodovar, N., Nougue, H., Launay, J. M., Solal, A. C. & Logeart, D. (2017) Sacubitril/valsartan in PARADIGM-HF, *Lancet Diabetes Endocrinol.* **5**, 495-496.

132. Nougue, H., Picard, F., Cohen Solal, A., Logeart, D., Launay, J. M. & Vodovar, N. (2023) Sacubitril/valsartan decreased cardiac and systemic hypoxia in chronic heart failure patients: a mechanistic study *under review*.

133. Sengenes, C., Berlan, M., De Glisezinski, I., Lafontan, M. & Galitzky, J. (2000) Natriuretic peptides: a new lipolytic pathway in human adipocytes, *FASEB J.* **14**, 1345-51.

134. Cacciatore, F., Amarelli, C., Maiello, C., Pratillo, M., Tosini, P., Mattucci, I., Salerno, G., Curcio, F., Elia, F., Mercurio, V., Golino, P., Bonaduce, D. & Abete, P. (2020) Effect of Sacubitril-Valsartan in reducing depression in patients with advanced heart failure, *J Affect Disord.* **272**, 132-137.

135. Dereli, S., Kilincel, O., Cerik, I. B. & Kaya, A. (2020) Impact of sacubitril/valsartan treatment on depression and anxiety in heart failure with reduced ejection fraction, *Acta Cardiol.* **75**, 774-782.

136. von Haehling, S., Arzt, M., Doehner, W., Edelmann, F., Evertz, R., Ebner, N., Herrmann-Lingen, C., Garfias Macedo, T., Koziolek, M., Noutsias, M., Schulze, P. C., Wachter, R., Hasenfuss, G. & Laufs, U. (2021) Improving exercise capacity and quality of life using non-invasive heart failure treatments: evidence from clinical trials, *Eur J Heart Fail.* **23**, 92-113.

137. Lecomte, J. M., Costentin, J., Vlaiculescu, A., Chaillet, P., Marcais-Collado, H., Llorens-Cortes, C., Leboyer, M. & Schwartz, J. C. (1986) Pharmacological properties of acetorphan, a parenterally active "enkephalinase" inhibitor, *J Pharmacol Exp Ther.* **237**, 937-44.

138. Griggs, D. W., Prinsen, M. J., Oliva, J., Campbell, M. A., Arnett, S. D., Tajfirouz, D., Ruminski, P. G., Yu, Y., Bond, B. R., Ji, Y., Neckermann, G., Choy, R. K., de Hostos, E. & Meyers, M. J. (2016) Pharmacologic Comparison of Clinical Neutral Endopeptidase Inhibitors in a Rat Model of Acute Secretory Diarrhea, *J Pharmacol Exp Ther.* **357**, 423-31.

139. Ronco, C., Grammaticopoulos, S., Rosner, M., De Cal, M., Soni, S., Lentini, P. & Piccinni, P. (2010) Oliguria, creatinine and other biomarkers of acute kidney injury, *Contrib Nephrol.* **164**, 118-127.

140. Zarbock, A., Kullmar, M., Ostermann, M., Lucchese, G., Baig, K., Cennamo, A., Rajani, R., McCorkell, S., Arndt, C., Wulf, H., Irqsusi, M., Monaco, F., Di Prima, A. L., Garcia Alvarez, M., Italiano, S., Miralles Bagan, J., Kunst, G., Nair, S., L'Acqua, C., Hoste, E., Vandenberghe, W.,

Honore, P. M., Kellum, J. A., Forni, L. G., Grieshaber, P., Massoth, C., Weiss, R., Gerss, J., Wempe, C. & Meersch, M. (2021) Prevention of Cardiac Surgery-Associated Acute Kidney Injury by Implementing the KDIGO Guidelines in High-Risk Patients Identified by Biomarkers: The PrevAKI-Multicenter Randomized Controlled Trial, *Anesth Analg.* **133**, 292-302.

141. Wang, Y. & Bellomo, R. (2017) Cardiac surgery-associated acute kidney injury: risk factors, pathophysiology and treatment, *Nat Rev Nephrol.* **13**, 697-711.

142. Nair, A. & Seelam, S. (2023) Urinary neprilysin - Another marker to predict postoperative acute kidney injury, *J Anaesthesiol Clin Pharmacol.* **39**, 143-144.

143. Damman, K., Gori, M., Claggett, B., Jhund, P. S., Senni, M., Lefkowitz, M. P., Prescott, M. F., Shi, V. C., Rouleau, J. L., Swedberg, K., Zile, M. R., Packer, M., Desai, A. S., Solomon, S. D. & McMurray, J. J. V. (2018) Renal Effects and Associated Outcomes During Angiotensin-Neprilysin Inhibition in Heart Failure, *JACC Heart Fail.* **6**, 489-498.

144. Packer, M., Claggett, B., Lefkowitz, M. P., McMurray, J. J. V., Rouleau, J. L., Solomon, S. D. & Zile, M. R. (2018) Effect of neprilysin inhibition on renal function in patients with type 2 diabetes and chronic heart failure who are receiving target doses of inhibitors of the renin-angiotensin system: a secondary analysis of the PARADIGM-HF trial, *Lancet Diabetes Endocrinol.* **6**, 547-554.

145. Habibi, J., Aroor, A. R., Das, N. A., Manrique-Acevedo, C. M., Johnson, M. S., Hayden, M. R., Nistala, R., Wiedmeyer, C., Chandrasekar, B. & DeMarco, V. G. (2019) The combination of a neprilysin inhibitor (sacubitril) and angiotensin-II receptor blocker (valsartan) attenuates glomerular and tubular injury in the Zucker Obese rat, *Cardiovasc Diabetol.* **18**, 40.

146. Legrand, M., Futier, E., Leone, M., Deniau, B., Mebazaa, A., Plaud, B., Coriat, P., Rossignol, P., Vicaut, E., Gayat, E. & investigators, S.-O.-N. s. (2019) Impact of renin-angiotensin system inhibitors continuation versus discontinuation on outcome after major surgery: protocol of a multicenter randomized, controlled trial (STOP-or-NOT trial), *Trials.* **20**, 160.